CONTROLLED RELEASE OF OXAMNIQUINE FROM POLYMER FILMS

Thesis submitted for the degree of

DOCTOR OF PHILOSOPHY

in the

FACULTY OF MEDICINE

in the

UNIVERSITY OF LONDON

by

RODGER PHILLIP BARNETT

Department of Pharmaceutics
School of Pharmacy
University of London

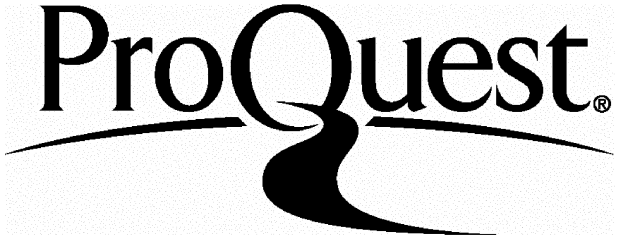

ABSTRACT OF THESIS

CONTROLLED RELEASE OF OXAMNIQUINE FROM POLYMER FILMS

A study has been made of the physicochemical properties of Eudragit Retard L (ERL) and Eudragit Retard S (ERS) copolymers that influence the release of the schistosomicidal agent, oxamniquine (Pfizer UK4271) when dispersed in the polymers.

Isolated films were produced by casting solutions of the mixed polymers in dichloromethane on to a mercury surface and allowing the solvent to evaporate. The presence or absence of crystallinity within the polymer films was determined by X-ray crystallography and samples of the isolated films were examined by scanning electron microscopy to study their surface characteristics. The glass transition temperatures of polymer films were determined by measurement of the surface hardness over a range of temperatures using a micro-indentation hardness tester.

A series of films containing dispersed oxamniquine were prepared and the diffusion of oxamniquine from the films into a buffered aqueous medium was measured. To extend the studies from these model systems to a suitable dosage form, the polymers containing dispersed oxamniquine were spray coated onto inert, spherical carbohydrate pellets in a laboratory scale fluidised bed coater/granulator.

The factors affecting the release of oxamniquine from the free films and coated pellets were critically evaluated. The parameters which were studied included the proportion of polymer ERL to ERS, the drug loading within the film, and the effect of plasticising agents. The plasticisers chosen were glyceryl triacetate, polyethylene glycol 400, and dimethyl, diethyl and dibutyl phthalates.

It was found that the release from coated pellets was faster than from the equivalent free films, and no direct correlation could be made between the model systems and formulated dosage forms. The data from the release profiles was optimised mathematically to arbitrary polynomials by computer. The fitted data were tested against various kinetic models to evaluate the possible mechanisms of release of oxamniquine from both the free films and coated pellets.

ACKNOWLEDGMENTS

I would like to express my sincere gratitude to Professor J E Carless and Dr M P Summers for their guidance and support throughout the course of this research and in the preparation of the manuscript.

My appreciation goes to Mr J E Jeffries and his staff of Pfizer Central Research Ltd for the provision of Oxamniquine and UK3883; the loan of equipment and the use of facilities at their pilot plant in Sandwich, Kent. Also to the technical staff of the Department of Pharmaceutics at The School of Pharmacy, University of London, for their help and assistance. Also to Röhm Pharma, Darmstadt for the gift of Eudragit RL and RS.

I am pleased to acknowledge the following people: Mr Wilf Baldeo of the Department of Pharmaceutical Chemistry at The School of Pharmacy for nuclear magnetic resonance and elemental analysis. Mr Malcolm Weinberg of Chelsea College University of London for assistance with scanning electron microscopy. Dr Ruth Osborn of Imperial College, University of London for X-ray crystallography. Dr Darico Butina of the Computational Chemistry Group, Glaxo Group Research for molecular modelling of oxamniquine. Finally to Dr Ian Winterborn and Dr Clive Walton of Glaxo Group Research for their support and encouragement.

I would also like to thank Miss Manda Freeman for her excellent work in typing this thesis, and Miss Gaynor Goldring for the numerous copies of photographs included in the text.

Finally, I would like to thank my wife Mandy and my parents for their interest, understanding and support to enable this work to be completed.

CONTENTS

Page Number

LIST OF FIGURES

Page Number

LIST OF TABLES

CHAPTER 1

INTRODUCTION AND LITERATURE REVIEW

1.1 Controlled Release

Over the years there have been several attempts to classify and apply a standard nomenclature to long acting dosage forms. BALLARD (1978) cited several terms which have been used in the literature to describe oral and injectable prolonged action dosage forms. These terms include continuous, controlled, programmed, protracted, repository, retard, spaced, sustained, long-term and timed release. This is one of several attempts which have been made to classify this type of prolonged action dosage form. (LAZARUS AND COOPER (1959); PETERS (1963 a, b); SHANGRAW (1967)). Many of these terms describe an essentially identical concept and lead to some confusion. BAKER AND LONSDALE (1974) and LANGER (1980) have drawn a distinction between sustained and controlled release. They stated that sustained release can be produced by several methods such as complexation, slow dissolving coatings and low solubility prodrugs, the release characteristics of these systems are sensitive to the environmental factors to which they are exposed. These include pH, gut motility and other variables along the gastrointestinal tract. Controlled release devices, however, have a release rate which is precisely determined by the characteristics of the device itself. KYDONIEUS (1980) has defined controlled release as

a technique or method in which active chemicals are made available to a specific target at a rate and with a duration designed to accomplish a specific effect. BANKER (1978) has extended this to state that controlling the release of drugs often involves the entrapment or association of the drug in a polymeric system. An engineering orientated definition is that controlled release is the permeation-moderated transfer of an active material from a reservoir to a target surface to maintain a predetermined concentration or emission level for a specified period of time (KYDONEIUS, 1980).

The design of controlled release device described in this thesis is a matrix system in which the polymer contains either dissolved solute or dispersed solute in equilibrium with dissolved solute. The solute is released by diffusion through the continuum of the matrix or pores within its structure (ROSEMAN AND CARDARELLI, 1980). When the whole matrix acts as the controlled release device, the matrix system is often termed a MONOLITH.

Monolithic devices have been developed to release steroids in microdoses for use in intravaginal, ring shaped, long term contraceptive devices containing a single steroid (MISHELL et al, 1970) and combination steroids (MISHELL et al, 1978). Monolithic devices containing steroids have also as subcutaneous implants (CHIEN et al, 1976). The main advantage with monolithic devices is claimed to be the simplicity and low cost of manufacture. In polymeric

systems, the active components and any excipients are mixed with the polymer and then fused together by moulding, extrusion, calendering or casting (HARRIS, 1976).

However, as will be discussed subsequently, it is not always possible to achieve zero order kinetics which is a desirable characteristic of controlled release.

1.1.1 Rationale For Controlled Release

Drugs administered periodically in conventional dosage forms such as tablets, capsules, topicals and parenterals may produce significant fluctuations of drug concentration in the systemic circulation or tissues (PAUL, 1976). This could lead to alternation between subtherapeutic and toxic levels of drug upon repeat administration, particularly if the drug has a narrow therapeutic index.

Conventional application of agricultural chemicals may provide initial concentrations of chemicals well in excess of requirements to ensure the presence of sufficient chemical for a practical time period, thus leading to wastage and possible toxicity.

Ideally, then, a controlled release system should maintain drug (or chemical) within a defined therapeutic range for the desired time. Figure 1 shows typical blood concentration levels which might be achieved following the administration of oral, intravenous and an ideal controlled

release dosage form.

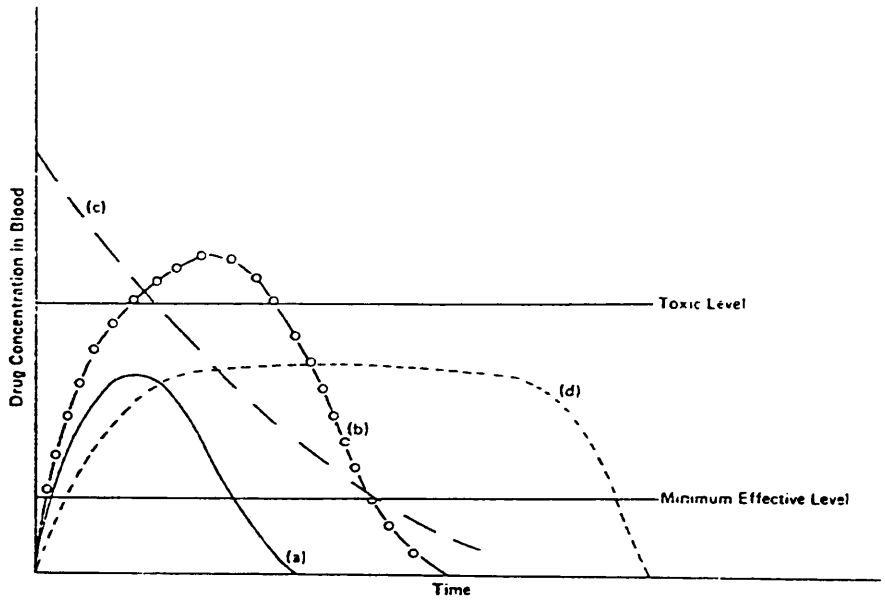

Figure 1 Typical drug level versus time profiles following the administration of various dosage forms.
(a) Standard oral dose. (b) Oral overdose. (c) IV injection. (d) Controlled release ideal dose. (Reproduced from KYDONEIUS, 1980)

With conventional dosage administration blood levels may be initially in the toxic range and side effects may be seen. As the concentration diminishes, a second dose is required to prevent blood levels falling below the minimum effective level. Characteristically the ideal controlled release profile shows a slower onset into the therapeutic range followed by a prolonged, constant level within this region and a slower tail off at the end of the life of the dosage form.

With controlled release dosage forms it is possible to programme the rate of effective administration into the

formulation. CHANDRASEKERAN et al (1983) have highlighted a number of drugs whose selectivity of action is related to the rate of administration. These include steroids, antitumour agents, hormones and narcotic analgesics. Pilocarpine and hyoscine have been developed as occular and transdermal controlled delivery systems with lower delivery rates than conventionally administered equivalents and reduced side effects (LANGER, 1980.)

Controlled release formulations may help to avoid 'first pass' metabolism of drugs in the liver and thus reduce the total amount of drug required for therapeutic effect (SHAW et al, 1975). ZAFFARONI (1973) has expressed the view that optimisation of existing drugs may replace new drug discovery. This is perhaps an extreme view, and the two activities should be seen as complementary.

Some of the advantages and disadvantages of controlled release are summarised as follows (LANGER, 1980; FANGER, 1974; ROBINSON, 1976).

1.1.1.1 Advantages

1. Plasma drug levels maintained in therapeutically desirable range.
2. Harmful side effects from systemic administration reduced or eliminated.
3. Patient compliance improved.
4. Drug administration improved in underprivileged (third world) areas where medical supervision may not be good.

5. Better administration of drugs with short half lives.

6. Potentially less expensive and less wasteful of drug.

7. More readily reversible in the case of adverse events.

8. Conversion of liquids to solids and flowable powders.

9. Taste masking of bitter substances.

10. Improvement of drug efficiency in the treatment of illness.

11. Special 'programmed' effects to release drugs at specific times during the day and night.

1.1.1.2 Disadvantages

1. Potential toxicity or lack of biocompatibility of the polymer or any polymer breakdown products.

2. Fate and toxicity of any additives included in the formulation of polymer matrices.

3. Expense resulting from material and development costs.

4. Surgical procedures may be required to implant or remove devices.

5. Pain resulting from the presence of implants.

6. Possibility of toxic effects if leaks or defects occur in devices. Stringent quality control and assurance is required during manufacture.

7. Cost, time and probability of securing government registration for controlled release.

1.1.2 Some Criteria For The Design Of Oral Controlled Release Dosage Forms

Compared with an implantable or transdermal controlled release dosage form, an oral controlled release dosage form has a shorter residence time at its site of action. Furthermore it is not reversible during that period. Special considerations have to be given to the design of such dosage forms.

The therapeutic index (TI) of a drug is the ratio of the toxic and minimum therapeutic plasma levels. Dosage forms designed to provide systemic therapy can be further rated by their ability to maintain the drug plasma concentration within the therapeutic range. THEEUWES AND BAYNE (1977) defined the dosage form index (DI) as the actual range of plasma concentrations achieved at steady state. Dosage form design for drugs is aimed at forcing DI $\leq$ TI.

Consideration must be given to whether a drug is suitable for inclusion in an oral controlled release dosage form. RITSCHEL (1973) has stated that there is no rational reason for using controlled release formulations of drugs with biological half lives of 8 or more hours. Similarly drugs with a half lives of 1 hour or less are difficult to formulate if their usual single dosage exceeds more than about 500mg.

The simplest model for the design of an oral controlled release dosage forms, is one similar to an intravenous infusion with an initial rapid intravenous injection as loading dose (GARCIA et al, 1978). For oral controlled release preparations both the initial and maintenance dose have an absorption step before entering the blood (GIBALDI AND PERRIER, 1975).

For a drug to be transferred from the gastrointestinal tract to the general circulation first involves the drug dissolving in the GI fluids. Bioavailability of drugs from

oral controlled release dosage forms may be rate limited by drug dissolution in the GI fluids. This rate limiting step may arise from the physical properties of the drug, the dosage or from physiological factors at the absorption site. Physiological factors that may influence drug bioavailability include gastric emptying time, intestinal mobility, specificity and surface area of absorption sites, blood flow to absorption sites, gastric secretions, metabolism, and the first pass effect. Controlled release dosage forms should ideally be designed to minimise the effects of these variables.

Gastric emtpying and factors affecting residence time in the stomach have been reviewed (BENET, 1973). Physical activity, emotional state, position of the body, volume and composition of meals, and drugs may affect gastric residence times, which may vary between 0 and 12 hours (WAGNER, 1961). Gastrointestinal motility and transit time are important experimental variables which should be considered when oral controlled release products are tested in vitro.

After the drug has crossed the gastrointestinal membrane, removal to the systemic circulation is dependent on blood flow. Changes in intestinal blood flow may affect the absorption of drugs in several ways depending on the lipophilicity of the drug. For controlled release preparations, the availability of a loading dose will depend more on adequate blood flow to the absorption site

than will the prolonged release dose.

The acidic medium in the stomach and enzymatic activity in the gastrointestinal tract may cause the degradation of some drugs before they can be absorbed. Drugs absorbed from the stomach and intestine will pass through the liver before reaching the systemic circulation. If a drug is metabolised in the liver or excreted into the bile, then a proportion of the dose may be lost. If this happens with a poorly designed controlled release preparation, systemic blood levels may be subtherapeutic. If, however, the first pass effect can be saturated, then a high loading dose and an increased maintenance dose may actually improve overall drug efficacy.

A well formulated controlled release preparation should be able to produce a release profile that overcomes potential physiological variability.

1.1.3 Methods of Achieving Controlled Release

Many physical and chemical systems have been developed to control the release of biologically active agents. KYDONEIUS (1980) has categorised polymeric systems which have been developed for controlled release. This classification is summarised in Table 1.

TABLE 1 **SUMMARY OF POLYMERIC SYSTEMS SUITABLE FOR CONTROLLED RELEASE**

1. PHYSICAL SYSTEMS

A. Reservoir systems with rate controlling membrane

1. Microencapsulation
2. Macroencapsulation
3. Membrane systems

B. Reservoir systems without rate controlling membrane

1. Hollow fibres
2. Porous polymeric sheets
3. Porous polymeric substrates and foams

C. Monolithic systems

1. Physically dissolved in non-porous, polymeric, or elastomeric matrix
2. Physically dispersed in nonporous, polymeric, or elastomeric matrix
   a. Nonerodible)
   b. Erodible) applies
   c. Environmental agent) to both
      ingression) C1 and C2
   d. Degradable)

D. Laminated structures

1. Reservoir layer chemically similar to outer control layers
2. Reservoir layer chemically dissimilar to outer control layers

E. Others

1. Osmotic pumps
2. Ion exchange resins

2. CHEMICAL SYSTEMS

A. Chemical erosion of the polymer matrix

B. Biological erosion of the polymer matrix

1. Heterogeneous erosion) applies to
2. Homogeneous erosion) both 2A and 2B

1.2 Controlled release from Matrix Dosage Forms

1.2.1 Factors Affecting the Performance of Matrix Systems

Much of the interest in matrix systems started from the innovative work of Takeru Higuchi who was studying percutaneous absorption of drugs from creams and ointments. HIGUCHI (1960) described cases where the rate limiting step to absorption was in the skin or the applied vehicle.
W I HIGUCHI (1962) applied the analysis of T Higuchi to data generated on the release of sodium radioiodide from hydrophilic ointment bases and demonstrated the validity of the models. T HIGUCHI (1963) extended the models to describe the release of drugs from matrices. He introduced the case of heterogeneous (granular) matrices where release of the drugs was through interconnecting capillaries within the matrix rather than through the matrix itself. Approximate expressions for the release of drugs from homogeneous and heterogeneous spherical matrices were also derived.

DESAI et al (1965, 1966 a, b, c) investigated in detail factors which influenced the release of solid drug dispersed in inert matrices. In a series of studies, it was found that although release from polyethylene matrices followed Higuchi's model on a qualitative and semiquantitative level, difficulties were encountered when a quantitative application of the theory to the data was

made. It was proposed that porosity and tortuosity were not independent of other factors in the model. In particular the porosity of the matrix was identified as comprising volume fractions due to dissolving drug, liberation of soluble excipients and entrapped air. Anomalous results would be obtained if experimental conditions were not defined to ensure that all of the available porosity was made available to the extracting solvent. This was most readily achieved by including a surfactant in the extraction medium. With polyvinyl chloride matrices anomalous results were obtained even using this technique. The cause was found to be entrapped air which could only be removed by vacuum pretreatment of the matrices. A similar effect was identified by KORSEMEYER et al (1983) with hydroxypropylmethyl cellulose matrices.

SINGH et al (1967 a, b) extended these experiments to include the effect of incorporating two drugs in the matrix. Studies were initially conducted using non-interacting drug mixtures. Two regions within the matrix were identified. The first region, in contact with the matrix-solvent boundary, was completely depleted of solid drug and contained only solutions of the drugs. The second region, further from the matrix-solvent interface contained solution of the faster moving drug in the presence of solid from the slower moving drug.

In a further study, two drugs which were known to form complexes in various stoichiometric ratios were chosen. In this case the regions within the matrix comprised mixtures of complexes in solution, and mixtures of complexes together with solid drug. Theoretical expressions for the release of the drugs were derived for each of these cases. Values for the tortuosity and porosity of the matrices were determined using the methods described by DESAI et al (1966 a). Good agreement was obtained between calculated and measured release rates. These studies are good examples of the complexity which may arise when more than one component is included in a matrix formulation. Comparable situations may occur when oxamniquine is incorporated into a plasticised matrix some form of interaction occurs within the matrix. LAPIDUS AND LORDI (1966, 1968) reported the release of drugs from hydrophilic gel forming matrices where contact with the extracting solvent causes swelling. Provided that the hydrated polymer does not disintegrate, the relationship between quantity released and $\sqrt{\text{time}}$ was linear and drug release was diffusion controlled. It was noted that where a water soluble excipient was included in the matrix formulation, diffusion of the excipient from the matrix reduced the effective tortuosity of the matrix and increased the apparent release rate of the drug.

ROSEMAN AND HIGUCHI (1970) studied the release of a sparingly soluble steroid incorporated into silicone polymer. It was found that including the effects of a static diffusion layer in contact with the matrix in the

model gave a better correlation of experimental results with predicted results. It was suggested that the partition coefficient of the drug between the extracting solvent and the matrix, drug concentration within the polymer, and agitation conditions are important factors in the release process. This has implications on the release profiles which could be expected in vivo, where slower observed release rates are likely to be due to diffusion boundary layers. ROSEMAN (1972) demonstrated that the solubility of a series of steroids in silicone polymer and their partition coefficient are sensitive functions of the steroid structure and influence the release profile of the drug from the polymer. At early times release was found to be dependent upon the matrix-boundary diffusion layer while at later times the release process was matrix controlled (i.e. followed the Higuchi model). Due to the low solubility of the steroids in the release medium and the necessity to maintain sink conditions throughout the duration of the experiment, each release determination could take several weeks to complete. CHIEN et al (1974) modified the experimental method by adding a cosolvent to the release medium increasing the solubility of the steroid. This experimental modification was shown not to alter the mechanism of drug release from the matrices.

CHIEN AND LAMBERT (1974) demonstrated that as the solubility of the drug in the eluting medium decreased, the drug release process changed from matrix control to partition control, and indicated the possibility of a

transition phase between these two processes at a critical value of the partition coefficient. CHIEN et al (1975) derived mathematical expressions to describe the effects of varying the volume fraction of cosolvent included in the eluting medium on the concentration gradients within the depletion zones and diffusion layers. It was concluded that the variation in solution solubility dictated the mechanism and rate of drug release from a drug dispersed within a polymer matrix. An alternative approach to the same problem was adopted by ROSEMAN AND YALKOWSKY (1976) who varied the solubility and partition coefficient by synthesising an homologous series of alkyl esters of para-aminobezoic acid. These compounds were incorporated into silicone matrices and the release into water studied. It was concluded that with the drug dispersed in the matrix a period of partition control precedes matrix control i.e. the overall release pattern is biphasic. The change of mechanism occurs gradually and a transition period exists. The overall balance of these phases is determined by solubility and partition coefficient of the drugs. It was claimed that this situation approximates to profiles which would be seen in vivo for an implanted controlled release device.

SCIARRA AND GIDWANI (1970, 1972) studied the release of several antiseptic agents dispersed in acrylic, polyamide and ethylcellulose films. They proposed that drug released followed an apparent first order or dissolution controlled model based on the Noyes-Whitney relationship rather than

the expected Higuchi matrix release model or the partition controlled model. No explanation for this unusual behaviour was given. DONBROW AND FRIEDMAN (1975a) re-examined the data using the mathematical manipulation of differential rate plots originally proposed by SCHWARTZ et al (1968) and proposed that, in practice, release was matrix controlled. The explanation proposed for this difference was that the duration over which the study had been conducted was insufficient to illustrate the true mechanism.

LEE (1980a) applied an integral method to moving boundary problems associated with drug release from polymeric matrices. The methods used by LEE (1980a) were also applied to the release from planar and spherical matrices into a constant finite volume (i.e. non sink conditions), as well as erodible planar matrices. The applicability of these equations to drug release from hydrogel matrices was also demonstrated (LEE, 1980b).

HALEBLAIN et al (1971) studied the release of steroids from silicone matrices and found the results to be incompatible with Higuchi's model. A dissolution rather than diffusion controlled mechanism was proposed. HIGUCHI (1967) considered dissolution controlled mechanisms as a heterogeneous reactions with mass transfer occurring through the movement of solute molecules from solid surfaces. CHIEN (1976) depicted the process of drug release from polymeric matrices as occurring in three

energy-activated steps

(a) dissociation of drug molecules from a crystal lattice

(b) solubilisation of drug molecules in the polymer matrix

(c) diffusion of drug molecules in the matrix.

CHANDRASEKARAN AND PAUL (1982) have proposed a model for dissolution controlled transport from dispersed matrices incorporating both dissolution and diffusion transport. Under appropriate boundary conditions, the approximated solutions, may be produced by the analytical method of Laplace transformations (CRANK, 1975) under dissolution limiting conditions or under diffusion control. The resulting equations produced by the diffusion controlled model equations are analogous to the model proposed by Higuchi.

FESSI et al (1982) have proposed a model and provided supporting data to show that the release of drugs from matrices which contained low drug content (less than saturation solubility x porosity) followed a square root release law as proposed by Higuchi. CHANDRASEKARAN AND HILLMAN (1980) have developed a model for drug release in which the polymer matrix is considered as a heterogeneous system comprising a continuous polymer phase and a discontinuous dispersed drug phase. In this way the release rate can be calculated from the density of the dispersed phase, the drug loading and the permeability of drug in the pure polymer.

Although this model appears to provide a relatively simple means of calculating release rates, factors such as changing composition of the disperse phase and phase interactions are not accounted for. CHANG AND HIMMELSTEIN (1990) have presented a mathematical model of simultaneous dissolution and diffusion-controlled release from non-swelling, non-erodible polymer matrices. The model, based on unsteady-state mass balances has been used to assess the potential to achieve controlled release from matrices by (i) altering geometry, (ii) balancing dissolution verus diffusion control, (iii) time dependent porosity change, (iv) position dependent drug loading and combinations of these effects.

As indicated previously, matrix formulations which demonstrate square root of time release kinetics when tested <u>in vitro</u> using sink conditions may perform very differently <u>in vivo</u> where static hydrodynamic boundary layers may determine the release kinetics. A number of approaches have been made to adapt matrix systems to produce time independent (zero order) kinetics. BORODKIN AND TUCKER (1975) prepared films of hydroxypropyl cellulose containing dispersed drugs which were shown to exhibit $\sqrt{t}$ time kinetics. Similar films were laminated with preformed mixed films of polyvinyl acetate and hydroxypropyl cellulose. These laminated films exhibited zero order release provided that unit thermodynamic activity of the drug was maintained at the interface between the films. The overall rate of release could be

altered by changing the composition of the mixed polymer layer. A similar effect was achieved by DONBROW AND SAMUELOV (1980) by laminating a drug free layer of ethylcellulose to a matrix layer of hydroxypropylcellulose containing various drugs. In these studies the effective release rate was varied by including either polyethylene glycol (PEG) or hydroxypropyl cellulose to the ethyl cellulose layer. Inclusion of the water soluble PEG increased the effective release rate from the composite film. BODMEIER AND PAERATAKUL (1990a) prepared laminated films comprising a reservoir and a drug free membrane prepared from aqueous latexes of Eudragit NE-30D, to obtain zero order release. Drug release was independent of loading where drug was dispersed, rather than dissolved in the reservoir layer. The release rate could be increased by including HPMC to the rate controlling membrane.

COLOMBO et al (1985) prepared small spherical matrices of polyvinyl alcohol containing drugs by compression, as a model for an oral multiple unit dosage form. These "mini-matrices" were demonstrated to give zero order release when the surface of the matrices were crosslinked.

Matrix systems termed 'swelling controlled' are capable of producing zero order release under certain conditions. Swelling controlled systems have been described (KORSMEYER AND PEPPAS, 1983) as initially solvent-free glassy polymers containing drugs, which in the presence of a thermodynamically compatible dissolution medium

(penetrant), swell. The glass transition temperature of the polymer is lowered in the swollen region producing a moving rubber/glass boundary, allowing the dispersed drug to diffuse outward. Approximate zero order kinetics are predicted when the velocity of the swelling interface is much smaller than the diffusion coefficient of the drug. Examples have been shown by GOOD (1978), HOPFENBERG AND HSU (1978) and HOPFENBERG et al (1981), although KORSMEYER AND PEPPAS (1981) were unable to demonstrate zero order kinetics, albeit predicted, from a cross linked polyvinyl alcohol matrix. This behaviour might be typical of hydrogel type polymers.

1.3 Eudragit Copolymers

1.3.1 Characteristics of Eudragit copolymers

Eudragit is a trade mark of Röhm Pharma, for a range of copolymers based on acrylic and methylacrylic acids, esters and salts. By altering the functionality of the co-monomers, the properties and potential applications of the copolymers can be varied. Table 2 summarises the properties and basic applications of Eudragit copolymers. It is possible to use any of the copolymers to coat whole tablets, pellets, granules and powders as well as in a granulating formulation under appropriate processing conditions to obtain the desired properties.

LEHMANN et al (1978) and LEHMANN AND DREHER (1979) coated small particles and granules with a range of Eudragit copolymers using fluidised bed conditions. They demonstrated that it was possible to obtain coated particles with the desired release profiles in which particles were not agglomerated, with coherent film layers covering all compact structures of particle surfaces, including sharp edges and corners of crystals. LEHMANN (1971) discussed the possibility of using Eudragits to produce oral programmed release dosage forms. Programmed release was defined as the controlled liberation of drugs with time at defined sites in the gastrointestinal tract, to obtain consistent therapeutic plasma and reduced side effects. Polymers such as Eudragit E, L and S contain pendant ionic groups which can be neutralised. Above a certain degree of neutralisation, these polymers begin to dissolve. These specific and markedly pH dependent properties allow controlled release of drugs in a specific section of the gastrointestinal tract. By contrast Eudragit RL and RS are pH independent, insoluble (LEHMANN, 1968) but permeable polymers, which when mixed together, will produce a coating which will release drug at a desired rate. LEHMANN proposed that the concept of programmed release could be produced using a combination of the two types of methacrylate which would localise both the site and rate of delivery.

TABLE 2 PROPERTIES AND APPLICATIONS OF EUDRAGIT COPOLYMERS

Polymer	Polymer Structure				Aqueous Solubility/ Permeability	Solvents/ Diluents	Description/Major Applications
	Repeating Unit	Substituents		Internal Ratio			
		R1	R2				
E	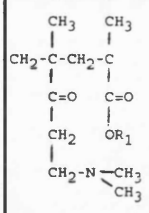	CH_2 or C_2H_5	-	-	Soluble at pHs up to 5, expandable and permeable above pH5	Organic	Cationic polymer. Rapidly disintegrating coatings for taste masking.
L and S	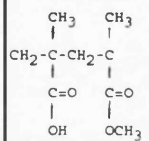	-	-	Carboxyl groups : esters is 1:1 in L 1:2 in S	L is soluble from pH6 upward. S is soluble from pH7 upward.	Organic & Plasticisers	Anionic polymer. Enteric coatings and pH dependent sustained release.
E30D	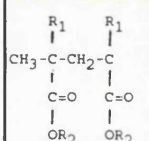	H,CH_3	CH_3, C_2H_5	-	Expandable with no additives. Permeable in combination with hydrophilic polymers.	Water	Neutral copolymer Delayed action preparations or as a rapidly disintegrating film.
L30D	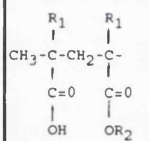	H,CH_3	CH_3, C_2H_5	Carboxyl groups : esters is 1:1	Soluble above pH5.5.	Water & Plasticisers	Gastric resistant enteric coatings. Anionic polymer.
RL and RS	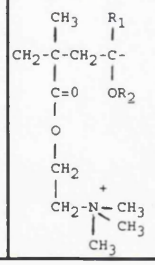	H,CH_3	CH_3, C_2H_5	Ammonium groups : neutral groups 1:20 in RL 1:40 in RS	Insoluble, RL is readily peremable, RS is poorly permeable.	Organic & Plasticisers	pH independent delayed action preparations.

1.3.2 Permeation Studies Involving Eudragit Copolymers

A number of studies have been conducted to evaluate the properties of Eudragits as film forming materials for use in controlled release applications.

GURNY et al (1976) prepared isolated films of Eudragit RL either by pouring onto a mercury substrate or by pneumatic

spraying onto a rotating disc. Dichloromethane was used as the solvent and glyceryl triacetate was evaluated as a plasticiser. Both poured and sprayed films swelled when immersed in simulated gastric or intestinal fluid, but not to the same extent as would be expected for hydrogel materials. Plasticised films swelled more than unplasticised films. Both sprayed and poured films swelled to around the same extent, but differences between the formulation and swelling medium were more marked with sprayed films. The diffusion of salicylic acid through each type of film was studied. As expected inclusion of glyceryl triacetate increased the permeability of both poured and sprayed films. The effect however was more marked when simulated intestinal juice was used as the permeation medium. Interestingly in these studies GURNY et al (1976) presoaked the films in drug free diffusion medium prior to the start of the experiment, to allow the films to hydrate to equilibrium. This would also have the effect of at least partially extracting the plasticiser from the films since it is readily water soluble. The actual diffusion experiments would therefore have been conducted using a partially deplasticised porous film. In a subsequent study, GURNY et al (1977 a) used a multiple regression model to analyse the effect of film thickness and plasticiser content for sprayed and poured films. It was attempted to describe the apparent permeability of the films as a quadratic function using plasticiser content and film thickness as independent variables. This approach was not found to be uniformly successful, which suggested that

other factors which were not controlled in this experimental model were also determinants in the resulting permeability.

LIPPOLD et al (1980) compared the permeability of cast films of Eudragit RS and ethylcellulose to carbutamide and chloramphenicol. Polyethylene glycol 1540 was included as a plasticiser in some formulations. Inclusion of increasing amounts of plasticiser results in increased diffusivity of the drug. Scanning electron microscopy demonstrated that the water soluble plasticiser is rapidly removed from the film after contact with aqueous extraction medium, resulting in a loose porous film structure. The diffusivity then depends on the solubility of the drugs in the network. The diffusivity is influenced considerably when ionised drugs interact with the ionised Eudragit membrane. In these studies, Eudragit RS/PM was used to prepare the films, which were cast onto mercury. This particular formulation of Eudragit contains a low level of talc intended as a lubricant for compression of matrices. It is possible that the presence of these particulates would influence the permeability of the resulting films.

As indicated in Section 1.4, preparation of isolated films by casting results in slow uniaxial removal of solvent. Upper and lower film surfaces developing on desolvation could differ in structure and therefore properties. ANDERSON et al (1973) observed that the permeation rate of urea through plasticised Eudragit RL membranes was greater

when the lower cast surface was the entry surface for the permeant. ABDEL-AZIZ et al (1975) prepared films of Eudragit RL and Eudragit RS cast onto PTFE moulds machined to give the best possible finish. This surface did, however, result in a core on the surface which could be detected and characterised using an electronic amplified stylus method (ABDEL-AZIZ, 1976) as well as by scanning electron microscopy. For both polymers the films were more permeable to urea when the lower (substrate contact) surface was used as the entry surface.

Exposure of the lower surface of Eudragit RL films to the permeant resulted in more numerous large, crater-like pores compared with fewer small blister like pores when the upper surface was exposed. Similar effects were observed with Eudragit RS, but the resulting pores were considerably smaller. It was not suggested that the pores were direct surface to surface channels but paths within the structure of the film. It was suggested that the non-homogeneous distribution of the pores could have resulted from non uniform drying conditions during film formation.

OKOR (1982a) examined the effect of mixing the two polymers on the permeability of urea through the films. The permeability of the films did not increase linearly with the ratio of the two polymers. Addition of less than 50% of Eudragit RL to Eudragit RS resulted in little permeability change, but with greater quantities of Eudragit RL the permeability increase was significant. In

contrast to ABDEL-AZIZ et al (1975), Okor felt that this permeability increase could not be related to the increase in swelling observed with films of increasing hydrophilicity. Instead, it was proposed that the permeability increase was related to an increase in the internal pore size, rather the number of pores.

It was proposed that the pore size was the result of balancing repulsive intermolecular forces due to increasing cation content with the cohesive forces involved in film formation.

OKOR AND ANDERSON (1978 a, b) also studied the effect of laminating preformed plasticised films of Eudragit RL and RS mixtures. When identical films were laminated and compared with single films of identical composition and thickness, the single film was generally more permeable than the laminate. This was likely to be due to increased diffusive resistance resulting from the formed boundary between the two films. When films of different composition were laminated, the permeability was found to depend on the arrangement of layers in the permeant stream. When the poorly permeable Eudragit RS was adjacent to the permeant stream, little change in permeability from a pure RS film was noted. The permeability could be moderated when Eudragit RL was adjacent to the permeant source.

1.3.3 Other Applications of Eudragit Copolymers

As indicated in Section 1.3.1, Eudragit Retard copolymers can also be used as compression excipients or granulating agents to produce controlled release without coating smaller particles. Examples of these studies have been reported in the literature by for example FARHADIEH et al (1971a, b), HANNULA (1983a, b), HANNULA AND IIVANAINEN (1983a, b) and NAIDOO AND MCGINITY (1985).

PONGPAIBUL et al (1984) prepared microspheres of indomethacin with Eudragit RS and Eudragit L using an emulsion-solvent evaporation method. Unusually, drug release followed zero order kinetics. It was proposed that the hydration and swelling of the microspheres resulted in an increased porosity which compensated for the increased diffusional path length. The release rate of drug from these microspheres could be altered by varying the ratio of the soluble to the swellable polymer, or by changing the solvent to polymer ratio which altered the porosity of the microsphere. MALAMATARIS AND AVGERINOS (1990) prepared Indomethacin microspheres. In contrast to PONGPAIBUL et al (1984) these workers found that drug loading efficiency was increased as the polymer content increased. The release pattern was found to be biphasic comprising a fast initial phase and a slow terminal phase. A matrix controlled model was found to be appropriate at higher drug : polymer ratios, whereas at lower ratios a form of dissolution control, termed the HIXSON-CROWELL cube root law was more

appropriate.

BENITA et al (1985) used Eudragit RL and RS to microencapsulate paracetamol using a solvent/non-solvent phase separation method. It was necessary to include another polymer, polyisobutylene to prevent aggregation of the microcapsules during preparation. The microcapsule membrane was found to control the release of paracetamol and it was possible that either a dissolution controlled or matrix controlled release model was appropriate. However, application of differential rate plots proposed for microcapsules (BENITA AND DONBROW, 1982; DONBROW AND BENITA, 1982) as well as for isolated polymer films (SCHWARTZ et al, 1968; DONBROW AND FRIEDMAN 1975a) demonstrated the release was dissolution controlled. The rate of release could be controlled by varying the quantity of coating polymer, or the particle size of the encapsulated drug i.e. the wall thickness and surface area of the microcapsules, or by varying the addition rate of the non-solvent phase.

EL-FATTAH et al (1984a) prepared co-precipitates of pheniramine aminosalicylate and various Eudragits by dissolving them in a common organic solvent followed by evaporation of the solvent and subsequent drying. Eudragit L, S, RL, RS, RLPM and RSPM as well as combinations of these polymers were tested. In all cases it was found that the co-precipitate, which was not the result of chemical interaction between the drug and Eudragit, provided some

measure of controlled release compared with an equivalent physical mixture of the drug and the polymer.

It was found that the insoluble, permeable Eudragit RL and RS were the least effective in controlling the release of the drug whereas the 'enteric' copolymers Eudragit L and S which are insoluble and impermeable below pHs 6 and 7 respectively did control the release over up to 7 hours, using a pH gradient 'half change' method to evaluate dissolution. Similar favourable results were obtained when the co-precipitates were compressed (EL-FATTAH et al, 1984b). LAUNO et al (1990) prepared co-precipitates of ampicillin with Eudragit RS to prepare matrix tablets with a sustaining effect.

Although intended primarily as solvent based polymers for matrix formulation, granulation and coating a number of novel applications for Eudragit have been reported in the literature. KAWASHIMA et al (1989) prepared coacervates with ibuprofen from ethanolic solution using a quasi emulsion solvent diffusion method to form microspheres. AKBUGA (1989) prepared spherical microspheres of frusemide, the release of which followed matrix controlled kinetics, using a spherical crystallisation technique. CHAFI et al (1988, 1989a, b, 1991) complexed drugs by polymerisation with an anhydride monomer. The resulting drug-polymer complex was subsequently dispersed in a Eudragit matrix. The resulting composition released drug on contact with

aqueous solutions independent of pH. Release kinetics were found to be diffusion controlled.

Pseudo-latices of Eudragit RL and RS prepared by direct emulsification in hot water without emulsifiers have been prepared commercially. Their potential for use in oral controlled delivery systems has been examined (LEHMANN AND DREHER, 1979, 1981; GOODHARD et al, 1984). BODMEIR AND PAERATKUL (1990b) indicated although drugs can be dissolved or dispersed in the latex, a more homogeneous dispersion could be obtained by first dissolving the drug in a water insoluble plasticiser. The addition of plasticiser reduced the temperature at which a film could be formed. If the drug dispersion in the matrix was monolithic then the mechanism of release was shown to depend on the concentration of plasticiser.

Pseudo-latices of Eudragit RL and RS have been prepared by solvent change techniques, to develop applications for these polymers in aqueous based systems. Pseudo-latices have been used to coat drug loaded pellets (CHANG et al, 1989) and as the basis for transdermal patches (JAIN et al, 1990). OKOR AND OBI (1990) prepared isolated films of an aqueous based coacervate of Eudragit RL impregnated onto a porous paper. The performance of the resulting film to control release compared favourably with films cast from organic solvents. Several studies have been conducted on the preparation of coacervates from ethanolic solutions of Eudragit RL and RS by the addition of water, which is a

non-solvent for these polymers. The resulting structure depended on the initial concentration of the polymer (OKOR, 1991) with gels forming at higher polymer concentration and fluids at lower concentrations. Addition of sodium chloride flocculated the stable dispersions to thixotropic gels. The concentration of sodium chloride required to achieve this was greater for the more ionic Eudragit RL.

Flocculated dispersions which were coacervated with a drug (salicylic acid) were dried. The resulting powder has been filled into capsules (OKOR 1990), or compressed with a suitable diluent (OKOR AND YAHAYA, 1990). Such systems have been shown to exhibit potential for controlled release.

OTH AND MOES (1989) prepared "coevaporates" of indomethacin with Eudragit RS and RL which were tabletted to form matrices. Indomethacin release was found to follow matrix controlled kinetics. Polymer films containing propranolol, prepared by dissolving the drug in aqueous colloidal dispersions of Eudragit RL and RS were examined by BODMEIER AND PAERATAKUL (1990b). The release from these latex based films was faster than from solvent cast films. Inclusion of a water soluble polymer further increased the drug release rate by preventing complete coalescence of the latex particles during film formation and consequent extraction of the plasticiser. WATTS et al (1991) prepared and harvested microspheres of Eudragit RS using an emulsion-solvent evaporation technique in both the presence

and absence of surfactants. Inclusion of the surfactant yielded microspheres with a greater porosity which promoted a more rapid release of drug. LEHR et al (1990) combined Eudragit RL with other acrylic polymers (carbomer and polycarbophil) as potential muco-adhesive polymer in-vitro. BARKAI et al (1990) incorporated Nifedipine into Eudragit RL and RS microspheres which were prepared. These microspheres were found to be of the 'film type' comprising a spherical micromatrix with an internal void space and a polymeric membrane of variable thickness containing either molecularly dispersed or solid drug. The kinetics of release of such microcapsules have proven difficult to characterise (BENITA et al, 1990). It would have been predicted that matrix controlled kinetics should be observed. However this was not the case as there were interactions between the drug and polymer in the membrane.

1.4 Formation and Properties of Polymer Films

Polymers represent a unique class of material which, due to their molecular structure, are able to form mechanically stable fibre and film structures when drawn or deposited from appropriate solvents. This section provides an overview of some of the factors affecting the formation, properties and testing of polymer films.

1.4.1 Forces in Polymer Films

In any pharmaceutical film coating operation where a polymer film is being applied to a substrate two sets of forces operate. Firstly, cohesion, which is the force between film forming polymer molecules, and secondly adhesion, which is the force between the film and the substrate. Clearly, when preparing an isolated film, it is necessary to minimise adhesive forces so that the formed film can be removed from the substrate.

Cohesion is the ability of contiguous surfaces of the same material, at a molecular or (polymer chain) supermolecular level, to form a strong bond which prevents or resists separation at the point of contact (BANKER 1966). To obtain high levels of cohesion, there must be high levels of cohesive strength between molecules, and the contiguous surfaces of the film material must coalesce on contact. Coalescence is the disappearance of boundary layers between adjacent polymer molecular layers and is described by diffusion theory. It involves the movement of one or more macromolecules between and within film layers under a number of conditions.

If there is adequate cohesive attraction between the molecules and sufficient diffusion and coalescence the overall result will be restoration of the polymer structure to a uniform non-laminated matrix at the contact zone. The degree of cohesion within a given polymer system will

influence the density and compactness of the film, and therefore the porosity and permeability, as well as mechanical properties.

Process factors which may influence film cohesion include (i) time in contact with surface (ii) contact surface temperature (iii) contact pressure (iv) coat thickness (v) coating solution concentration. Not all of these factors may be controlled in typical pharmaceutical coating operations.

In addition, several formulation factors may influence film cohesion. These include polymer chemistry (stereo-chemistry and functionality), polymer structure (molecular order and crystallinity), choice of solvent, inclusion of plasticisers and dispersed solids within the film.

1.4.2 Methods of Preparation of Free Films

Polymer films can be made by two fundamentally different techniques - by melt or sinter fabrication or by casting from solution (ALLCOCK AND LAMPE, 1981).

Melt processes are suitable for polymers that are thermally stable above their melting or softening temperature. Films are fabricated by a combination of heat and pressure typically as a unit process (melt pressing) or a continuous process (melt extrusion). These methods often involve cooling on both surfaces to form the film. Since the

cooling is unlikely to be identically balanced, some degree of asymmetry is imposed upon the resulting film structure (HOPFENBERG, 1978).

In solution casting, the polymer is dissolved in a suitable solvent (or combination of solvents) to form a viscous solution. The solution is then poured onto a non-adhesive surface, and the solvent allowed to evaporate. The dry film can then be peeled from the flat surface. Once again some degree of asymmetry may be expected, since the solvent is removed unidirectionally (HOPFENBERG, 1978).

CARNELL AND CASSIDY (1961) have reviewed methods for the preparation of thick membranes. In this instance a thick membrane is taken to be 1μm to 5mm thick. Methods which were cited included casting onto a rotating cylinder, the addition of a release agent coated onto metal plate, and a water soluble polymer precoated onto plates as a parting agent. The use of metal retaining rings placed onto mercury contained in glass dishes was described as a methods of preparing flexible collodion membranes.

KANIG AND GOODMAN (1962) prepared films using the Gardner Ultra Applicator. This device draws a wet film of a defined thickness onto a suitable surface using a suitable 'doctor' blade. Similar apparatus has been used to prepare films by a number of workers (MUNDEN et al, 1964; FITES et al, 1970; SPITAEL AND KINGET, 1977a; BANKER et al, 1966a).

As an alternative to solution spreading methods it is possible to simply pour the polymer solution onto a suitable inert surface.

Potential substrates for the preparation of such films are polytetrafluoroethylene, float glass, brass, 'Formica', polyethylene and mercury (ABDEL-AZIZ, 1976; SAMUELOV et al, 1979), plexiglass (perspex), siliconised plexiglass and aluminium (GURNY, 1976). Paraffin wax film (PARAFILM) has been used as a substrate for sprayed isolated silicone derived films containing polyethylene glycols (LI AND PECK, 1989). For special applications such as the preparation of Angström thick films, water has been used as a casting substrate (CARNELL AND CASSIDY, 1961).

Much of the preliminary work in these studies involved identifying suitable methods which could be used for the preparation of free films of Eudragit Retard.

1.4.3 Effect of Casting Solvent

It is important that a suitable solvent is chosen so that the good films of the polymers can be cast and that subsequently the polymer can be applied to the surface of pellets in a state allowing maximum use to be made of its properties. Solvation of a polymer requires that the cohesive forces between polymer macromolecules are overcome by attractions between solute and solvent molecules. If a polymer has a high degree of crystallinity, then the

greater will be the intermolecular cohesive forces, and the more difficult it will be to solvate such a polymer.

Dissolution of a polymer takes place in two distinct stages. In the first stage the polymer imbibes solvent and expands to form a swollen gel. The second stage involves the breakdown of the gel to give a solution of the polymer in the solvent. It is this second stage which does not occur when a polymer is crosslinked, highly crystalline, or has strong hydrogen bonding throughout its structure. Thus for film preparation and coating applications the most suitable polymers are those which are substantially (or totally) amorphous and which have been modified to minimise intermolecular interaction. Typically polymers for pharmaceutical applications are polyfunctional polyelectrolytes. The rate, extent and pH of ionisation of these polymers will determine the application for the polymer.

BANKER (1966) has indicated how the functionality of a polymer influences its solution properties and film characteristics. When a charged polymer becomes ionised mutual repulsion of the charged groups will repel one another causing stretching of the polymer chain backbone. This will increase the interaction between polymer and solvent. This may be a point of note for Eudragit RL and RS which differ only in the extent of charged group substitution.

On a qualitative level, a liquid will be a 'good' solvent for the polymer if the solvent physically and chemically resembles the polymer that it is dissolving. Thermodynamically, dissolution occurs when in the equation

$$\Delta G = \Delta H - T\Delta S \qquad (1)$$

the free energy of mixing, ΔG is negative. If the entropy of mixing, ΔS, is positive then the sign and magnitude of ΔG is determined by the heat of mixing ΔH. For non polar molecules, and in the absence of hydrogen bonding ΔH is positive. HILDEBRAND AND SCOTT (1950) defined a quantity called the cohesive energy densitive density δ^2 by the equation

$$\delta^2 = \frac{Eo}{Vo} \qquad (2)$$

where Eo is the latent energy of vaporisation for a volume Vo of substance.

The quantity reflects the energy required to overcome the cohesive forces present to vaporise a substance. If the adhesive forces between polymer and solvent are to be similar to the cohesive forces of the polymer and solvent, then it follows that the cohesive energy densities should be similar. If the heat of mixing per unit volume for polymers is the same as that derived for small molecules then, as shown by HILDEBRAND AND SCOTT (1950)

$$\Delta H = V(1-V)(\delta_1-\delta_2)^2 \qquad (3)$$

where V is the volume fraction of polymer; δ_1^2 and δ_2^2 are the cohesive energy densities and δ_1, δ_2 the solubility parameters of the solvent and polymer respectively.

The solubility parameter approach can fail where there is evidence of strong polymer-solvent interactions, but it is useful information which can be supplemented by an examination of other effects (BURRELL, 1975).

The solubility parameter of solvents can be readily determined from calorimetry experiments. However, the solubility of parameter of polymers is often determined indirectly by mixing a known weight of polymer in a selected solvent and observing the resultant mixture. If that mixture is single phase and free from gel particles, then the polymer is judged 'soluble'. This procedure is performed for a range of solvents capable of poor, moderate and strong hydrogen bonding. The solubility parameter of the polymer is taken as the mid point of the solubility parameters of the solvents in which the polymer is soluble. It is also possible to assess the solubility parameter by examining properties such as swelling or intrinsic viscosity, which are assumed to be at a maximum when the solubility parameter of the polymer is equal to that of the solvent. This assessment can also be made using a range of solvents (KENT AND ROWE, 1978).

The use of a mixed solvent system for polymers presents further difficulties. Mixed solvents may be essential for copolymers of chemically different polymers. SPITAEL AND KINGET (1977b, 1980) compared the effect of using mixed and single solvents. Where a mixed solvent was used in which the polymer was insoluble in the slower evaporating solvent, the polymer precipitated from the solution to form a non-cohesive, brittle and opaque mixture. This was avoided by using an azeotropic mixture of the two solvents, such that the composition of the solvent mixture remained constant during the evaporation of the solvent. It was also noted that even when a single solvent was used, increasing the evaporation rate by using a pneumatic spray resulted in a 'droplet structure' in the film and reduced its overall mechanical strength. TAMBA VEMBA et al (1980) examined the effect of a range of cosolvents added to Freon 21 on the appearance, mechanical strength and water vapour permeability of ethylcellulose films. The nature of the cosolvent clearly influenced the cohesion of the polymer chains and was reflected in whether a transparent or translucent film was formed, which was mechanically strong and resisted the passage of water vapour.

One interesting observation made was that films cast from certain solvent mixtures were at ambient relative humidity, opaque and apparently non-cohesive. However, when cast in an enclosed low humidity environment, the resulting films were transparent. The effect was therefore a combination of high humidity and the solvent composition. GILLARD et

al (1980) identified the presence of 'molecular regions' of precipitated ethylcellulose within a homogeneous structure using scanning electron microscopy. It was proposed that the presence of water during the gelling stage of film formation resulted in the formation of a second phase. After evaporation of the solvent the resulting film was in two phases resulting in an opaque appearance. SPROCKEL et al (1990) identified a similar influence of the relative humidity of the casting environment on the barrier properties of cellulosic films to water vapour.

JOHNSTON AND SOURIRAJAN (1973) demonstrated that the permeability of polymer films may be affected by altering the casting solvent composition. ABDEL AZIZ et al (1974) investigated the effect of including up to 10% of methanol or ethanol in the casting solvent for Eudragit films. The surface differences effect described previously was reduced and the overall permeability of the film was increased. Inclusion of ethanol in the casting solvent caused an apparently dense surface layer of the films to be replaced with a porous layer. The internal layer which comprised a sponge like structure with discontinuous pores was replaced with more contiguous channel-like structure between the two surfaces of the film (ABDEL AZIZ AND ANDERSON, 1976). Two possible reasons were suggested for this effect. Firstly, the less volatile mixture of solvent containing alcohol produced higher temperatures within the forming polymer which deaggregated the chains. Secondly, since both Eudragit RL and Eudragit RS are less soluble in ethanol,

the consequent decrease in polymer solvation and molecular dispersion resulted in decreased film cohesive strength and more near-continuous surface to surface channels to form. Although no proposals were made as to which of the two effects predominated, it is likely that the solubility effect was most responsible for the change in internal structure.

AZOURY et al (1988) found significant differences in the hydration properties of films cast from ethanol and chloroform and ethanol in the presence of various quantities of PEG were attributed to structural or chemical differences induced by the casting solvent. The hydrophilic solvent resulted in films with a more porous, ordered and less dense structure than those cast from the hydrophobic solvent. NIXON AND WONG (1990) prepared cast films of ethylcellulose from solvents, and found them to be smooth and non-porous examined by scanning electron microscopy. Solvent evaporation methods were found to produce films with a denser polymer structure than those prepared by temperature induced formation.

1.4.4 The Effect of Plasticisers

Two types of plasticisation of polymers are possible. These are termed internal and external plasticisation. In both cases the effect is to extend, dilute and soften the polymer structure, reducing cohesion within the structure. Internal plasticisation achieves this chemically,

copolymerising the structure with small compatible molecules. The studies described in this thesis involved only external plasticisation in which a substance is added to the polymer structure and may be physiochemically associated with it.

Plasticisers may be defined (BANKER, 1966) as substantially non-volatile, high boiling, non-separating substances which when added to another material changes certain physical and mechanical properties of that material. Plasticisers are added to polymers for several reasons, of which reduced brittleness, improved flexibility, toughness, strength and tear resistance are notable. The proposed mechanism for these changes is thought to be a decrease in the intermolecular forces along the polymer chain hence a reduction in cohesion, which reduces the tensile strength and glass transition temperature.

Essentially, plasticisers should be compatible with the polymer and remain permanent within the structure. Thus the plasticiser should as far as possible resemble the polymer which it is plasticising. Since plasticisers reduce the intermolecular forces within the polymer structure, their use is limited to completely or mostly amorphous polymers. Clearly the plasticiser must be compatible with all components in the film forming mixture. The permanence requirement for plasticisers relates to the potential to resist changes in physical and mechanical stability with time. ANDERSON AND ABDEL AZIZ (1976) found

that approximately 50% of the plasticiser content of Eudragit films was lost after six months storage in a desiccator. This resulted in changes to the permeability and plasticity of the films. For the more hydrophilic Eudragit RL the change was less critical since the polymer more readily hydrates during permeation. PICKARD (1979) reported similar effects for the storage of mixed ethylcellulose/hydroxypropyl methylcellulose films plasticised with propylene glycol, stored at controlled ambient conditions. The water vapour permeability of the films diminished with time ultimately equalling the permeability of unplasticised films stored similarly. The observations were consistent with a loss of plasticiser from the films. This was not the case when the films were stored under a control condition enclosed in an environment saturated with propylene glycol vapour. Although plasticisers generally are high boiling substances, as small molecules, they exert a high vapour pressure and are subject to phase separation and subsequent loss.

By decreasing cohesion and increasing segmental mobility, plasticisers should be expected to increase the permeability of polymer films. This effect has been demonstrated by, amongst others, COLLETTA AND RUBIN (1964), FITES et al (1970), SHAH AND SHETH (1972) and DONBROW AND FRIEDMAN (1974) who also demonstrated that polyethylene glycol 4000 is extracted rapidly from ethylcellulose membranes. DONBROW AND FRIEDMAN (1975b) proposed that the enhancement of permeation of ethylcellulose films to

benzoic and salicylic acid by PEG4000 could arise as a result of

(a) altering the properties of the film homogeneously, changing the balance between the configuration of crystalline and amorphous regions

(b) increasing the porosity of the film

(c) formation of a network of surface to surface channels

(d) acting as a carrier forming complexes which transport permeants across the membrane.

These mechanisms would not necessarily have to act uniquely. In a series of experiments (b) was identified as being the most likely mechanism since channels are not apparently formed in the film and benzoates and salicylates do not form complexes with PEG4000 in aqueous media independently of the film environment.

SPITAEL AND KINGET (1977b) evaluated the effects of including polyethylene glycol (PEG), dibutyl phthalate (DBP) or acetyl triethyl citrate (ATC) in isolated films of cellulose acetate phthalate (CAP). They found that inclusion of the readily water soluble PEG resulted in the most significant permeability increase compared with the insoluble plasticisers DBP and ATC. Incorporation of any of the plasticisers into isolated films prepared by

pneumatic spraying had little or no effect on the permeability of the films. It was proposed that sprayed films were more heterogeneous and that plasticisers would not therefore result in increased porosity.

DELPORTE AND JAMINET (1978 a) studied the effects of incorporating the hydrophobic plasticisers diethyl phthalate and ATC on the water vapour permeability of CAP. They determined that the plasticisers reduced the water vapour permeability of the films, that the effect of film thickness was more marked in the presence of plasticiser, and that there was an optimum level of plasticiser which achieved this effect. LACHMAN AND DRUBULIS (1964) proposed that at low levels plasticisers fill intermolecular spaces and therefore reduce the permeability by restricting the diffusivity of permeants. However, at higher concentrations, when the plasticiser completely fills intermolecular spaces, the effect is that of a diluent and permeability is increased. ZATZ et al (1969) provided a more attractive theory that in unplasticised insoluble films, water acts as both a permeant and plasticiser, solvating polar groups within the polymer. When a plasticiser is introduced, there are polar/polar and non-polar/non-polar interactions set up within the film. The polar interactions between polymer and plasticiser effectively solvate the polymer, and at low concentrations reduce the effectiveness of the water in increasing the overall permeability. However, plasticisers also increase the chain mobility which increases the permeability of the

polymer. The overall effect can therefore be considered as the net result of those opposing effects.

DELPORTE AND JAMINET (1978b) examined a water soluble coating composed of hydroxypropyl methylcellulose and ethylcellulose (4:1). Although ethylcellulose is insoluble, the film remains soluble because of the low proportion of EC. The effect of water soluble plasticisers glyceryl triacetate, glycerol and insoluble plasticisers, ATC, diethyl phthalate and Myvacet 7-00 on the water vapour permeability of the films was evaluated.

Unlike the insoluble film, the effect of plasticisers on the permeability was only very slight and not readily predictable. Plasticisers did not, in general, reduce the water vapour permeability of the films. Furthermore, the water vapour permeability was not influenced by film thickness.

OKOR AND ANDERSON (1979) mixed a hydrophillic and a hydrophobic plasticiser, glyceryl triacetate and glyceryl tributyrate in Eudragit RL films. Unexpectedly permeability to urea increased as the proportion of the less soluble glyceryl tributyrate was increased, even though the readily extractable glyceryl triacetate would be expected to provide more available pore space after extraction. Subsequently it was shown (OKOR, 1982b) that the rate of urea permeation through Eudragit RS films decreased as the proportion of glyceryl tributyrate was

increased in the plasticiser mixture. It was considered the former effect was due to increased porosity resulting from extraction of the water miscible plasticiser whereas the latter effect was due to the ability of glyceryl tributyrate to promote the swelling of the film and porosity.

In conclusion LAGUNA et al (1975) have considered properties of polymers, plasticisers and solvents and concluded that many formulations which are actually used are not well researched which results in work being considerably prolonged. It is desirable to consider the properties of all of the components in the formulation together rather than as individual entities. They also consider that future development of coating formulations lies in optimising conditions for current agents rather than the development of new agents.

1.5 Formation and Properties of Applied Coatings

The application of coatings to tablets, pills and capsules has been known since the end of the 18th Century. Since that time it has gradually evolved from an art into a science. Four methods have emerged as a result.

1. Manual application in a standard coating pan.
2. Automatic application in a standard coating pan.
3. Automatic application in a fluidised bed.
4. Compression coating.

Of these methods, automatic application in coating pans and the fluidised bed are methods of choice for the application of polymer films. In particular this review will focus on the fluidised bed method, which was used to prepare applied coatings in these studies.

1.5.1 Development of Fluidised Bed Coating Technology

Fluid bed technology was first developed for rapid and intensive drying of powdered and granular materials. It is now routinely applied to the coating and encapsulation of fine particles and agglomerates as well as the aggregation of fine materials to form granules.

The fluidisation process entails separating a particle bed into discrete entities under a stream of dried gas, application of a solution or suspension of coating material, spreading of the coating uniformly over the surface of the particles, and drying whilst still in suspension. The process is repeated continuously until a coating of the required thickness is built up (ROBINSON et al, 1968).

The original apparatus of WURSTER (1959) comprised a vertical column, constricted at the bottom and expanded at the top. The air velocity in the constricted region was sufficient to propel particles upward. In the expanded region, the air velocity was considerably reduced so that particles fell into the working region of the column.

Calculations were made for the air velocity necessary to fluidise particles of varying density, which was controlled by a constant speed blower and adjustable plates within the column. The atomiser was placed below the working region of the column, and coating solution was sprayed co-currently with the air stream. Drying time was controlled by adjusting either the temperature of the fluidising air or the atomisation conditions.

SINGISER AND LOWENTHAL (1961) reported a slight variation to the basic Wurster design, including a funnel shaped constriction which produced a slightly different fluidisation pattern. CALDWELL AND ROSEN (1964) modified the design further to eliminate the need for support screens, by delivering the particles to be coated via a side arm directly into the fluidising air stream. The coating solution was delivered out of the fluidised air stream, counter-current to the flow of particles. The claimed advantages of this system were the ability to handle large quantities of coating material and to coat with tacky solutions. ROBINSON et al (1968) altered the basic design of the system in order to reduce the minimum coatable particle size. In this design solid particles were blown from a fluidised bed by a turbulent gas jet and the discrete particles transported through a converging cone into a coating application zone. The particles were coated with a spray delivered counter-currently and at a greater velocity than the upward moving particles. The velocity differential removed wetted solids from the

coating area to the fluidised bed outside of the coating zone, where they were able to dry. This process is repeated in a continuous cycle. Using this system it was possible to coat particles as small as 15μm diameter.

WOLKOFF et al (1968) evaluated a miniature air suspension apparatus which permitted the processing of small quantities (several grams) of material rather than the kilogram quantities which had been used in previous studies. Similarly, FRIEDMAN AND DONBROW (1978) reported the design and use of a laboratory scale fluidiser to coat small batches of granules with ethyl cellulose.

1.5.2 Solvent and Temperature Selection

For any solvent based coating process, a rate limiting factor is the removal of solvent i.e. the drying of the coating. The use of large amounts of air in Wurster processes results in the rapid removal of solvent from the applied film. For aqueous based coatings water removal is a function of the humidity, temperature and the volume throughput of the process air. This information is summarised in psychrometric charts for water. In larger scale processes, if the inlet fluidising air is unconditioned for moisture, a weather effect can lead to seasonal variations in the performance of fluid bed processes (JONES, 1985).

With organic solvent based coatings, similar principles apply except that no solvent is present in the ambient air. Evaporative cooling occurs around the surface of the pellets until saturation is reached. Residual water or solvent in the coating layer will probably affect the film forming process. The situation is more complex when a mixed solvent system is used for coating.

The choice of solvent for the process depends upon a number of factors. A rapid drying solvent may be required in a particular process. The boiling point of the solvent is not necessarily a reliable indicator of evaporation rate. Other factors to consider include solubility and compatibility with the polymer (which may be predicted from a knowledge of solubility parameters) as well as cost, safety and toxicity of any residues in the product (HALL AND PONDELL, 1980).

As a result of evaporative cooling, a temperature profile exists within the chamber during the coating process. Air is hottest at the inlet, cooler in the vicinity of the spray and coolest at the top of the bed and around the air outlet. For this reason it is possible to heat the process air to a temperature higher than would be expected from solvent boiling point data alone. When the temperature differential across the bed decreases, this is an indication that moisture or solvent content has been reduced to a critical level. At this point, no free surface moisture is present and the temperature starts to

rise further (SEAGER et al, 1976) in two distinct phases. The first phase of unsaturated surface drying is frequently characterised by a linear relationship between the rate of drying and the water content. In the second phase internal fluid controls drying. This may be characterised by a slow non-linear rate of solvent loss (HARBERT, 1974). It is important to stop drying at this point to prevent over-drying. The use of temperature probes at the air inlet and outlet points may be used to automate coating processes (KULLING AND SIMON, 1980) and reduce the risk of overdrying or underdrying of the coated material. Drying may also be controlled by measurement of relative humidity in the particle bed (COOPER et al, 1961).

GURNY et al (1977b) considered fluidisation temperature and atomisation pressure to be key process variables and plasticiser content of the film to be the key formulation variable in a study on the factors which influence fluidised bed processes. They used a multiple linear regression model, considering up to 2 way interactions, to model the relative effects of these variables. Dissolution of 63% of the active ingredient in either simulated gastric or intestinal media was used as the response variable. Four coating thicknesses were used, but this was not included in the regression model. It was interesting to note that the main effects were significant in both cases, but interactions were less important when simulated intestinal medium was used as the dissolution medium.

1.5.3 Advantages and Disadvantages of Fluidised Bed Coating

1.5.3.1 Advantages

1. Simple to operate; close control of coating conditions which may be automated.
2. Reproducible provided that coating conditions are defined.
3. Rapid. Very good drying conditions achieved within chamber.
4. Flexible. Able to coat a wide range of particle sizes and shapes with a variety of coating agents which may be water or solvent based.
5. Completely enclosed. Pollution control and solvent recovery may be built into process (SIMON, 1978).
6. Range of designs to coat loads from 2g to greater than 30Kg.

1.5.3.2 Disadvantages

1. Unable to coat very small particles (less than 75μm).
2. Possibility of electrostatic buildup within chamber and consequent powder explosion.
3. Risk of explosion, particularly with solvent based processes (SIMON, 1978).

1.5.4 Practical Applications of Coating

There are many examples of fluid bed coating applications reported in the literature. COLLETTA AND RUBIN (1964) coated 20 mesh aspirin particles with a mixture of ethylcellulose and methylcellulose to prepare sustained release coated crystals with an even and reproducible coating of film. FRIEDMAN AND DONBROW (1978) coated granules containing salicylic acid or caffeine with an

ethylcellulose/polyethylene glycol coating to produce homogeneous sustained release coated granules on a small (30-100g) scale. Subsequently FRIEDMAN et al (1979) prepared placebo lactose granules coated with caffeine or salicylic acid dispersed in an ethylcellulose film. Release of drug from the granules was found to conform to the matrix control (Higuchi) model when the quantity of drug contained in the film was less than the estimated solubility of drug in the film. When the drug loading exceeded the solubility, microcrystals were present, which were observed by scanning electron microscopy which resulted in a higher than predicted drug release rate. MEHTA AND JONES (1985) compared coatings prepared from aqueous based and organic based polymers using a range of coating equipment. Coatings prepared in fluidised bed equipment were found to be better than those prepared in conventional or modified coating pans in respect of their homogeneity. Coatings prepared in a Wurster type chamber were better than those prepared in a top-spray fluidised bed, particularly for organic solvent based coatings.

LEHMANN et al (1978) and LEHMANN AND DREHER (1979) have demonstrated that it is possible to coat small and irregular particles with organic solvent based Eudragit polymers providing delayed release and enteric coatings. Coatings, which were prepared using fluidised bed techniques were shown to be applied uniformly even around sharp corners resulting from fractured crystals. It was claimed that coatings of Eudragit retard polymers were

sufficiently flexible so as not to need plasticisers in the formulation.

Considerable interest has arisen in changing from solvent based to water based coatings in recent years, primarily for reasons of reducing emissions and industrial safety issues (PONDELL, 1984). The penalty to be paid is that the choice of polymer and plasticisers is restricted to those which are either water soluble or water dispersible. Although water is not a hazard itself, it may have a deleterious effect on active ingredients or water soluble granules or tablets which may be coated. Core penetration, or failure to form a distinct boundary between the granule or tablet and the film coating is more likely to occur with aqueous based coatings (MEHTA AND JONES, 1985). Microbiological proliferation may occur during solution preparation and on storage. Changes to the way in which coatings are applied, and the type of equipment used, may be necessary with aqueous based coatings (PONDELL, 1984).

LEHMANN (1975, 1982, 1984) has described applications of aqueous based Eudragit pseudolatices, primarily to produce matrix tablets with either delayed release or enteric properties. It does not appear that a suitable acrylic polymer of this type is available for coating granules which themselves display controlled release properties.

Recently aqueous pseudo-latex dispersions of Eudragit RL and Eudragit RS have been prepared and used for coating

(CHANG AND HSIAO, 1989).

1.5.5 Correlation Between Isolated Films and Applied Films

In these studies, isolated films of Eudragit were used as possible models for applied films spray coated onto inert Non-Pareil pellets. A number of studies, for example PATEL et al (1964), LACHMAN AND DRUBULIS (1964), LAPPAS AND MCKEEHAN (1965) have made conclusions about the performance of coatings based on results obtained from experiments using isolated films. BANKER et al (1966 a) have suggested that such conclusions may not be entirely valid. In their studies, plasticisers did not significantly affect the water vapour permeability of hydroxypropyl cellulose films or mixed hydroxypropyl methyl cellulose/ethylcellulose mixed films. Also the permeabilities of the two film types were themselves similar. In a subsequent study (BANKER et al, 1966b), it was shown that films with identical water vapour permeabilites did not impart identical properties when applied to tablet cores.

GURNY et al (1977c) coated granules containing salicylic acid, prepared by marumerisation, with Eudragit RL films plasticised with glyceryl triacetate but did not compare them with similar isolated films prepared previously (GURNY et al, 1976). The release from the applied coatings was studied in vitro and theoretical plasma levels simulated by computer.

1.6 Methods of Measuring Drug Release

The development of new dosage forms requires extensive *in vitro* testing to characterise performance during development to ensure reproducibility during scale up, and ultimately in quality control testing of the final dosage form. The pre-requisites for any *in vitro* method are that it should be simple to execute, easy to standardise, have the minimum practical number of system variables and in the long term be amenable to automation.

Classical methods of characterising drug release involve measuring the permeability coefficient during steady state and evaluating the diffusion coefficient by the time lag method (CRANK AND PARK, 1968). These and other methods often assume that the concentration of drug in the elution medium is negligible throughout the experiment i.e. sink conditions exist. GIBALDI AND FELDMAN (1967) have considered that sink conditions equate to drug concentrations not exceeding 10-20% of the drug solubility in the eluting medium. This may be achieved by various means. ROSEMAN AND HIGUCHI (1970) pumped water continuously at a rate of 60 litres/day to evaluate the release of low solubility steroids. CHIEN *et al* (1974) utilised a solvent mixture of water with polyethylene glycol 400 as the eluting medium; DESAI *et al* (1965) included a surfactant at low concentration although the objective of this was not to increase solubility but to expose the maximum porosity of the matrix. In these

studies the pH of eluting medium was chosen to maintain sink conditions through the time period of release.

Measuring the release of drugs from films involves the use of some kind of a diffusion cell in which the film is mounted and the elution medium passes across the surfaces of the film. When a device is immersed in a stationary elution medium, a diffusion layer will be established at the surface. The significance of such diffusion layers is discussed in Chapter 5. LEVICH (1962) derived an equation to calculate the effective thickness of the diffusion layer of a rotating system (i.e. where a device is rotated in the elution medium or the medium is forced to rotate around a device).

Cell and system designs are often designed to eliminate as far as possible unwanted boundary layers. Frequently hydrodynamics are controlled by the in vitro method used, and are affected by the geometry of any vessels, the volume of liquid and the speed and form of motion caused by the agitator (GOULD, 1983).

There are numerous designs of diffusion cell. Some of the designs which have been cited in literature are those of GONZALES et al (1967), SPILMAN et al (1976) and FITES et al (1970). The cell design used for these studies was a commercially available cell designed by STRICKER (1969, 1971) for simulation in vitro of the bioavailability of drugs. The systems described can be either closed or open.

In closed recirculating systems, a fixed volume of eluent circulates across the system under test, through a continuous monitoring system and then returns to bulk. In open systems, fluid passes across the test system only once, is analysed and then is rejected to waste. Where continuous analysis is not possible, for example where two components are being released and a flow through analysis such as spectroscopy or fluorimetry is not possible because of interactions, it may be necessary to adopt a sampling programme to take aliquots at specified intervals. The disadvantage of such a system, unless it is fully automated, is the length of time over which it is practical to monitor drug release.

The release of drugs from coated pellets is measured using a dissolution apparatus arrangement with either a rotating paddle or rotating basket arrangement. Precise descriptions of this sort of equipment are provided in the pharmacopoeia such as the BP and USP. The precise control of hydrodynamics in such rotatory systems can be difficult and may be affected by liquid agitation characteristics, system geometries, as well as any irregularities with the performance of the apparatus (GOULD, 1983).

1.7 Glass Transition Temperatures

1.7.1 Glass Transitions and Polymer Structure

The glass transition point of a polymer is a fundamental characteristic which affects both the physico-chemical and physical properties of that polymer.

PETERS (1968) has stated that chain mobility should be curtailed when the temperature drops below the glass transition point (Tg). The ease of diffusive hole formation depends upon the segmental chain mobility and on the cohesive energy of the polymer. Diffusion of molecules of comparable size to the monomer segments requires the co-operative movement of polymer segments to create the necessary diffusive holes. KUMINS AND ROTEMAN (1961) have argued that above the glass transition, the number of holes present does not change significantly, but their size changes. In this way the amplitude of segmental oscillations or rotations increases. Thus, with the diffusion of small molecules, the effect of the glass transition might be minor since the molecules are roughly equally likely to encounter a hole of adequate size both above and below Tg. With the diffusion of larger molecules the size becomes more important and an effect of the glass transition can be seen.

Upon heating, polymers pass through the glass transition temperature, and change from the glassy state to either a

rubbery or flexible state depending upon the nature of the polymer. There is no sharp discontinuity in physical properties, but a gradual change in order.

PARK (1968) has described the difference between the glassy and rubbery states in terms of the effects of response to changes in condition. For example if temperature falls, then a decrease in volume occurs. A rubbery polymer will rapidly reach a new equilibrium volume whereas in the glassy state, this will not occur. The glassy state can be considered as a non-equilibrium time-dependent state.

In a glassy polymer the stress developed after the application of a given strain decays slowly with time. If, for instance, such a strain is induced by impact, this impact is focussed on relatively few chemical bonds. Cracks therefore propagate rapidly as both covalent bonds and Van der Waals attractions are broken and a rigid glassy polymer therefore shatters. Bond breakage is one of the few mechanisms by which a glassy polymer can dissipate energy. By contrast elastomers absorb energy which is converted into harmless molecular motions.

Different transition behaviours are exhibited by amorphous and crystalline polymers on heating. Amorphous polymers pass from the glassy state through rubbery gum-like and finally liquid states. Crystalline polymers, by contrast, change from glasses to flexible thermoplastics and will remain in that state until the crystalline melting point is

reached after which the polymer liquifies.

Knowledge of the glass transition temperature of polymers is important to drug release studies since the difference between experimental temperature and glass transition temperature provides an assessment of the free volume of the structure and hence its diffusional characteristics (FLYNN, 1974).

1.7.2 Measurement of Glass Transitions

There is often a discontinuity in temperature related physical properties at the glass transition temperature, and it is this discontinuity which is used to determine the value. WENDLANDT AND GALLAGHER (1981) have described thermal methods used to measure the glass transition. Differential Scanning Calorimetry (DSC) measures changes in heat absorption of a sample compared with a reference during heating. Differential Thermal Analysis measures the temperature difference between the sample and a reference material whilst heating with a constant rate of temperature increase. Glass transitions are, however, second order transitions, which means that the specific heat capacity of a sample rather than the enthalpy changes. These specific heat capacity changes are sometimes very small and may be masked by 'drifts' in the instrument baseline, which can lead to difficulties in detecting glass transitions by thermal methods. Several other techniques have been used

to detect glass transition. These include

1. Dilatometry, in which the rate of change of the volume of a polymer sample immersed in a liquid which is a non-solvent for the polymer and any additives is measured.

2. Torsonial Rigidity. A polymer sample is impregnated onto an inert glass braid. The fibre is suspended in a torsional pendulum, and the damping frequency and period of the pendulum are measured.

3. Penetration (Indentation) Techniques. A point or sphere is rested on the surface of a polymer sample. The movement of the indenter is measured and amplified. Above Tg, the polymer is softer and the indenter will penetrate deeper.

4. Nuclear Magnetic Resonance. Broad shifts in the nuclear magnetic resonance spectrum of polymers can be detected, as in the glass transition region the polymer is transformed from a solid to a pseudo liquid.

LEE AND KNIGHT (1965) have discussed reasons for the inconsistencies which occur in the measurement of glass transition temperatures. They concluded that the main factors were the failure to enable near equilibrium conditions during measurement and the use of too great a

rate of temperature change, exceeding the rate of change in molecular arrangement. The first problem is difficult to overcome, but the second may be addressed by employing slower heating rate. This is not practical unless the approximate transition temperature is known and measurements are made over a narrow temperature range. In a comparative study PORTER AND RIDGWAY (1983) found that a penetration method based on hardness determination yielded results which were closer to predicted values than differential scanning calorimetry.

SEYMOUR AND MINTER (1980) measured the change in dielectric relaxation of plasticised cellulose ester polymers with temperature. They identified an event or loss process which appeared in plasticised polymers and which was characteristic of the molecular structure and concentration of the polymer. This loss process was seen in addition to Tg, and was claimed to be useful for characterising plasticiser efficiency.

1.8 Aims and Approach

The objective of the work described in this thesis was to investigate factors leading to the design of an oral controlled release dosage form of oxamniquine using Eudragit Retard copolymers.

If successful it would be possible to develop a programmed

release dosage form to overcome the variable systemic serum concentrations (KAYE, 1978) associated with gut wall metabolism (KAYE AND ROBERTS, 1980) of oxamniquine produced on conventional dosing.

The approach taken was to develop a model system comprising monolithic polymer films containing oxamniquine prepared by casting polymer solutions onto an inert substrate.

The model system was applied to a potential dosage form in which films of similar composition were spray coated onto inert pellets using a fluidised bed process. It was envisaged that mixtures of coated pellets in a single unit such as a capsule would provide the required release profile.

The composition of both the films and pellet coatings was varied to evaluate some of the underlying trends and possible mechanisms of release in-vitro. The surface structure and microstructure of the films was studied to examine these effects further.

CHAPTER 2

RAW MATERIALS

2.1 Eudragit Retard Copolymers

2.1.1 Introduction

Eudragit Retard copolymers are synthesised by emulsion polymerisation from acrylic and methacrylic acid esters with a low content of quarternary ammonium substitution. The two copolymers in the series are designated RL and RS, which relate to the German words "leichtdurch-lässig" (freely permeable) and "swerdurchlässig" (slightly permeable). The chemical structure of the Eudragit retard copolymers is shown in Figure 2.

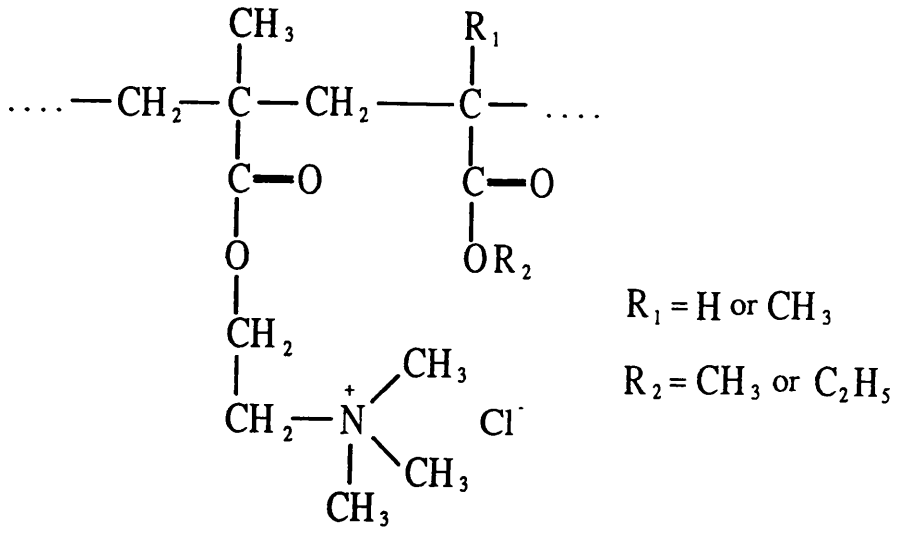

Figure 2 Chemical structure of Eudragit Retard copolymers

The molar ratio of the ammonium groups to the remaining neutral (meth)acrylic acid esters is 1:20 for Eudragit RL and 1:40 for Eudragit RS. The quarternary ammonium groups are present in the polymers as salts which are fully dissociated between pH2 and pH8. Films formed from Eudragit RL and RS are insoluble in water, but swell in water over the range of physiological pH, and are permeable both to water vapour and drugs. The permeability may be regulated by mixing the two polymers in the film.

2.1.2 Eudragit RS

Experimental work was carried out using Eudragit RS manufactured by Röhm Pharma GMBH, Weiterstadt, West Germany. The material was used as received.

2.1.2.1 Elemental Analysis

The elemental composition of the supplied material was determined by microchemical analysis using a Carlo Erba 1106 Elemental Analyser.

Assuming the average molecular weight of the neutral monomeric units to be 100.13, and the molecular weight of the substituted unit to be 207.73 it is possible to calculate the expected elememtal composition.

The experimentally determined composition differed in carbon, hydrogen and nitrogen content from the calculated

composition by less than 1%, based on a ratio of neutral to charged groups of 39 to 1, which confirms the information given in the manufacturers literature.

2.1.2.2 Infra-Red Spectroscopy

The infra-red spectrum of Eudragit RS was determined using the potassium bromide disc method described in Chapter 3. Although the absorption bands are relatively broad, characteristic features are present which confirm the general structure of the polymer.

2.1.3 Eudragit RL

Eudragit RL used in these studies was manufactured by Röhm Pharm, GMBH, Weiterstadt, W. Germany. The material was used as received.

2.1.3.1 Elemental Analysis

The elemental composition of the supplied material was determined by microchemical analysis. The experimental method, and calculation of the expected elemental compositions were as detailed in Section 2.1.2.1.

The experimentally determined composition differed in carbon, hydrogen and nitrogen content from the calculated composition by less than 1%, based on a ratio of neutral to charged groups of 19 to 1, which confirms the information

given in the manufacturers literature.

2.1.3.2 Infra-Red Spectroscopy

The infra-red spectrum of Eudragit RL was determined using the potassium bromide disc method (see Section 3.1.1.). The spectrum is similar to that obtained for Eudragit RS. The absorption bands were slightly less broad, particularly the C-O stretches in the spectrum of Eudragit RL, compared with Eudragit RS.

2.1.4 Discussion and General Information

The similarity between the infra-red spectra of Eudragits RL and RS suggests that the molecular structures are similar. The elemental analysis data shows that the nitrogen content of Eudragit RL is twice that of Eudragit RS. This suggests that the only difference between Eudragit RL and RS is the extent of quarternary ammonium substitution, within the bounds of the information obtained.

2.2 Dichloromethane

Dichloromethane, used as solvent for casting isolated films and spray coating of pellets was of General Purpose Reagent grade obtained from BDH Limited, Poole, England and was used as received.

2.3 Plasticisers

Glyceryl triacetate (triacetin; GTA), Polyethylene Glycol 400 (PEG 400), Dimethyl Phthalate (DMP), Diethyl Phthalate (DEP) and Di-n-butyl Phthalate (Dibutyl Phthalate; DBP) used as plasticisers in isolated films and applied coatings were of General Purpose Reagent grade obtained from BDH Limited, Poole, England and were used as received.

2.4 Mercury

Mercury was used as a casting substrate to prepare free films, was of Analar grade obtained from BDH Limited, Poole, England.

When exposed to the air mercury attracted dust and other airborne contaminants. After each use the mercury was cleaned by draining through a filter paper cone punctured at its apex. Contaminated mercury was retained in the filter paper. The residual mercury which still had the contaminants on the surface was washed through a column containing 0.1N Nitric Acid. Periodically the entire lot of mercury was washed through fresh 0.1N Nitric Acid.

2.5 Buffer Salts and Solutions

Citric Acid dihydrate and di-Sodium hydrogen orthophosphate dihydrate (Sörenson's salt) used to prepare pH6.0 Citric

Acid-Phosphate buffer solution were of Analar and General Purpose Reagent grade respectively. They were obtained from BDH Ltd, Poole and used as received.

Water was double distilled from an all-glass still and used within 24 hours of collection.

Prepared buffer solutions were stored in a refrigerator to prevent microbial growth and used within 14 days of preparation.

2.6 HPLC Reagents

2.6.1 Acetonitrile

Acetonitrile (methyl cyanide) was of Liquid Chromatography grade, obtained from BDH Limited, Poole, England and was used without further purification.

2.6.2 Ammonium Acetate

Ammonium Acetate was of Analar grade, obtained from BDH Limited, Poole, England and was used as received.

2.6.3 HPLC Separation Columns

The main analytical column used was a 30cm long pre-packed μ-Bondapak-CN Column obtained from Waters Associates (Mass.

USA). A pre-column packed with 30-38 μm pellicular Co-Pell PAC packing (Whatman Inc), which is compatible with the main column was used.

2.7 Nupareil Pellets

Nupareil pellets (E. Mendell, Inc) were received as two size fractions: 14-18 US Mesh (Lot NJ509A) and 20-25 US Mesh (Lot NJ509D).

2.8 Oxamniquine

Oxamniquine was supplied by Pfizer Central Research Ltd from batch 403 OX 501. It was used as received without further purification. It was stored at ambient temperature with protection from light.

The molecular structure was confirmed by elemental analysis, NMR and IR spectroscopy.

2.8.1 Elemental Analysis

The elemental composition of oxamniquine was determined by microchemical analysis as described previously.

Table 3 shows the theoretical and measured elemental compositions of oxamniquine. The theoretical composition was calculated using the empirical formula $C_{14}\ H_{21}\ N_3\ O_3$.

TABLE 3 **ELEMENTAL COMPOSITION OF OXAMNIQUINE**

Element	% Theoretical	% Measured	% Difference
C	60.18	60.38	+0.20
H	7.59	7.51	-0.08
N	15.04	15.15	+0.11
O	17.18	-	-

The close agreement between the theoretical and measured compositions confirms that the empirical formula is C_{14} H_{21} N_3 O_3.

2.8.2 Nuclear Magnetic Resonance

The NMR spectrum of oxamniquine was obtained as described in Chapter 3. The characteristic features of the NMR spectrum are summarised in Table 4.

TABLE 4 **FEATURES OF THE NMR SPECTRUM OF OXAMNIQUINE**

Peak Position δ (ppm)	Number of Protons (from integral)	Assignment of peak and comment
7.20	2	Aromatic protons at C-5 and C-8 (para position)
5.15	1	Proton at nitrogen in 1-position
4.74	2	Methylene protons of CH_2OH group
COMPLEX MULTIPLET	9	Ring methylenes, ring methine, side chain methane, side chain -NH, isopropyl methine
1.12 and 1.05	6	Doublet, characteristic of protons in isopropyl group

A sharp peak was also observed at δ 7.33 ppm. This was due to trace contamination of protonated chloroform in the deuterated chloroform solvent. The peak was therefore ignored.

Only 20 of the 21 protons were detected in the spectrum. The likely explanation is that the proton on the aliphatic hydoxymethyl group gave rise to a broad peak which was masked underneath other sharp peaks.

2.8.3 Infra-Red Spectroscopy

The infra-red spectrum of oxamniquine was obtained using the method described in Section 3.1.1. The main features of the spectrum are summarised in Table 5.

TABLE 5 MAIN FEATURES OF THE INFRA-RED SPECTRUM OF OXAMNIQUINE

Absorption Band (cm^{-1})	Assignment and comments
3310	-OH and secondary NH
1625	C=C stretching modes
1515 and 1360	Symmetric and asymmetric stretching frequencies
1460 and 1380	C-H bending of CH_3 groups
1050	C-O stretching in $-CH_2OH$ groups

CHAPTER 3

EXPERIMENTAL PROCEDURES

3.1 Spectroscopy

3.1.1 Infra-red

The infra-red spectra of oxamniquine, Eudragit RL and RS were determined in the solid state using the compressed disc method described in the British Pharmacopoeia 1980. Potassium chloride used as carrier was of infra-red spectroscopy grade (BDH Limited, Poole, England). Discs were mounted in a suitable holder and scanned in the range 2.5 - 16 micrometers (4000 - 600cm^{-1}) using a Perkin Elmer 928 double beam infra-red spectrophotometer.

3.1.2 Nuclear Magnetic Resonance

The nuclear magnetic resonance (NMR) spectrum of oxamniquine was obtained using an approximately 10mg cm^{-3} solution of the material in deuterated chloroform. Tetramethyl silane (TMS) was added as internal standard. The spectrum was obtained using a Bruker WP80-SY, Fourier transform NMR using energy supplied at 80.133 MHz. 128 energy pulses were applied and the field ionisation decay spectrum was recorded in a digitised form. The spectrum and an integral trace of peak areas were recorded on a chart recorder.

3.2 Decomposition of Oxamniquine by Thin-Layer Chromatography (TLC)

3.2.1 Introduction

A feature of the structure of oxamniquine is the strong ultra-violet chromophore arising from extensive electron delocalisation in the quinoline nucleus. Any side chain degradation would be unlikely to affect the UV absorption characteristics. Thus a complex mixture of degradation products of oxamniquine together with the parent drug may be indistinguishable from oxamniquine in solution when assayed by a non-specific technique such as UV spectrophotometry.

A TLC assay was supplied by Pfizer Ltd to demonstrate the instability of oxamniquine in acidic solution. Solutions of oxamniquine in 0.1N methanolic hydrochloric acid were stored for 24 hours at 37°C and spotted onto 250μm thick Kieselgel G_{F254} plates and developed using a mobile phase comprising Toluene:Methanol:Acetone:Glacial Acetic Acid (16:4:4:1 parts by volume) until the solvent front had run for 15cm.

The assay did not separate oxamniquine from degradation products which remained on the baseline and was therefore not capable of indicating the extent of decomposition.

3.2.2 Extraction Procedure and Analysis

Buffered aqueous solutions of oxamniquine were quenched with about 50ml of ammonia solution (35% NH_3, Analar Grade, BDH Limited, Poole, England), which raised the pH of the solution to about 12.2 and extracted with a total of 100ml of diethyl ether (Analar grade, BDH Limited, Poole, England) in 3 aliquots. The bulk of the ether was removed by evaporating the solution over a hot water bath. Final traces of ether were removed by storing the sample at 35°C overnight in a vacuum oven. Samples were prepared for TLC by reconstitution with 5ml of chloroform (Analar Grade, BDH Limited, Poole, England).

TLC plates were spread with a 250 μm thick layer of silica gel G_{F254}. The plates were heated at 100°C for 20 minutes to remove excess slurry water, but the silica gel was not activated. Prepared plates were spotted with 10μl of test solution.

The mobile phase was composed of n-butanol:glacial acetic acid:water (4:2:1 parts by volume). The solvent front was allowed to run for a distance of 15cm from the baseline. The plates were dried and viewed under UV light at 254nm.

A solution of oxamniquine in chloroform as internal standard was run on each plate. It was verified that the extraction process did not cause degradation, by preparing

and extracting a solution of oxamniquine in pH3.0 glycine/hydrochloric acid buffer. No components separated by TLC from this preparation.

The extent of degradation was assessed in a semi-quantitative manner by spotting 10µl of oxamniquine solutions in chloroform at concentrations ranging from 8mgcm^{-3} to 0.008mgcm^{-3} onto a TLC plate and developing as previously described. As expected, the optical density of the spot diminished as the concentration decreased. The intensity of spots on plates were assessed visually and compared with the control plate. It was assumed that the optical density properties of all separated components were identical to oxamniquine.

3.3 Analytical Methods for Determination of Oxamniquine

3.3.1 UV-Spectrophotometry

A scan of the absorbance spectrum from 180nm to 300nm of a 10mcg cm^{-3} solution of oxamniquine in pH6.0 Citric Acid-Phosphate buffer was made using a Pye Unicam SP1800 double beam recording spectrophotometer with optically matched 1cm path silica cells of 2ml capacity. pH6.0 Citric Acid-Phosphate buffer was used in the reference cell. The wavelength of maximum absorption (λmax at pH6.0) was 246nm. A series of solutions of oxamniquine of concentrations ranging from 1mcg cm^{-3} to 20mcg cm^{-3} were prepared in pH6.0 Citric Acid-Phosphate buffer. The absorbances of these

solutions were measured in duplicate at 246nm. The calibration graph was linear over this concentration range, ($A_{1\%,\ 1cm}$ = 5688.3).

A calibration graph for oxamniquine in methanol (Pronalys grade, Fisons Ltd) was linear over the same concentration range, ($A_{1\%,\ 1cm}$ = 6636.9). The wavelength of maximum UV absorbance of oxamniquine in methanol was 250nm. In the release studies described in Chapter 5 oxamniquine release was monitored continuously using a Cecil CE272 single beam ultraviolet spectrophotometer fitted with an 75µl silica flow through cell. The absorbance against concentration calibration was obtained before commencing diffusion experiments by pumping solutions of oxamniquine of concentrations between from 1mcg cm^{-3} and 20mcg cm^{-3} in pH6.0 Citric Acid-Phosphate buffer through the cell and recording the absorbances. The calibration graph for this flow through system was linear over this concentration range. ($A_{1\%,\ 1cm}$ = 5669.2 λ max = 246nm).

3.3.2 High Performance Liquid Chromatography

It was found that the phthalate esters, used as plasticisers in both free films and coated pellets, had strong ultraviolet absorbances at the wavelength used to determine oxamniquine concentration and therefore interfered with the UV assay. Reverse phase HPLC was used to separate these interfering components.

The analytical conditions (Pfizer Ltd, personal communication 1982) used are summarised in Table 6.

TABLE 6 **CONDITIONS USED IN THE PFIZER HPLC ASSAY OF OXAMNIQUINE**

COLUMN	μ-Bondapak-CN (Waters Associates)
MOBILE PHASE	Acetonitrile/0.05M Ammonium acetate solution (70:30 parts by volume)
FLOW RATE	1.5ml min^{-1}
DETECTION	Ultraviolet absorption at 251nm
CALIBRATION	External standard, plotting detector response against concentration
RETENTION TIME	3.6 min

These conditions were reproduced using an ACS 300/02 rapid oscillating single piston pump (Applied Chromatography Systems, Ltd), with a Valco valve injector port fitted with a 25μl injection loop. The detector was a Cecil CE2012 reference channel variable wavelength UV monitor set at 251nm with an 8μl stainless steel flow cell with silica windows. The spectrophotometer was adapted to allow the column to be mounted directly into the cell compartment. Absorption peaks were recorded on a Servoscribe 1S potentiometric recorder. The chromatogram of a 15mcg cm^{-3} solution of oxamniquine in pH6.0 Citric Acid-Phosphate buffer is shown in Figure 3.

The assay was modified in order to separate the phthalate esters from oxamniquine. The composition of the mobile phase was altered to Acetonitrile/0.05M ammonium acetate

solution (60:40 parts by volume). This reduced the retention time of the phthalate esters without altering the retention of oxamniquine. 10mcg cm^{-3} of 1,2,3,4-Tetrahydro-2-isopropylaminomethyl-7-nitro-6 methyl quinoline methane sulphonate (Pfizer UK3883) was added as internal standard. UK3883 is the direct precursor of oxamniquine (see Section 4.1).

To prolong the life of the analytical column a short precolumn was included in the system between the injection port and the main column inlet. The precolumn was packed with Co-Pell PAC packing (Whatman Inc) which has a cyano function stationary phase bonded to 30-38μm pellicular packing.

The separation of oxamniquine from phthalate esters was successful using these conditions. A typical chromatogram is shown in Figure 4.

The system was calibrated with oxamniquine solutions in pH6.0 Citric Acid-Phosphate buffer containing between 1mcg cm^{-3} and 20mcg cm^{-3} oxamniquine with UK3883 added as internal standard at a concentration of 10mcg cm^{-3}. The solutions were injected onto the column in duplicate and the heights of the absorbance peaks of oxamniquine and UK3883 recorded. The calibration graph is linear over this concentration range (response factor f_x = 1.63).

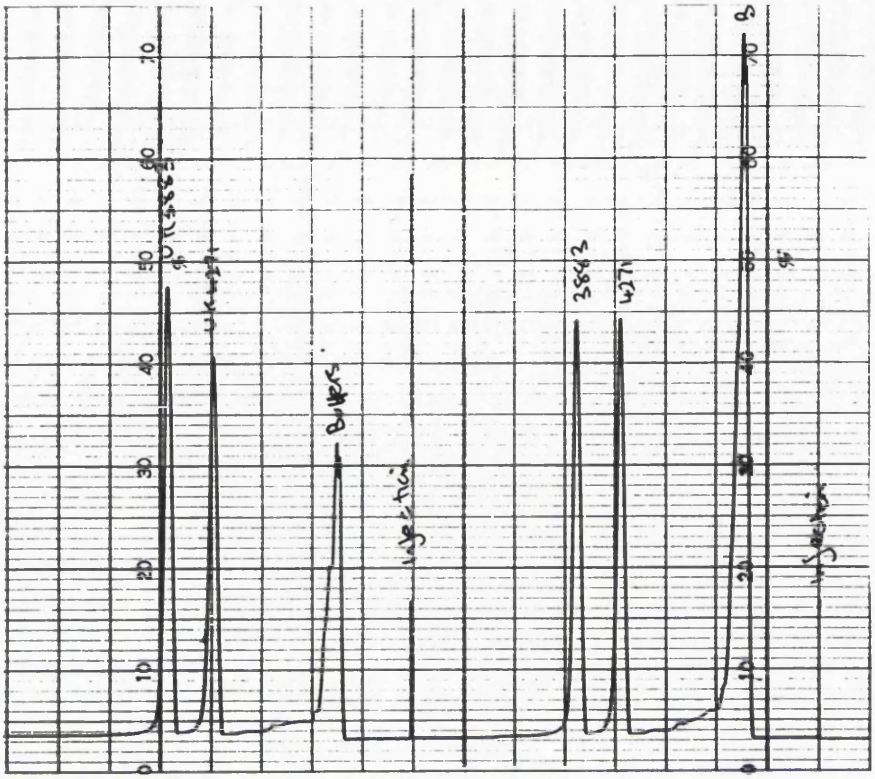

FIG 3: HPLC CHROMATOGRAM OF A 15 MICROGRAM PER ML SOLUTION OF OXAMNIQUINE IN pH6.0 CITRIC ACID-PHOSPHATE BUFFER SOLUTION

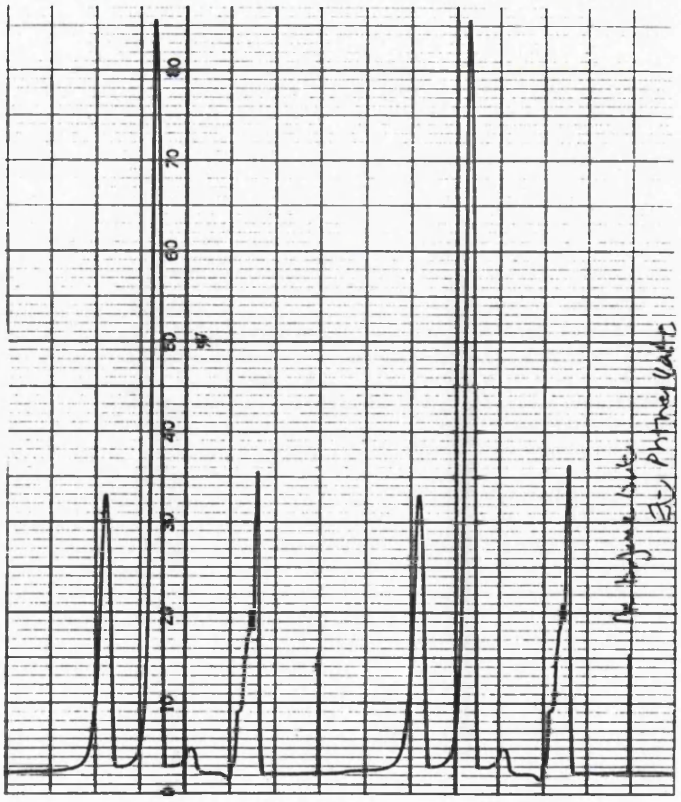

FIG 4: HPLC CHROMATOGRAM SHOWING THE SEPARATION OF OXAMNIQUINE FROM PHTHALATE ESTERS

The good resolution and response linearity of this HPLC assay made it suitable for the determination of oxamniquine in pH6.0 Citric Acid-Phosphate buffer solution. It was also found to be suitable for the determination of dimethyl or diethyl phthalate in the concentration range 1 to 50mcg cm^{-3} in this buffer. The calibration graphs for dimethyl phthalate and diethyl phthalate determinations were linear over this concentration range (f_x, DMP = 0.42, f_x, DEP = 0.48). Dibutyl phthalate was not sufficiently soluble in pH6.0 Citric Acid-Phosphate buffer to prepare suitable solutions to produce a calibration graph.

3.4 Solubility of Oxamniquine

3.4.1 pH-Solubility Profile of Oxamniquine

The pH-solubility profile of oxamniquine at 37°C was determined by measuring the equilibrium solubility of oxamniquine in aqueous buffers. Potassium Chloride/Hydrochloric Acid buffer (pH1.0 and 2.0), Citric Acid/Phosphate buffer (pH3.0 to 8.0) or Glycine/NaOH buffer (pH9.0 and 10.0) were used. Buffers were prepared according to forumulae given in Geigy Scientific Tables (1984). The pH of the buffers was measured using a Philips PW9410 digital pH-meter.

Oxamniquine has two amine groups, in the quinoline nucleus and in the side chain substituent (see Chapter 4). At a given pH the two amine groups will be ionised to different

extents. The variation of ionisation with pH might alter the wavelength of maximum absorbance at different pHs. If this effect were significant, it would not be possible to make all of the solubility determinations at a single wavelength, independent of the pH.

Solutions containing 50mcg cm^{-3} oxamniquine were prepared in buffer solutions of pH1.0, 3.0, 5.2 and 7.1. Dilutions of these solutions with buffer were made to give solutions containing 5, 10 and 15mcg cm^{-3} oxamniquine.

The UV absorbance of each of the solutions was measured in the range 200-340nm using a Perkin-Elmer 554 double beam scanning spectrophotometer. The cells used were optically matched silica (Spectrosil) with a 1cm path length and a capacity of about 1ml. In each case, the appropriate buffer solution was used as a reference, and a background correction spectrum using buffer in both the sample and reference cells was made in the range 200-340nm. A second spectrum of each solution was made, and the first derivative of absorbance with respect to wavelength ($dA/d\lambda$) was plotted against wavelength. This gave another method of determining λ_{max}, since when $\lambda=\lambda_{max}$, the first derivative $dA/d\lambda$ is zero. It was found that λ_{max} for oxamniquine occurs at 246nm, independent of both the pH and the concentration of the solution.

3.4.1.1 Solubility Determination

Excess oxamniquine was added to 15cm^3 aliquots of each buffer solution in screw capped glass vials with foil lid liners. The vials were fixed to a rotating wheel assembly which was totally immersed in a constant temperature water bath at 37°C. The samples were allowed to attain equilibrium by rotating for a period of 5 days. After this time, the samples were removed from the bath and filtered through 0.45μm pore size cellulose filter discs (Millipore Corp) into clean screw capped glass vials, which had been previously warmed to 37°C until they were required. The filtered samples were stored at 37°C before analysis. The pH of the filtered solutions was measured to determine any change from the original pH of the buffer.

Each filtrate from the solubility experiment was diluted using the appropriate buffer solution and the UV absorbance measured. Concentrations were obtained from a previously determined calibration graph and the equilibrium solubilities in the original solutions were calculated assuming that any breakdown products assayed as oxamniquine. All experiments were performed in triplicate and the mean values of equilibrium solubility calculated.

3.4.2 Solubility of Oxamniquine in Water Miscible Plasticisers

A potential problem in determining the solubility of drugs in different solvents by UV spectrophotometry is that the

solvent may have a significant absorbance at the same wavelength used to determine the drug concentration.

To check whether interference occurred with the plasticisers used in the diffusion studies the absorbances of 10mg cm^{-3} solutions of glyceryl triacetate (GTA), polyethylene glycol 400 (PEG 400), dimethyl phthalate (DMP), diethyl phthalate (DEP) and dibutyl phthalate (DBP) in methanol were prepared. The UV absorbances of these solutions at 250nm were measured as described previously using methanol in the reference cell. The water soluble plasticisers, GTA and PEG 400 did not absorb at this wavelength whereas three phthalate esters exhibited strong absorbance.

The equilibrium solubility of oxamniquine in GTA and PEG 400 was determined using the method described in Section 3.4.1. The drug/plasticiser mixture was rotated for 24 hours at 25°C, after which the mixtures were filtered free of solid drug through Whatman 54 filter paper. Methanol was used as diluent to prepare solutions of suitable concentration for measurement of UV absorption.

3.4.3 Partitioning of Oxamniquine Between Aqueous Buffer and Water Immiscible Plasticisers

The partition coefficient of oxamniquine between pH6.0 Citric acid-phosphate buffer and the three phthalate ester plasticisers was measured to give an indication of the

relative solubility of the drug in these plasticisers.

It was impossible to measure the equilibrium solubility of oxamniquine as described in Section 3.4.1 in the phthalate esters and assay by direct UV spectrophotometry since the phthalates interfered with the assay for oxamniquine. Furthermore, it was not possible to determine the oxamniquine concentration in filtered and diluted solutions by HPLC, because the intensity of the phthalate peak masked the oxamniquine peak.

A saturated solution of oxamniquine in pH6.0 Citric acid-phosphate buffer at ambient temperature was prepared by shaking excess oxamniquine with the buffer overnight. Excess solid drug was removed by filtering the suspension through a cellulose filter of 0.45μm pore size (Millipore Corp). The clear filtrate was retained. 5.0cm^3 of the filtrate and 5.0cm^3 of the appropriate phthalate ester were measured into screw capped vials. The two immiscible phases were homogenised on a vortex mixer and fixed to a rotating wheel assembly in an incubator at 37°C. The samples were rotated in the incubator for 72 hours with periodic removal to rehomogenise the two phases on the vortex mixer.

After 72 hours, the vials were removed from the incubator and centrifuged for 15 minutes to separate the aqueous and organic phases. The aqueous (upper) phase was carefully removed using a Pasteur pipette. Appropriate dilutions

were made with pH6.0 Citric acid-phosphate buffer and the oxamniquine content determined by HPLC. Since the concentration of phthalate ester in the aqueous phase was low, peak resolution occurred and quantitative measurements of both the oxamniquine and phthalate content of the aqueous phase were possible. The concentration of oxamniquine in the aqueous solution before partitioning was similarly determined. The oxamniquine content in the organic phase was calculated by difference.

To determine the effect of the initial concentration of oxamniquine in the aqueous phase, the experiment was repeated using the filtrate of the saturated solution of oxamniquine diluted to 50%$^{v}/_{v}$ and 25%$^{v}/_{v}$ with pH6.0 Citric acid-phosphate buffer as the aqueous phase. All of the experiments were conducted in triplicate.

3.4.4 Diffusion Coefficient of Oxamniquine in Aqueous Buffer

The diffusion coefficient of oxamniquine in pH6.0 Citric acid-phosphate buffer was determined using the filter paper diaphragm cell technique described by CADMAN et al (1981).

A 0.45μm pore size cellulose filter (Millipore Corp) was used as the diffusion membrane. The lower compartment of the cell contained a 996.6mcg cm^{-3} (3.566×10^{-3}M) solution of oxamniquine in pH6.0 Citric acid-phosphate buffer, which had been warmed to 37°C.

25ml of pH6.0 Citric acid-phosphate buffer, previously warmed to 37°C was pipetted into the upper compartment and the magnetic stirrer switched on. After equilibration for 10 minutes, 5ml of solution was pipetted from the upper compartment, and a stop watch started (T=0 minutes). A further sample was withdrawn at T=25 minutes. The samples were analysed for oxamniquine by UV-spectrophotometry. The experiment was conducted in triplicate, using a fresh membrane each time.

A calibration constant for the cell was obtained by performing experiments with aqueous solutions of potassium chloride at 25°C in the lower compartment. The potassium chloride was analysed by flame photometry, using a Corning 400 filter flame photometer.

3.5 Preparation of Free Films of Eudragit Copolymers

3.5.1 Methods Used to Prepare Free Films

Although apparently simple, the preparation and isolation of reproducible free films of Eudragit RL and RS presented considerable difficulties. These polymers are known to form brittle, mechanically poor films, and to overcome this, the manufacturers recommend that plasticisers are included in films (ROHM PHARMA 1979 a, b). A suitable casting method was required, so that any formulation of film, including unplasticised films, could be prepared and removed from the casting surface without damaging the film.

Film casting involves pouring a solution of the polymer together with any additives onto a suitable inert substrate, and allowing the solvent to evaporate. After evaporation a coherent film should remain, which can then be removed from the surface. Since the rate of solvent evaporation may dramatically affect the properties of the film (BANKER (1966), SPITAEL AND KINGET (1977a)), solvent removal should not be accelerated as a means of preparing films more rapidly.

Various substrates were evaluated as candidates for film casting templates. Shallow circular PTFE moulds (diameter 5.8cm; depth 1.0mm), similar to those described by ABDEL-AZIZ et al (1975) were machined from PTFE sheet on a lathe using a slightly radiused single point turning tool. This gave the best possible finish with minimum core indentation. Deeper moulds were similarly machined from PTFE sheet (8.5cm diameter; 1.5cm deep).

Initial attempts were made to cast films of Eudragit from solution in dichloromethane. The concentration of polymer was 25mg cm^{-3}, and 2.5mg cm^{-3} of GTA was added as plasticiser (ABDEL-AZIZ AND ANDERSON 1976). The solvent was evaporated overnight leaving a clear, transparent film in the mould. Static surface attraction between the film and the mould made removal of the film very difficult. The films produced by this process were about 30μm thick, measured by micrometry. It was apparent, upon visual inspection, that the removal process had damaged the film

by stretching, and that such films would not be suitable for diffusion studies. When the plasticiser was excluded, and a film cast from a 25mg cm^{-3} solution of Eudragit in dichloromethane, it was impossible to remove the film from the mould without breaking it.

Other surfaces which were tested included glass plate, and glass plate coated with polydimethylsiloxane 350cps (silicone 200, Dow Corning, Michagan USA) as described by PICKARD (1979). Although films formed on the substrate, removal of the film from the surface proved difficult or impossible. Furthermore, repeated applications of dichloromethane to the silicone-treated glass appeared to strip away the silicone coating from the plate.

An alternative method to casting onto a solid substrate, is to float the polymer solution onto a suitable liquid surface. The film, once formed, can be removed from the surface by draining the fluid substrate from underneath the film. Clearly the liquid chosen must be completely inert to the polymer, the casting solvent and any additives included in the film formulation.

Mercury was chosen as an inert substrate for casting Eudragit films. Approximately 1 to 1.2 Kg of mercury was poured into a glass crystallising dish (diameter 14.0cm, depth 75mm). Films were prepared by pouring the required polymer solution into Dural retaining rings (internal diameter 8.80cm; wall thickness 0.79cm; height 1.98cm)

which were placed in the mercury. The interior wall of the ring was highly polished and the top and bottom faces were squared to ensure uniform contact between the ring and the base of the dish. Prior to casting, the mercury was cleaned as described in Chapter 2.

The film casting dishes were placed on a formica laminated, adjustable levelling table, covered with a perspex lid. Films were cast at ambient temperature. The relative humidity of the environment was controlled at about 40%RH, by placing trays of coarse, self indicating, silica gel (BDH Limited, Poole, England) alongside the dishes. Humidity was measured using a hair hygrometer fixed to the wall of the lid. The perspex lid helped to maintain the environment by excluding circulating air.

The solvent was evaporated overnight to dryness, after which the formed film was removed from the mercury by holding the ring and draining the mercury from underneath the film. The film, which remained attached to the ring, was thicker around the circumference of the ring (see Section 3.5.2) than in the centre.

The film was cut away from the ring using a single-edged razor blade, and a disc of diameter 3.82cm was cut out from the centre of the film using a punch and die razor edged cutter.

Films were stored in plastic Petri dishes, interleaved with

sheets of siliconised paper. The Petri dishes were kept in a desiccator over silica gel for at least 24 hours prior to being used for diffusion studies.

3.5.2 Composition of Polymer Solution

The choice of casting solvent used in the formation of polymeric films can have a marked effect on both the structure and properties of the films formed (ABDEL-AZIZ, 1976). If a mixed solvent system is used, careful consideration must be given to the relative evaporation rates of the solvents in the mixture and the solubility of the polymer in the individual components in the solvent blend. If the polymer is not very soluble in the individual components of the mixture, but dissolves readily in the solvent blend, then upon evaporation of the solvent the polymer may precipitate, rather than form a cohesive film (PORTER, 1980). Even when polymer films are cast from a single solvent, the microstructure of the films can depend on the volatility of the casting solvent (KOLONITS, 1968).

Eudragit RL and RS will dissolve in a wide range of solvents. For these studies, dichloromethane was used as the casting solvent because it readily dissolved both Eudragit RL and RS, was volatile but was not flammable.

Another important factor which must be considered is concentration of the polymer in the film forming solution.

BANKER (1966) stated that at low polymer concentrations, segmental diffusion of the polymer will be promoted during film formation resulting in a more cohesive film. However, if the solution is too dilute then the time for film formation to occur will be increased considerably, or an excessively large volume of solution will be required to produce a given thickness of polymer film.

The large contact angle between the mercury and the Dural ring, used in the casting process created a "gully" which could trap a reservoir of the film forming solution. The concentration of polymer in the film-forming solution was chosen so that at least 25ml of polymer solution was poured to produce a given thickness of film.

Polymer solutions containing 100mg cm^{-3} of either Eudragit RL or Eudragit RS in dichloromethane were prepared by shaking the polymer granules with sufficient solvent in a stoppered conical flask for 1 to 2 hours until the polymer has completely dissolved. The solution was then transferred to a volumetric flask and adjusted to final volume. Polymer solutions were refrigerated until they were required. Since all of the plasticisers used were completely miscible with dichloromethane, solutions containing 500mg cm^{-3} of each of the plasticisers in dichloromethane were also prepared. Plasticiser solutions were also refrigerated until required.

Film forming solutions, in general, contained a total of

50mg cm^{-3} of the polymers dissolved in dichloromethane. Film forming solutions were prepared by mixing the solutions of polymers and plasticiser, dissolving the oxamniquine and diluting as necessary, using appropriate volumetric glassware.

A series of films which did not contain oxamniquine were cast for use in the studies on diffusion of oxamniquine through polymer films (see Chapter 5). The films were prepared as described previously except that the total concentration of polymer in the film-forming solution was 20mg cm^{-3}.

3.5.3 Determination of Film Thickness

Several techniques have been described in the literature for the determination of film thickness. The suitability of a particular method will depend upon the nature of the film, the order of magnitude of its thickness, its mechanical handling properties, and whether or not it can be isolated from the substrate.

The most convenient means of determining the thickness of mechanically stable, isolated films is by micrometry, and this technique has been adopted by several workers (FITES et al 1970, KANIG AND GOODMAN 1962, SHAH AND SHETH 1972, GURNY et al 1976, ABDEL-AZIZ 1976). Micrometry was chosen to measure the thickness of the films used in these studies.

Films were sandwiched between two glass slides and 20 measurements of the thickness of this sandwich were made using a micrometer with faces of 3.14mm^2 diameter and a low-torque clutch (Tesa SA, Switzerland). The thickness of the two slides was determined previously by the same method and the film thickness calculated by difference. Use of this technique minimised compression of the film by direct contact with the micrometer faces. Comparable measurements of film thickness were made using the micrometer directly on the surface of the film. The use of a micrometer with a low face area reduced the likelihood of measuring only the thickest parts of the film by being able to take more discrete measurements over the surface of the film.

The results from micrometry were verified by light microscopy. Embedment and sectioning of the films using wax or acrylic resin mountants was attempted, but this failed since the film was either affected by the embedment process or was damaged when sectioning was attempted. The sections for microscopy were prepared by cutting a thin strip of film which then mounted edge upwards on a glass slide using double sided adhesive tape. The thickness was measured directly using a calibrated eyepiece graticule.

Typically matrix films produced by the methods described were 40μm +/- 5μm thick.

3.6 Diffusion Studies on Free Films

The diffusion cell from the Sartorious Absorption Simulator used in these studies is illustrated in Figure 5.

The film is positioned between two silicone O-rings, located in grooves in the cell faces. The two halves of the cell are clamped together with perspex screw nuts. The interior faces of the cell in contact with the film are of ridged design, to permit the distribution of fluid uniformly across the faces of the film. The cell gives an exposed film cell area of $12cm^2$ per surface.

The Absorption Simulator has polycarbonate reservoir solution containers of 100ml capacity, which are surrounded by metal insulating jackets, and the solutions heated to $39°C \pm 1°C$ by heaters located underneath the base of the jackets. The reservoir liquids are stirred magnetically and are pumped across the faces of the film with a built-in two channel peristaltic pump, which pumps liquid at approximately $14ml/min^{-1}$. The solutions are pumped through 'distribution heads' which are fitted with sampling taps permitting the withdrawal of aliquots of the solutions if required. All connections between the diffusion cell, distribution head, and peristaltic pumps were made with Tygon inert plastic tubing (Grade R3603; Norton Plastics Inc).

The equipment was adapted to continuously measure the

release of oxamniquine from a single surface of cast films. A 1 litre glass USP design dissolution vessel, thermostatted to 37°C ± 0.5°C with rotary paddle stirring at 100rpm (G B Caleva Ltd, Ascot) was substituted for one of the reservoirs described previously. This was connected through the Absorption Simulator pump and diffusion cell via the distribution head to a UV Spectrophotometer (CE272, Cecil Instruments) fitted with a 75 µl Spectrosil flow through cell (Specac Ltd).

pH6.0 ± 0.1 Citric Acid/Phosphate buffer solution was prepared according to the formula given in GEIGY SCIENTIFIC TABLES (1984). Since air entrapment within the UV cell or diffusion cell can lead to erroneous results, buffer solutions were de-aerated by heating in a covered beaker until boiling just occurred, and then cooled. Deaeration by this method did not affect the clarity or pH of the solution and did not cause any precipitation of the buffer salts.

The required quantity of buffer solution was measured into the dissolution vessel and placed in the water bath. The liquid was circulated through the pump and UV cell for 1 hour to ensure that the liquid was at equilibrium temperature through the flow path.

The test film was carefully placed on the silicone 'O' ring in the lower half of the cell. The upper half was placed in position and clamped using the four perspex retaining

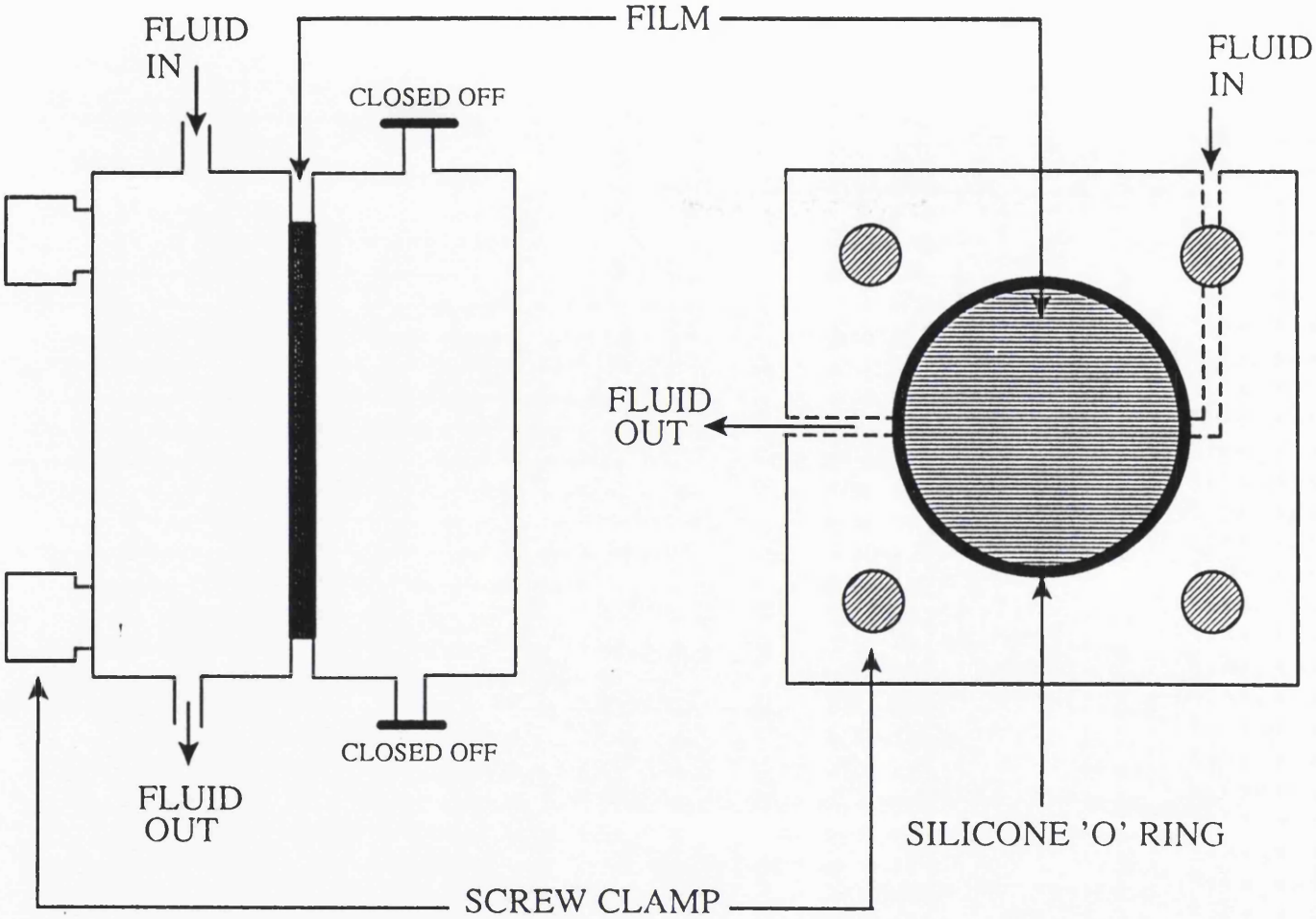

FIG 5: SCHEMATIC DIAGRAM OF THE SARTORIUS SIMULATOR DIFFUSION CELL

screws, ensuring that firm even pressure was applied by the screws. Connections were made so as to pump the reservoir fluid across one face of the film. A length of tubing was connected between the inlet and outlet ports of the cell serving the other side of the film. The absence of any liquid in this tube indicated that the film remained intact throughout the experiment. The absence of any air bubbles in contact with the surface being extracted was checked visually. The release of oxamniquine from the film into the reservoir was followed by UV-spectrophotometry for a period of at least 6 hours.

This method was followed for all film compositions except those containing phthalate ester plasticisers. For these studies samples of the solution were removed from the reservoir parallel to and at the same height as the stirrer blade at appropriate intervals, and analysed by HPLC as described in Section 3.3.2. For these studies UK3883 was added as internal standard to the buffer solution in the reservoir at a concentration of 10 mcg cm^{-3}.

3.7 Preparation of Coated Pellets

The equipment used to prepare coated pellets was an Aeromatic STREA-1 laboratory size fluid bed unit (Aeromatic Ltd, Bubendorf, Switzerland). This is a small scale unit capable of coating batches of between 200 gram and 4Kg. It is fitted with a perspex coating chamber with a counter-current spray gun which has the advantage that the process

can be directly observed, and altered if required. This arrangement is more usually used for spray granulation processes. Also the choice of carrier is limited to water based applications or solvents which do not destroy the surface of the perspex coating chamber. An all stainless steel chamber with a fixed position spray gun in the base of chamber spraying co-current to the fluidised bed was used. A glass window bonded into the straight section of the chamber allows a limited view of the fluidising bed. This apparatus is shown in Figure 6. The base of the chamber was attached to a perforated metal screen which acted as a support for a fine metal gauze. These screens retained the particles in the chamber whilst directing an even air distribution across the bed. The base plate was not of the Wurster design, but the perforations in the base plate were of uniform diameter arranged concentrically.

To prevent the loss of fluidised solid through the exhaust at the top of the apparatus a guard mesh was fixed to the top of the chamber. This allowed the passage to exhaust of particles less than around 500μm and also provided an exhaust outlet for the fluidising air and solvent vapour from the coating solution. The exhaust outlet was connected to flame-proofed exhaust handling facilities. Rubber rims around the lid of the apparatus and the upper mesh ensured that an efficient seal was made when the top section of the apparatus was closed. The design of nozzle shown in Figure 7 was a central circular orifice of diameter 0.25mm through which the solution was delivered,

FIG 6: AEROMATIC STREA-1 WITH STAINLESS STEEL COATING CHAMBER

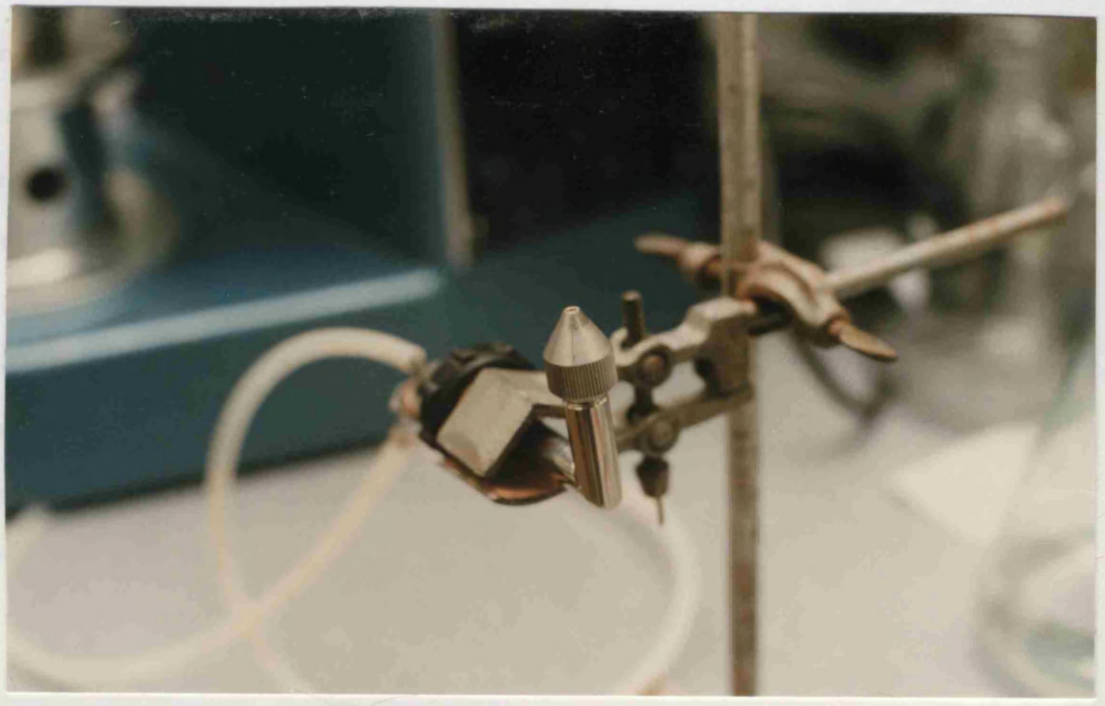

FIG 7: DELIVERY NOZZLE USED IN AEROMATIC STREA-1 COATING CHAMBER

surrounded by a concentric orifice leading to the supply of high pressure atomising air. The nozzle was connected to a source of compressed air capable of providing about 690 KPa (100psig) pressure at the outlet. This external high pressure line was connected to the Aeromatic pumping set which reduced the air pressure and regulated the supply of air to the nozzle at pressures between 0 and 400 KPa (0 to 60 psig).The coating solution was fed from the reservoir to the atomiser through silicone rubber tubing using a Watson Marlow MHRE peristaltic pump. The flow rate of solution was measured for coating solutions of different compositions.

The fluidising air stream was produced by a single phase motor which drew ambient air through a fibre glass pre-filter over a heating element to warm it to the desired temperature. The warm air then passed through the support grid into the particle bed. The volume of air passing into the chamber was controlled by altering the fan capacity. This was controlled from a dial calibrated in arbitrary divisions.

The coating process was monitored by measuring the inlet and outlet air temperatures, and the air volume flow through the bed. The state of the fluidised bed was assessed visually through the glass window in the chamber.

3.8 Drug Release From Coated Pellets

Oxamniquine release from coated pellets was measured continuously using a similar method to that used for free films. A USP rotating basket dissolution apparatus was used. The required weight of coated pellets were placed in the basket which was lowered into the extraction medium. Where phthalate plasticised coatings were used, the dissolution medium was sampled and analysed. A preliminary experiment indicated that the rotation speed of the basket between 25rpm and 200 rpm did not affect the release of oxamniquine from the pellets, other than at high rotational speeds, where there was a tendency to introduce air bubbles into the buffer solution which could be seen as spikes in the UV trace as the solution passed through the flow cell. Therefore a constant rotation speed of 100rpm was used for all experiments.

3.9 Measurement of Glass Transition Temperature of Cast Films by Surface Hardness

The glass transition temperature of polymer films was determined by measuring their change in Brinnell hardness number with temperature. The apparatus used was a pneumatic microindentation hardness tester (Research Equipment [London] Ltd) which was developed by MONK AND WRIGHT (1965) for testing the surface hardness of paint films. The apparatus is shown in Figure 8.

FIG 8: MICROINDENTATION HARDNESS TESTER

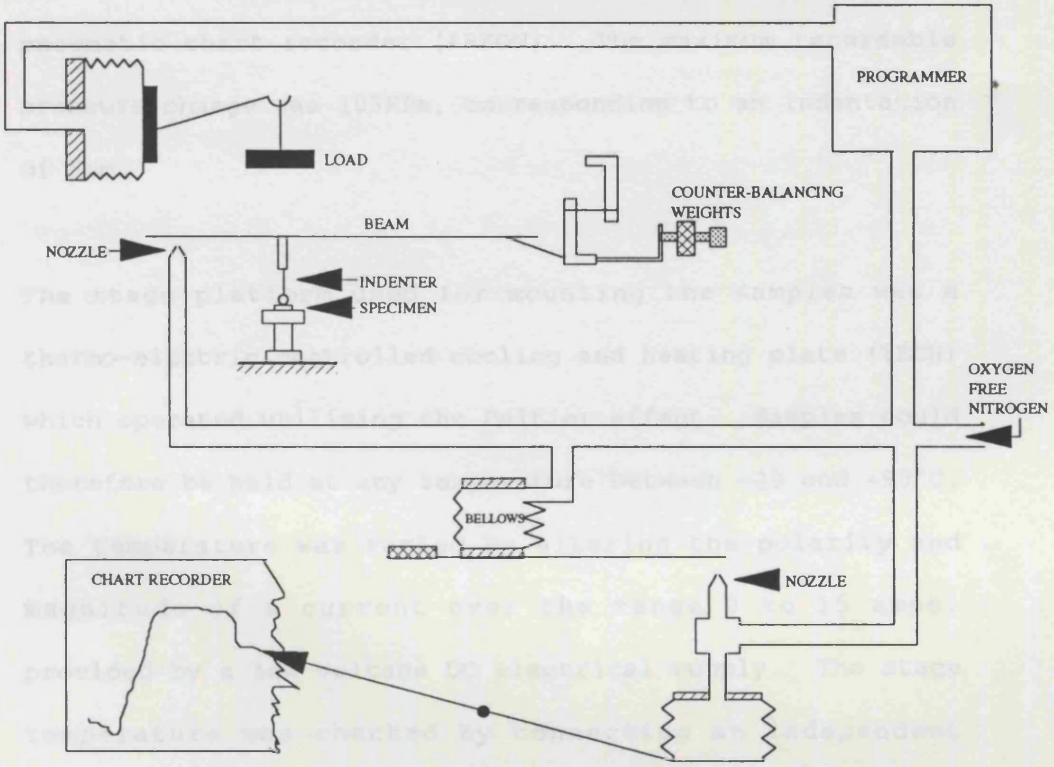

FIG 9: SCHEMATIC DIGRAM OF THE PNEUMATIC FLOW CIRCUIT OF THE MICROINDENTATION HARDNESS TESTER

The equipment consisted of a ball ended sapphire needle, 1.55mm in diameter which was allowed to rest on the surface of the sample under a load of about 0.1g. A specific load was then applied and the indentation of the sample was followed for a period of 75 seconds after which the load was removed automatically from the sample. The recovery of the sample was followed for a further period of 75 seconds.

The indenter movements were monitored by a two stage pneumatic amplification system consisting of flappers and nozzles powered by oxygen free-nitrogen at approximately 138KPa. Figure 9 shows a schematic diagram of the pneumatic flow circuit. Changes in the position of the indenter, corresponding to the indentation of the sample, gave rise to pressure changes within the pneumatic system. These changes, suitably amplified, were recorded on a pneumatic chart recorder (ARKON). The maximum recordable pressure change was 103KPa, corresponding to an indentation of 6μm.

The stage platform used for mounting the samples was a thermo-electric controlled cooling and heating plate (TECH) which operated utilising the Peltier effect. Samples could therefore be held at any temperature between -20 and +90°C. The temperature was varied by altering the polarity and magnitude of a current over the range 0 to 15 amps, provided by a low voltage DC electrical supply. The stage temperature was checked by connecting an independent thermocouple leading to a high precision electronic

thermometer to the stage. Since measurements were made at temperatures below the dew point of the ambient laboratory atmosphere the apparatus was completely enclosed in a glove box along with trays of phosphorus pentoxide desiccant (BDH Limited, Poole, England), which maintained a relative humidity less than 20%. The humidity was measured using a hair hygrometer and the atmosphere allowed to stabilise for 24 hours prior to using the equipment.

3.9.1 Calibration

The instrument was calibrated by measuring the pressure changes in the system caused by an indentation of known magnitude. The beam was first balanced using the counter balance weights so that the recorder showed a full scale deflection of 6μm. A 20g weight was then loaded and lowered onto the beam. The needle was lowered to touch a non-indentable specimen (a glass microscope slide) and the recorder set to zero. A fine adjusting screw was then rotated to simulate 1, 2, 3, 4, 5 and 6μm penetration depths, and the readings on the recorder were noted. This procedure was repeated 3 times.

The calibration curve obtained is shown in Figure 10.

3.9.2 Sample Testing

Samples were prepared so as to give good thermal contact with the TECH plate.

FIG 10: INDENTATION CALIBRATION CURVE FOR PNEUMATIC MICROINDENTATION HARDNESS TESTER

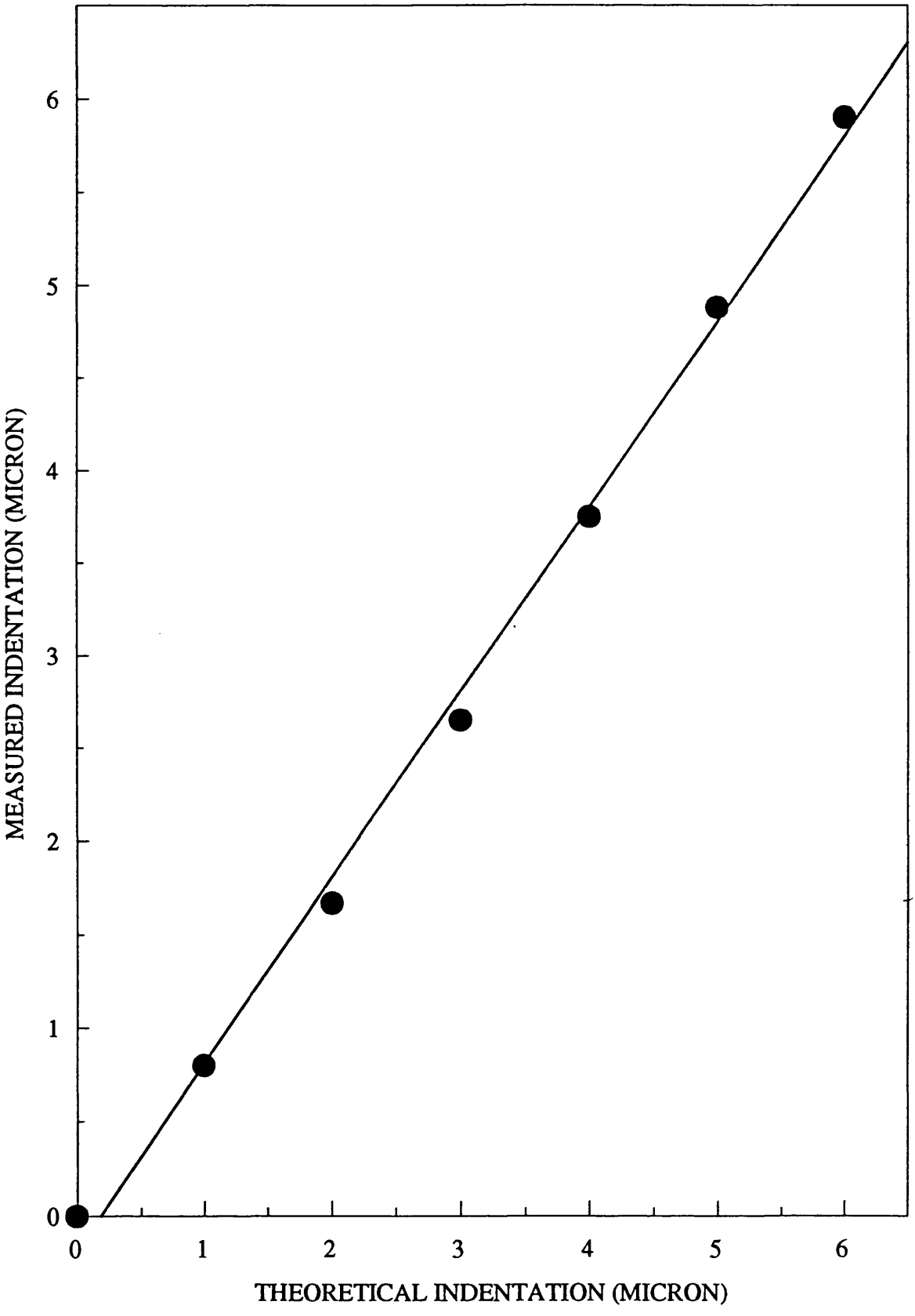

Films were cast from an 80mg cm^{-3} solution of the polymers in dichloromethane, onto circular Dural discs (diameter 3.18cm). About $2cm^{-3}$ of the solution was poured into each disc and the solvent allowed to evaporate. This gave a film of at least 50μm depth to prevent interference of the substrate with the indentation measurement because the depth of penetration would be considerably less than the thickness of the film. For each sample, measurements of indentation and recovery, under a suitable load, were taken over a range of temperatures from approximately -20°C to +40°C. The temperature was incremented in steps of about 5°C, and the sample was allowed to equilibrate for about 10 minutes before readings were taken. For each temperature five individual measurements of indentation and recovery were taken.

3.10 X-Ray Diffraction Studies

Film samples for X-ray diffraction were prepared by casting onto mercury as described in Section 3.5. Powder samples were prepared by trituration and serial dilution using a glass pestle and mortar.

The X-ray diffraction analysis was carried out using a Nonius MK2 self focussing Guinier-Wolff camera (Imperial College, University of London).

The reflected X-rays could be focussed onto four samples

simultaneously to allow the comparison of band intensities. Quartz monochromated copper radiation was used as the source in the apparatus. Film samples were mounted onto clear adhesive tape in suitable holders to facilitate loading into the diffractometer. Powder samples were spread lightly over the adhesive tape in similar holders.

3.11 Scanning Electron Microscopy

The surface structures of free polymer films and polymer films which had been applied to spherical pellets were examined using scanning electron microscopy. The microscope used was a Philips 501B scanning electron microscope.

Films were prepared by casting onto mercury as described in Section 3.5. For these studies films containing equal proportions of Eudragit RL and RS with 10% w/w of plasticiser and 5% w/w oxamniquine (relative to total polymer weight) were examined. Films containing GTA, PEG 400 and DBP as plasticiser were prepared.

Identical films were prepared and the oxamniquine content subsequently extracted by mounting them in an adapted ointment diffusion cell and washing the upper (air exposed) surface with pH6.0 Citric acid-phosphate buffer at 37°C for 18 hours.

Examples from each type of film were cut out using a razor

blade and mounted onto glass slides using double-sided pressure sensitive adhesive tape. Prepared samples were stored in a desiccator over silica gel before examination by SEM. Immediately before examination, samples were sputter coated with gold/palladium mixture in vacuo using a Polaron E5100 sputter-coater.

Both the upper (air exposed) surface and the lower (mercury contact) surface of the initial and extracted films were examined in at least two fields of view at magnifications ranging from x220 to x13,800.

The surface structure of the polymer film coating the pellets was also examined using scanning electron microscopy. In addition several pellets were sectioned into two hemispheres and examined using scanning electron microscopy so that the interface between the film and the pellet core could be viewed.

CHAPTER 4

CHARACTERISATION OF OXAMNIQUINE

4.1 Discovery of Oxamniquine

Oxamniquine (UK4271) is a discovery of Pfizer Central Research Ltd UK. It was discovered as a result of research into cyclic analogues of Mirasan.

This displayed schistosomicidal activity in primates (RICHARDS AND FOSTER, 1969). Oxamniquine is believed to be the active metabolite of a parent compound, UK3883 (Figure 11) and is produced from microbial hydroxylation of the 6-methyl group in that compound.

The chemical synthesis of UK3883 has been described by BAXTER AND RICHARDS (1971). The schistosomicidal activity of UK3883 and UK4271 have been described by BAXTER AND RICHARDS (1972).

Oxamniquine is effective only against S.mansoni and can be given orally over a 3 day course. It was previously given as a single dose by intramuscular injection but this caused severe pain on injection. It is well tolerated with no serious side effects and gives good cure rates (MARTINDALE, 1989).

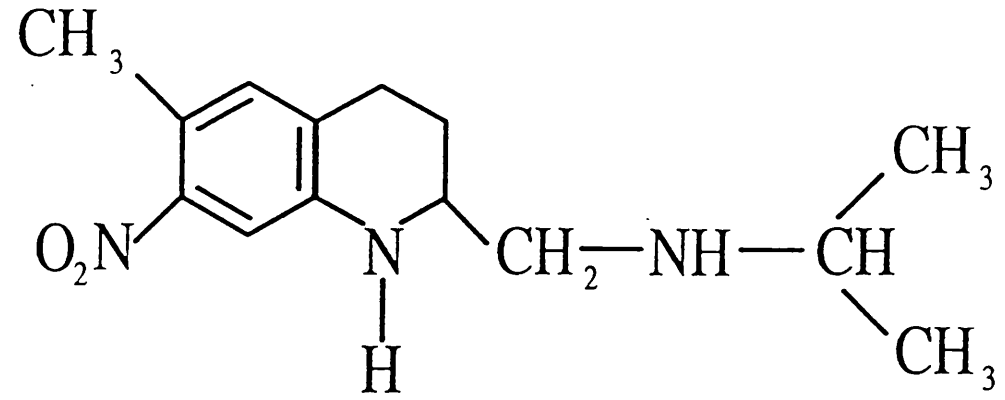

UK3883

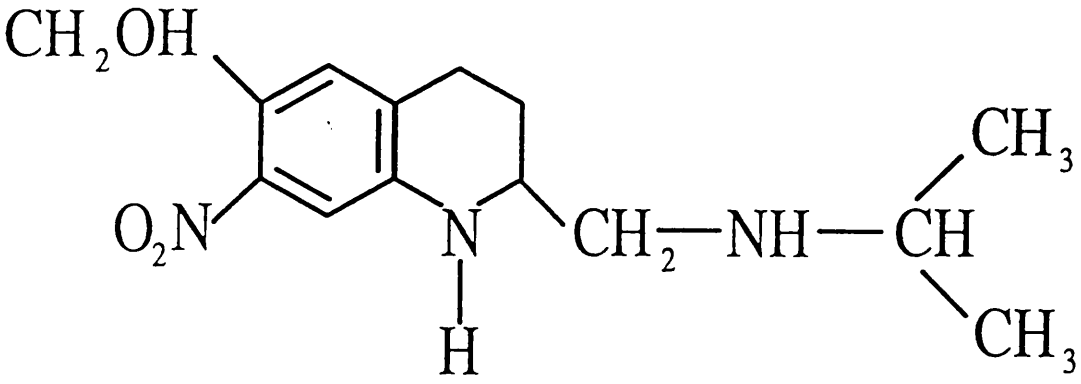

OXAMNIQUINE, UK4271

Figure 11 Structures of Oxamniquine (UK4271) and UK3883

4.3 Variation of Oxamniquine Solubility with pH

The relationship between solubility of oxamniquine (in the presence of any degradation products) and pH was determined by measuring the concentration of oxamniquine solutions in

various buffers of pH from 1 to 10 as described in Chapter 3. Oxamniquine solubility in distilled water was determined similarly.

Figure 12 shows the relationship between pH and oxamniquine solubility.

Dissociation constants for a molecule may be determined by potentiometric titration. However, where the compound is poorly water soluble this technique is not applicable. KREBS AND SPEAKMAN (1945) have described a method by which dissociation constants can be calculated from solubility data. Equation 4 shows the solution for a sparingly soluble base.

$$\log \left(\frac{S}{S_o} - 1\right) = (pK_w - pK'_B) - pH \qquad (4)$$

In equation 13, B represents the sparingly soluble base which gives to the ion BH^+; S is the solubility at any given pH and S_o is the intrinsic solubility.

$\log \left(\frac{S}{S_o} - 1\right)$ is termed the solubility function.

If the intrinsic solubility S_o of oxamniquine is assumed to be the solubility in water (0.30mg cm^{-3}) then the solubility function can be calculated from the solubility at any given pH. This assumption is reasonable since the pH of the saturated solution of oxamniquine in water is sufficiently high that the drug will not be ionised. Figure 13 shows the solubility function plotted against pH

FIG 12: pH-SOLUBILITY PROFILE OF OXAMNIQUINE: GRAPH OF SATURATION SOLUBILITY AGAINST pH OF SATURATED SOLUTIONS AT 37C

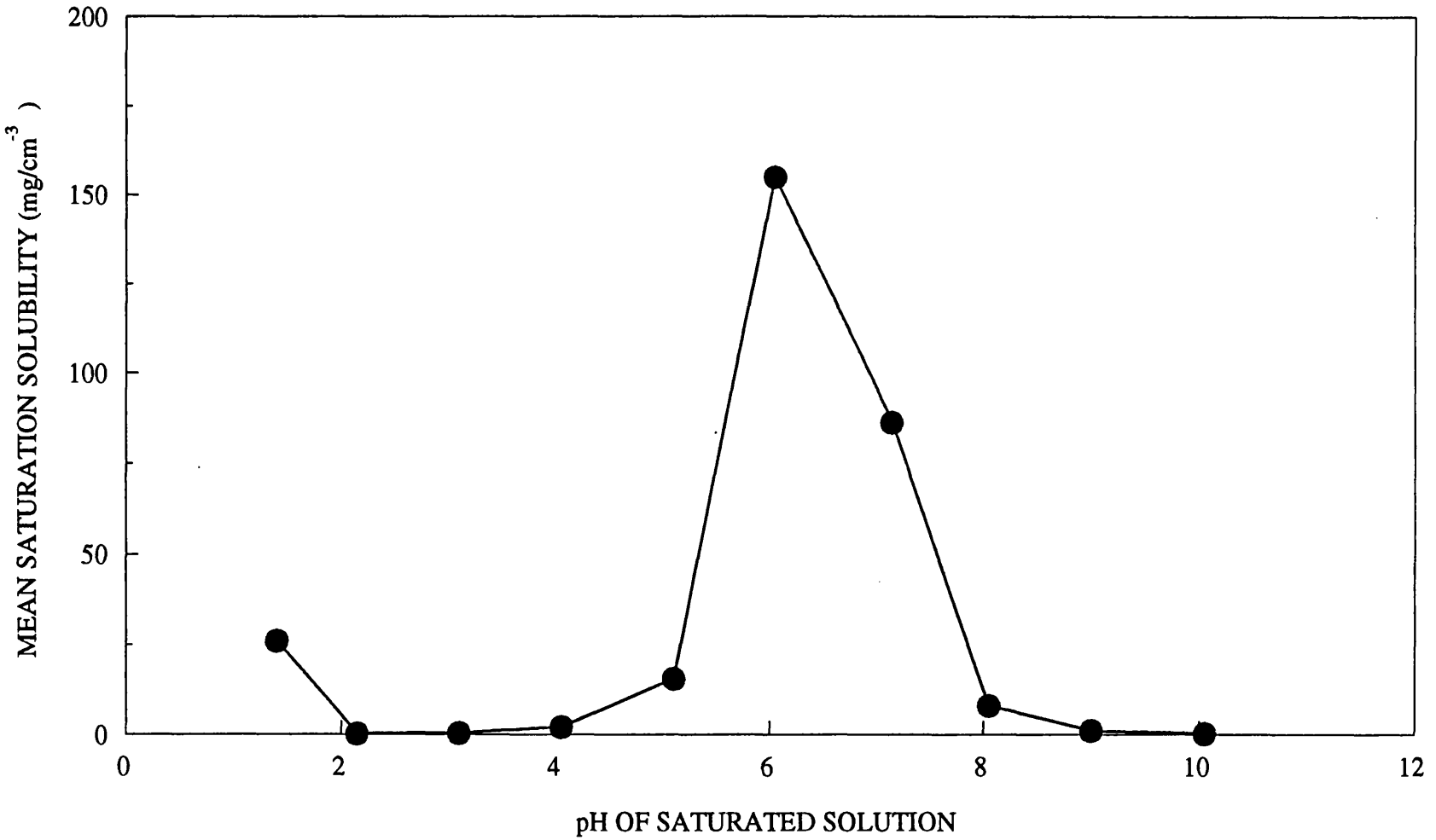

OXAMNIQUINE WAS ASSAYED IN THE PRESENCE OF DEGRADATION PRODUCTS

of the saturated solution.

From Figure 13, the value solubility function is zero at pH1.85, pH3.55 and pH9.55. Oxamniquine has two ionizable centres, the nitrogen on the isopropylaminomethyl side chain and the nitrogen of the quinoline nucleus. KOFITSEKPO (1980) determined pKa values for oxamniquine of 9.53 and 3.28. By analogy with various aliphatic and aromatic compounds, PFIZER LTD (internal report, 1969) have predicted pK values in the range 9-10 for the side chain nitrogen and 1-2 for the ring nitrogen. Values of 8.2 and 2.0 were determined by titration of oxamniquine monomethane sulphonate with hydrochloric acid or sodium hydroxide.

The actual pKa values determined in these studies are 3.55 for the quinoline nitrogen and 9.55 for the side chain nitrogen. The apparent pKa at 1.85 may be due to experimental error or to the degradation of oxamniquine which occurs in acidic solutions (see Section 4.5).

4.3 pH Related Degradation of Oxamniquine In Aqueous Solution

The decomposition of oxamniquine at 37°C in aqueous buffer solutions ranging from pH1 to pH8 was studied. Preliminary stability studies conducted by Pfizer (PFIZER LTD., 1969) indicated that oxamniquine is unstable in acidic solution and that solutions of oxamniquine in 0.1M hydrochloric and at 37°C decompose with a half life of approximately 4 hours. No other studies of the relationship between the

FIG 13: pH-SOLUBILITY PROFILE OF OXAMNIQUINE: GRAPH OF SOLUBILITY FUNCTION AGAINST pH OF SATURATED SOLUTIONS AT 37C

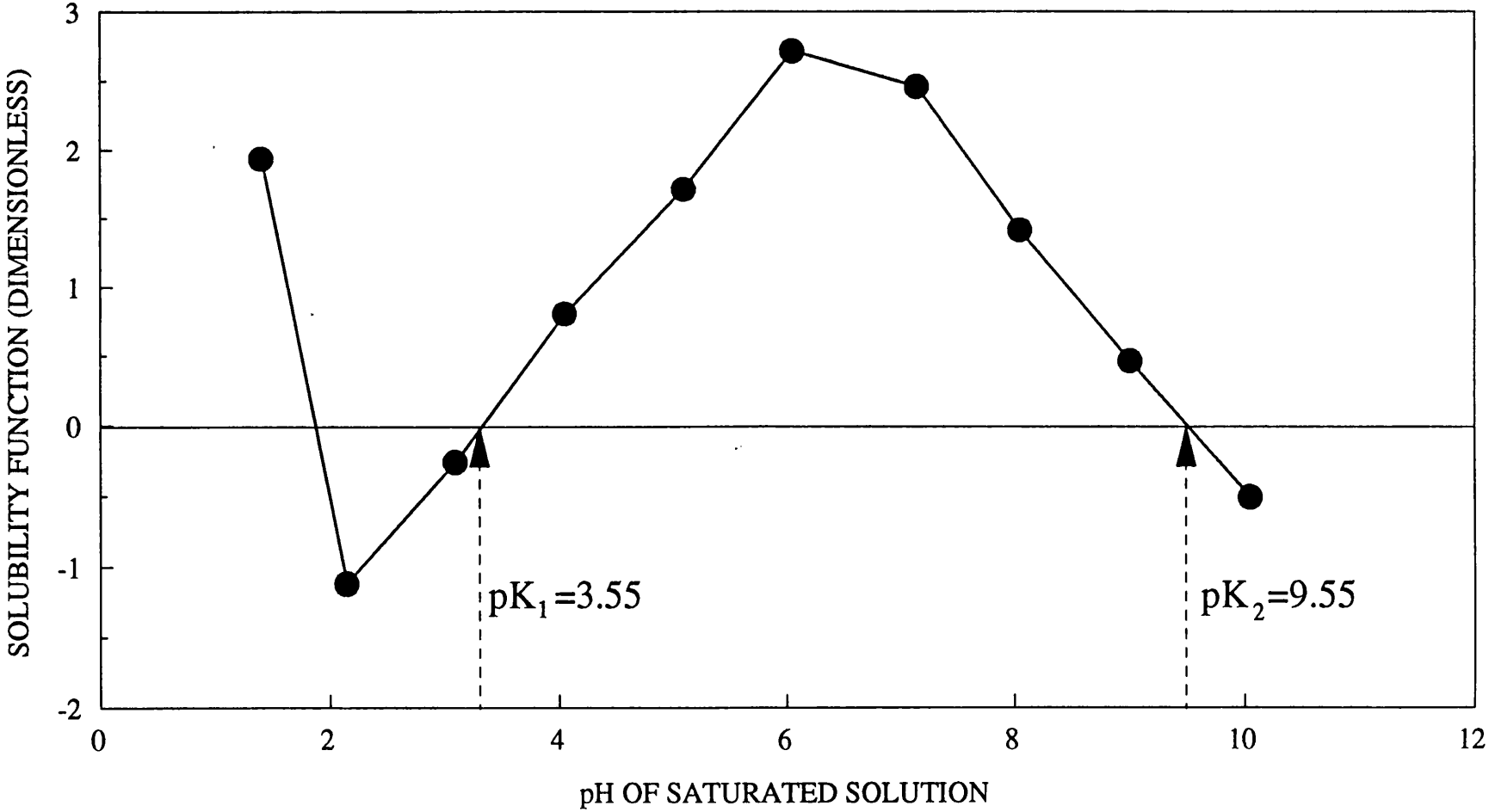

OXAMNIQUINE WAS ASSAYED IN THE PRESENCE OF DEGRADATION PRODUCTS

decomposition of oxamniquine and pH of aqueous solutions have been reported in the literature.

A series of buffer solutions were prepared to give solutions with pH ranging 1.0 to 8.0 in steps of pH1.0.

Buffer solutions were prepared according to formulae given in GEIGY SCIENTIFIC TABLES (1984). Potassium chloride/hydrochloric acid buffer was used for pH1.0; glycine/hydrochloric acid buffer for pH2.0 and 3.0; sodium citrate/hydrochloric acid buffer for pH4.0; Citric Acid/Phosphate buffer (McIlvaine) for pH's 5.0 to 7.0 and Phosphate buffer (Sorenson) for pH8.0.

Stock solutions for buffers and prepared buffer solutions were kept refrigerated (2°C - 8°C) to prevent microbial growth.

Solutions containing 8.00 $\pm$0.01mgcm^{-3} oxamniquine in each of the buffer solutions were prepared and the pH of each solution measured using a Pye Unicam PW9410 digital pH meter. Dissolution of the drug was aided by sonication in an ultrasonic bath.

For each solution, 6 aliquots each of 15cm^3 were distributed into 20cm^3 clear glass ampoules which were then sealed with an air headspace. The ampoules were stored in a water bath at 37°C for either 24 hours or 7 days without protection from light. Experiments were carried out in

duplicate.

In this study, the thin layer chromatographic (TLC) method which separated oxamniquine from decomposition products in aqueous solution, described in Chapter 3, was used.

4.3.1 Results

Table 7 summarises the TLC results obtained after storage of oxamniquine solutions in aqueous buffers ranging for 24 hours at 37°C. The results are summarised in Table 7. Up to 8 components were seen as a result of the degradation. The most extensive degradation occurred at acidic pHs, notably at pH1.0. Only traces of separated components were observed for solutions stored at pH5.

TABLE 7 **SUMMARY OF TLC RESULTS FOR OXAMNIQUINE STORED IN AQUEOUS BUFFERS FOR 24 HOURS**

Position of Component		pH of buffer solution							
R_F	R_X	1.0	2.0	3.0	4.0	5.0	6.0	7.0	8.0
0.00	0.00	+++	+	+					
0.04	0.09	+++							
0.07	0.18		+						
0.10	0.24	+++		+					
0.18	0.45	+++	+		+	+			
0.23	0.58	+	++	++					
0.28	0.71	++	+	+	+				
OXAMNIQUINE									
0.40	1.00	+++	+++	+++	+++	+++	+++	+++	+++
0.51	1.28	+	+	+					

+++ = 8 to 20 mcg of component on plate) assessed
++ = 4 to 8 mcg of component on plate) visually
+ = <4 mcg of component on plate)

After storage of oxamniquine solutions in aqueous buffers for 7 days at 37°C, the pattern of separated components was similar to that seen after 24 hours storage. Additionally, traces of separated components were observed after 7 days storage in pH6.0 and pH7.0 buffer, which suggests some degradation occurs in solutions of oxamniquine stored at near neutral pH.

4.3.2 Conclusions

This study demonstrated that oxamniquine is unstable in acidic solution. Decomposition appears to extensive in pH1.0 buffer, with apparently 7 components separating out from the solution in this buffer within 24 hours at 37°C. Decomposition is less extensive in neutral or alkaline solutions.

The UV assay is not specific for oxamniquine in the presence of its decomposition products.

Based on considerations from the degradation and solubility experiments, pH6.0 buffer was chosen as an extraction medium for the diffusion studies on oxamniquine. At this pH, sink conditions can be maintained throughout the duration of release experiments without oxamniquine decomposing in the extraction medium.

4.4 Solubility of Oxamniquine in Plasticisers

A number of factors may affect the release profile of drugs which are dispersed or dissolved in plasticised films. These include:

(1) The relative affinity of the plasticiser for the polymer
(2) The solubility of the plasticiser in the surrounding extraction medium
(3) The solubility of the drug in the plasticiser

The permanence of the plasticiser in the polymer matrix in the presence of the dissolution medium, the amount of drug extracted if the plasticiser is extracted simultaneously from the film, and the proportion of drug dissolved in the film are influenced by these factors.

To assess some of these effects the solubility of oxamniquine in the water miscible plasticisers used in these studies, glyceryl triacetate and polyethylene glycol 400 was measured.

For the three partially miscible plasticisers, dimethyl phthalate, diethyl phthalate and dibutyl phthalate, the partition coefficient of the drug between the plasticiser and pH6.0 Citric Acid-Phosphate buffer, was measured.

4.4.1 Solubility in Water Miscible Plasticisers

The solubility of oxamniquine in GTA and PEG 400 was determined as described in Section 3.4.2. The results are summarised in Table 8.

TABLE 8 SOLUBILITY OF OXAMNIQUINE IN WATER MISCIBLE PLASTICISERS

Plasticiser	Solubility of oxamniquine ($mgcm^{-3}$)	
	INDIVIDUALS	MEAN ± S.D.
Glyceryl Triacetate	1.46, 1.53, 1.47	1.49 ± 0.04
Polyethylene Glycol 400	10.48, 10.48, 10.18	10.38 ± 0.17

4.4.2 Partition Coefficient of Oxamniquine Between Water Immiscible Plasticisers and Aqueous Buffer

To assess the affinity of oxamniquine for DMP, DEP and DBP the partition coefficient of oxamniquine between the plasticisers and pH6.0 Citric Acid-Phosphate buffer was determined as described in Chapter 3.

The measured partition coefficient was dependent on the initial concentration of oxamniquine in the aqueous buffer. This suggests that oxamniquine associates in one of the phases, most likely the phthalate plasticiser phase. Furthermore, oxamniquine is partially ionised in the aqueous buffer phase. The distribution law of partitioning of solute between immiscible solvents applies only to the concentration of the species common to both phases i.e. the unasscciated unionised molecules of oxamniquine.

Equation 5 relates the molar concentration of unionised oxamniquine to the total molar concentration of oxamniquine in the buffer phase after partitioning.

$$C'_{AQ} = 0.0736\ C_{AQ} \qquad (5)$$

where C'_{AQ} is the molar concentration of unionised oxamniquine at pH6.0 and C_{AQ} is the total molar concentration in the aqueous buffer.

If association of oxamniquine into multiple molecules occurs in the plasticiser phase, an equilibrium will be set up as follows:

$$n\,(Ox) \rightleftharpoons (Ox)_n$$

If the measured concentration of oxamniquine in the plasticiser phase is C_p, then the concentration of unassociated oxamniquine in the phthalate phase, $C'p$, is given by

$$C'_p = n\sqrt{(\alpha C_p / n\kappa)} \qquad (6)$$

where n = number of associated molecules

α = degree of association

κ = association equilibrium constant

Equations 5 and 6 may be combined to form an equation which is applicable to partitioning of a drug between an aqueous phase where the drug dissociates and a plasticiser where the drug associates. A general equation is produced which relates the measured concentrations of oxamniquine in the aqueous buffer and phthalate phases, C_{AQ} and C_p:

$$\log C_{AQ} = \frac{1}{n} \log Cp + \log K'' \qquad (7)$$

where n = number of individual molecules which associate

K'' = is an apparent partition coefficient linearly related to the true partition coefficient

Log C_{AQ} is plotted against log Cp for each of the plasticisers in Figure 14. The results of regression analysis on these data are summarised in Table 9.

TABLE 9 **SUMMARY OF REGRESSION ANALYSIS FOR OXAMNIQUINE PARTITIONING EXPERIMENT**

Plasticiser	Correlation Coefficient of Line	Association Number, n (1/slope)	Apparent Partition Coefficient, K'' (M)
Dimethyl Phthalate	0.9975	1.7	0.6430
Diethyl Phthalate	0.9991	2.1	0.5130
Dibutyl Phthalate	0.9958	1.8	0.8032

For each of the plasticisers, the association number is close to 2 indicating that oxamniquine dimerises in the plasticiser phases. The apparent partition coefficient,

K'', allows the plasticisers to be placed in a rank order of their affinity for oxamniquine when partitioned from pH6.0 Citric Acid-Phosphate buffer. This rank order is

Dibutyl Phthalate > Dimethyl Phthalate > Diethyl Phthalate

However, in terms of the aqueous miscibility of these plasticisers, they are ranked

Dimethyl Phthalate > Diethyl Phthalate > Dibutyl Phthalate

Since the release of oxamniquine from plasticised films depends upon a combination of these factors, it is not simple to predict the effect of the plasticisers on the rate of release.

4.5 Diffusion Coefficient of Oxamniquine in Aqueous Buffer

4.5.1 Introduction

The diffusion coefficient of oxamniquine at 37°C in pH6.0 Citric Acid-Phosphate buffer was measured. These conditions were chosen as they were the principle conditions used to study the release of oxamniquine from free films and coated pellets. A knowledge of the diffusion coefficient of the drug in the dissolution medium permits a comparison of the retarding effect of the formulation. It is also possible to calculate the

FIG 14: PARTITIONING OF OXAMNIQUINE BETWEEN pH6.0 CITRIC ACID-PHOSPHATE BUFFER AND PHTHALATE ESTER PLASTICISERS

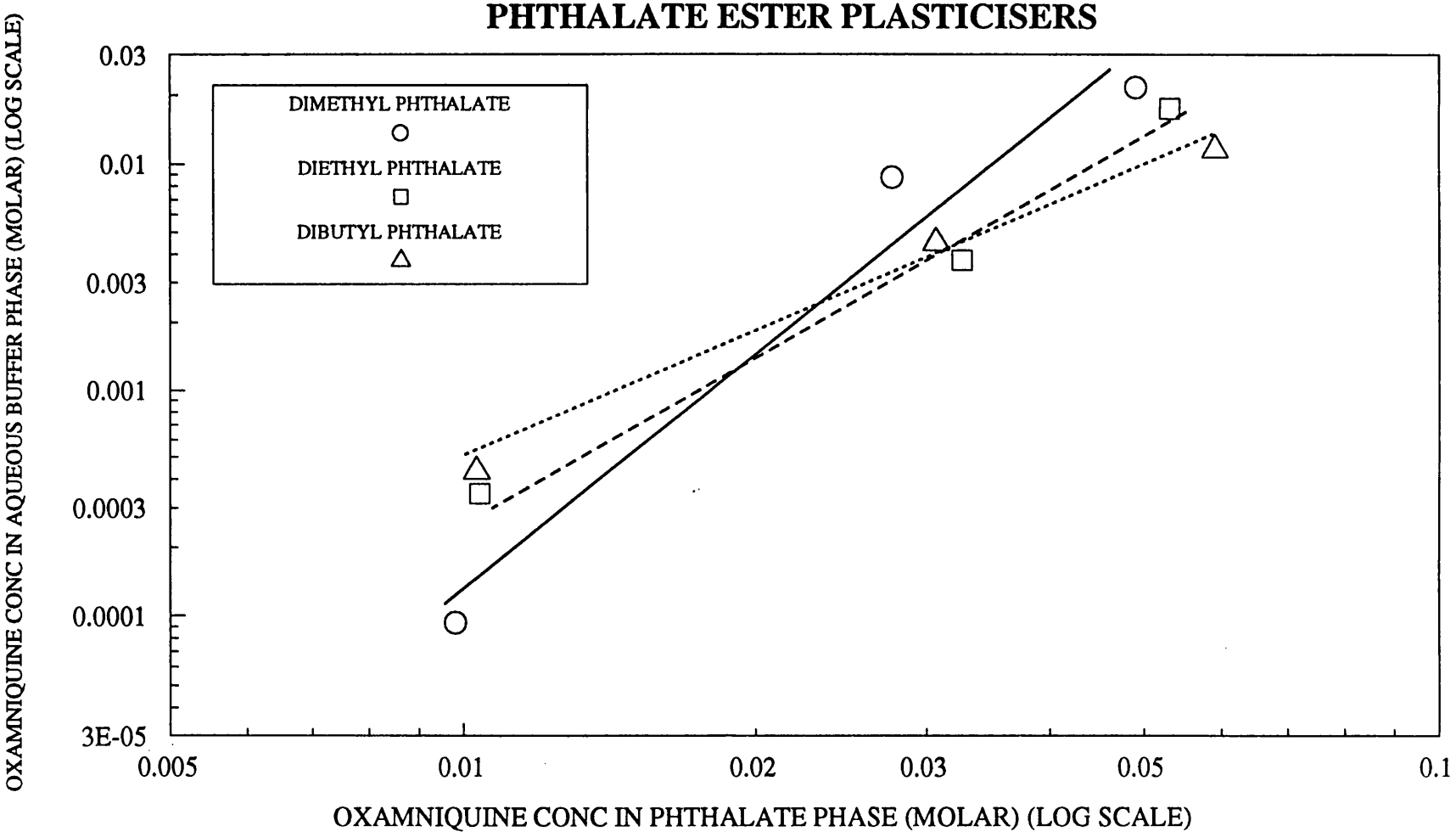

effective diffusing radius of the drug, which can be compared with the dimensions of the molecule calculated by molecular graphics.

4.5.2 Results

The diffusion coefficient, D, was calculated from the following equation (ROBINSON AND STOKES, 1965).

$$D = \frac{1}{\beta t} \ln \left[\frac{C_1 - C_2}{C_3 - C_4} \right] \qquad (17)$$

where C_1= drug concentration in lower compartment at t=0 mins
C_2= drug concentration in upper compartment at t=0 mins
C_3= drug concentration in lower compartment at t=25 mins
C_4= drug concentration in upper compartment at t=25 mins

β is a calibration constant for the cell related to cell dimensions and the porosity of the diaphragm membrane.

The concentration of drug in the lower compartment is the difference between the initial concentration and the measured concentration at each time period. The cell calibration constant was determined by repeating the experiment with a drug of known diffusion coefficient. For these studies potassium chloride in water at 25°C was used. The results are summarised in Table 10.

The effective volume of lower compartment is 12.276ml. Standard diffusion coefficients for aqueous potassium chloride solutions at 25°C (WEAST, 1988) are for 0.1M KCl, $D = 1.844 \times 10^{-5}$ cm^2 s^{-1}, and for 0.01M KCl, $D = 1.917 \times 10^{-5}$ cm^2 s^{-1}.

TABLE 10 **CONCENTRATION DATA USED TO CALIBRATE DIFFUSION CELL WITH POTASSIUM CHLORIDE SOLUTIONS**

Compartment concentration (mM)				t (secs)	β/cm^{-2}
at t=0		at t=t			
C_1	C_2	C_3	C_4		
88.64	5.58	63.91	20.76	900	39.46
88.68	5.56	64.29	20.53	900	38.66
88.68	5.56	64.16	20.61	900	38.95
8.81	0.58	5.40	2.68	1,500	38.50
8.84	0.57	5.42	2.67	1,500	38.29
8.76	0.61	5.30	2.73	1,500	40.14

Mean β = $39.00cm^{-2}$
s.d. = $0.69cm^{-2}$
c.v. = 1.77%

The concentration of the donor solution of oxamniquine was 996 mcg/cm^3 (3.566mM). Table 11 summarises the results of the diffusion coefficient determination.

TABLE 11 **CONCENTRATION DATA USED TO DETERMINE THE DIFFUSION COEFFICIENT FOR OXAMNIQUINE IN pH6.0 CITRIC ACID/PHOSPHATE BUFFER**

Compartment concentration (mM)				D cm^{-2}/sec
at t=0		at t=t		
C_1	C_2	C_3	C_4	
3.201	0.179	2.485	0.619	8.235×10^{-6}
3.246	0.157	2.475	0.631	8.814×10^{-6}
3.225	0.167	2.423	0.660	8.717×10^{-6}

$D_{MEAN} = 8.589 \times 10^{-6}$ cm^2/sec
s.d. = 3.101×10^{-7} cm^2/sec
c.v. = 3.61%

It is possible to calculate the diffusional radius of a molecule from its diffusion coefficient. For a spherical

particle, Stokes equation (Eq 9) relates the frictional coefficient to the radius.

$$f = 6\pi\eta r \qquad (9)$$

f = frictional coefficient of the particle
η = viscosity of the medium

$1/f$ = velocity of the particle under unit force.

The Einstein equation relates velocity under unit force, V_A to the diffusion coefficient.

$$V_A = \frac{1}{f} = \frac{D}{KT} \qquad (10)$$

K = Boltzmann constant
T = Temperature (K)

Combining the two equations produces the well known Stokes-Einstein equation.

$$D = \frac{KT}{6\pi\eta r} \qquad (11)$$

Substituting data

$K = 1.38 \times 10^{-23}\ JK^{-1}$

$T = 310.1K$

η = viscosity of medium

$= 1.009 \times 10^{-3}\ Nsm^{-2}$

$D = 8.589 \times 10^{-10}\ m^2/sec$

$$r = \frac{1.38 \times 10^{-23} \times 310.1}{6\pi \times 1.009 \times 10^{-3} \times 8.589 \times 10^{-10}}$$

$= 2.62 \times 10^{-10}\ m$

$= \underline{0.26\ nm}$

The effective diffusional diameter is therefore 0.52nm (5.2 Angstrom).

The spatial structure of oxamniquine was generated using SYBYL molecular modelling software running on a Silicon Graphics workstation, model IRIS 4D/25TG. Figure 15 shows 'spatial' representations of oxamniquine. The molecular diameter across the para hydrogens in aromatic ring of the quinoline nucleus in 5.2 Angstrom which agrees with the value calculated from the diffusion experiments. The overall length of the molecule from the nitro group to the end of the isopropylaminomethyl group is 12.3 Angstrom. These dimensions indicate the preferred orientation of oxamniquine as an effective cylinder and demonstrates that oxamniquine does not apparently hydrate with an associated sheath of water molecules when dissolved in pH6.0 Citric Acid-Phosphate buffer solution.

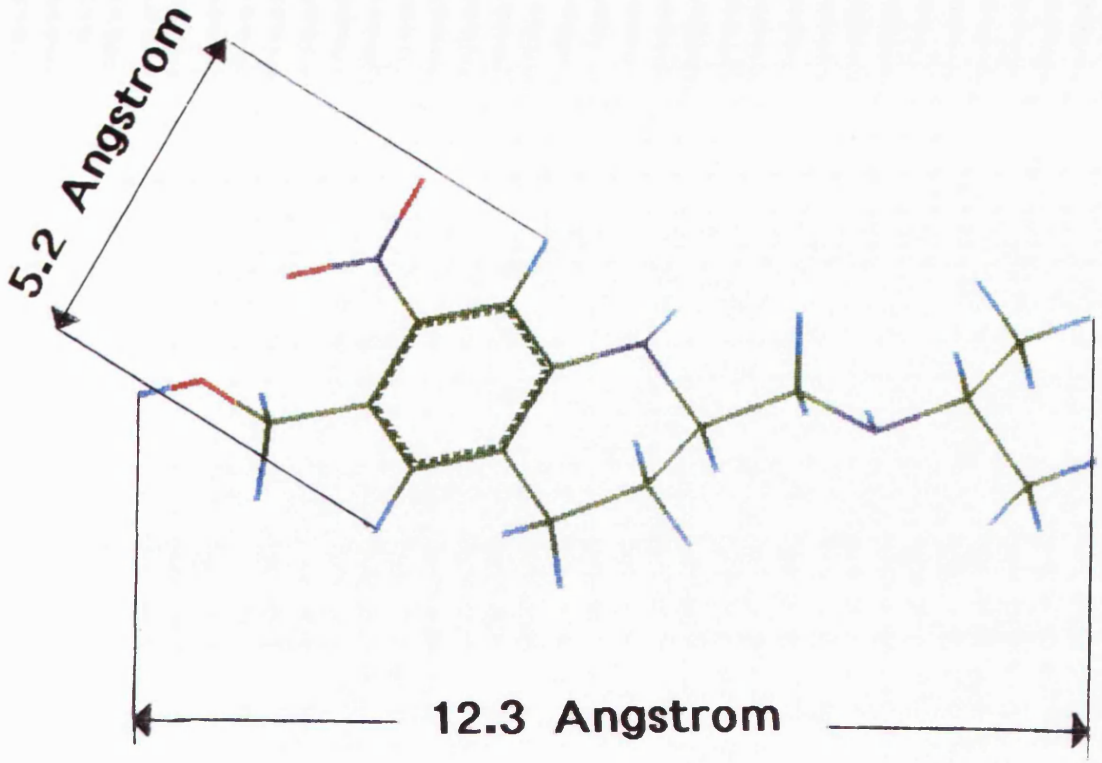

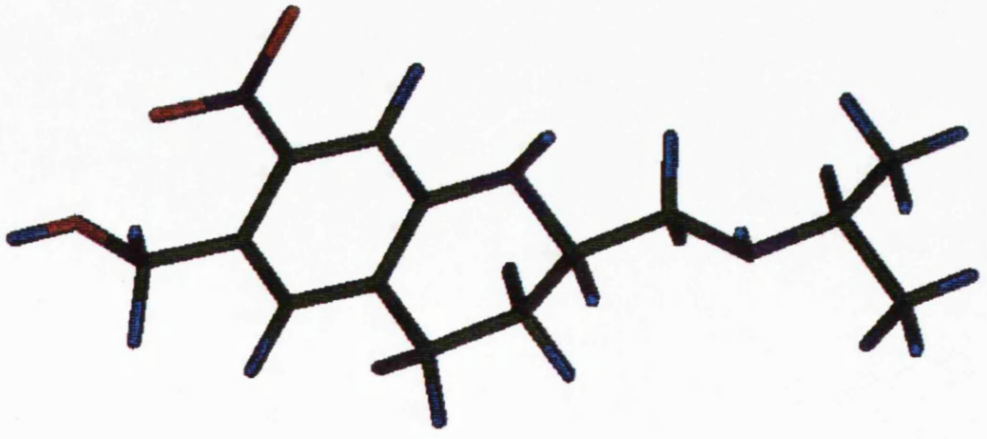

FIG 15: SPATIAL REPRESENTATION OF OXAMNIQUINE

CHAPTER 5

RESULTS AND DISCUSSION

5.1 Introduction

In this chapter the results of release studies on oxamniquine dispersed in isolated matrix films are presented and contrasted with the release of oxamniquine from similar films coated onto inert pellets. A number of factors affecting the release of oxamnquine from these systems are critically evaluated. Consideration is also given to possible mechanisms of release. Some of the physical properties of isolated films are also considered.

5.2 Preparation of Free Films

Difficulties were encountered in producing and isolating free films of Eudragit. Attempts to reproduce the methods of ABDEL-AZIZ et al (1975) were generally unsuccessful in that films could not be readily removed from PTFE casting moulds without stretching or cracking.

For these studies films were prepared by casting solutions of the polymers and additives from organic solvents onto mercury. Films of any composition could be prepared and isolated for use in release studies.

Dichloromethane was used as the casting solvent for the films prepared for these studies since the polymers, plasticisers and oxamniquine were readily soluble. Current practice in coating technology is towards aqueous dispersions or solutions of polymers which avoids the need for using flammable solvents. Dichloromethane would not now be considered an acceptable solvent as it is possibly carcinogenic.

5.2.1 Film Formulations Tested

The composition of free films prepared was varied to study the following:

1) The variation of the ratio of Eudragit RL and Eudragit RS included in the film.
2) The effect of the inclusion of plasticiser in the film.
3) The effect of the nature of the plasticiser incorporated into the film.
4) The effect of the casting surface used to form the film.

The compositions of the films are summarised in Table 12. The codes used to describe film formulations correspond (as far as possible) with the codes used to describe the composition of coatings applied to inert pellets (see Section 5.3.3).

TABLE 12 **COMPOSITIONS OF FILM FORMULATIONS TESTED**

Composition of Film % w/w	Formulation Code									
	A1	B1	B4	C1	D1	D2	D3	D4	F1	F2
Eudragit RL	43.48	86.96	-	47.62	43.48	43.48	43.48	43.48	43.48	43.48
Eudragit RS	43.48	-	86.96	47.62	43.48	43.48	43.48	43.48	43.48	43.48
Oxamniquine	4.35	4.35	4.35	4.76	4.35	4.35	4.35	4.35	4.35	4.35
Glyceryl Triacetate	8.70	8.70	8.70	-	-	-	-	-	8.70	8.70
Polyethylene Glycol 400	-	-	-	-	8.70	-	-	-	-	-
Dimethyl Phthalate	-	-	-	-	-	8.70	-	-	-	-
Diethyl Phthalate	-	-	-	-	-	-	8.70	-	-	-
Di-n-butyl Phthalate	-	-	-	-	-	-	-	8.70	-	-
Cast on Mercury Air exposed surface desorbed	✓	✓	✓	✓	✓	✓	✓	✓		
Cast on Mercury Mercury contact surface desorbed									✓	
Cast on PTFE Air exposed surface desorbed										✓

5.3 Spray Coating of Placebo Pellets

The method used for coating polymer films containing oxamniquine to placebo pellets in a laboratory scale fluidised bed coater was generally successful, since a coherent film apparently formed on the pellets. The apparatus used for the coating and the coating process have been described in Chapter 3.

As a general observation the films produced by the coating process appeared undamaged and were not readily removed from the pellet cores. The coatings were not 'powdery' in appearance which would have suggested spray drying of polymer and oxamniquine powders on the surface of the pellets. There was no obvious evidence of attrition of the pellets from the coating process.

The development of the process used to prepare coatings is described in Section 5.3.3.

5.3.1 Characterisation of Uncoated Pellets

The size distribution of the uncoated Nu-pareil pellets was determined by sieve analysis. 50g samples from each batch were separated through a nest of Endecotts test sieves which was agitated for 20 minutes on an Endecotts sieve shaker. Three separate samples were taken from each size fraction. The results are summarised in Tables 13 and 14.

Samples of 14-18 US Mesh pellets were tested to evaluate their ability to withstand abrasion during mechanical processing. A version of the Roche friabilator was used. This consisted of a circular plastic chamber, 20cm diameter fitted with steps inside the circumference. 20 glass spheres, each 0.5cm in diameter were placed in the chamber to increase the abrasion effect. Three 15g samples of the pellets were tested by rotating the chamber for 15 minutes at 24 revolutions per minute. The size distribution of the abraided samples was determined by sieve analysis as described above. The results are summarised in Table 15.

TABLE 13 **SIEVE ANALYSIS OF NU-PAREIL PELLETS 14-18 US MESH**

Sieve Aperture µm	Weight Percentage of Pellets Retained on Sieve			Mean Weight Percentage Retained	Mean Cumulative Percentage Oversize
	(1)	(2)	(3)		
2000	0.00	0.00	0.00	0.00	0.00
1400	6.10	5.93	5.98	6.00	6.00
1200	59.65	61.26	63.94	61.62	67.62
1000	33.66	32.01	29.68	31.78	99.40
841	0.39	0.40	0.40	0.40	99.80
710	0.00	0.20	0.00	0.07	99.87
Fines (<710)	0.20	0.20	0.00	0.13	100.00

TABLE 14 **SIEVE ANALYSIS OF NU-PAREIL PELLETS 20-25 US MESH**

Sieve Aperture μm	Weight Percentage of Pellets Retained on Sieve			Mean Weight Percentage Retained	Mean Cumulative Percentage Oversize
	(1)	(2)	(3)		
1200	0.00	0.00	0.00	0.00	0.00
1000	0.20	0.00	0.00	0.07	0.07
841	22.91	25.80	25.95	24.89	24.96
710	69.32	66.20	67.66	67.73	92.69
500	7.57	8.00	6.39	7.32	100.00
353	0.00	0.00	0.00	0.00	100.00
150	0.00	0.00	0.00	0.00	100.00
<150 (Fines)	0.00	0.00	0.00	0.00	100.00

TABLE 15 **SIEVE ANALYSIS OF NU-PAREIL PELLETS 14-18 US MESH AFTER ABRASION TEST**

Sieve Aperature μm	Weight Percentage of Pellets Retained on Sieve			Mean Weight Percentage Retained	Mean Cumulative Percentage Oversize
	(1)	(2)	(3)		
1700	0.00	0.00	0.00	0.00	0.00
1400	5.79	6.21	5.82	5.94	5.94
1200	60.45	64.66	63.00	62.70	68.64
1000	32.76	28.46	30.31	30.51	99.15
850	0.60	0.53	0.60	0.58	99.73
710	0.27	0.07	0.13	0.16	99.89
600	0.00	0.00	0.00	0.00	99.89
425	0.00	0.00	0.00	0.00	99.89
300	0.00	0.00	0.00	0.00	99.89
<300 (Fines)	0.13	0.07	0.13	0.11	100.00

From the distributions shown in Tables 13 to 15, it is possible to calculate pellet sizes corresponding to the median, lower quartile and upper quartile. The results of these calculations are shown in Table 16.

The lower quartile, median and upper quartile sizes shown in Table 16 for the 14-18 US Mesh pellets before and after abrasion demonstrate that there was no significant abrasion of the uncoated pellets, and that they are able to withstand moderate mechanical handling.

TABLE 16 **FRACTILE PARAMETERS FOR NU-PAREIL PELLETS**

Fractile	20-25 US Mesh	14-18 US Mesh Before Abrasion	14-18 US Mesh After Abrasion
Lower Quartile	743μm	1153μm	1162μm
Median	792μm	1256μm	1258μm
Upper Quartile	840μm	1337μm	1338μm

5.3.2 Calculation of Coating Requirements for Nu-Pareil Pellets

5.3.2.1 14-18 US Mesh Pellets

Ten random samples of twenty pellets were taken from the batch and weighed. The mean weight for 20 pellets was

0.0336g (s.d.1.743 x 10^{-3}g). Taking the average diameter of the pellets to be 0.12cm (the middle of the size fraction range) and assuming the pellets to be spherical, the average surface area of a pellet is 0.045cm^2.

Based on the average weight for 20 pellets, the average number of pellets per 500g load is 297,619 pellets, and the total surface area for coverage is 13,393cm^2.

To coat with 5mg polymer per square centimetre of pellet surface, the total requirement of polymer would be 66.97g of polymer.

An excess of polymer was sprayed onto the pellets to allow for possible loss of material in the coating process and 70.0g of polymer was applied per 500g of pellets as a 50mg cm^{-3} polymer solution to give the required coverage of polymer.

5.3.2.2 <u>20-25 US Mesh Pellets</u>

Ten random samples of fifty pellets were taken from the batch and weighed. The mean weight for 50 pellets was 0.0208g (s.d.3.665 x 10^{-4}g). Taking the average diameter of the pellets to be 0.0775cm (the middle of the size fraction range), and assuming the pellets to be spherical, the average surface area of a pellet is 0.01887cm^2.

Based on the average weight for 50 pellets, the average

number of pellets per 500g load is 1,201,923 pellets, and the total surface area for coverage is 22,680.3cm^2.

To coat with 5mg polymer per square centimetre of pellet surface, the total requirement of polymer would be 113.40g of polymer.

An excess of polymer was sprayed onto the pellets to allow for possible loss of material in the coating process and 115g of polymer was applied per 500g of pellets as a 5% w/v polymer solution to give the required coverage of polymer.

5.3.2.3 30-35 US Mesh Pellets

30-35 US mesh pellets were also examined for suitability for coating using the Aeromatic STREA-1. It was found that excessive quantities of the pellets were lost through the guard meshes in the base and top of the chamber. The mesh could not be restricted as this would impede the solvent extract.

Furthermore, the quantity of solution and consequent coating time necessary to apply a comparable thickness of coating to the pellet core was considered to be impractical.

5.3.3 Coating Process Development

A process capable of coating pellets evenly with polymer

film was required to ensure that the release of oxamniquine dispersed in the film is controlled by the coating. The quality of the coating is determined by the characteristics of fluidisation and atomisation as well as by the composition of the coating solution.

Figure 16 illustrates the dynamics of the coating process which can be broken down as follows:

1. Droplet formation
2. Contact/spreading
3. Coalescence
4. Core penetration
5. Evaporation

The total coating process involves the application of multiple coats to individual pellets, so that stages 1 to 5 all occur simultaneously throughout the process.

Figure 17, derived from data given by HALL AND PONDELL (1980), shows the percentage of coating required to produce a 100μm thick layer on particles between 0.044 and 4mm uncoated diameter (325 - 5 US Mesh). The calculations used to derive this plot assumed that the density of the uncoated particle was $1.3gcm^{-3}$ and the density of the coating material was $1.0gcm^{-3}$. From Figure 17 the addition of 5% of coating material to 1.2mm diameter pellets should result in a 100μm thick membrane.

FIG 16: DYNAMICS OF THE FLUIDISED BED COATING PROCESS

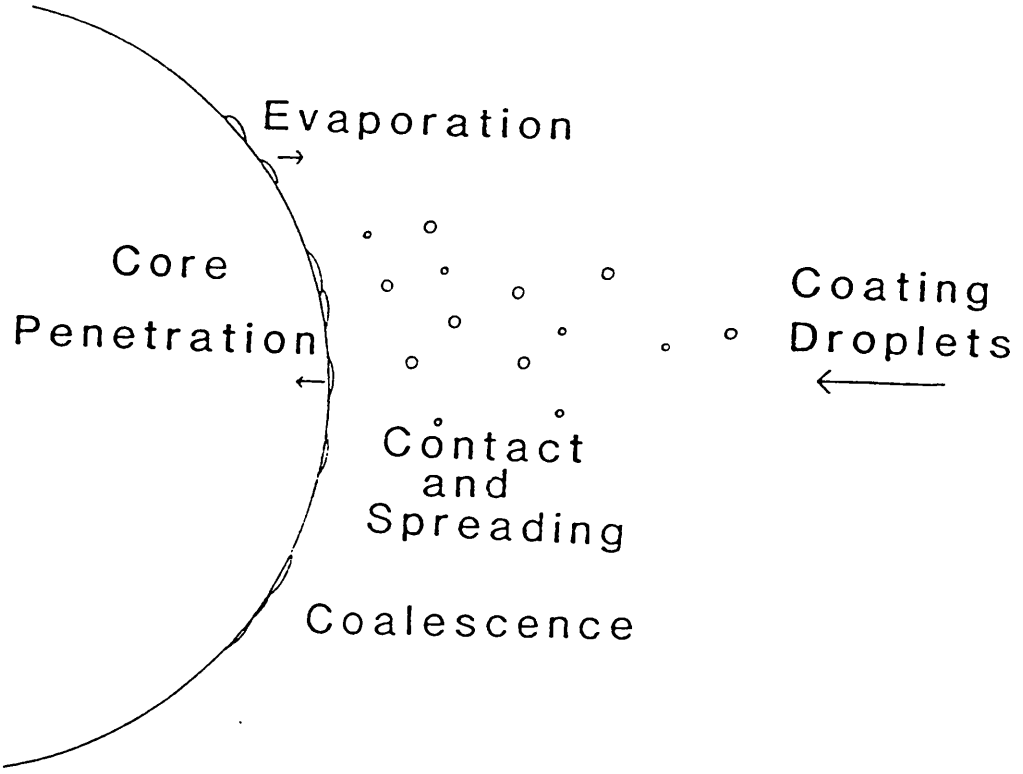

FIG 17: RELATIONSHIP BETWEEN PARTICLE SIZE AND QUANTITY OF COATING REQUIRED TO PRODUCE A 100 MICRON THICK COAT

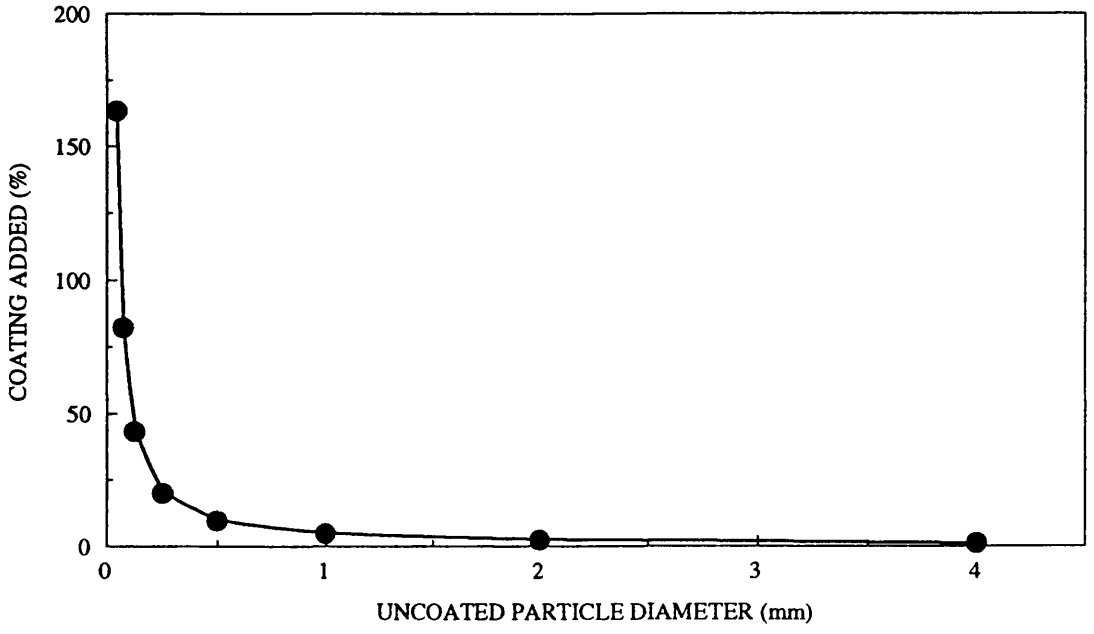

DATA FROM HALL AND PONDELL (1980)

For spray coating, a limiting factor in encapsulating solid particles is the size of the atomised droplets. When the droplets are large relative to the size of the particles, the particles are overwetted and may agglomerate or stick together. Larger droplets also result slower drying of the solvent which may also lead to particle agglomeration. Very small droplets may result in premature spray drying of the coating solution.

Figure 18 illustrates the typical droplet size produced by hydraulic nozzles and air atomising nozzles (JONES, 1985). Air atomising nozzles tend to produce finer droplets. The droplet size formed will vary with the liquid being atomised, the design of the nozzle and the rate of supply of liquid to the nozzle.

The duration of the coating process must be sufficiently short to minimise abrasion of uncoated and partially coated pellets in the chamber. The time taken to complete the process of applying a fixed quantity of coating to a batch of pellets may be reduced by increasing the concentration of the coating solution increasing the delivery rate of solution to the nozzle. Table 17 summarises some possible operating conditions to achieve this. Several preliminary experiments were conducted to derive a satisfactory process. It was found that solutions containing 100mg cm^{-3} polymer in dichloromethane were too viscous and rapidly blocked the atomising nozzle.

FIG 18: TYPICAL DROPLET SIZES PRODUCED BY HYDRAULIC AND AIR ATOMISING NOZZLES

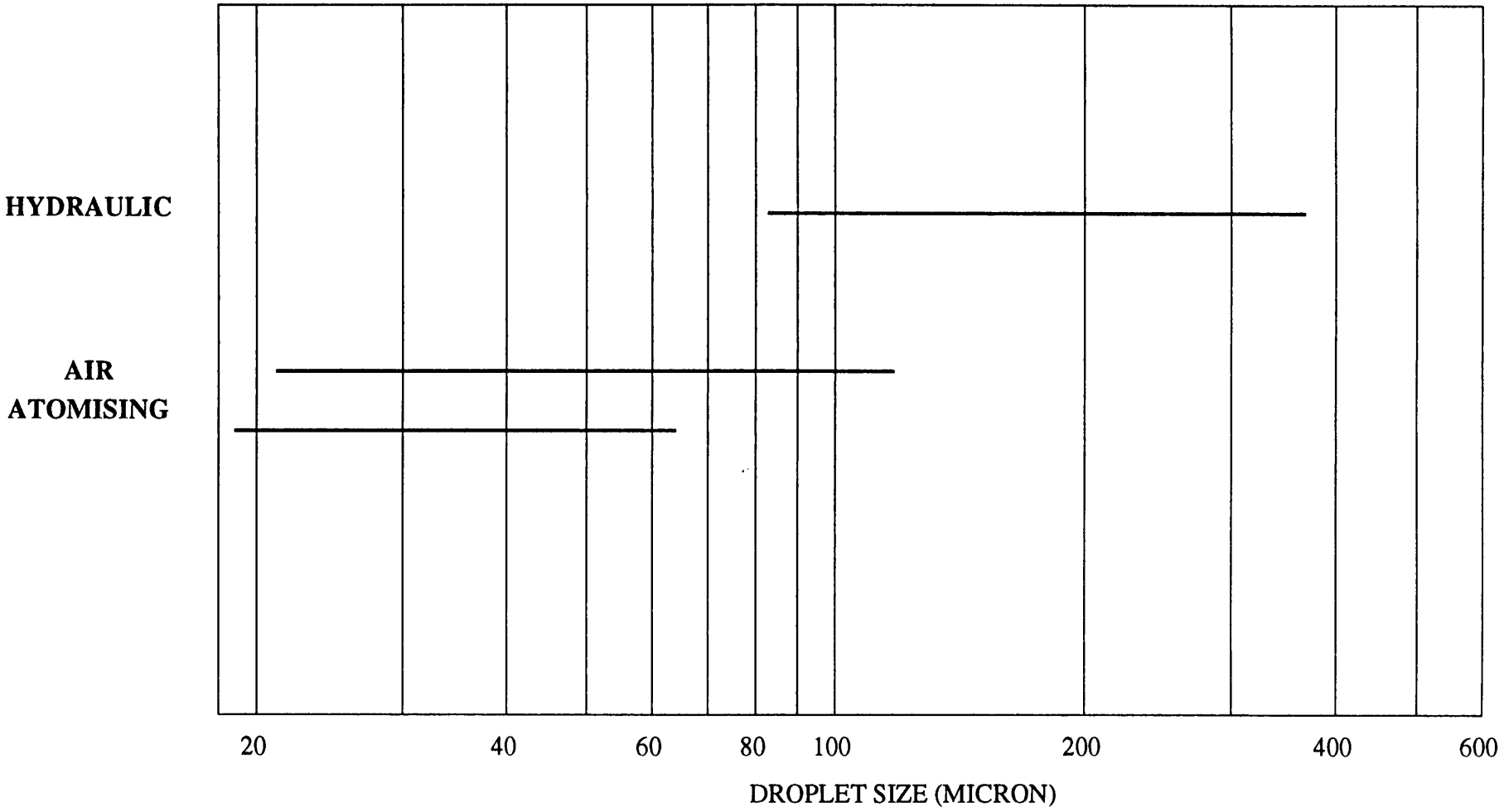

TABLE 17 **TIME TAKEN TO APPLY 70G OF POLYMER COATING FROM SOLUTIONS OF DIFFERENT CONCENTRATIONS APPLIED AT VARIOUS RATES**

Flow Rate of Solution to Nozzle	Concentration of Polymer Solution		
	10mg cm^{-3}	50mg cm^{-3}	100mg cm^{-3}
5cm^3 min^{-1}	1400 mins	280 mins	140 mins
10cm^3 min^{-1}	700 mins	140 mins	70 mins
15cm^3 min^{-1}	467 mins	93 mins	47 mins
25cm^3 min^{-1}	280 mins	56 mins	28 mins

Blockage did not occur with either 50mg cm^{-3} or 10mg cm^{-3} polymer solutions. 50mg cm^{-3} solutions of polymer were chosen in preference to reduce the coating time.

The characteristics of the atomising nozzle were evaluated by spraying aliquots of solution onto a blotting paper target mounted 30cm away from the spray nozzle. The nozzle was removed from the chamber and arranged so that the spray was horizontal to the target.

Ideally the spray pattern observed should be a core comprising a coalesced zone of small droplets with relatively few large isolated droplets outside of the central core. The spray pattern within the coating chamber will be a well defined coating zone consisting of large numbers of small droplets with minimal impact and loss of coating material to the walls of the chamber.

Also under these conditions, the droplet size should not be

excessively large which would lead to overwetting of the pellets, slower drying of the coating and possible agglomeration of the pellets within the chamber. The spray pattern was satisfactory when a coating solution containing 50mg cm^{-3} of polymer solution, delivered to the nozzle at 25cm^3 min^{-1} was sprayed at an atomising pressure of 276 KPa.

Dichloromethane is non-flammable, has a moderate boiling point and a high evaporation rate, which makes it a suitable solvent for this process. In modern industrial practice, dichloromethane would not be considered favourably in spray coating processes.

It was observed that the temperature of the process air leaving the chamber was lower than the preset air inlet temperature. This is due to evaporative cooling of the solvent. In a Wurster process an air distribution plate would be located in the base of the chamber and a partition, which defines the coating zone, within the chamber. Outside of the partition, coated particles descend in the fluidising air stream before being drawn into the coating zone. A temperature gradient exists outside of the partition, being cooler near to the top of the partition. The particle flow and temperature gradient within the coating chamber of the Aeromatic STREA-1, which is not a Wurster design is simpler, with particles rising and falling as a function of the volume and velocity of the air flow. It might be expected that in this type of

coating apparatus a temperature gradient occurs with the warmest point at the air inlet and the coolest point at the air outlet. There will also be localised cool points at the surface of pellets from which solvent is evaporating as a result of evaporative cooling.

In preliminary coating experiments the temperature of the process air was set to 50°C. During coating, the recorded outlet air temperature was 40°C. After coating was complete the outlet air temperature climbed to 50°C as the coated pellets dried. At this point the atomising air was turned off and the fluidising air maintained for a further hour to allow coated pellets to dry. Reducing the process air temperature to 40°C or less resulted in process failure due to agglomeration of the pellets.

5.3.4 Coating Formulations Tested

The composition of the coating applied to the pellets was varied to study the following effects:

i) Variation of the ratio of Eudragit RL to Eudragit RS in the coating

ii) Variation of the quantity of plasticiser in the coating

iii) The effect of different plasticiser types

iv) Variation of the oxamniquine loading in the coating

v) Diameter of the uncoated pellets.

The compositions of the coatings tested are summarised in Table 18.

TABLE 18 **FORMULATIONS OF THE COATINGS APPLIED TO INERT NU-PAREIL PELLETS**

Composition of Film % w/w	Formulation Code														
	A1	A2	B1	B2	B3	B4	C1	C2	C3	D1	D2	D3	D4	E1	E2
Eudragit RL	43.48	43.48	86.96	69.57	17.39	-	47.62	45.45	40.00	43.48	43.48	43.48	43.48	41.67	40.00
Eudragit RS	43.48	43.48	-	17.39	69.57	86.96	47.62	45.45	40.00	43.48	43.48	43.48	43.48	41.67	40.00
Oxamniquine	4.35	4.35	4.35	4.35	4.35	4.35	4.76	4.55	4.00	4.35	4.35	4.35	4.35	8.33	12.00
Glyceryl Triacetate	8.70	8.70	8.70	8.70	8.70	8.70	-	4.55	16.00	-	-	-	-	8.33	8.00
Polyethylene Glycol 400	-	-	-	-	-	-	-	-	-	8.70	-	-	-	-	-
Dimethyl Phthalate	-	-	-	-	-	-	-	-	-	-	8.70	-	-	-	-
Diethyl Phthalate	-	-	-	-	-	-	-	-	-	-	-	8.70	-	-	-
Di-n-butyl Phthalate	-	-	-	-	-	-	-	-	-	-	-	-	8.70	-	-
Pellet size (US Mesh)	14-18	20-25	14-18	14-18	14-18	14-18	14-18	14-18	14-18	14-18	14-18	14-18	14-18	14-18	14-18
Coating level of Polymer $mgcm^{-2}$	5	5	5	5	5	5	5	5	5	5	5	5	5	5	5

5.3.5 Coating Process Efficiency

All of the film formulations detailed in Table 18 were applied to the Nu-Pareil pellets using the process described in Chapter 3. After the coating was applied, and the pellets dried in the chamber, the batch of material was removed and weighed. The efficiency of the coating process was evaluated by expressing the recorded weight of the batch as a percentage of the input weight of polymer, oxamniquine, plasticiser and pellets. The results are summarised in Table 19.

The coating efficiency is an expression of the loss of material from the process. Typical losses in a fluidised bed coating process might be loss of fines abraded from the bed to the exhaust system, coating material impinging onto the walls of the chamber, coating material 'spray-dried' before impacting onto pellets. Optimisation of the atomisation conditions, fluidisation conditions and bed temperature clearly increase the process efficiency (JONES 1985).

Typically, the efficiency of a fluidised bed spray process is better than a similar operation using an air spray process in a conventional coating pan. PORTER (1980) sprayed Cellulose Acetate Phthalate and Polyvinyl Acetate Phthalate films onto inert tablet cores using an air spray process in a coating pan. The average coating efficiency was found to be 65%. This is considerably lower than the

92% obtained using the fluidised bed air spray process. The efficiency of fluidised bed processes is generally accepted to be very high, and under the control of a properly optimised process, negligible losses of coating material may be expected.

TABLE 19 **EFFICIENCY OF THE COATING PROCESS FOR DIFFERENT COATING FORMULATIONS**

FORMULATION	COATING EFFICIENCY %
A1	85.8
A2	81.9
B1	96.1
B2	93.2
B3	93.6
B4	92.4
C1	89.4
C2	89.9
C3	91.2
D1	90.4
D2	93.8
D3	92.7
D4	93.3
E1	97.1
E2	93.6
Mean (±s.d.)	91.6 (±3.9)

The pellets were examined visually after completion of the coating process. There were no obvious defects present in the coatings which might have resulted from incompatibilities of the components, internal stresses within the coatings, overdrying and excessively rapid drying such as blistering, sweating and 'orange-peel' appearance (ELLIS et al 1976).

5.4 Mathematical Models of Drug Release

A major factor considered in this thesis is the mechanism of oxamniquine release from Eudragit films and how this is affected by film formulations.

A number of mathematical models have been developed to describe the release of drugs from diffusion or dissolution controlled systems. These are frequently based on Ficks Laws of Diffusion. Diffusion, which is the transport of matter within a system by random molecular motion was described in a phenomenological equation by A Fick in 1855 (CRANK, 1975). Fick's original observations were made for the transfer of heat in materials, but parallels have been drawn to describe diffusion phenomena.

The rate of transfer of a diffusing substance through a unit area of a section is proportional to the concentration gradient measured normal to that section, thus

$$J = -D\frac{\partial c}{\partial x} \qquad (12)$$

J = rate of transfer per unit area
D = diffusion coefficient
$\frac{\partial c}{\partial x}$ = concentration gradient with respect to distance

The negative sign expresses the fact that diffusion takes place along a diminishing concentration gradient. This is the simplest mathematical expression of FICKS FIRST LAW and assumes that

(1) the diffusion coefficient is constant

(2) diffusion takes place in one direction only

(3) the medium is isotropic i.e. diffusion properties are identical in all directions.

Diffusion models have been developed for various cases where not all of these assumptions can be made.

The fundamental differential equation of diffusion in an isotropic medium (FICKS SECOND LAW) may be derived by equating the rate at which the amount of diffusing substance accumulates in an element of volume with the net rate of transfer of diffusing substance through that element. This yields equation 13.

$$\frac{\partial C}{\partial t} = D\frac{\partial^2 C}{\partial x^2} \qquad (13)$$

This equation expresses that the rate of change of concentration with time at a particular point is proportional to the rate of change of concentration at that point. The assumptions stated in the expression of Ficks First Law hold for this statement of Ficks Second Law.

Equation 13 is a second order, partial differential equation in three variables, which cannot be solved directly. Solutions to the equation are usually in the form of series of error functions or trigonometrical terms, are obtained by defining limiting boundary conditions specific to the particular problem and applying standard mathematical techniques such as Laplace Transformation or

separation of variables (CRANK, 1975).

Non-disintegrating and non-eroding matrix or monolithic devices may be broadly divided into two classes. The solute may be either totally dissolved within the matrix or may contain solute within the matrix in excess of its solubility and in equilibrium with dissolved solute (BAKER AND LONSDALE, 1974). The release kinetics of monolithic devices containing dissolved and dispersed drugs are different and will be considered separately. The following sections detail the mathematical background to some of the models to demonstrate how their validity may be checked for the particular systems studied.

5.4.1 Drug totally dissolved within the matrix

This system may be described mathematically as the solution to Ficks Second Law for a membrane which has a constant solute concentration at the surfaces and an initial drug distribution described by a function of the position within the membrane. A limiting case of this model occurs where the solute is initially dissolved uniformly throughout the membrane at concentration C_o.

If Q_t is the quantity of drug in the membrane at time t, and Q_∞ the quantity of drug after infinite time, then an integrated form of the equation can be written

$$\frac{Q_t}{Q_\infty} = 1 \sum_{o}^{\infty} \frac{8}{(2n+1)^2\pi^2} \exp\left[-D(2n+1)^2\pi^2 t/4l^2\right] \qquad (14)$$

This equation describe the behaviour of the system for the release of the last 40-60% of the solute. The corresponding solution which best describes the release of the first 40-60% of solute is

$$\frac{Q_t}{Q_\infty} = 2\left[\frac{Dt}{l^2}\right]^{1/2}\left[\pi^{-1/2} + 2\sum_{1}^{\infty}(-1)^n \text{ ierfc } \frac{nl}{\sqrt{(Dt)}}\right] \qquad (15)$$

Where ierf c is the error function in c.

Equations are too clumsy for routine use and can be reduced to two expressions which approximate to the exact solutions by better than 1% (BAKER AND LONSDALE, 1974). For early times

$$0 \leq \frac{Q_t}{Q_\infty} \leq 0.6$$

$$\frac{Q_t}{Q_\infty} = 2\left[\frac{Dt}{l^2}\right]^{1/2} \qquad (16)$$

and for late times

$$0.4 \leq \frac{Q_t}{Q_\infty} \leq 1.0$$

$$\frac{Q_t}{Q_\infty} = 1 - \frac{8}{\pi^2}\exp\left[\frac{-\pi^2 Dt}{l^2}\right] \qquad (17)$$

The interpretation of equations 16 and 17 is that for a matrix system containing only dissolved drug, the release pattern will be biphasic, with the first 40-60% release in manner clearly dependent on $\sqrt{t}$, and the remainder released in an exponentially decaying manner. These approximations are shown graphically in Figure 30, which illustrates their different regions of application.

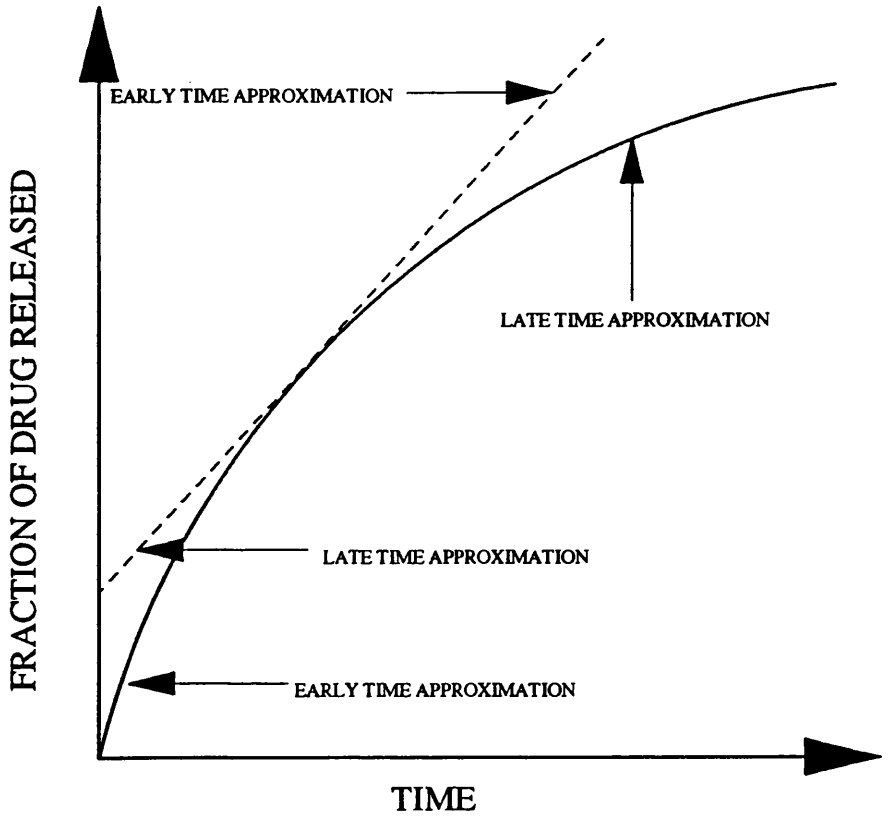

Figure 19 Fraction of drug released from a plane membrane as a function of time using early and late time approximations.

5.4.2 Drug Dispersed Within the Matrix

Matrices of this type contain finely divided solute particles which are uniformly dispersed or suspended within the matrix phase. The dispersed solute is in equilibrium with dissolved solute. Of these, homogeneous matrices have a non-granular matrix phase, and diffusion occurs through the matrix continuum. Heterogeneous matrices, by contrast, have a granular polymer phase, and release of the solute occurs only through pores or capillaries. It is possible that intermediate types exist and that the structure of the polymer may change with time if leachable components are

removed, leaving voids. The two types of matrix are shown schematically in Figure 20.

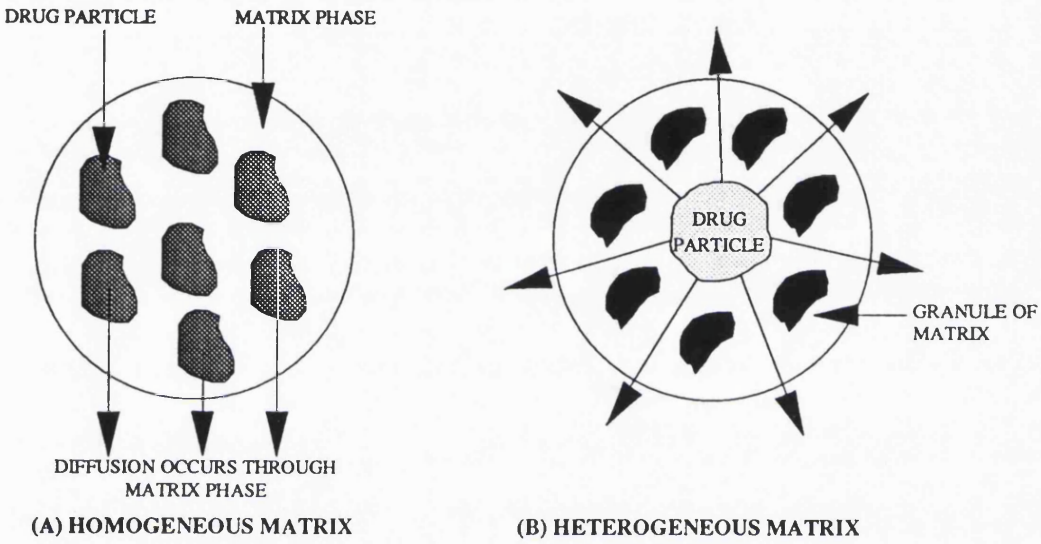

Figure 20 Schematic Representation of the Two Classes of Matrix.

HIGUCHI (1960) presented equations to describe the release of drugs from ointments, where the rate controlling step to drug absorption is in the ointment phase rather than the skin. The derivation of these equations was detailed by HIGUCHI (1961).

Assume that a concentration profile exists within a matrix containing suspended drug which is in contact with a perfect sink. Figure 21 shows:

(i) the concentration profile after some time t and

(ii) the concentration profile after time (t + dt)

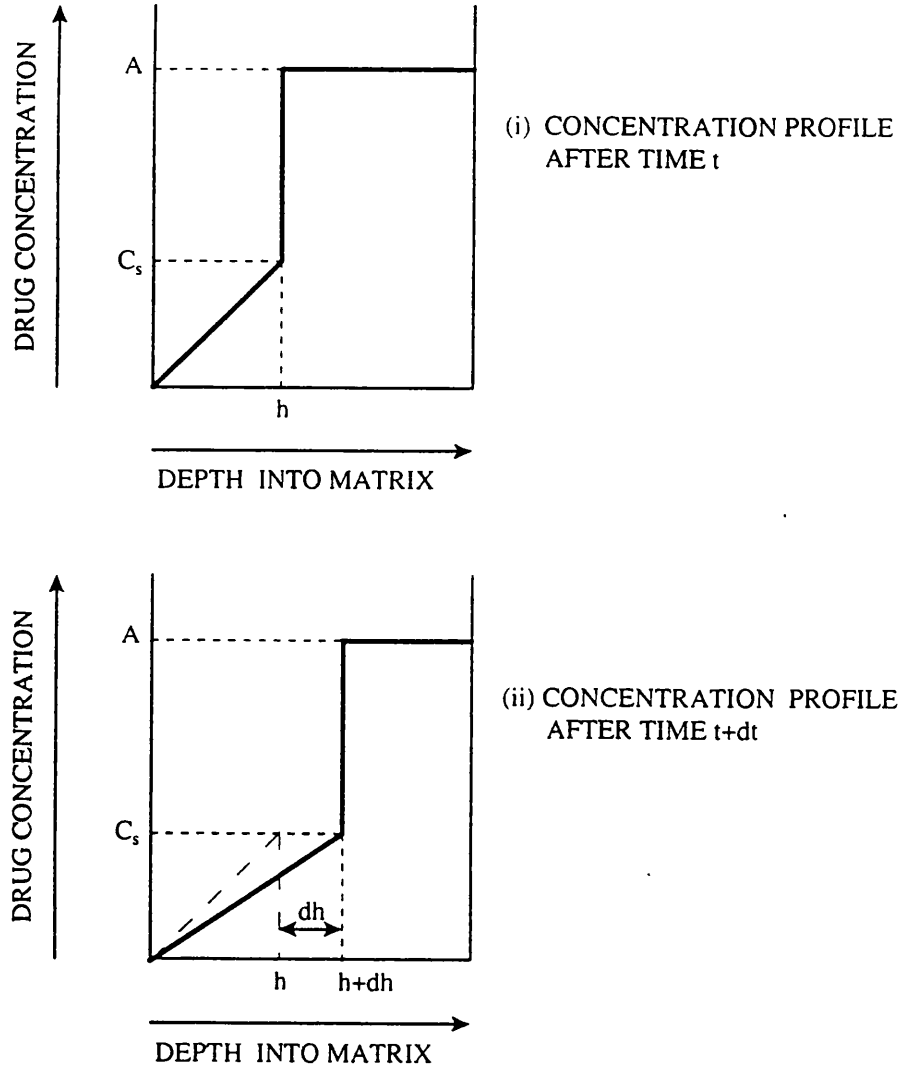

C_S = saturation solubility in matrix

A = total drug loading in matrix

Figure 21 Concentration Profiles Within a Matrix

Figure 21 (i)shows that after time t, there is a surface zone 0<x<h in which all of the drug has dissolved. After time t+dt, Figure 21 (ii) shows that this zone has receded further into the depth of the matrix by a distance dh.

From Figure 21 (i), the total amount of drug released, Q,

after time t, is given by

$$Q = Ah - \tfrac{1}{2} C_s h.$$

After time t+dt, the amount of drug released Q+dQ, with the boundary at depth h+dh is

$$Q+dQ = A(h+dh) - \tfrac{1}{2} C_s (h+dh)$$

Hence $dQ = Adh - \tfrac{1}{2} C_s dh$.

By application of Ficks First Law to the depleted zone

$$\frac{dQ}{dt} = \frac{DC_s}{h}$$

Hence $\frac{dQ}{dt} = A\frac{dh}{dt} - \frac{1}{2} C_s \frac{dh}{dt} = \frac{DC_s}{h}$

and $dt = \frac{(2A - C_s)}{2DC_s} h\, dh$

By integration

$$t = \frac{(2A - C_s)}{4DC_s} h^2 + K$$

where K is the constant of integration. However, K=0 since h=o when t=o.

Thus

$$h = 2 \left[\frac{DC_s t}{(2A-C_s)}\right]^{1/2}$$

Substituting this equation into the original expression for Q to eliminate h gives

$$Q = (2A-C_s)\sqrt{\frac{DC_s t}{(2A-C_s)}}$$

or

$$Q = \sqrt{D(2A-C_s)C_s t} \qquad (18)$$

HIGUCHI (1963) has described the analogy between ointment bases, for which this equation was originally derived and sustained release matrices. This model predicts that the amount of drug released is linear with $\sqrt{t}$ provided there is excess suspended drug within the matrix. In developing the model, several assumptions have been made

(1) The drug concentration profile shows a sharp discontinuity at the point of depletion, with none of the suspended phase dissolving until the environmental concentration falls below C_s.

(2) The transfer of solute from the dispersed to dissolved state is rapid compared with the subsequent elimination of the solute by diffusion. This largely depends on the state of dispersion of the drug in the suspended phase.

(3) The concentration profile in the zone of depletion $o \leq x \leq h$ is assumed to be linear. This is a reasonable assumption if $A >> C_s$. In this case undissolved drug at the depletion boundary acts as a source of constant thermodynamic activity.

(4) A linear profile exists between the perfect sink, x=o and the boundary x=h. Under these conditions Ficks First Law is assumed to apply. This is known as the PSEUDOSTEADY STATE assumption implicit in this model.

For granular matrices the equation describing the model becomes

$$Q = \sqrt{\frac{D_A}{\tau} \epsilon (2A-\epsilon C_A) C_A t} \qquad (19)$$

where ϵ is the porosity of the matrix

τ is the tortuosity of the matrix

D_A is the diffusion coefficient in the fluid filled channels

C_A is the saturation concentration in the fluid filled channels

PAUL AND McSPADDEN (1976) examined the pseudosteady state assumption at the limit A-> C_S and found that the result did not precisely match the prediction of the classical theory for $A<C_S$. This discrepancy (11.3% low) was removed by applying Ficks Second Law to the region $0<x<h$ illustrated in Figure 21, resulting in equation 20,

$$Q_T = \alpha \sqrt{2DC_S(A-C_S)t} \qquad (20)$$

which is similar to equation 19, and demonstrates the validity of the pseudosteady approximation in the limit $A>>C_S$.

5.4.3 Effect of Boundary Layers

ROSEMAN AND HIGUCHI, W.I. (1970) extended the model of HIGUCHI,T. (1963) to include the effects of boundary layers

as additional diffusional resistance. This is an important consideration, since although boundary layers can be eliminated <u>in vitro</u> by effective stirring of the eluting medium, boundary layers of indeterminate thickness can be formed with some devices placed <u>in vivo</u>. These boundary layers may, in extreme cases, become rate limiting in drug release from the devices.

A diagram which illustrates this model for release from a planar matrix is shown in Figure 22.

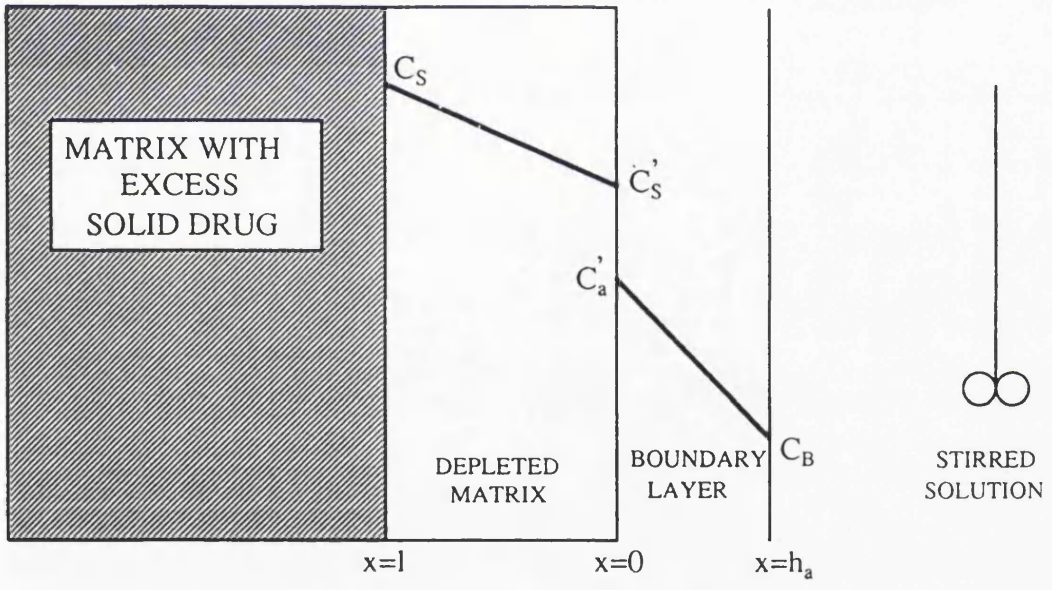

Figure 22 Diagram illustrating release from a planar matrix including boundary layer and partitioning effects.

In this model steady state approximations have been made

for the depleted zone of the matrix and across the boundary layer. A partition step at the matrix/solution boundary has also been included in the model.

Assuming sink conditions exist i.e. $C_{B(t)}=0$, expressions may be derived which describe the release of drugs from matrices as follows

$$l^2 + \frac{2D_e\ h_a\ l}{K\ D_a} = \frac{4\ C_s\ D_e}{(2A-C_s)}\ t \qquad (21)$$

$$\text{and } Q = \frac{(A-C_s)l}{2} \qquad (22)$$

where D_a =diffusion coefficient in the extraction medium

A = drug loading concentration in the matrix

D_e= effective diffusion coefficient in the matrix.

CHIEN AND LAMBERT (1974) identified two possible mechanisms for drug release from matrices.

For a 'matrix controlled' process

$$l^2 >> \frac{2\ D_e\ h_a\ l}{KD_a}$$

$$\text{and} \qquad Q = \sqrt{D_e\ (2A-C_s)C_s t} \qquad (23)$$

which is analogous to the model developed by HIGUCHI (1963).

However, for a 'partition control' process

$$l^2 << \frac{4\ C_s\ D_e}{K\ D_a}\ t$$

and $$Q = \frac{K\ D_a\ C_s}{h_a}\ t \qquad (24)$$

Partition control of drug release arises when the dissolution of drug into the elution medium is the rate limiting step compared with dissolution of the drug into the polymer phase, and may be expected when the partition coefficient between the elution medium and the polymer phase is relatively small. The nature of the controlling mechanism can be deduced from plots of Q against $\sqrt{t}$.

A transition region exists, in which the release mechanism is neither truly partition controlled nor matrix controlled.

The nature of the permeating agent also influences the release mechanism. ROSEMAN AND YALKOWSKY (1976) studied the release of a series of alkyl p-aminobenzoic acid esters to evaluate the effect of drug lipophilicity and boundary layer effects. Drugs which have a large partition coefficient between the matrix and the elution medium will exhibit a period of zero order release before the onset of matrix-controlled kinetics. This is therefore a biphasic release mechanism. The duration of zero order release depends upon the initial drug loading, the boundary layer resistance and the permeability of the drug through the matrix.

The concept can also be applied to matrices containing any dissolved drug. The release pattern in such cases would be triphasic with a zero order period followed by $t^{-1/2}$ dependent phase and then by an exponential phase.

SCIARRA and GIDWANI (1970, 1972) studied the release of gentian violet and cetylpyridinium chloride dispersed in various acrylic, polyamide and ethylcellulose films. The data were analysed using a dissolution control model based on the classical Noyes-Whitney equation. This model is actually a special case of the classical first order model. (CRANK, 1975; FLYNN et al, 1974.)

$$\log X = \log A_o - \frac{kt}{2.303} \qquad (25)$$

X = amount of drug remaining in the film

A_o = initial drug loading in the film

If this model was applicable then a plot of log X vs t should be linear; and this was found to be so by SCIARRA AND GIDWANI. However DONBROW AND FRIEDMAN (1975a), analysed the same data and demonstrated that they also fitted the matrix controlled model of Higuchi. The latter workers proposed a test to critically distinguish between the two possible mechanisms.

Considering the equation arising from Higuchi model (equation 18)

$$Q = \sqrt{D(2A-C_s)C_s t}$$

If $K = \sqrt{D(2A-C_s)C_s}$ then

$$Q = Kt^{1/2}$$

and $$2Q \frac{dQ}{dt} = K^2 \qquad (26)$$

so that a plot of $\frac{dQ}{dt}$ against $1/Q$ is linear.

However, for the dissolution type mechanism

$$X = A-Q$$

Thus

$$\ln (A-Q) = \ln A - Kt$$

and $$\frac{dQ}{dt} = KA - KQ \qquad (27)$$

so that a plot of $\frac{dQ}{dt}$ against Q is linear.

Using this test Donbrow and Friedman demonstrated the diffusion controlled matrix model fitted Sciarra and Gidwani's data more closely than the dissolution controlled model. This treatment can be described as the differential rate plot method.

From the foregoing discussion, it is possible that one of a number of physicochemical models may describe the release of oxamniquine from Eudragit films. However, it must be remembered that many of these models were developed for matrix systems, such as filled silicone polymers which did not change significantly over the period of drug release.

5.5 Release of Oxamniquine from Free Films

5.5.1 The Effect of Polymer Ratio

Mixed films of Eudragit RL and Eudragit RS were prepared by dissolving granules of the polymers in dichloromethane and pouring the solution onto mercury. Figure 23 shows the effect of increasing the proportion of Eudragit RL in films containing 5%$^{w}/_{w}$ oxamniquine and plasticised with 10%$^{w}/_{w}$ glyceryl triacetate. The results shown are the mean of at least 3 films. The release of oxamniquine was found to be reproducible to within 5% of the mean. As the proportion of Eudragit RL in the film is increased, oxamniquine is released substantially faster from the film. This has been reported previously (BARNETT, CARLESS and SUMMERS, 1984). Figure 24 shows the time taken to release between 10 and 50% of the oxamniquine content of the films plotted as a function of Eudragit RS content of the film. The release from films containing only Eudragit RL is approximately 12 times faster than from films containing any Eudragit RS.

This observation is in general agreement with other workers who have examined the properties of Eudragit RL and Eudragit RS. ANDERSON AND ABDEL-AZIZ (1976) found that the transmission of urea through Eudragit films was slower in films prepared from Eudragit RS than in those prepared from Eudragit RL. BENITA et al (1985) produced microcapsules of paracetamol with Eudragit RL or Eudragit RS with similar findings.

FIG 23:THE EFFECT OF POLYMER RATIO ON THE RELEASE OF OXAMNIQUINE FROM POLYMER FILMS: GRAPH OF FRACTION RELEASED AGAINST TIME

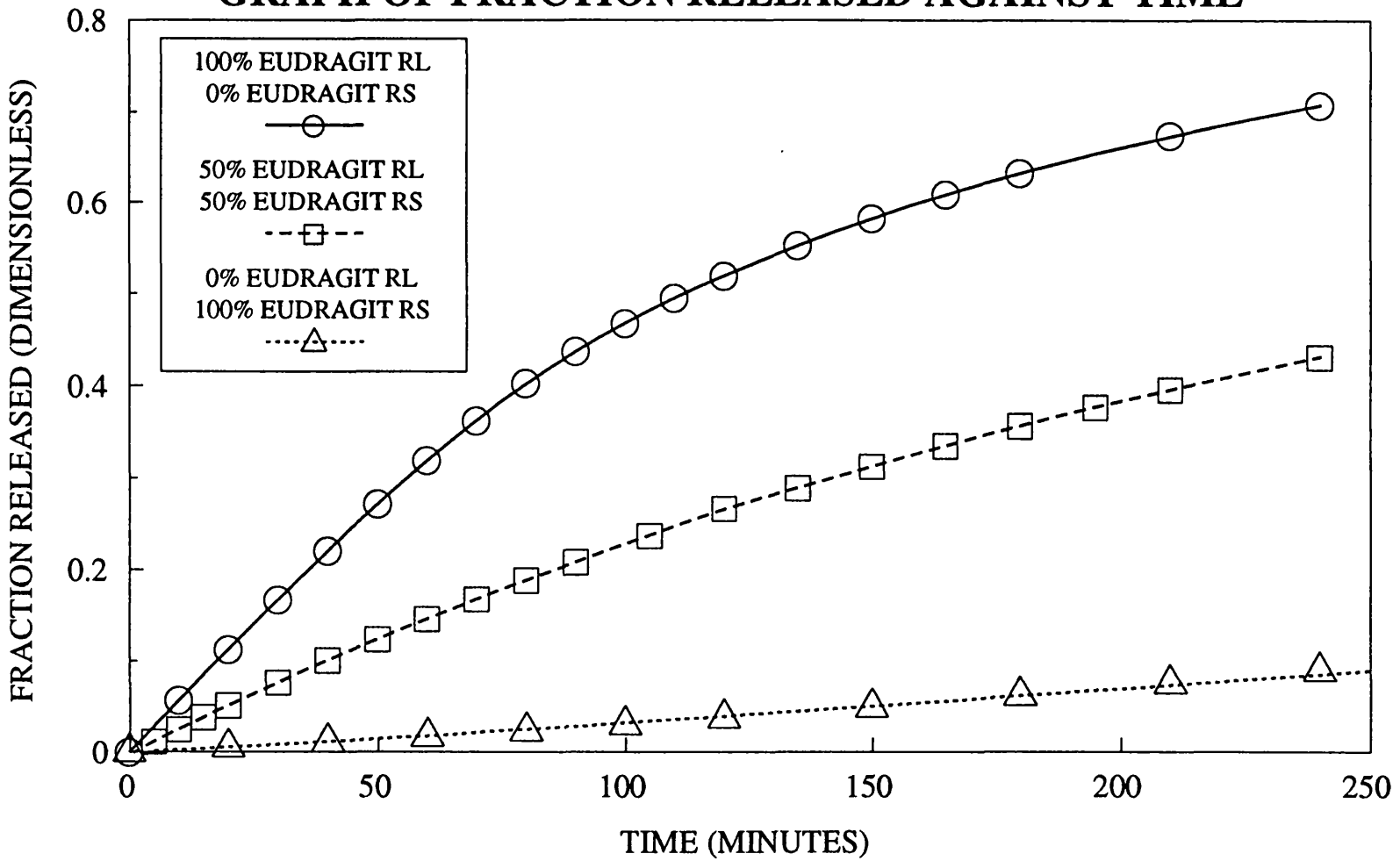

FILMS CONTAINED 10% GLYCERYL TRIACETATE AND
5% OXAMNIQUINE RELATIVE TO POLYMER WEIGHT

FIG 24:THE EFFECT OF POLYMER RATIO ON THE TIME TAKEN TO RELEASE OXAMNIQUINE FROM FREE FILMS

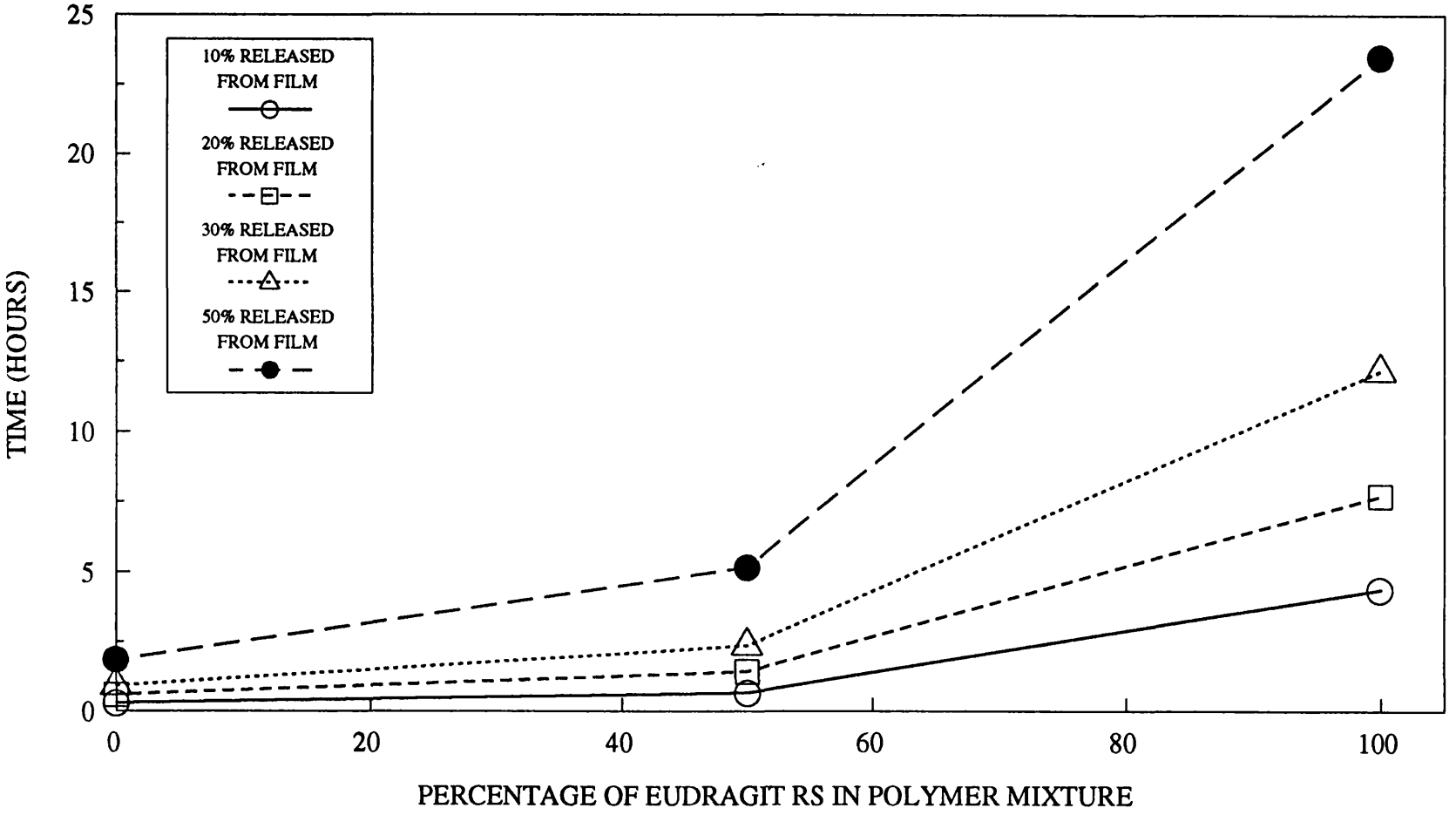

FILMS CONTAINED 10% GLYCERYL TRIACETATE AND
5% OXAMNIQUINE RELATIVE TO POLYMER WEIGHT

FIG 25: THE EFFECT OF POLYMER RATIO ON THE RELEASE OF OXAMNIQUINE FROM FREE FILMS: GRAPH OF RATE OF FRACTIONAL RELEASE AGAINST TIME

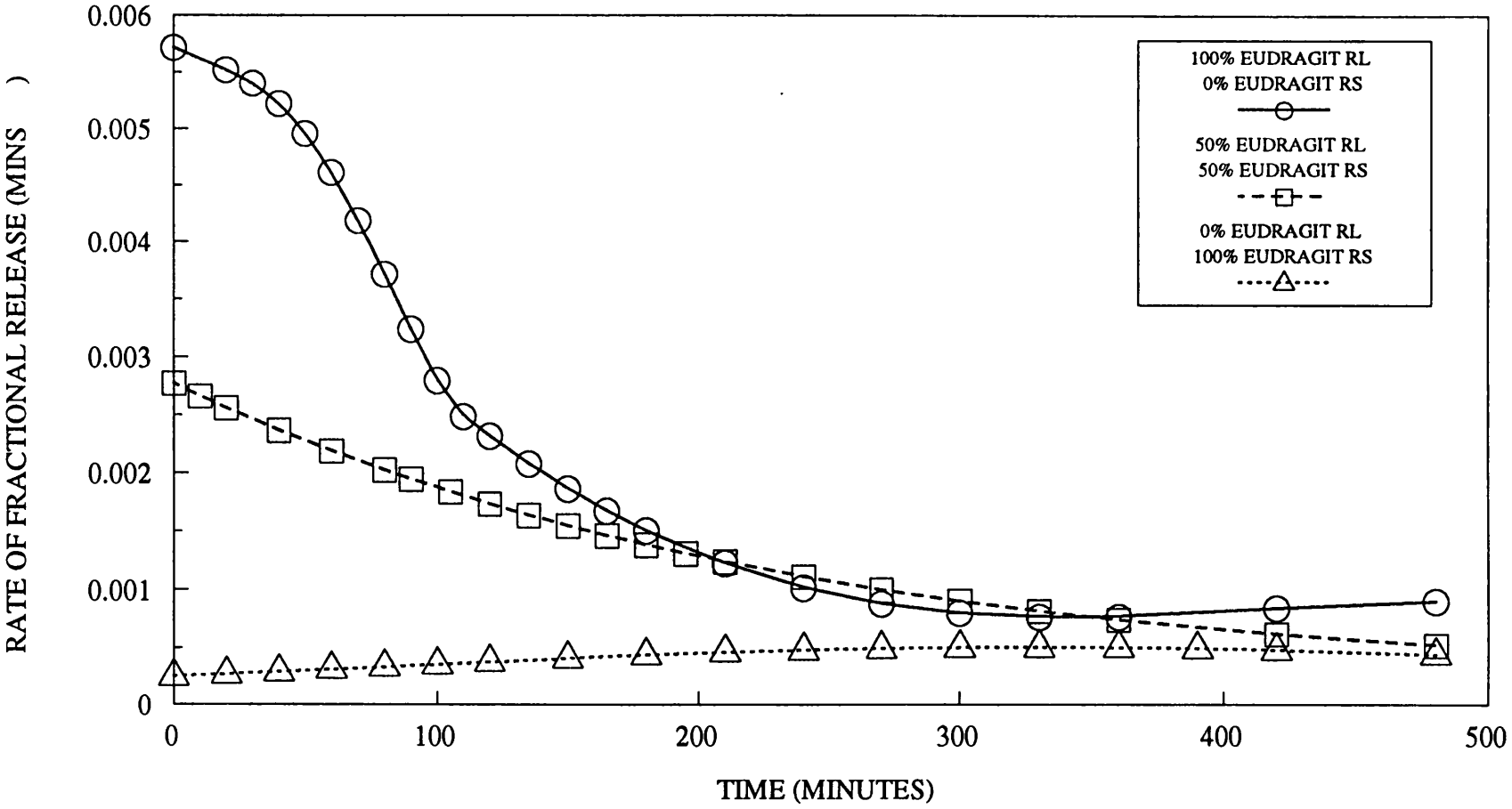

FILMS CONTAINED 10% GLYCERYL TRIACETATE
AND 5% OXAMNIQUINE RELATIVE TO POLYMER WEIGHT

EL-FATTEH et al (1984b) prepared co-precipitates of pheniramine aminosalicylate with Eudragit RL and RS and found that release of the drug was slower from the Eudragit RS co-precipitate than from the Eudragit RL co-precipitate. However, comparing ERL and ERS co-precipitates the decrease in release rate was only about 0.2 times, which is less significant than films examined in these studies. A difference is envisaged between a polymer film system and a co-precipitate even though both formulations have been produced by evaporation from organic solution. In a polymer film evaporation of the solvent results in a structured cohesive arrangement of polymer chains containing dispersed or dissolved drug. In a co-precipitate, as solvent evaporates and dissolved components exceed their solubility, and precipitate from solution forming a non-ordered but intimate mixture. The cohesive film structure may retard the release of drug compared with the co-precipitate. Precipitation may occur where a non eutectic mixture of solvents is used to dissolve a polymer which is poorly soluble in the least volatile solvent.

Figure 25 shows the calculated rate of release of oxamniquine as a function of time. The data for these curves were generated using a computer curve fitting routine based on Chebyshev series polynomials from the NAG algorithm library. The early release rates of oxamniquine from the film formulations increase with the proportion of Eudragit RL in the film. The varying shape of the rate of release curves suggests that the release mechanism of

oxamniquine from these films may vary with the ratio of the polymers. It is appropriate to examine possible mechanisms of release of oxamniquine from these films.

It may be expected that a film system of this type would be described by the matrix control model described by HIGUCHI (1963). Figure 26 shows the fractional release of oxamniquine plotted against √(time) for films containing different compositions of polymers. If the release from these films was described by Higuchi's model this relationship would be linear.

Figure 26 illustrates that the matrix controlled model does not adequately describe the release of oxamniquine from these films, since the relationship is not linear at early times as would be expected.

An extension to the matrix controlled model is the inclusion of a partition effect at the membrane-solution interface which has been described by ROSEMAN AND HIGUCHI (1970) and ROSEMAN AND YALKOWSKY (1976). If this model were applicable then a constant release (zero order) followed by $t^{-1/2}$ decay would be observed. Figure 27 shows a typical release plot for a system described by this model containing dispersed drug.

FIG 26: THE EFFECT OF POLYMER RATIO ON THE RELEASE OF OXAMNIQUINE FROM FREE FILMS: GRAPH OF FRACTION RELEASED AGAINST ROOT TIME

PLOT TO EVALUATE THE MATRIX CONTROLLED MODEL

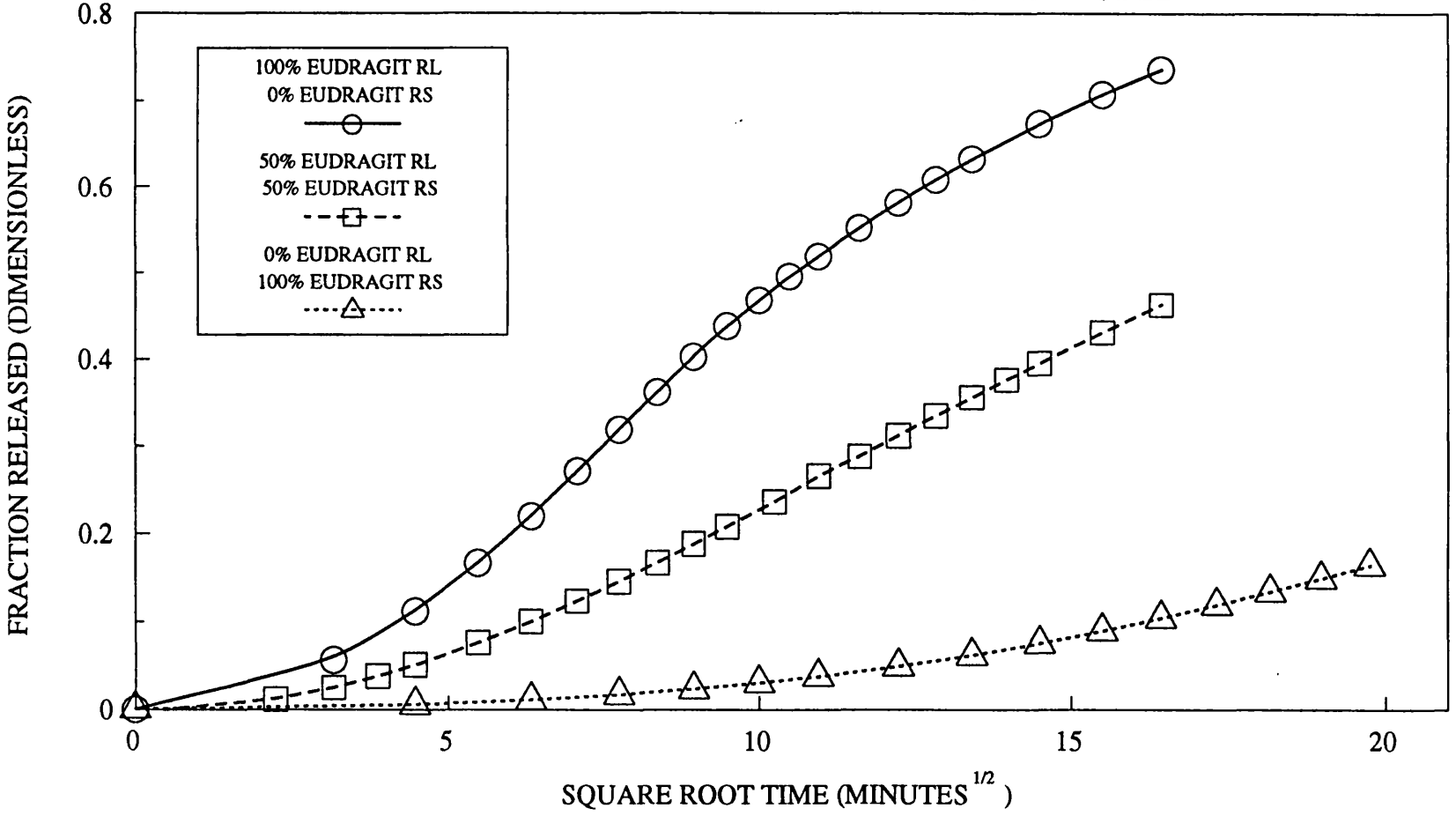

FILMS CONTAINED 10% GLYCERYL TRIACETATE
AND 5% OXAMNIQUINE RELATIVE TO POLYMER WEIGHT

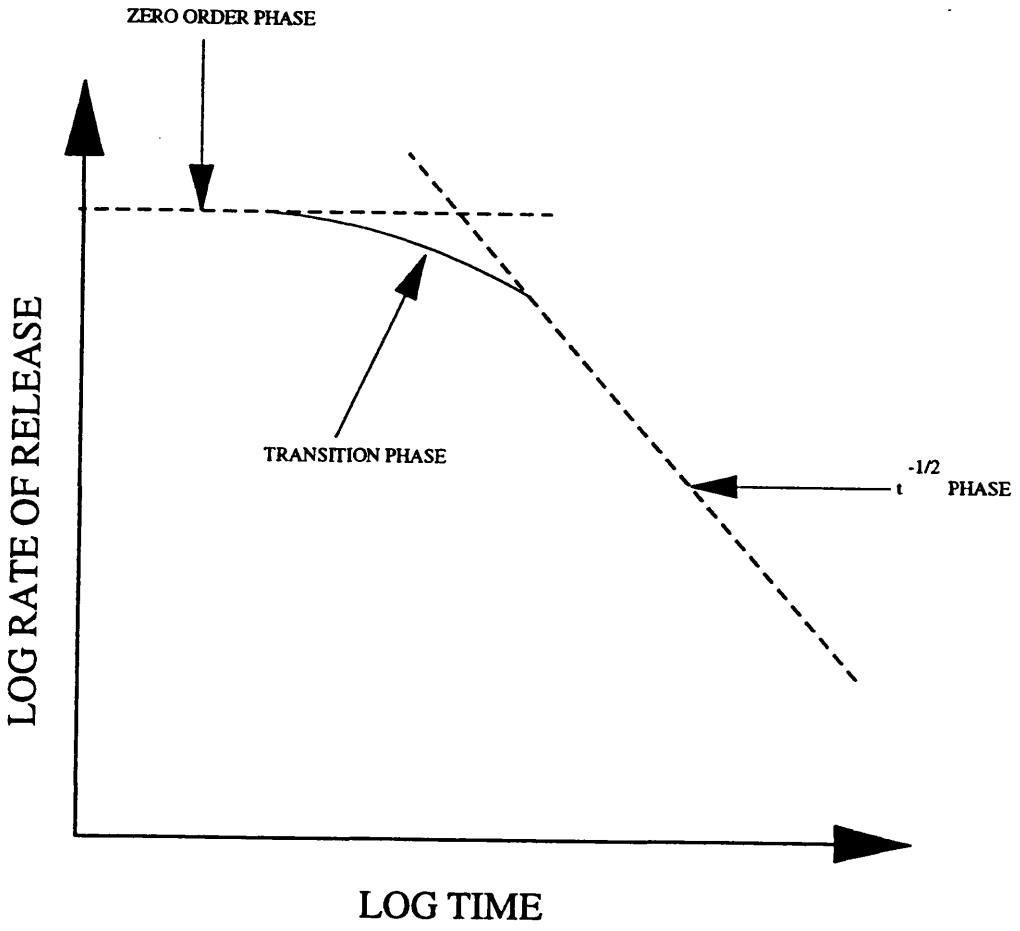

Figure 27 Release rate-time behaviour for a typical matrix with diffusion layer (after ROSEMAN AND YALKOWSKY (1976))

Figure 28 examines whether this model describes the release of oxamniquine from Eudragit films. Since no significant constant release phase is apparent, it can be concluded that this model is not appropriate.

It is possible that the oxaminiquine release may be described by a first order model similar to that used by SCIARRA AND GIDWANI (1970, 1972). Figures 29 and 30 show the fraction of oxamniquine retained in the film (log scale) plotted against time. A biphasic relationship is apparent for each of the polymer compositions tested. The points where the change in rate of release occurs are summarised in Table 20.

FIG 28: THE EFFECT OF POLYMER RATIO ON THE RELEASE OF OXAMNIQUINE FROM FREE FILMS: GRAPH OF LOG RATE OF FRACTIONAL RELEASE AGAINST LOG TIME

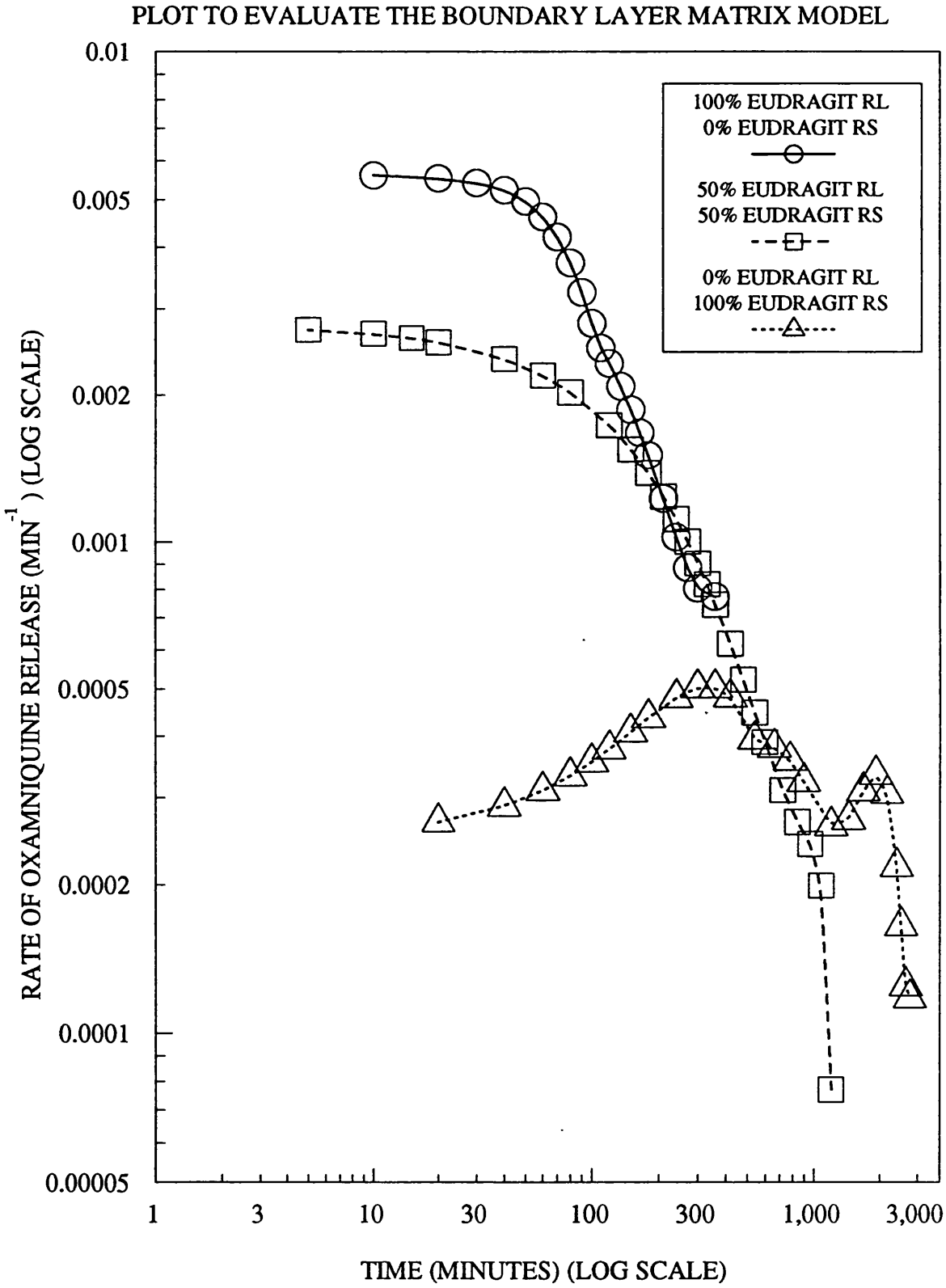

FILMS CONTAINED 10% GLYCERYL TRIACETATE AND
5% OXAMNIQUINE RELATIVE TO TOTAL POLYMER WEIGHT.

FIG 29: THE EFFECT OF POLYMER RATIO ON THE RELEASE OF OXAMNIQUINE FROM FREE FILMS: GRAPH OF LOG FRACTION REMAINING IN FILM AGAINST TIME

I. FILMS CONTAINING EUDRAGIT RL

PLOT TO TEST THE VALIDITY OF THE DISSOLUTION CONTROLLED MODEL.

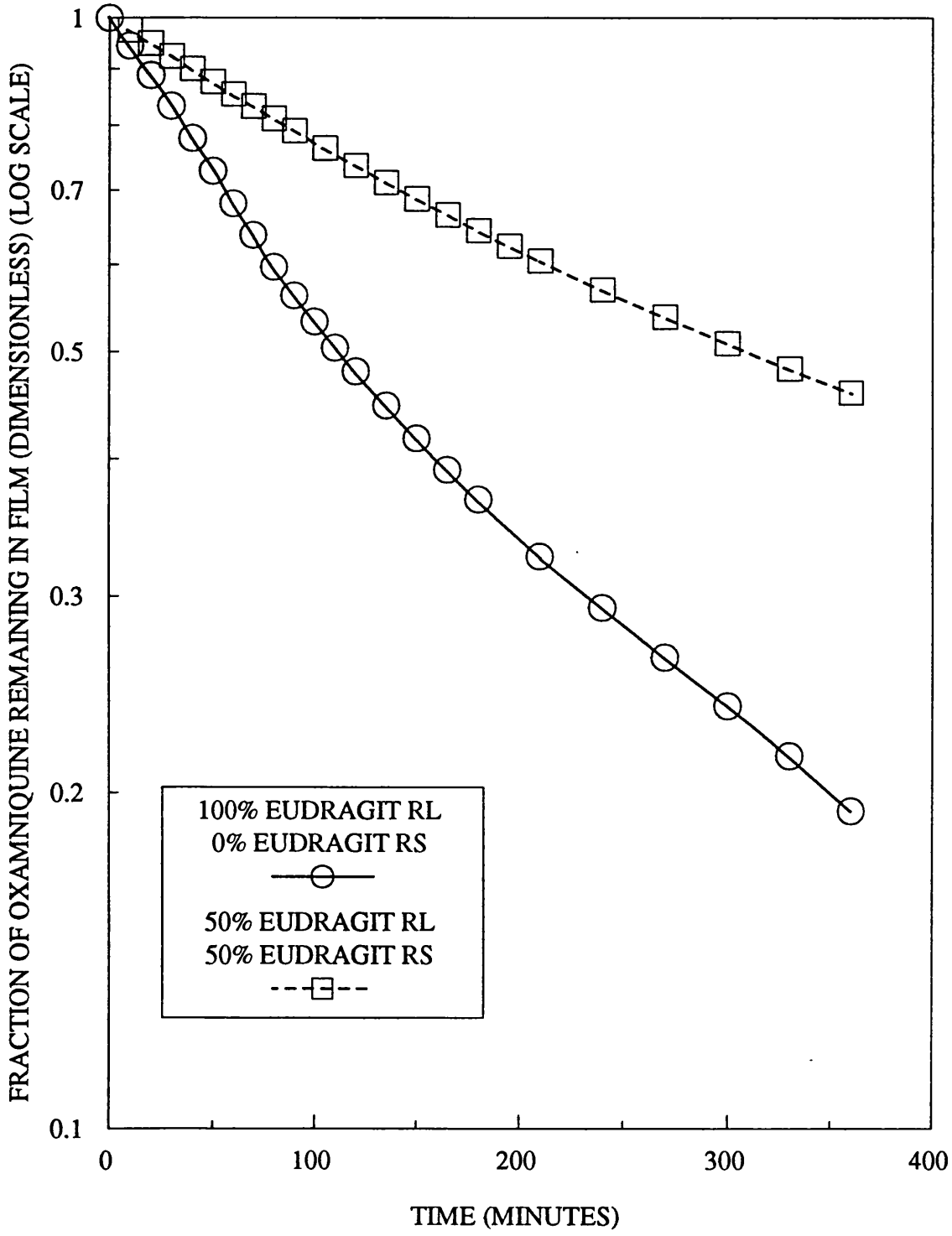

FILMS CONTAINED 10% GLYCERYL TRIACETATE AND 5% OXAMNIQUINE RELATIVE TO TOTAL POLYMER WEIGHT.

FIG 30: THE EFFECT OF POLYMER RATIO ON THE RELEASE OF OXAMNIQUINE FROM FREE FILMS: GRAPH OF LOG FRACTION REMAINING IN FILM AGAINST TIME

II. EUDRAGIT RS FILMS

PLOT TO TEST THE VALIDITY OF THE DISSOLUTION CONTROLLED MODEL.

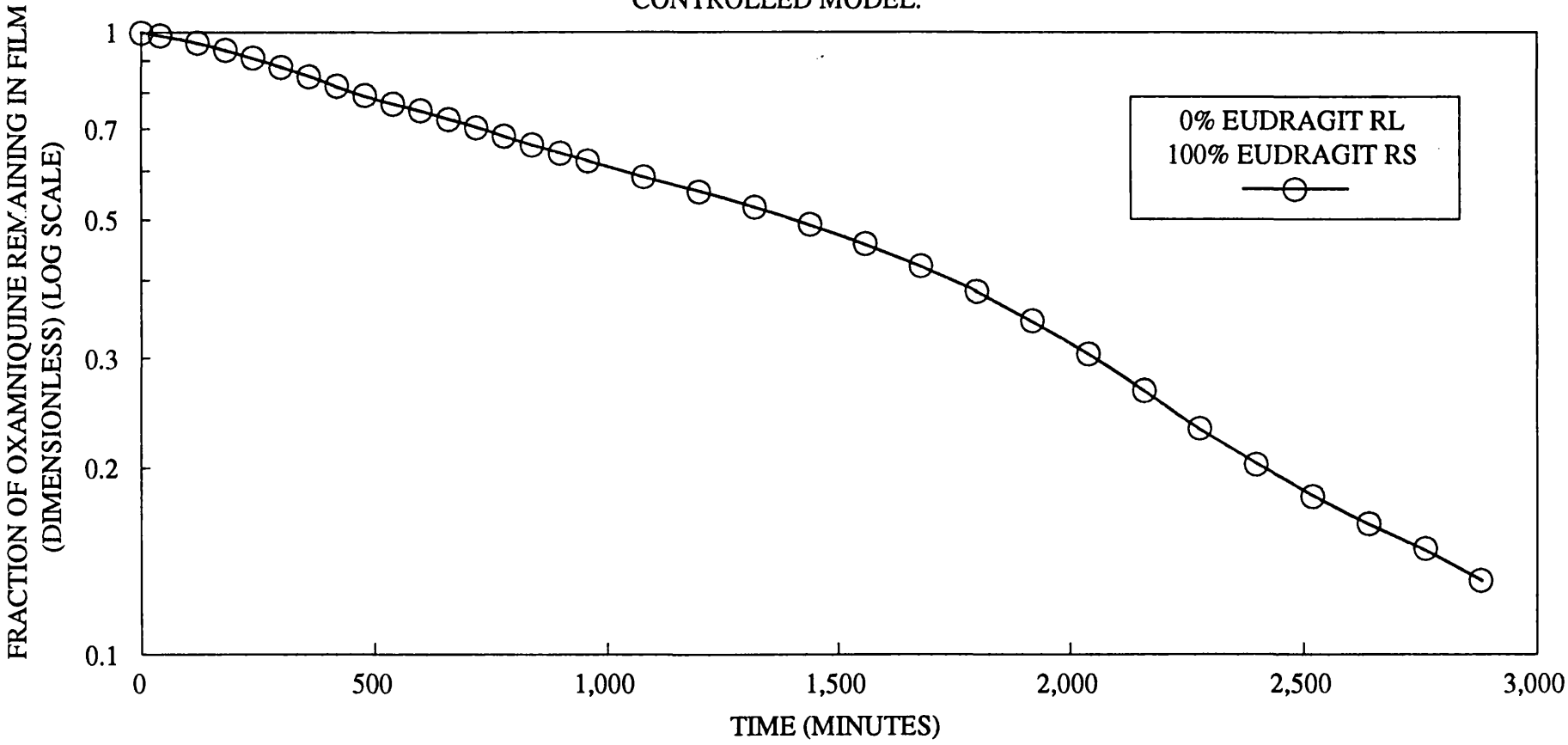

FILMS CONTAINED 10% GLYCERYL TRIACETATE AND
5% OXAMNIQUINE RELATIVE TO TOTAL POLYMER WEIGHT.

TABLE 20 **RATE CHANGE POINTS FOR LOG (FRACTION RETAINED) AGAINST TIME GRAPH FOR FIRST ORDER RELEASE MADE FOR OXAMNIQUINE RELEASE FROM POLYMER FILMS**

Ratio of Eudragit RL to Eudragit RS	Fraction of Oxamniquine Remaining in Film	Time Elapsed
	At Rate Change Point	
1:0	0.463	120 mins
1:1	0.660	166 mins
0:1	0.435	1675 mins

The increased rate of release of oxamniquine from films containing increased proportions of Eudragit RL may be due to the higher proportion of cationic groups which makes the film more hydrophillic and encourages oxamniquine release. Figure 31 shows the release rate of oxamniquine from Eudragit RS films as a function of time over an extended time scale. The release rate appears to vary as a polynomial. This may be due to the hydrophobicity of the polymer resulting from low degree of cationic substitution. The maxima and minima represent relatively small changes in the release rate occurring with time.

The apparent biphasic release of oxamniquine from these films is an unexpected effect. A possible explanation may be given in terms of relative affinities between oxamniquine, glyceryl triacetate and Eudragit.

External plasticisers included in polymer films should ideally be permanently retained in the film (BANKER 1966).

Glyceryl triacetate is miscible with water and will therefore be extracted with oxamniquine from the exposed surface of film. It was not possible in these experiments to measure the release of glyceryl triacetate from the films simultaneously with oxamniquine. Glyceryl triacetate may have different affinities for Eudragit RL compared with Eudragit RS which would affect its release from composite films. The solubility of oxamniquine in glyceryl triacetate has been measured as 1.5mg cm^{-3}. Therefore oxamniquine will be partially dissolved in the plasticiser within the film structure and will be released along with the glyceryl triacetate. It is possible that the release of oxamniquine can be considered in two phases

(i) Release along with glyceryl triacetate from the plasticised film

(ii) Release from the hydrated, porous, unplasticised matrix after the platiciser has been removed.

It is probable that the transition between these phases would occur at different times depending on the composition of the film.

The release of plasticisers from the films will be discussed further in this Chapter.

FIG 31: THE EFFECT OF POLYMER RATIO ON THE RELEASE OF OXAMNIQUINE FROM FREE FILMS: GRAPH OF RATE OF FRACTIONAL RELEASE AGAINST TIME FOR EUDRAGIT RS FILMS

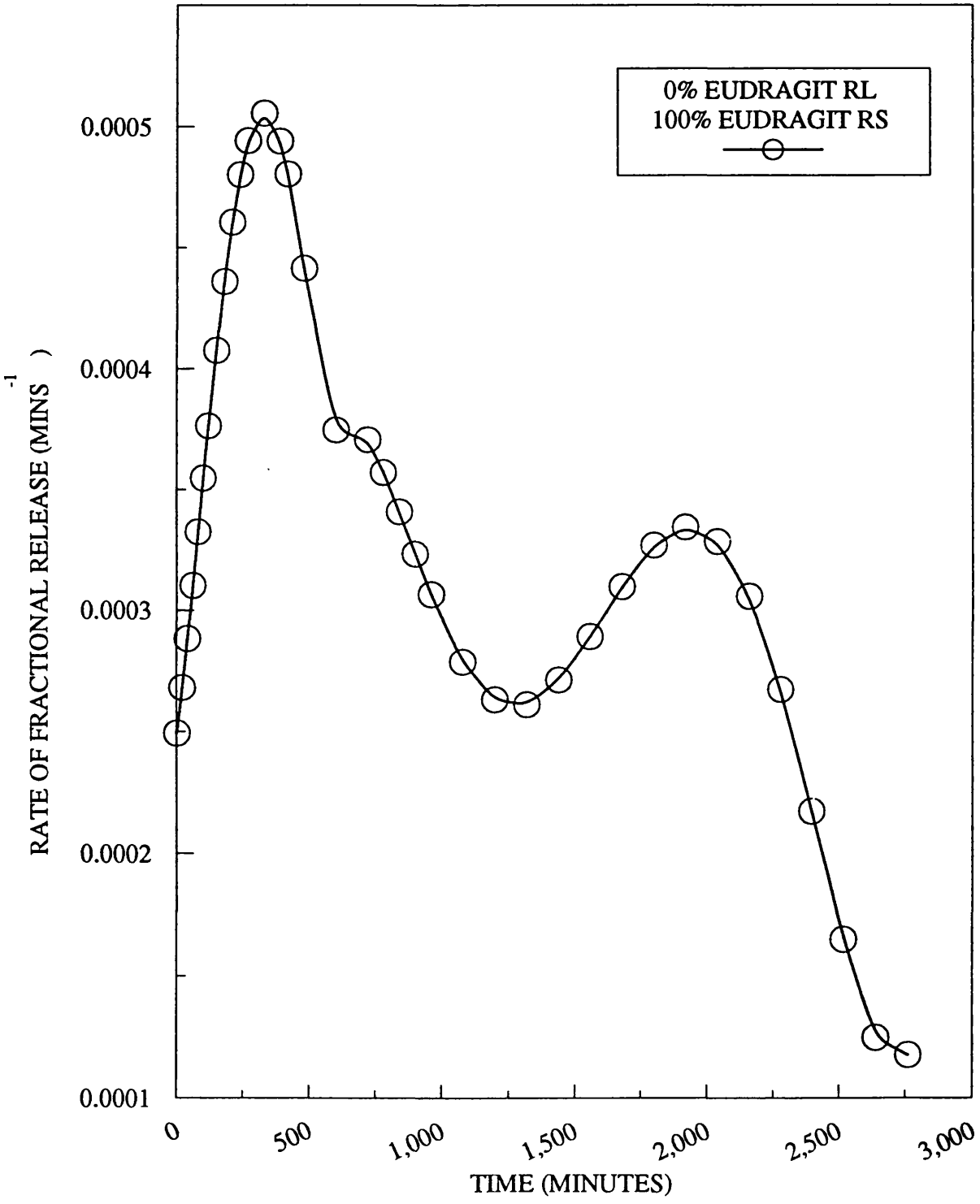

FILMS CONTAINED 10% GLYCERYL TRIACETATE AND
5% OXAMNIQUINE RELATIVE TO TOTAL POLYMER WEIGHT.

It is interesting to examine the data more closely using the method suggested by DONBROW AND FRIEDMAN (1975a). Figure 32 shows the rate of release of oxamniquine plotted as function of the reciprocal fraction released from the film for each of the polymer compositions to test the applicability of the matrix controlled model. Since these graphs are not linear the matrix controlled model is not applicable. Figure 33 shows the rate of release plotted as a function of the fraction released. This should be linear if the mechanism of release is described by the first order (dissolution control) model.

For each of the formulations, the first order test plots show an apparent biphasic pattern. It is likely that the experimental system does not comply with the assumptions which this model makes, and that the apparent first order release pattern is not a simple Noyes-Whitney dissolution effect. The defect must be in the assumption of the constant K in equation 25. K must incorporate the diffusion coefficient of the drug in the polymer. Although assumed to be constant in many models, it is likely that the diffusion coefficient is time dependent and affected by interactions between polymers, plasticisers and drug. It is also known that Eudragit RL and Eudragit RS undergo a limited amount of swelling when hydrated (GURNY et al, 1976). Although the extent of swelling is considerably less than methacrylate hydrogels, it does represent another time dependent process which complicates the model.

FIG 32: THE EFFECT OF POLYMER RATIO ON THE RELEASE OF OXAMNIQUINE FROM FREE FILMS: GRAPH OF RATE OF FRACTIONAL RELEASE AGAINST RECIPROCAL FRACTION RELEASED

DIFFERENTIAL RATE PLOT TO TEST THE VALIDITY OF THE MATRIX CONTROLLED MODEL

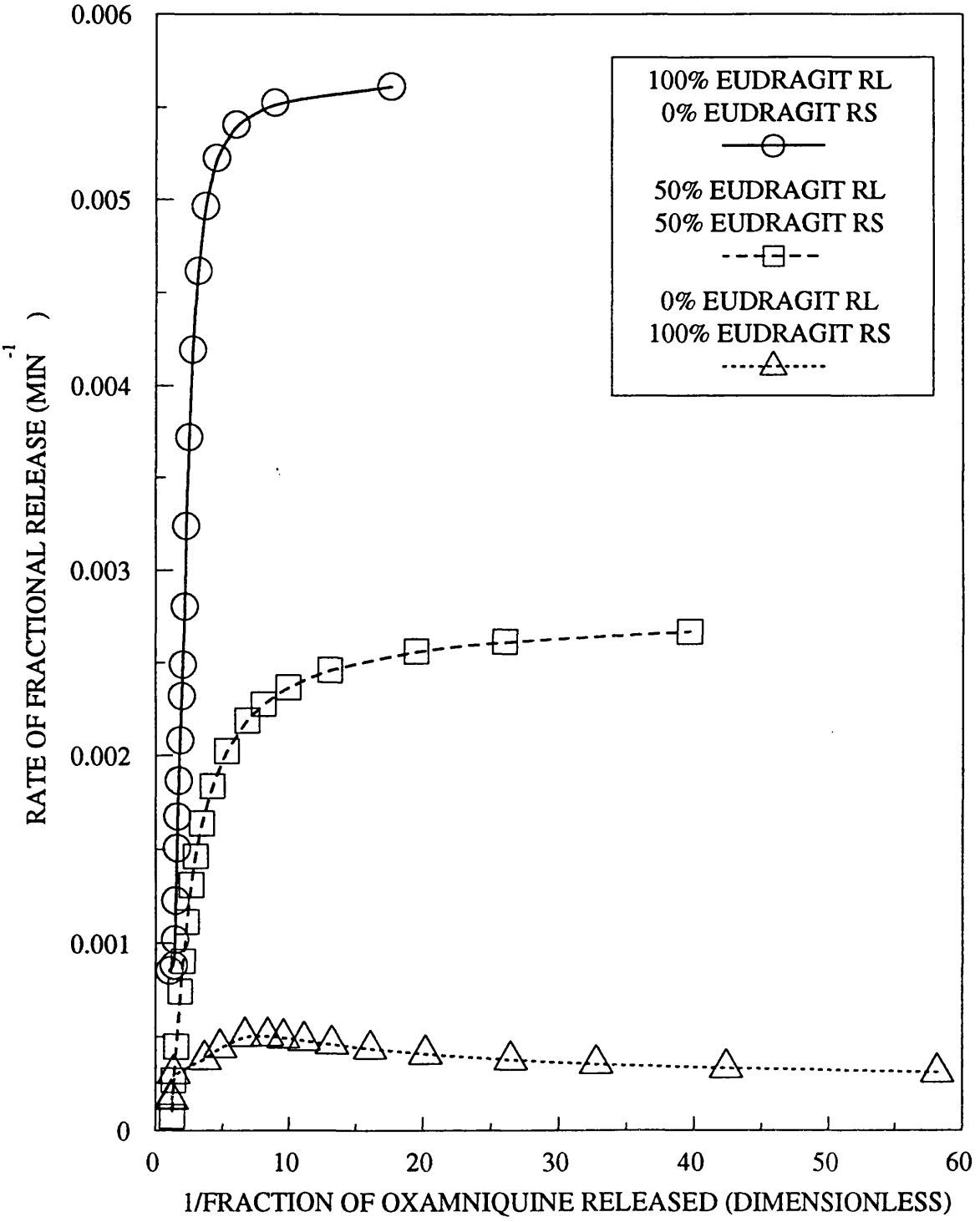

FILMS CONTAINED 10% GLYCERYL TRIACETATE AND 5% OXAMNIQUINE RELATIVE TO TOTAL POLYMER WEIGHT.

FIG 33: THE EFFECT OF POLYMER RATIO ON THE RELEASE OF OXAMNIQUINE FROM FREE FILMS: GRAPH OF RATE OF FRACTIONAL RELEASE AGAINST RECIPROCAL FRACTION RELEASED

DIFFERENTIAL RATE PLOT TO TEST THE VALIDITY OF THE MATRIX CONTROLLED MODEL

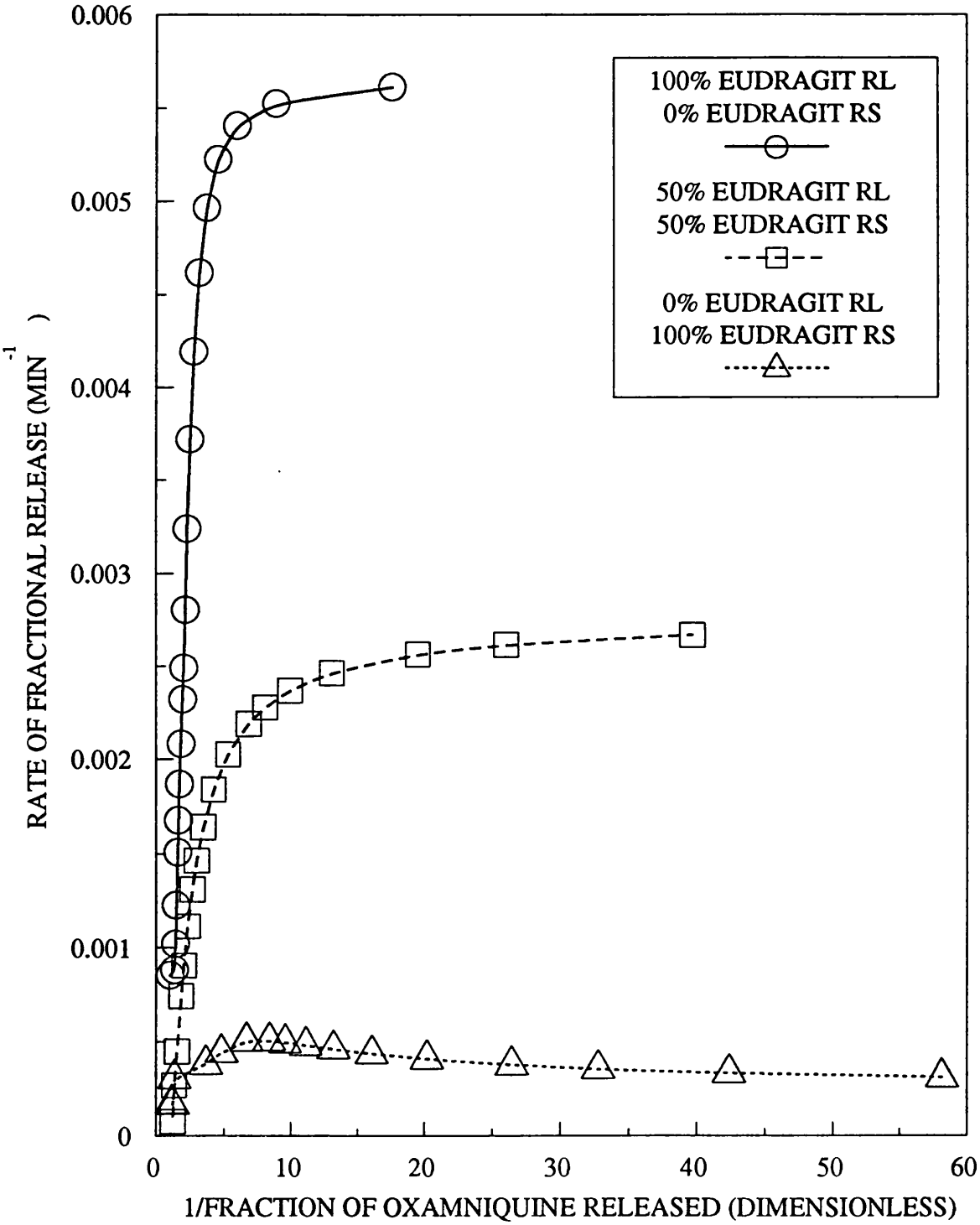

FILMS CONTAINED 10% GLYCERYL TRIACETATE AND
5% OXAMNIQUINE RELATIVE TO TOTAL POLYMER WEIGHT.

5.5.2 The Effect of Desorption Surface

Previous workers have reported surface asymmetry in studies on permeation of drugs through Eudragit films (ABDEL-AZIZ et al, 1975; ANDERSON et al, 1973: OKOR AND ANDERSON, 1978 a, b). Films reported in the literature were produced on a solid mould surface such as Teflon or Polythene. It is possible that contact between the polymer and mould surface may leave impressions on the film, which would cause variations in surface structure and differences in the permeability of different surfaces of the film.

In these studies, the drug substance is contained within the film structure, which has been prepared from a solution. Mercury was used as a casting substrate. The mercury was cleaned before films were cast, to eliminate any surface imperfections caused by dust or other contaminants. Films were cast in a closed, controlled humidity environment arranged to eliminate vibrational disturbances during film formation. It was considered that this was the best method for preparing uniform films. Any evidence of surface differences was therefore of interest in these studies.

To examine the effect of surface differences oxamniquine release was measured from the air exposed and mercury contact surfaces of films prepared from equal proportions of Eudragit RL and RS with 10% w/w glyceryl triacetate and 5% w/w oxamniquine. Figure 34 shows that oxamniquine is

released more quickly from the mercury contact surface. This is illustrated further in Figure 35 which shows the rate of release of oxamniquine plotted against time. The initial release rate from the mercury contact surface is higher than from the air exposed surface. The release rates are equal after approximately 120 minutes, corresponding to 26% and 39% of the oxamniquine released from the air exposed and mercury contact surfaces respectively. This finding is in broad agreement with the literature cited where it is claimed the lower surface of Eudragit films was more permeable to drugs.

The probable reason for the permeability asymmetry is the casting process itself. Typically, the polymer solution is cast onto the substrate and the solvent is removed uniaxially. This uniaxial removal of mass (and possibly heat) from the film gives rises to a degree of permeability asymmetry (HOPFENBERG 1978). The higher permeability of the mercury surface suggests that the microstructure of the film is apparently less dense in this region. This could be a function of the supermolecular lamination which occurs as the solvent is removed from the polymer during film formation.

It is interesting to examine whether the permeability asymmetry is associated with differences in the mechanism of drug release from the film surface. Figure 36 shows the fraction of oxamniquine released from the film as a function of $\sqrt{t}$ time to test the validity of the matrix

controlled model. The curvature of this graph suggests that this model is not applicable. Plotting the log fraction of oxamniquine remaining against time (Figure 37) produces a similar biphasic pattern to the air surface which suggests a similar first order type model. In contrast,however, the graph of rate of release against fraction released (Figure 38) is sigmoidal. The implicit assumptions in differential rate plot model are apparently not valid under these conditions. This surprising observation may be another consequence of the surface differences phenomenon as well as an effect of more rapid release from the mercury contact surface.

It is considered that release from the air exposed surface is more relevant to release from coatings applied to the surface of inert pellets. Therefore subsequent release studies were performed using the air exposed surface only.

FIG 34: THE EFFECT OF FILM SURFACE ON THE RELEASE OF OXAMNIQUINE FROM FREE FILMS: GRAPH OF FRACTION RELEASED AGAINST TIME

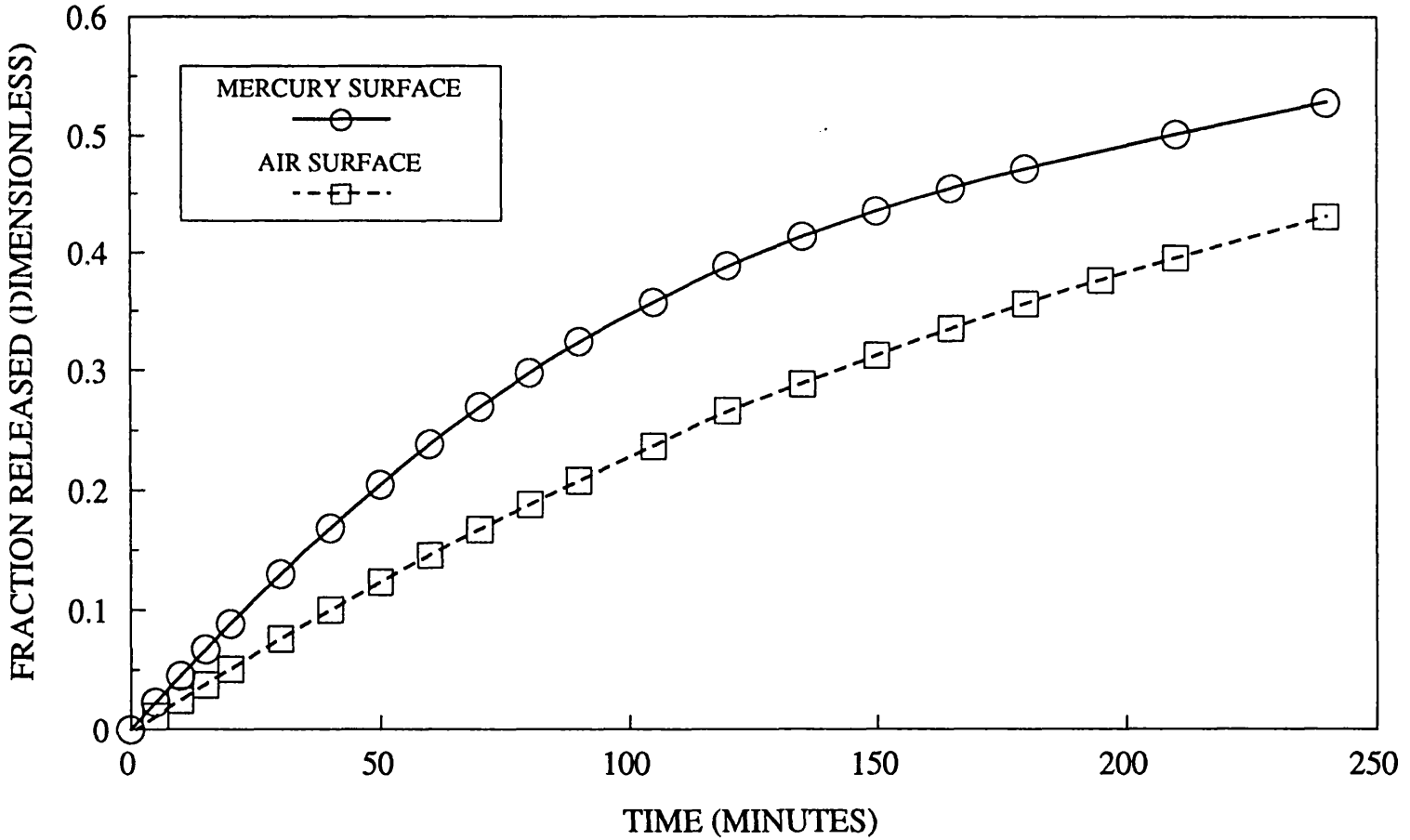

FILMS CONTAINED EQUAL PROPORTIONS OF
EUDRAGIT RL AND RS WITH 10% GLYCERYL TRIACETATE
AND 5% OXAMNIQUINE RELATIVE TO POLYMER WEIGHT

FIG 35: THE EFFECT OF FILM SURFACE ON THE RELEASE OF OXAMNIQUINE FROM FREE FILMS: GRAPH OF RATE OF FRACTIONAL RELEASE AGAINST TIME

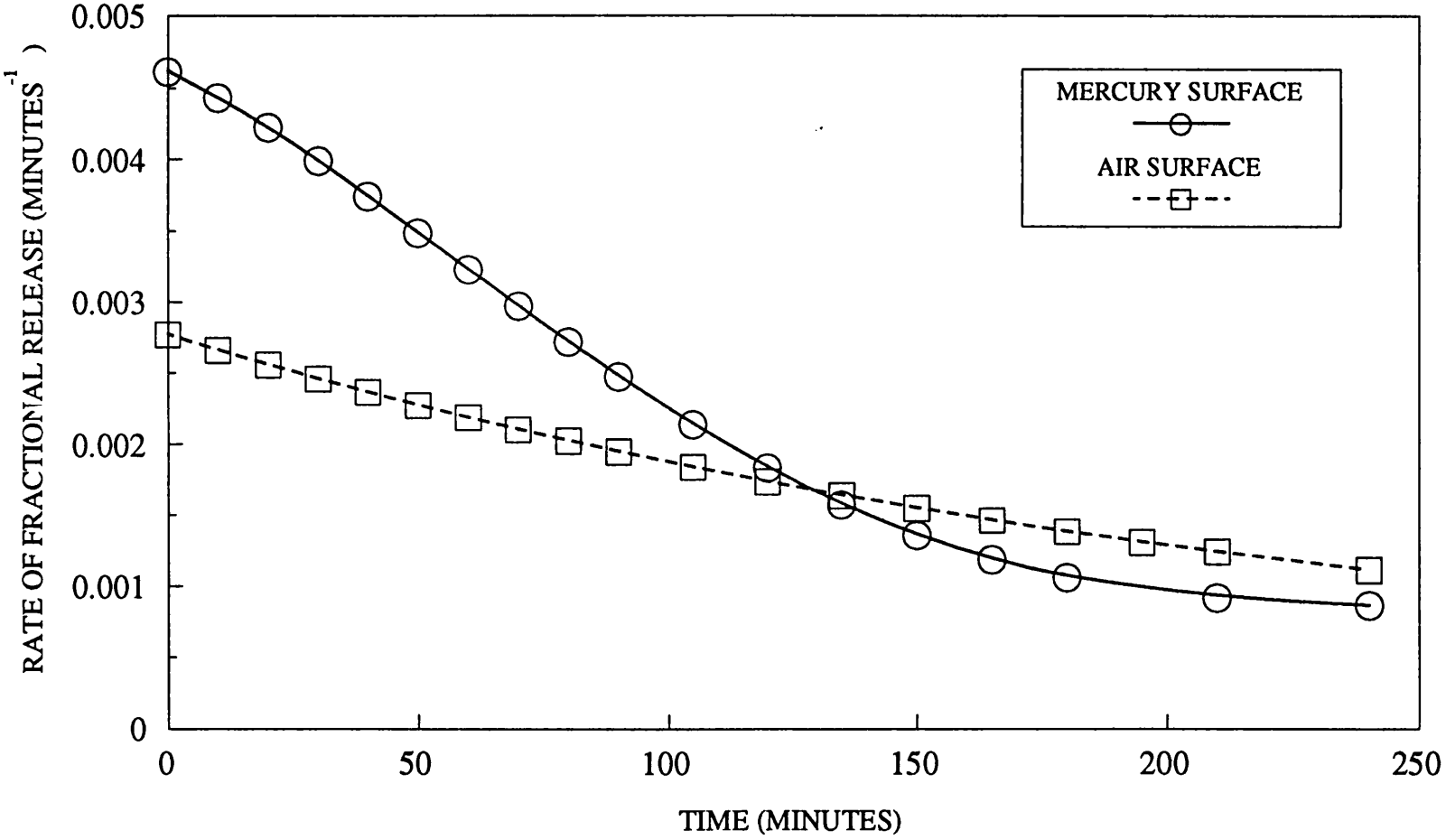

FILMS CONTAINED EQUAL PROPORTIONS OF EUDRAGIT RL AND RS WITH 10% GLYCERYL TRIACETATE AND 5% OXAMNIQUINE RELATIVE TO POLYMER WEIGHT

FIG 36: THE EFFECT OF FILM SURFACE ON THE RELEASE OF OXAMNIQUINE FROM FREE FILMS: GRAPH OF FRACTION RELEASED AGAINST SQUARE ROOT OF TIME

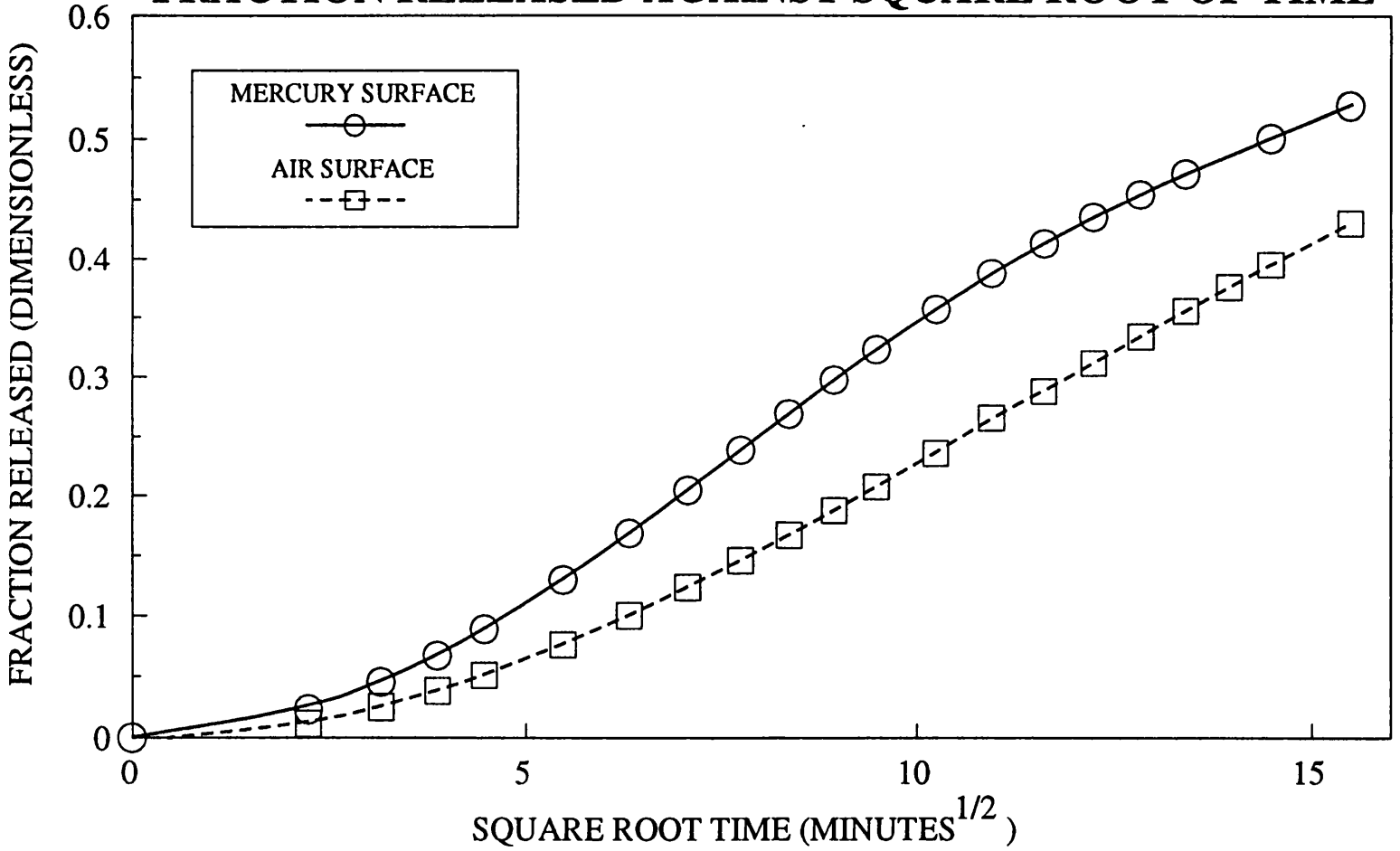

FILMS CONTAINED EQUAL PROPORTIONS OF EUDRAGIT RL AND RS WITH 10% GLYCERYL TRIACETATE AND 5% OXAMNIQUINE RELATIVE TO POLYMER WEIGHT

TO TEST THE VALIDITY OF THE MATRIX CONTROLLED MODEL

FIG 37: THE EFFECT OF FILM SURFACE ON THE RELEASE OF OXAMNIQUINE FROM FREE FILMS. GRAPH OF LOG FRACTION REMAINING AGAINST TIME

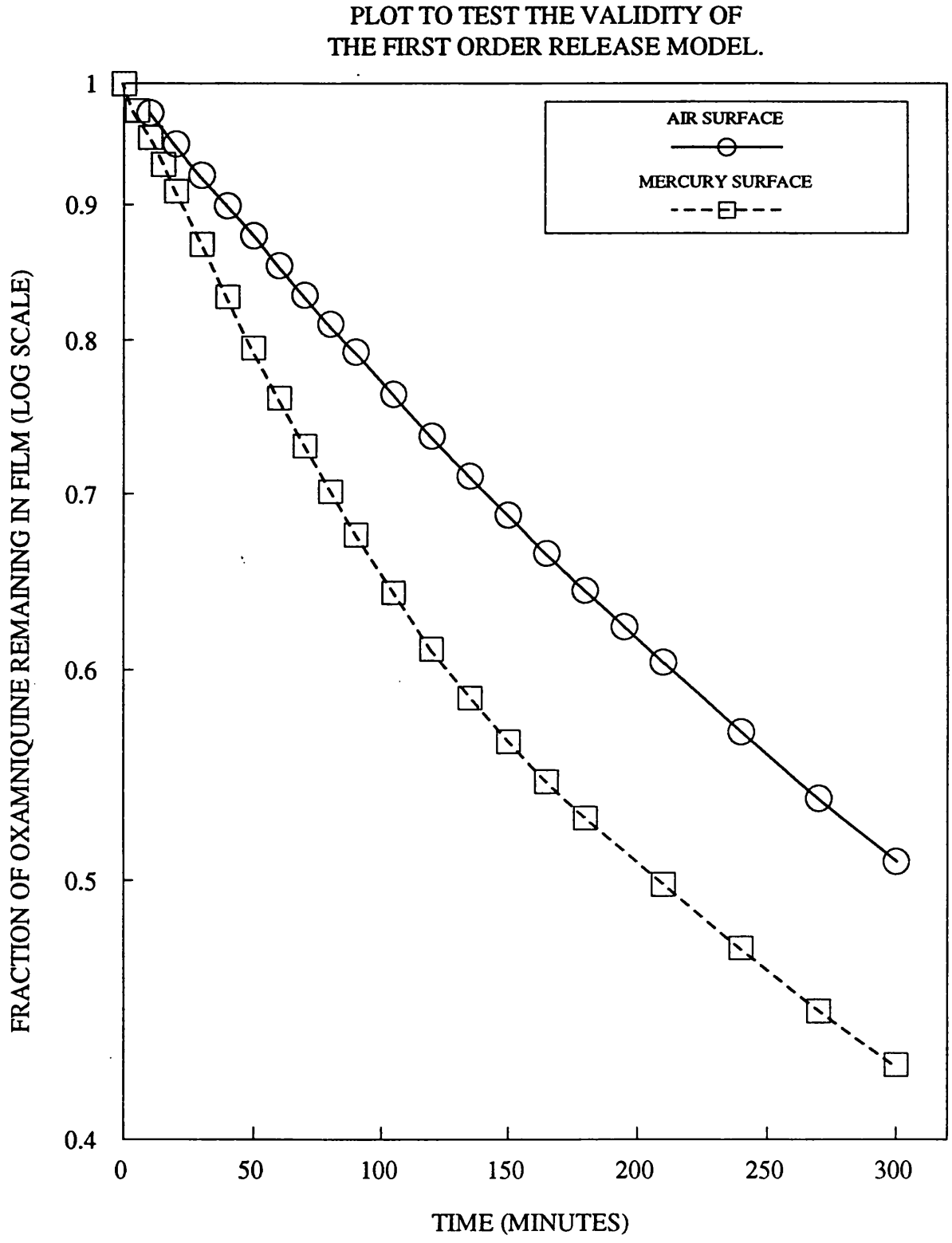

FILMS CONTAINED EQUAL PROPORTIONS OF EUDRAGIT RL AND RS WITH 10% GLYCERYL TRIACETATE AND 5% OXAMNIQUINE RELATIVE TO POLYMER WEIGHT

FIG 38: THE EFFECT OF FILM SURFACE ON THE RELEASE OF OXAMNIQUINE FROM FREE FILMS: GRAPH OF RATE OF FRACTIONAL RELEASE AGAINST FRACTION RELEASED

DIFFERENTIAL RATE PLOT TO TEST THE VALIDITY
OF THE FIRST ORDER RELEASE MODEL

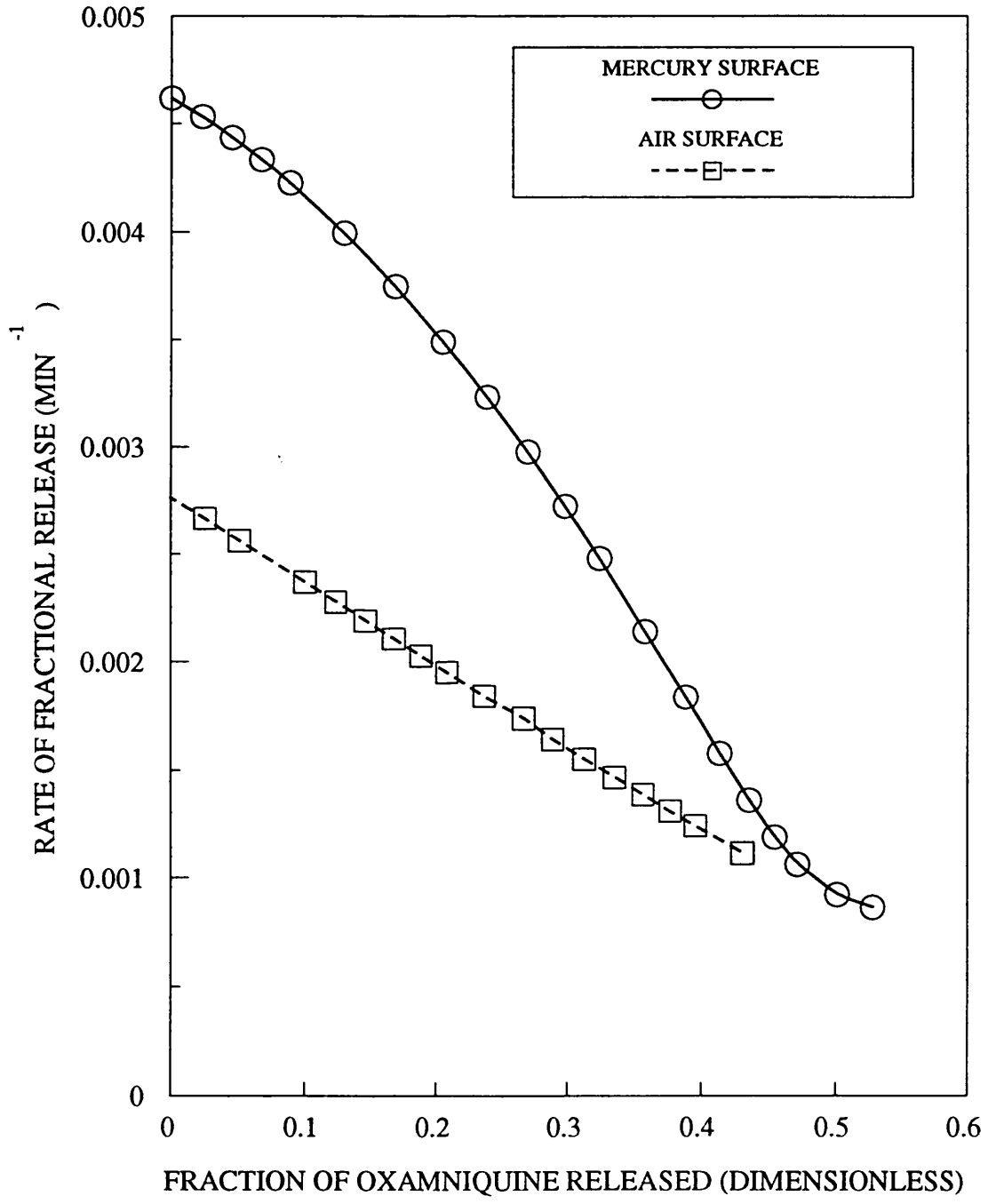

FILMS CONTAINED EQUAL PROPORTIONS OF
EUDRAGIT RL AND RS WITH 10% GLYCERYL TRIACETATE
AND 5% OXAMNIQUINE RELATIVE TO POLYMER WEIGHT

5.5.3 The Effect of Plasticisers

An essential part of these studies was the use and choice of plasticisers in the film. On formation of the polymeric film, the plasticiser is dispersed throughout the film and may be physico-chemically associated with the polymer. Plasticisers may not be dispersed homogeneously throughout the film, since more polar plasticisers will interact preferentially with polar regions of the polymer (LAGUNA et al, 1975). The effect of this in Eudragit polymers is that more polar plasticisers would be preferentially attracted to the areas of charge associated with the quarternary ammonium groups in the polymer. The supermolecular structure of the polymer film will be influenced by the presence of plasticiser.

The basic requirements of any plasticiser in a polymer film are compatibility and permanence. The plasticiser must be miscible with the polymer, which suggests similar intermolecular forces must exist in the two components. The most effective plasticisers will therefore resemble most closely in structure the polymers that they plasticise. Evidence of plasticiser incompatibility may be a bloom on the film surface, or areas of non-uniformity within the film structure where pockets of plasticiser have aggregated or separated from the film. None of the film formulations prepared in these studies showed evidence of such physical incompatibility.

The plasticisers selected for these studies can be broadly classified as either water miscible or water immiscible. Since plasticisers are intended to be 'permanent' within the film structure the water solubility of the plasticiser will determine the fate of the plasticiser when the film is in contact with aqueous solutions.

To make a valid study the effect of plasticisers, it was necessary to prepare unplasticised films of similar composition as a reference. In the literature it is claimed that it was not possible to produce unplasticised Eudragit films (ABDEL-AZIZ 1976). However, in their work films were prepared by casting onto a machined PTFE surface. Considerable effort to reproduce the method of preparation described by Abdel-Aziz and co-workers failed to produce suitable films which could be used in these studies. Static attraction between films and the PTFE surface made it very difficult to isolate formed films without damaging them. In particular unplasticised films were very glassy and easily broken on removal from the moulds. It was considered impossible to produce unplasticised films by this method. LIPPOLD et al (1980) reported the production of unplasticised films by casting onto mercury using similar methods to those described in this thesis. However, in these studies, EUDRAGIT RS/PM was used as the starting material. Eudragit RS/PM is finely powdered polymer blended with 2% w/w of talc as a glidant. It is not possible to predict the effect of talc on film

formation and its subsequent properties.

For these studies, glyceryl triacetate and PEG 400 were selected as examples of water miscible plasticisers. The homologous series of alkyl phthalate esters, dimethyl, diethyl and dibutyl phthalate were selected as examples of water immiscible plasticisers.

Figures 39 and 40 show the effect of plasticisers on the release of oxamniquine from films containing equal proportions of Eudragit RL and Eudragit RS and 10% w/w of plasticiser with respect to the total polymer content. The results shown are the mean of at least three films. Inclusion of plasticisers accelerates the release of oxamniquine from the films. However, the extent to which each of the plasticisers increases the rate of release of oxamniquine from the films is not obviously predictable. Figures 41 and 42 show the rate of oxamniquine release from different plasticised films plotted against time.

Examining Figures 39 to 42 allows the plasticisers to be grouped in a rank order based on rate of release of oxamniquine from the films. This is summarised in Table 21.

Unplasticised films released oxamniquine more slowly than any of the plasticised films. This effect is not unexpected since plasticisers are effective in reducing interactions between polymer chains and increasing the

TABLE 21 **PLASTICISERS TESTED WITH EUDRAGIT FILMS CONTAINING OXAMNIQUINE ARRANGED IN INCREASING ORDER OF OXAMNIQUINE RELEASE**

GLYCERYL TRIACETATE
DIETHYL PHTHALATE
DIMETHYL PHTHALATE
DIBUTYL PHTHALATE
POLYETHYLENE GLYCOL 400

possibility of interchain slippage. More flexible movement between the polymer chains permits the removal of oxamniquine by diffusion.

Two factors will, in particular, influence the relative effects that the different plasticisers have on the release of oxamniquine from Eudragit films. These factors are the solubility of oxamniquine in the plasticiser and the aqueous solubility of the plasticiser itself.

5.5.3.1 Solubility of the Plasticiser in Water

The aqueous solubility of the plasticiser will affect the rate at which it is removed from the film during the release experiments. Clearly the more soluble the plasticiser the more rapidly it will be removed from the film.

FIG 39: THE EFFECT OF PLASTICISERS ON THE RELEASE OF OXAMNIQUINE FROM FREE FILMS: GRAPH OF FRACTION RELEASED AGAINST TIME I

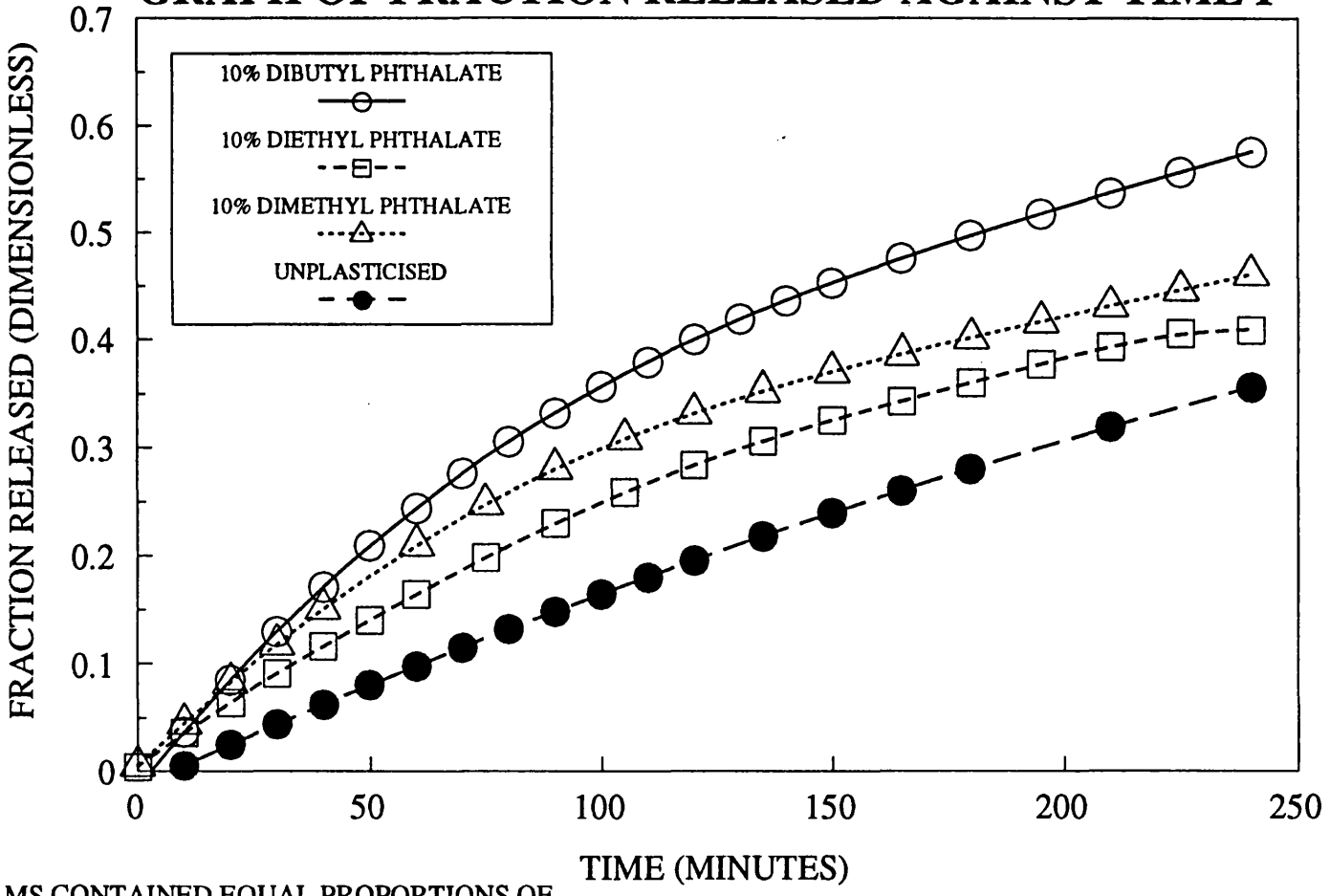

FILMS CONTAINED EQUAL PROPORTIONS OF EUDRAGIT RL AND RS WITH 5% OXAMNIQUINE RELATIVE TO POLYMER WEIGHT

FIG 40: THE EFFECT OF PLASTICISERS ON THE RELEASE OF OXAMNIQUINE FROM FREE FILMS: GRAPH OF FRACTION RELEASED AGAINST TIME II

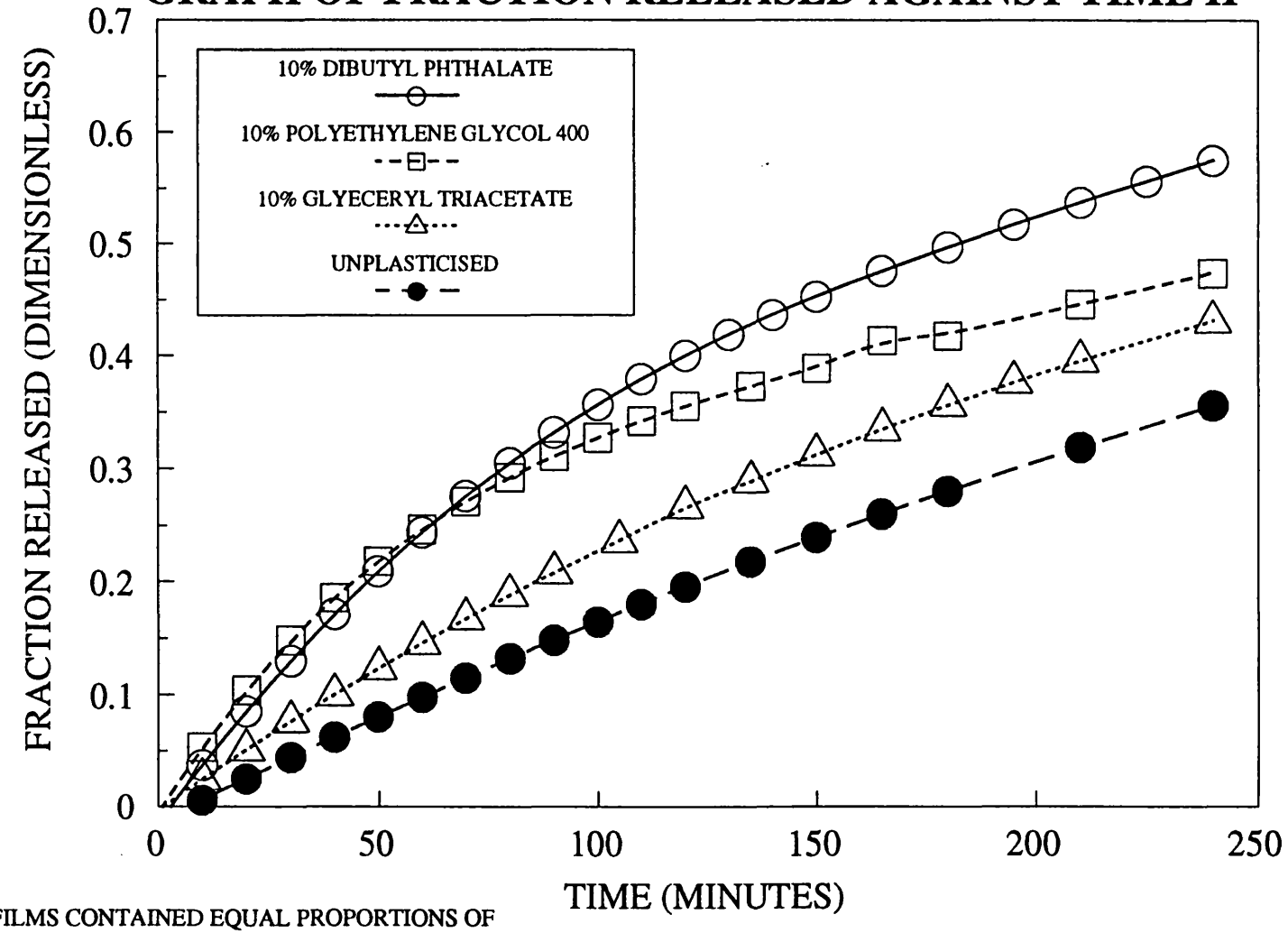

FILMS CONTAINED EQUAL PROPORTIONS OF EUDRAGIT RL AND RS WITH 5% OXAMNIQUINE RELATIVE TO POLYMER WEIGHT

FIG 41: THE EFFECT OF PLASTICISERS ON THE RELEASE OF OXAMNIQUINE FROM FREE FILMS: GRAPH OF RATE OF FRACTIONAL RELEASE AGAINST TIME I

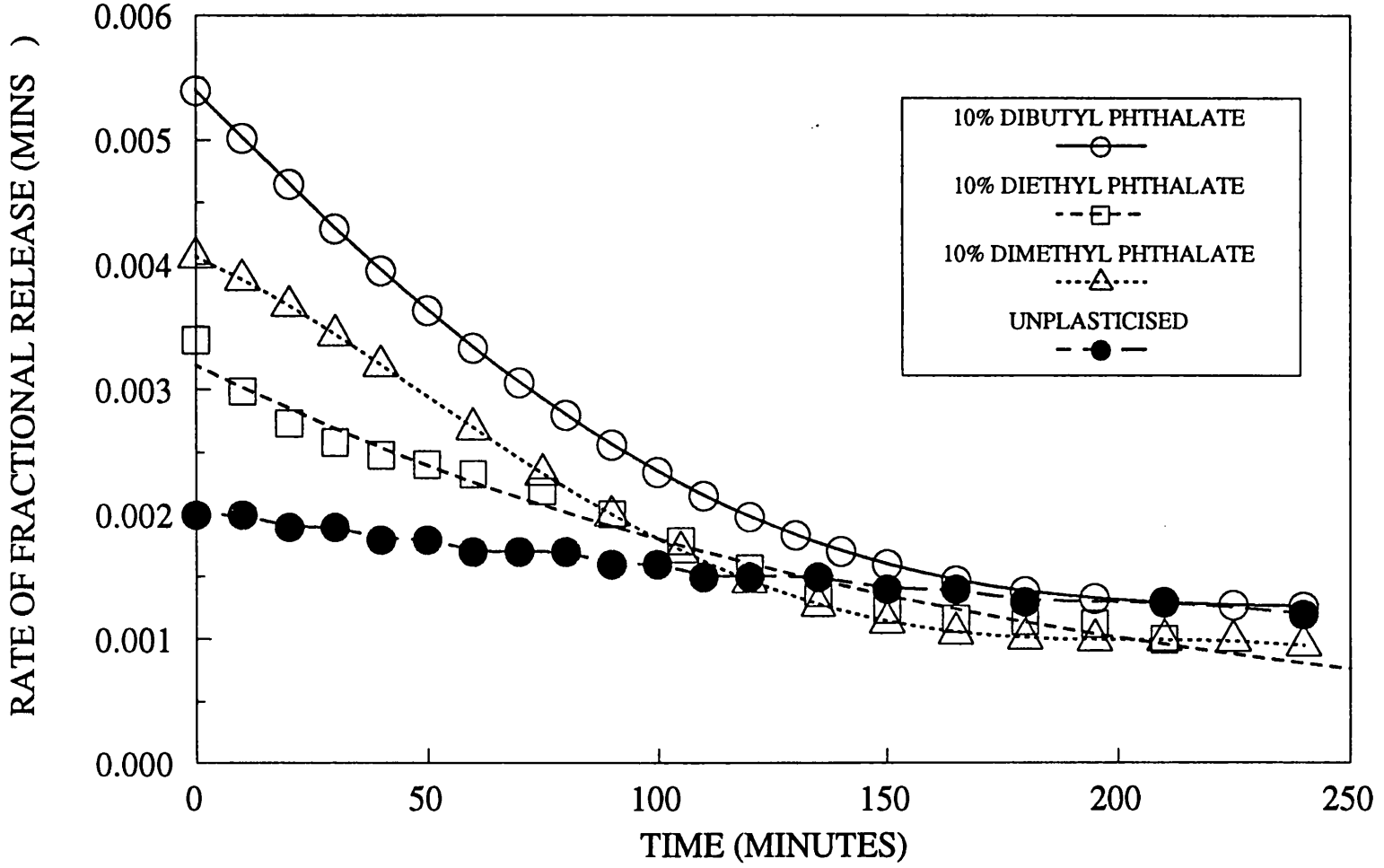

FILMS CONTAINED EQUAL PROPORTIONS OF EUDRAGIT RL AND RS WITH 5% OXAMNIQUINE RELATIVE TO POLYMER WEIGHT

FIG 42: THE EFFECT OF PLASTICISERS ON THE RELEASE OF OXAMNIQUINE FROM FREE FILMS: GRAPH OF RATE OF FRACTIONAL RELEASE AGAINST TIME II

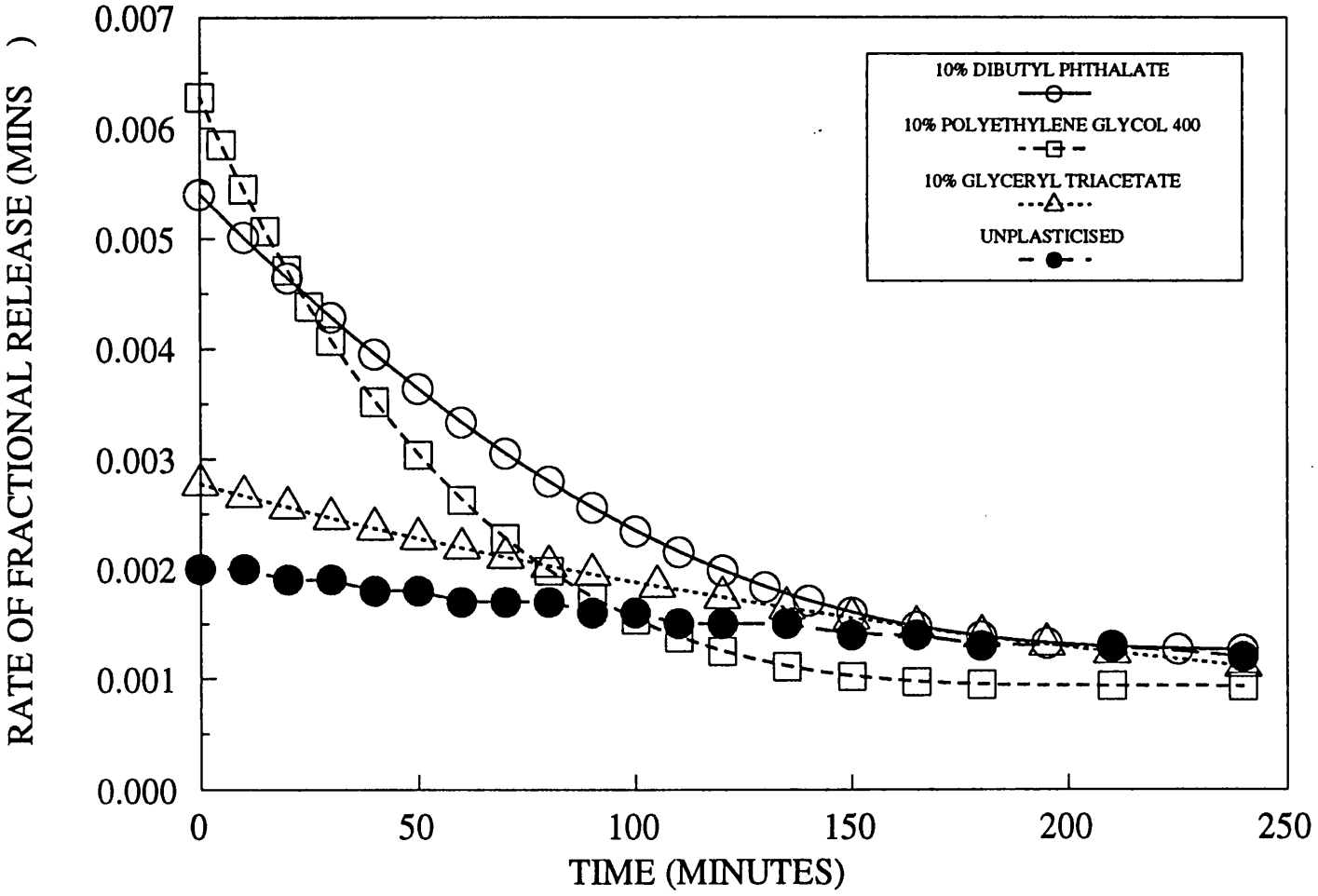

FILMS CONTAINED EQUAL PROPORTIONS OF EUDRAGIT RL AND RS WITH 5% OXAMNIQUINE RELATIVE TO POLYMER WEIGHT

As the plasticiser is removed, it leaves a porous, skeleton structure, filled with the leaching medium. This structure will be associated with a different rate of release of oxamniquine from the film.

The problem becomes more complex with the phthalate plasticisers which are only partially miscible with water. These plasticisers will be removed more slowly from the film than water soluble plasticisers. Additionally, oxamniquine will be partitioned within the membrane between the plasticiser and the aqueous leaching medium. During the time course of the release, increasing amounts of plasticiser will be removed from the films, leaving behind the porous skeleton filled with the aqueous medium, in a similar way to films plasticised with water soluble plasticisers.

Where the plasticiser is substantially immiscible with water, similar effects may occur but the plasticiser will be removed from the film very slowly. This is the case with films plasticised with dibutyl phthalate. Unplasticised films are comparable in that they should not change during the course of an experiment as a result of plasticiser extraction. In Section 5.5.3.2 it is shown that the model for predicting first order behaviour is valid for a substantial proportion of oxamniquine release. It is suggested that although oxamniquine is released from Eudragit films by a first order mechanism, the model derived to distinguish dissolution control from matrix

control kinetics only describes the behaviour of films where the composition does not change substantially as oxamniquine is released.

5.5.3.2 Solubility of Oxamniquine in the Plasticiser

In Chapter 4 results were presented for the solubility of oxamniquine in glyceryl triacetate and PEG 400. Partition coefficients of oxamniquine between dimethyl, diethyl, dibutyl phthalate and pH6.0 citric acid-phosphate buffer were also determined. The solubility of oxamniquine in these plasticisers has a fundamental effect on the release of oxamniquine from plasticised films.

While plasticiser is present within the film, it is capable of acting as carrier for dissolved oxamniquine from the film. The maximum concentration of oxamniquine dissolved in the plasticiser is the saturated solubility of oxamniquine in the plasticiser.

It was also demonstrated that when partitioned between phthalate plasticisers and aqueous buffer oxamniquine exists as dimers in the phthalate rich phase. Release of oxamniquine from plasticised films is therefore a complex, dynamic situation in which oxamniquine is removed dissolved in the plasticiser as through aqueous buffer filled pores which develop in the membrane. Additionally, there may be partitioning of oxamniquine within the membrane. The overall situation is summarised in Figure 43.

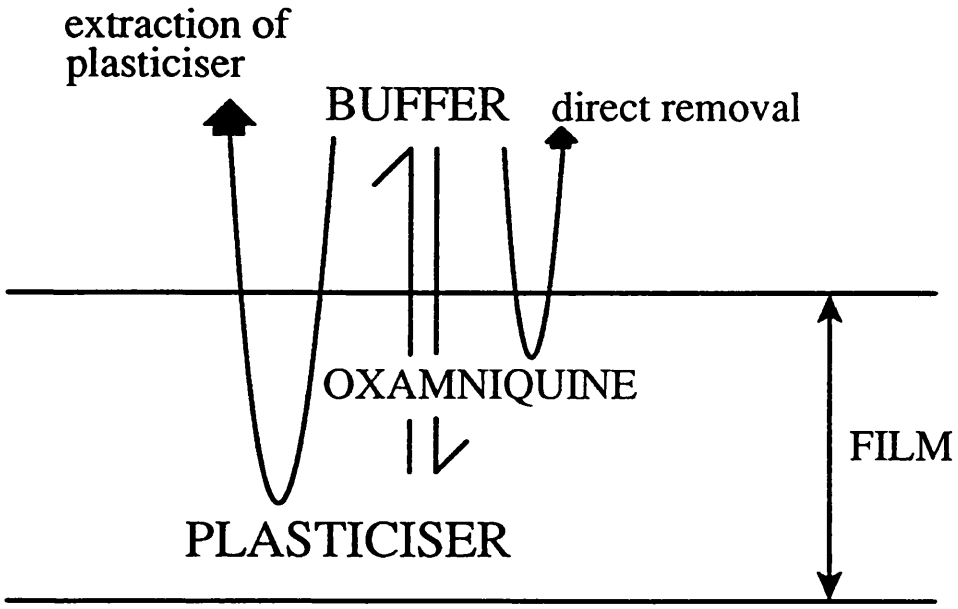

Figure 43 Summary of possible mechanisms of oxamniquine release from plasticised films.

Oxamniquine is approximately eight times more soluble in PEG 400 than in glyceryl triacetate. If release follows the proposed mechanism, and is dependent upon simultaneous loss of plasticiser and drug whilst the plasticiser is present in the film, oxamniquine will be removed more rapidly from the film containing PEG 400. In films plasticised with PEG 400, the rate of release, shown in Figure 42, diminishes rapidly compared with the glyceryl triacetate plasticised films. This would occur if, in addition, PEG 400 itself was extracted from the film more rapidly than glyceryl triacetate. Eventually the rate of oxamniquine release from the two types of film are similar. It is probable that at this time, all of the plasticiser has been removed from the film and oxamniquine is released through fluid filled pores within the film.

It is interesting to determine whether different plasticisers affect the state in which oxamniquine is present in the film (i.e. dissolved or dispersed) and whether the kinetics of oxamniquine release are affected. The possibility of oxamniquine partitioning between phthalate plasticisers and aqueous buffer within the films was proposed. It is therefore possible that a partition layer external to the diffusing surface may be set up and influence the kinetics of oxamniquine release from these films.

Figure 44 shows the fraction of oxamniquine released as a function of $\sqrt{time}$ to test the matrix controlled model. The initial portion of the graph is curved but after approximately 30% of the drug has been released, the relationship is linear. Typically, for matrix controlled kinetics, the release of the first 60-70% of the contents of the matrix is described by Higuchi's equation, which suggests that this model is not applicable to these films. Figure 45 shows a graph of log (fraction of oxamniquine remaining) against time which demonstrates that the dissolution controlled model more appropriately describes the release of oxamniquine from the films. The release from unplasticised films is not biphasic as seen with films plasticised with glyceryl triacetate. This supports the theory that the biphasic release pattern corresponds firstly to release from a plasticised film followed by release from the porous hydrated matrix from which the plasticiser has been extracted. Since there is no

plasticiser present in unplasticised films there is nothing corresponding to the first phase described above.

The rates of release from the unplasticised film and the second phase of the glyceryl triacetate plasticised film are comparable. It is unlikely that these rates would be identical since the porous structure remaining after the glyceryl triacetate has been removed will be different to an unplasticised film.

Figures 46 and 47 show the differential rate plots for films. Figure 46 suggests that oxamniquine release is dissolution controlled for approximately 40% of the oxamniquine content, equivalent to approximately 280 minutes. The original data suggest that dissolution control extends well beyond this time. Therefore the assumptions made in deriving the differential rate plots may not be completely valid even for unplasticised films. Figure 44 shows the fraction of oxamniquine released from films plasticised with PEG 400 plotted against $\sqrt{t}$ime. The sigmoidal shape of this curve shows that the matrix controlled model is not valid. The dissolution controlled model is examined in Figures 45 and 46. The release pattern is biphasic, but the curve has a different shape from previous examples which indicates that the release mechanism may be different. A possible explanation for this is that the structure or composition of the film is changing rapidly as PEG 400 is removed from the film.

FIG 44: THE EFFECT OF PLASTICISERS ON THE RELEASE OF OXAMNIQUINE FROM FREE FILMS: GRAPH OF FRACTION RELEASED AGAINST SQUARE ROOT TIME

I WATER MISCIBLE PLASTICISERS

PLOT TO TEST THE VALIDITY OF THE MATRIX CONTROLLED MODEL

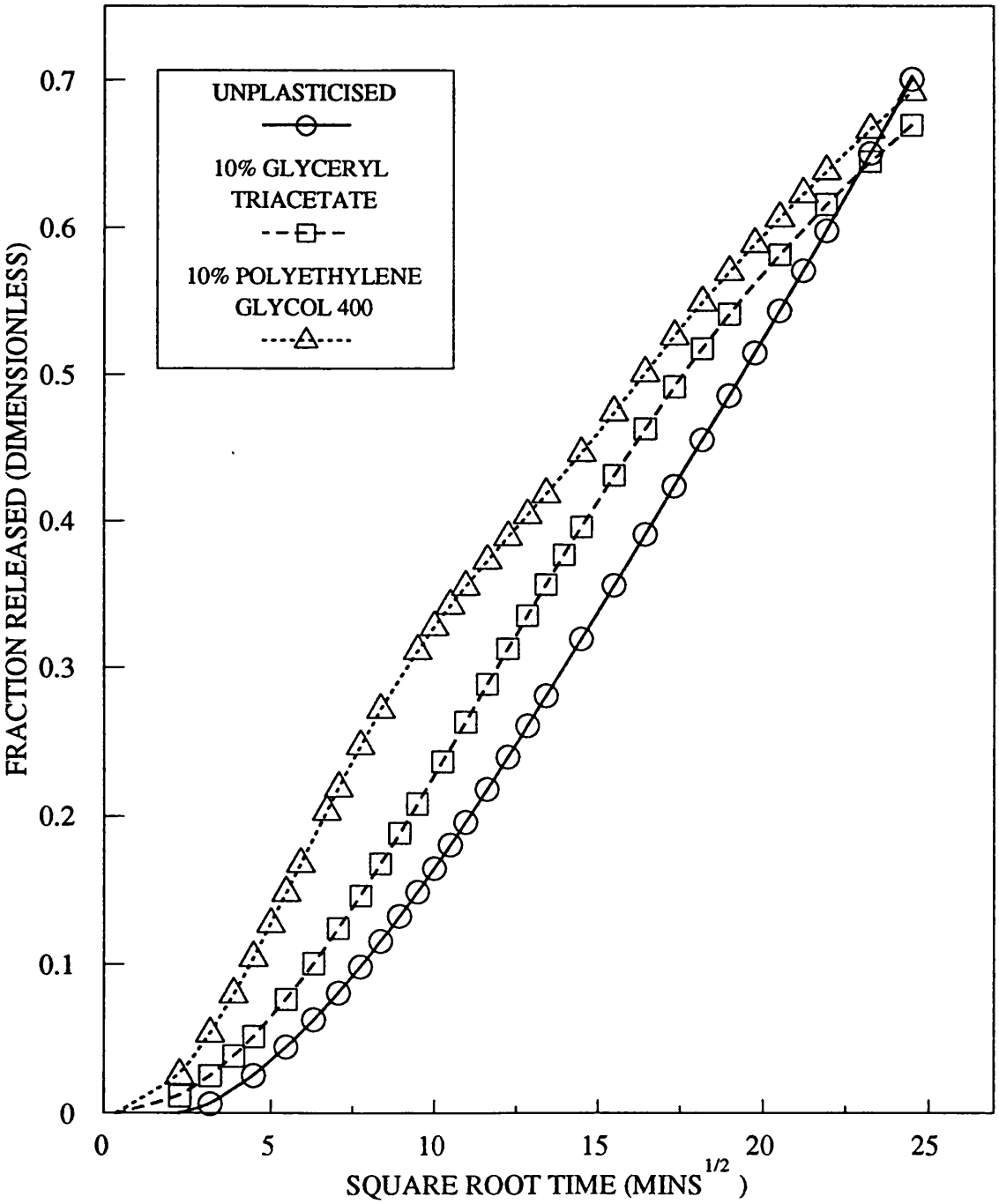

FILMS CONTAINED EQUAL PROPORTIONS OF EUDRAGIT RL AND RS WITH 5% OXAMNIQUINE RELATIVE TO POLYMER WEIGHT

FIG 45:THE EFFECT OF PLASTICISERS ON THE RELEASE OF OXAMNIQUINE FROM FREE FILMS: GRAPH OF LOG FRACTION REMAINING IN FILM AGAINST TIME

I WATER MISCIBLE PLASTICISERS

PLOT TO TEST THE VALIDITY OF THE DISSOLUTION CONTROLLED MODEL

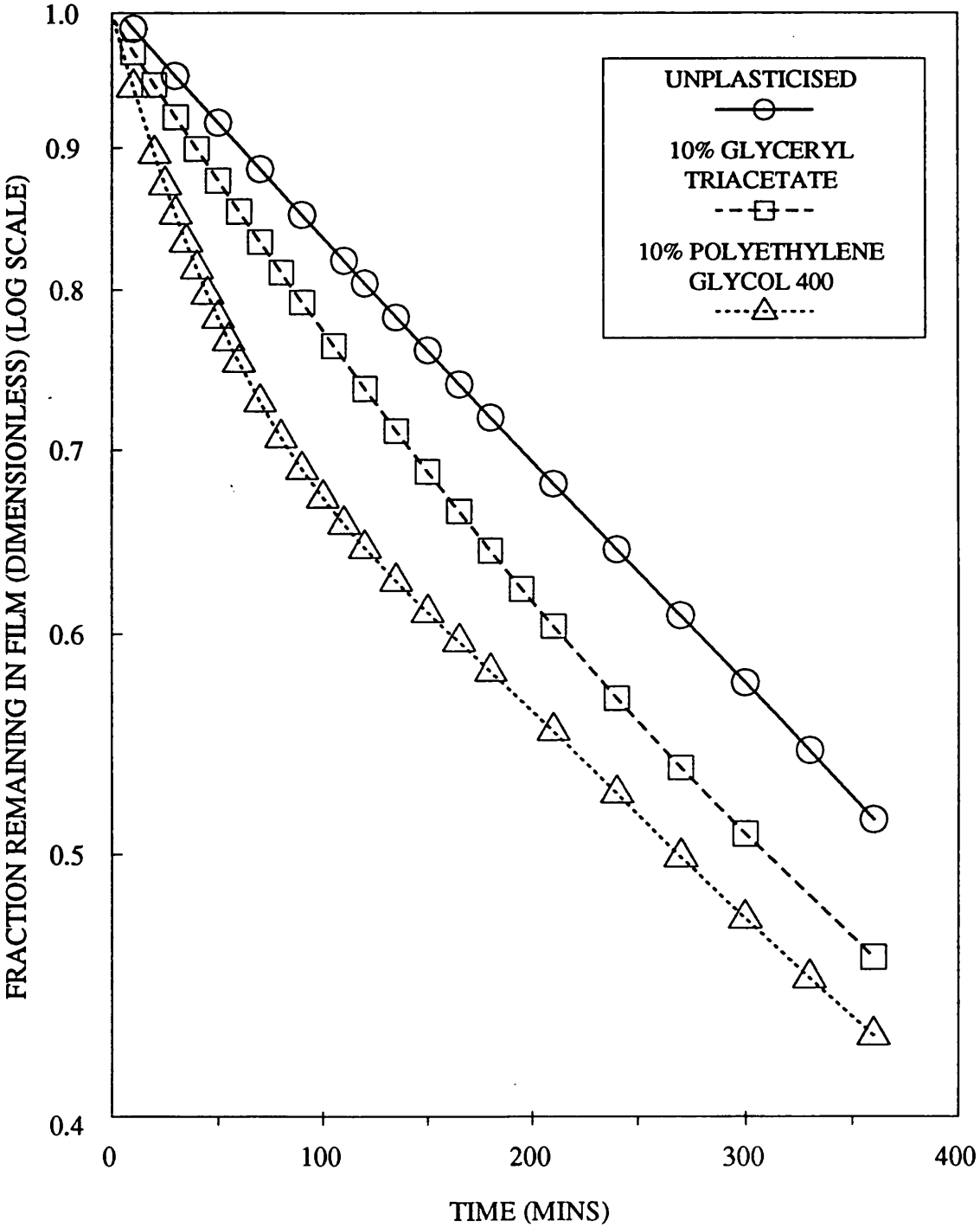

FILMS CONTAINED EQUAL PROPORTIONS OF EUDRAGIT RL AND RS WITH 5% OXAMNIQUINE RELATIVE TO POLYMER WEIGHT

FIG 46:THE EFFECT OF PLASTICISERS ON THE RELEASE OF OXAMNIQUINE FROM FREE FILMS: GRAPH OF RATE OF FRACTIONAL RELEASE AGAINST FRACTION RELEASED

I WATER MISCIBLE PLASTICISERS

DIFFERENTIAL RATE PLOT TO TEST THE VALIDITY OF THE DISSOLUTION CONTROLLED MODEL

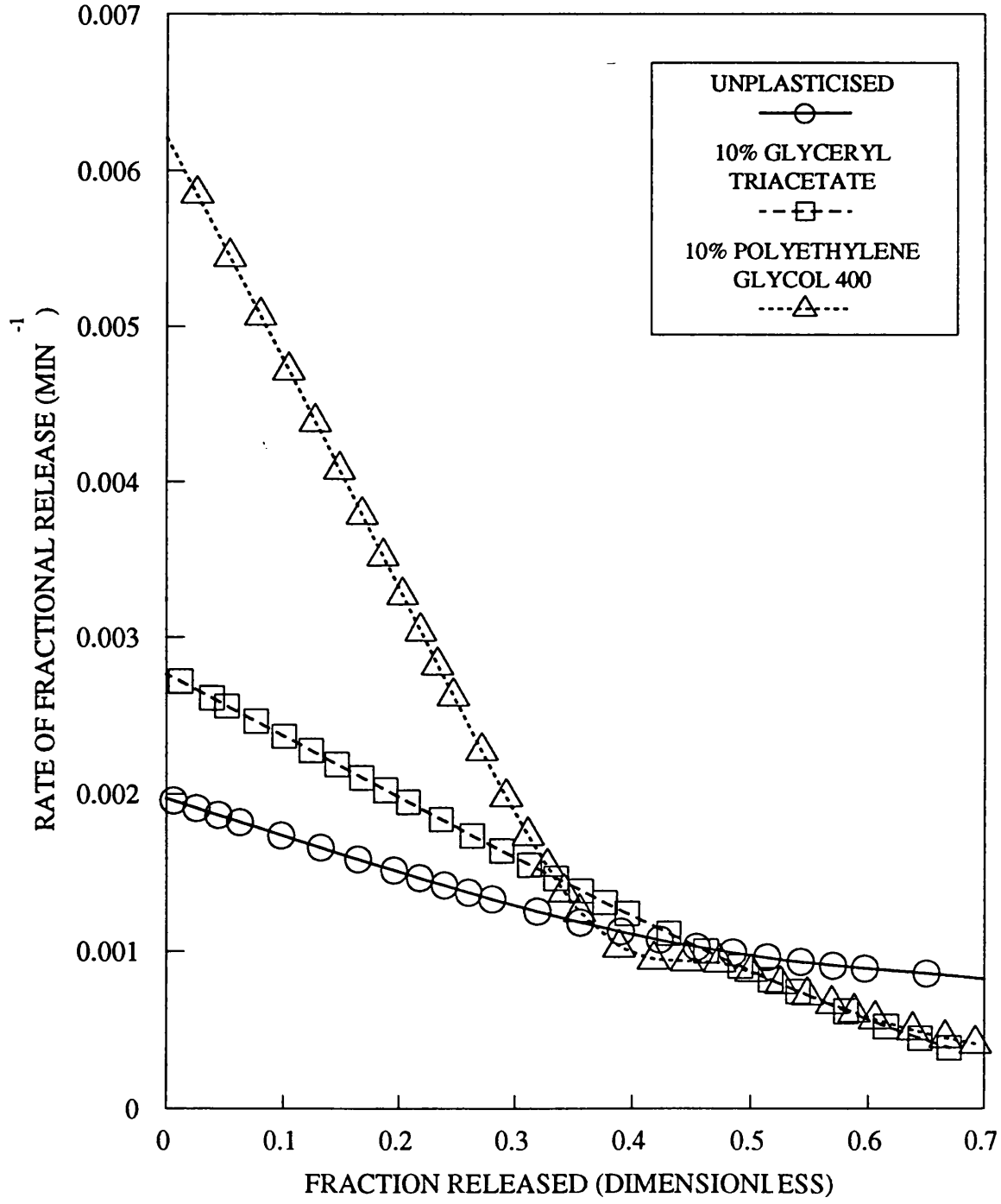

FILMS CONTAINED EQUAL PROPORTIONS OF EUDRAGIT RL AND RS WITH 5% OXAMNIQUINE RELATIVE TO POLYMER WEIGHT

FIG 47:THE EFFECT OF PLASTICISERS ON THE RELEASE OF OXAMNIQUINE FROM FREE FILMS: GRAPH OF RATE OF FRACTIONAL RELEASE AGAINST RECIPROCAL FRACTION RELEASED

I WATER MISCIBLE PLASTICISERS

DIFFERENTIAL RATE PLOT TO TEST THE VALIDITY OF THE MATRIX CONTROLLED MODEL

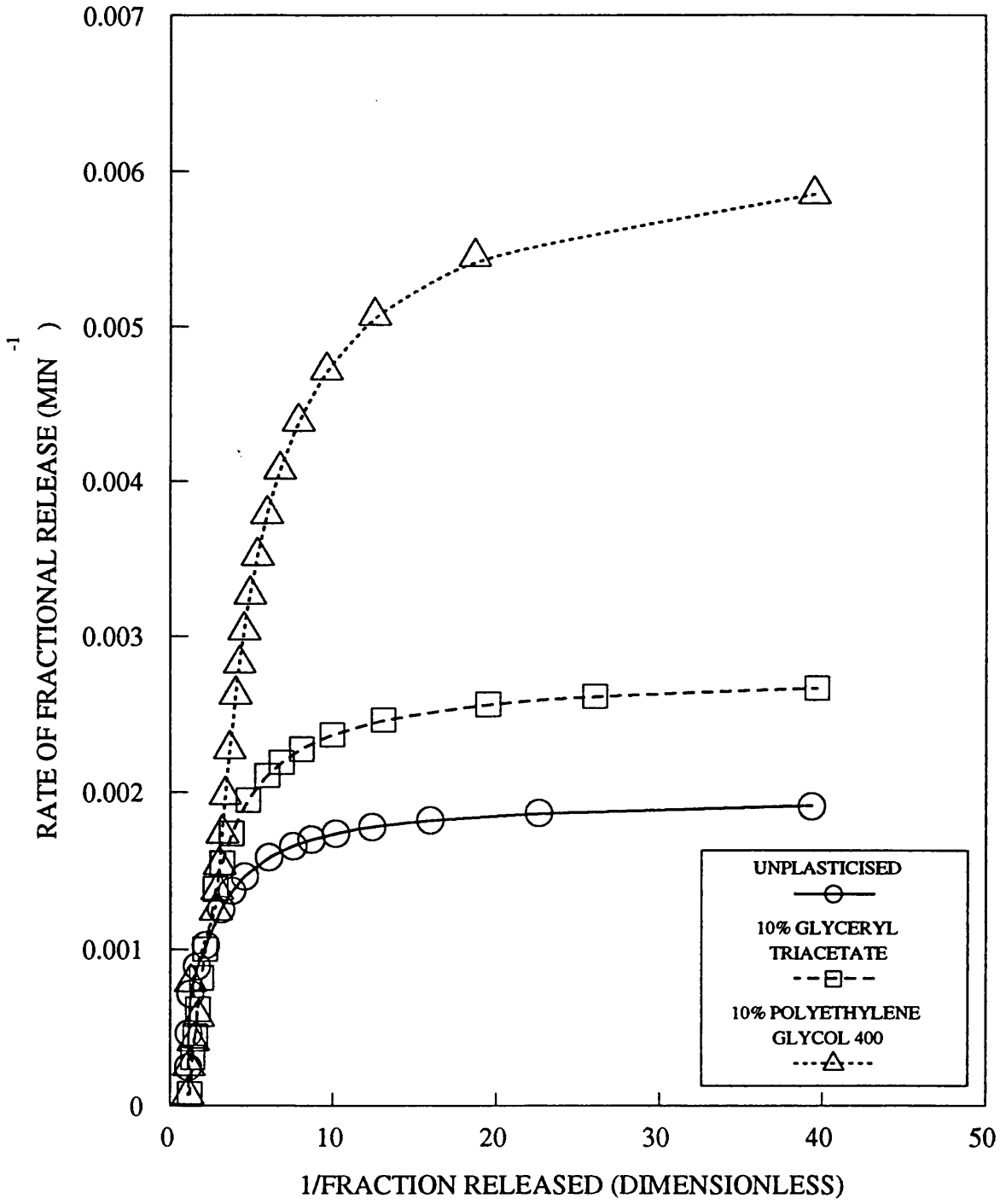

FILMS CONTAINED EQUAL PROPORTIONS OF EUDRAGIT RL AND RS WITH 5% OXAMNIQUINE RELATIVE TO POLYMER WEIGHT

It has been shown that glyceryl triacetate and PEG 400 impart significantly different release properties to films. For these water miscible plasticisers the rate at which oxamniquine is released from the films depends upon the mutual solubilities of the drug in the plasticisers and the plasticiser in the penetrating medium.

As indicated previously phthalate plasticisers are partially soluble in water with dimethyl phthalate the most soluble and dibutyl phthalate substantially insoluble in water. Oxamniquine therefore partitions between the aqueous medium and the plasticiser within the film. The apparent partition coefficients of oxamniquine between the phthalate esters and aqueous buffer were determined. The plasticisers were placed in a rank order of their affinity for oxamniquine which was

DIBUTYL PHTHALATE > DIMETHYL PHTHALATE > DIETHYL PHTHALATE

Figures 39 and 41 show that the rate of oxamniquine release from films containing these plasticisers correlates with this rank order of the affinity of oxamniquine for the plasticisers.

This correlation suggests that partitioning of oxamniquine between the plasticiser and aqueous buffer within the film matrix removes oxamniquine more efficiently than diffusion within fluid filled pores which remain after the plasticiser has been removed. This is further illustrated

in Figure 42 which shows that oxamniquine release from films plasticised with dibutyl phthalate is faster than from films plasticised with the hydrophillic PEG 400. Also, after 4 hours of release, a greater fraction of oxamniquine has been extracted from the films containing the hydrophobic plasticiser.

The mechanism of release from films containing phthalate plasticisers is interesting because of the complex way in which oxamniquine is expected to behave within the films and possibly in a boundary layer surrounding the film. Mathematical models describing release kinetics have been derived for idealised situations, so it is of value to test the applicability of some of these models to this situation.

Figure 48 shows the fraction of oxamniquine released plotted against $\sqrt{\text{time}}$. Since this relationship is not linear oxamniquine release does not appear to be matrix controlled.

As partitioning of oxamniquine within the membrane is part of the proposed descriptive model for phthalate plasticised films, it is possible that the models of ROSEMAN AND HIGUCHI (1970) and ROSEMAN AND YALKOWSKY (1976), which include partitioning at the membrane solution interface may be applicable. Figure 49 shows a plot of log (rate of fractional release) against log time for films plasticised with phthalate plasticisers to test this model. If the

FIG 48: THE EFFECT OF PLASTICISERS ON THE RELEASE OF OXAMNIQUINE FROM FREE FILMS: GRAPH OF FRACTION RELEASED AGAINST ROOT TIME

II WATER IMMISCIBLE PLASTICISERS

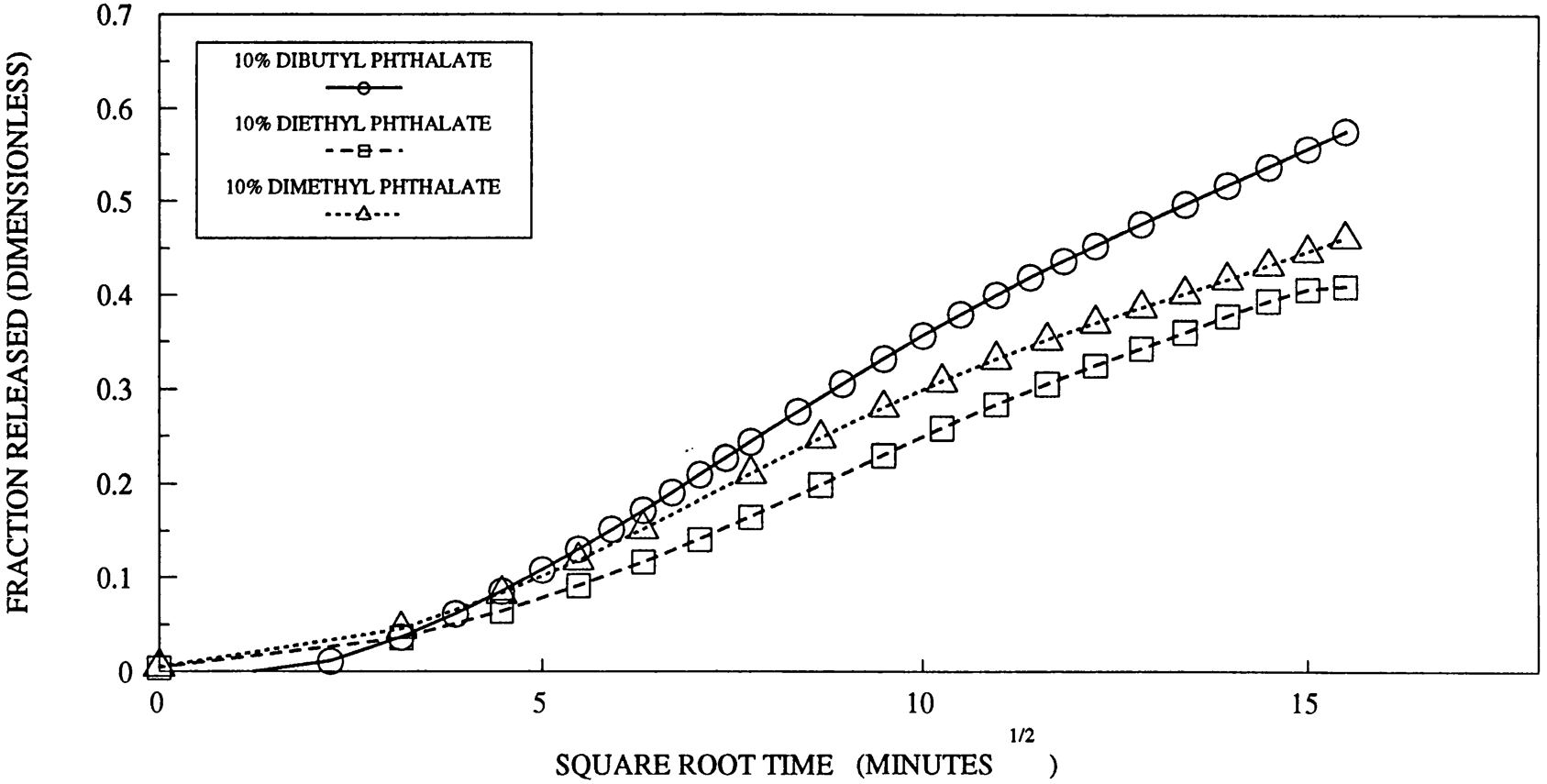

FILMS CONTAINED EQUAL PROPORTIONS OF EUDRAGIT RL AND RS WITH 5% OXAMNIQUINE RELATIVE TO POLYMER WEIGHT

PLOT TO EVALUATE THE VALIDITY OF THE MATRIX CONTROLLED MODEL

data fitted this model, the initial portion of the curve would be linear with a slope of zero, representing partition controlled release where the rate limiting step is passage of the drug through a static diffusion layer. As this is absent it can be concluded that this model is not applicable. It is likely that the removal of plasticiser from the films or the plasticiser within the films does not form a static boundary layer which limits the diffusion of oxamniquine. It is also possible that the hydrodynamics of the diffusion cell effectively disrupt the boundary by mixing as the aqueous buffer is pumped across the surface of the film.

Figure 50 shows graphs of the fraction of oxamniquine remaining in the films plotted against time to test the first order dissolution model. In each case the films exhibit similar biphasic release patterns to other plasticised films. Although the effect might have been predicted for films plasticised with dimethyl and diethyl phthalates which are partially miscible with the aqueous buffer; it would not be expected for films plasticised with dibutyl phthalate, which is virtually immiscible with water and is not therefore expected to be removed from the films. The biphasic release pattern suggests that the DBP plasticised films undergo some change during release of oxamniquine. The nature of this change is not obvious and requires further investigation.

Since it is proposed that oxamniquine release is

dissolution controlled, it is appropriate to examine the differential rate plot for dissolution controlled kinetics. The relevant graphs are shown in Figure 51.

Considering the data for the first 50% of oxamniquine release, Donbrow and Friedmans model applies well to unplasticised films and films containing dibutyl phthalate where it is expected that no change in film structure occurs during oxamniquine release. The model also applies well to films plasticised with glyceryl triacetate which is released relatively slowly. There is an adequate fit to the data generated from films containing other plasticisers, sufficient only to distinguish between dissolution and matrix controlled kinetics.

5.6 Diffusion of Oxamniquine through Films Containing Phthalate Plasticisers

In Section 5.5 results were presented for the release of oxamniquine from films plasticised with phthalate esters. It was found that the nature of oxamniquine release from these films was not readily predictable. Although the main objective of these studies was to identify factors which influenced the release of oxamniquine from monolithic film, it was considered relevant to examine the effects of phthalate plasticisers on the permeation of oxamniquine through films possibly to explain the results obtained.

FIG 49: THE EFFECT OF PLASTICISERS ON THE RELEASE OF OXAMNIQUINE FROM FREE FILMS: GRAPH OF LOG RATE OF FRACTIONAL RELEASE AGAINST LOG TIME

PLOT TO EVALUATE THE EFFECT OF PARTITIONING

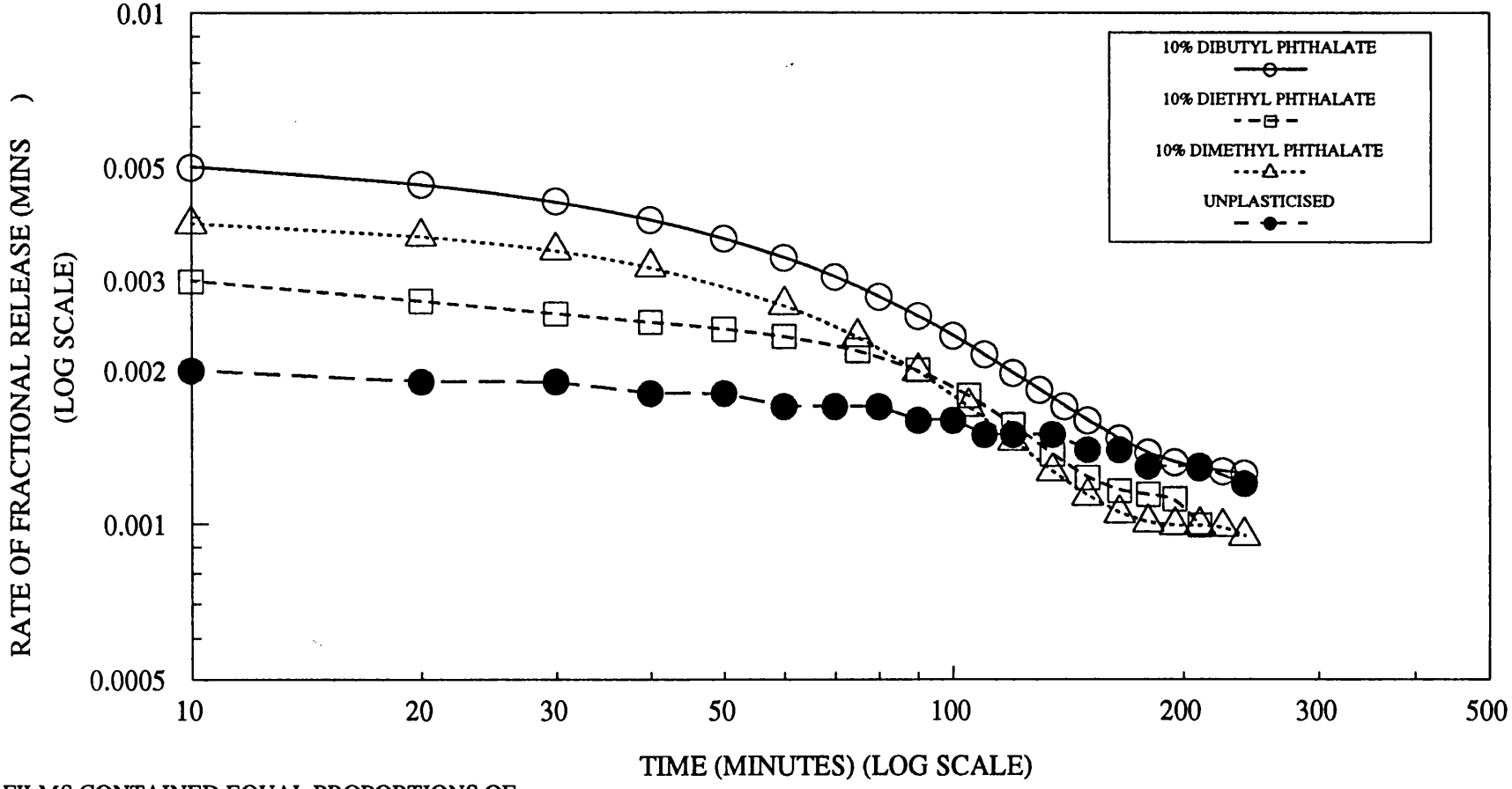

FILMS CONTAINED EQUAL PROPORTIONS OF EUDRAGIT RL AND RS WITH 5% OXAMNIQUINE RELATIVE TO POLYMER WEIGHT

FIG 50: THE EFFECT OF PLASTICISERS ON THE RELEASE OF OXAMNIQUINE FROM FREE FILMS: GRAPH OF LOG FRACTION REMAINING AGAINST TIME II WATER IMMISCIBLE PLASTICISERS

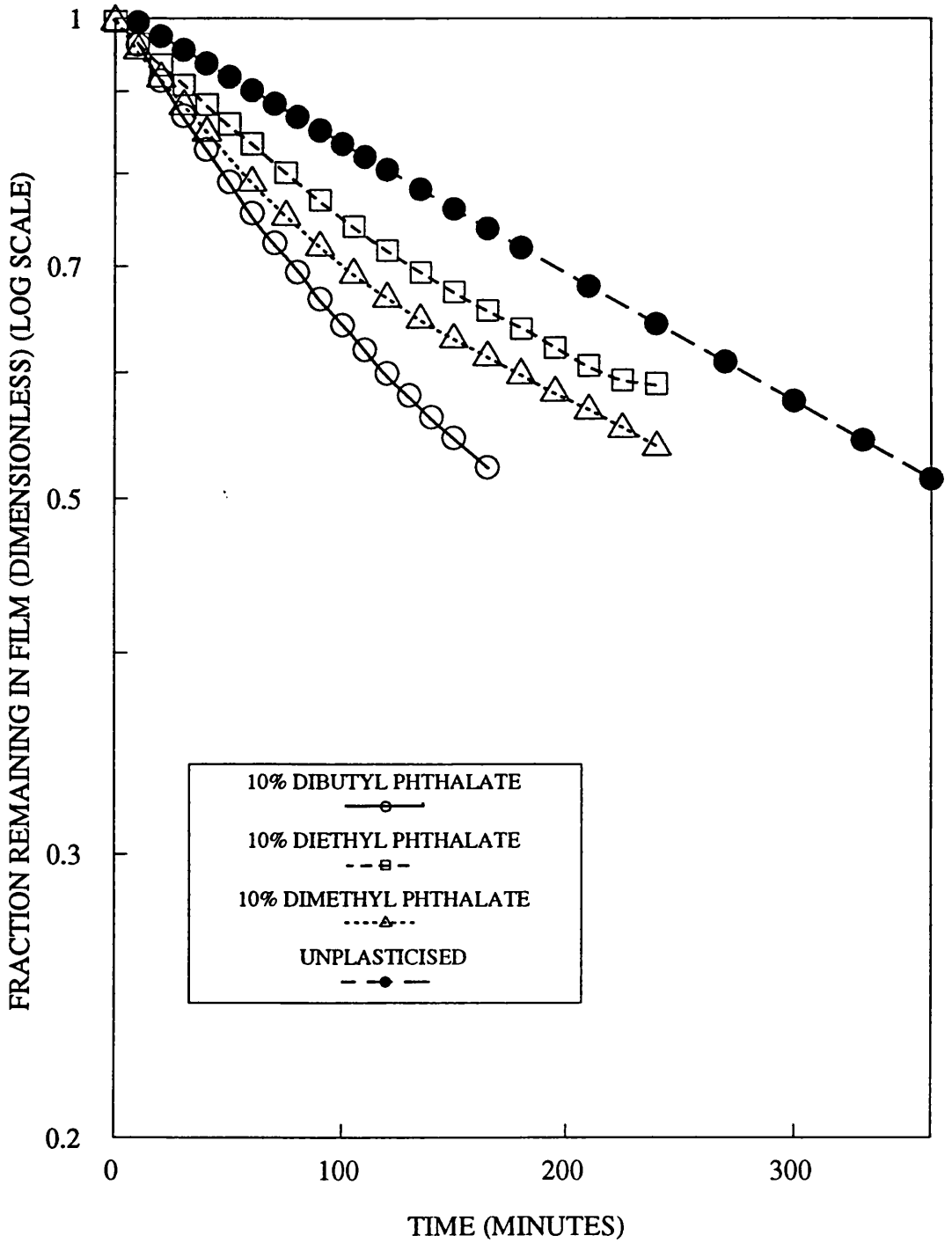

FILMS CONTAINED EQUAL PROPORTIONS OF EUDRAGIT RL AND RS WITH 5% OXAMNIQUINE RELATIVE TO POLYMER WEIGHT

FIG 51: THE EFFECT OF PHTHALATE PLASTICISERS ON RELEASE OF OXAMNIQUINE FROM FREE FILMS: GRAPH OF RATE OF FRACTIONAL RELEASE AGAINST FRACTION RELEASED

PLOT TO TEST THE VALIDITY OF THE
DISSOLUTION CONTROLLED MODEL.

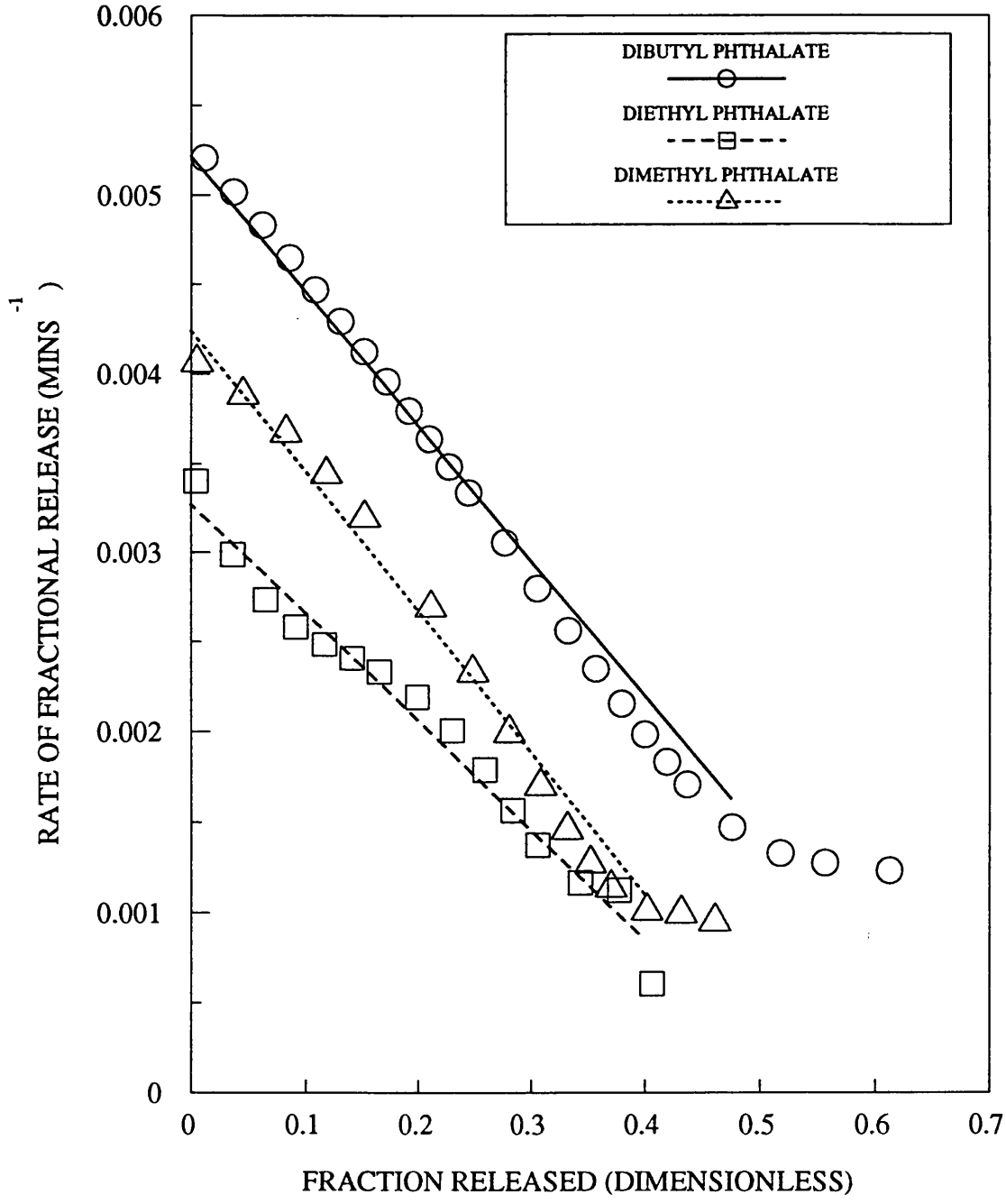

FILMS CONTAINED EQUAL PROPORTIONS OF
EUDRAGIT RL AND RS WITH 10% PLASTICISER AND
5% OXAMNIQUINE RELATIVE TO POLYMER WEIGHT

5.6.1 Theoretical Considerations

Consider the case of a non-porous, homogeneous polymer membrane. Transport of a permeating species occurs by dissolution in the polymer at one interface, followed by diffusion down a gradient of thermodynamic activity and then release at the other interface. This is termed a solution-diffusion membrane.

Transport through these membranes is described by Ficks First Law, which for diffusion in one dimension can be expressed by equation 28.

$$J = \frac{dM_t}{Adt} = \frac{-DdC_m}{dx} \qquad (28)$$

where J is the flux of material (usually expressed in $gcm^{-2}sec^{-1}$), dC_m/dx is the concentration gradient, D is the diffusion coefficient, A the effective area available for diffusion. The minus sign expresses the fact that diffusion occurs down a concentration gradient. This is illustrated in Figure 52.

The concentration gradient described by Ficks First Law applies to the inner surfaces of the membrane i.e. $Cm_{(o)}$ and $Cm_{(1)}$ rather than in the bulk solution C_o and C_1.

These concentrations are related by the distribution coefficient K, which is analogous to the partition coefficient between two immiscible solutions.

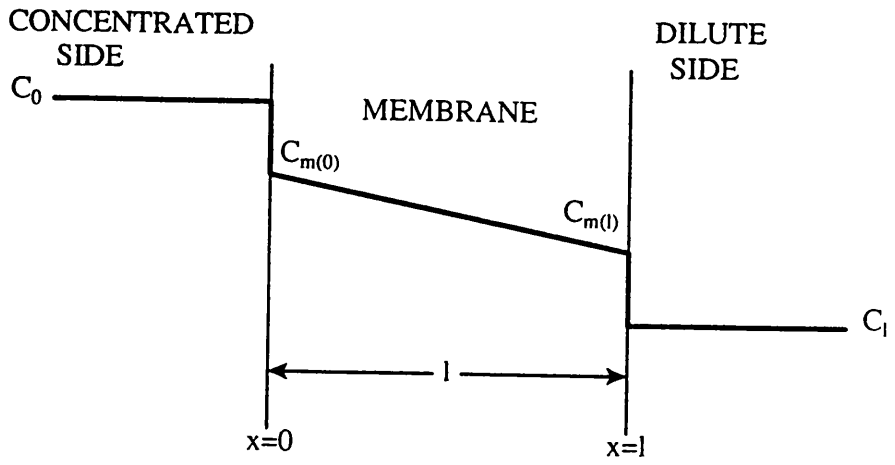

Figure 52 Concentration gradient within a solution-diffusion membrane of thickness l, also showing partitioning at the solution membrane interface.

It is possible to establish steady state conditions within the membrane if the activity of the drug at the upstream surface is constant. A convenient value for constant activity is unity and this may be achieved by having a saturated solution in contact with excess drug or a pure liquid in contact with the membrane at the upstream surface. Under these conditions, equation 28 can be integrated to give

$$J = \frac{DK\Delta C}{l} \text{ or } \frac{dM_t}{dt} = \frac{ADK\Delta C}{l} \qquad (29)$$

where ΔC is difference in concentration of the solutions on either side of the membrane.

The permeability coefficient P is defined as the product of the distribution and diffusion constants.

i.e. $P = DK$

It is therefore possible to deduce the permeability coefficient from steady state permeability measurements.

Before steady state conditions are established a period exists where the permeation rate is either higher or lower than the steady state rate. For a fresh membrane placed in contact with a reservoir containing drug, a finite time will elapse while the steady state concentration gradient is established within the membrane. During this period the release rate will be lower than expected. However, if a membrane which has been equilibrated with drug is placed in contact with a similar reservoir then a higher than expected release rate will be observed before steady state is established. These effects are respectively termed the TIME LAG and BURST EFFECT.

Ficks Second Law can then be solved in terms of trigonometrical series using appropriate boundary conditions to obtain an expression relating concentration and time.

This expression can then be integrated with respect to time using the appropriate boundary conditions to obtain the total quantity of diffusant which has passed through the membrane in time t.

$$\frac{M_t}{lC_1} = \frac{Dt}{l^2} - \frac{1}{6} = \frac{2}{\pi^2} \sum_{n=o}^{\infty} \frac{(-1)^n}{n^2} \exp\left(-Dn^2\pi^2 t/l^2\right) \qquad (30)$$

At steady state i.e. at long times t->∞ and the exponential terms disappears and equation 30 approaches

$$M_t = \frac{DC_1}{1}\left(t-\frac{1^2}{6D}\right) \qquad (31)$$

which when extrapolated to $M_t=0$ gives

$$t = T_{Lag} = \frac{1^2}{6D} \qquad (32)$$

BARRER (1951) used this relationship to derive the diffusion coefficient D from steady state measurements. All of the foregoing arguments assume that the diffusion coefficient D does not vary with time, position or diffusant concentration over the course of the experiment. If the diffusion coefficient is not constant then the mathematical treatment is different (CRANK 1975).

5.6.2 Results

Figure 53 shows graphs of the quantity of oxamniquine which has permeated through films containing equal proportions of Eudragit RL and Eudragit RS. Films were either unplasticised or plasticised with 20% w/w of dimethyl, diethyl or dibutyl phthalate. Figure 54 shows the data for unplasticised films over a longer time base. Data reported are the mean of three determinations on fresh films. In general results were reproducible to within ±10% of the mean. However, at low oxamniquine concentrations, variation between films was greater which may reflect

FIG 53: THE EFFECT OF PHTHALATE PLASTICISERS ON THE PERMEATION OF OXAMNIQUINE THROUGH EUDRAGIT FILMS: GRAPH OF AMOUNT PERMEATED AGAINST TIME

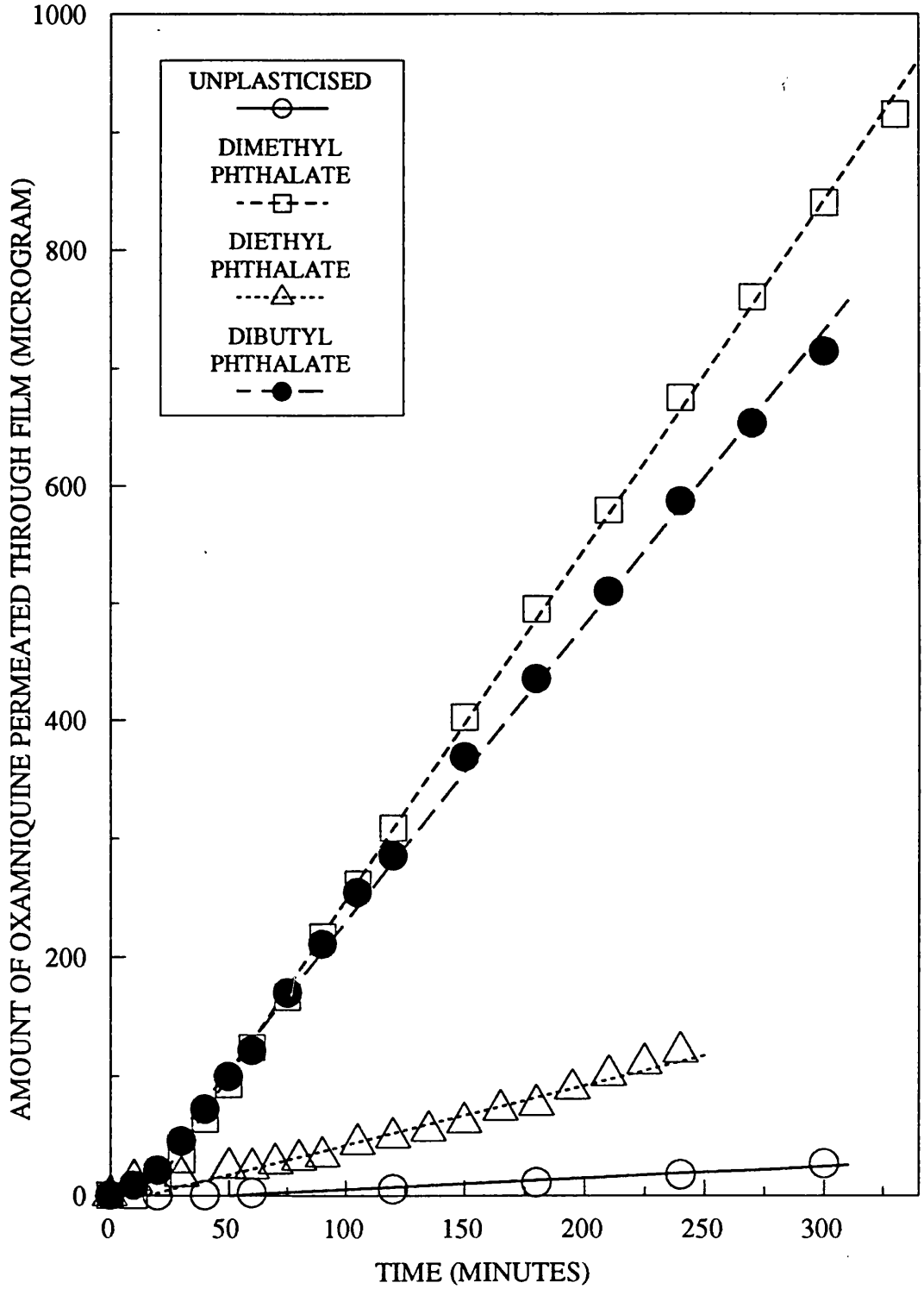

FILMS CONTAINED EQUAL PROPORTIONS OF EUDRAGIT RL AND RS WITH 20% PLASTICISER RELATIVE TO TOTAL POLYMER WEIGHT.

FIG 54: PERMEATION OF OXAMNIQUINE THROUGH UNPLASTICISED EUDRAGIT FILMS: GRAPH OF AMOUNT PERMEATED AGAINST TIME

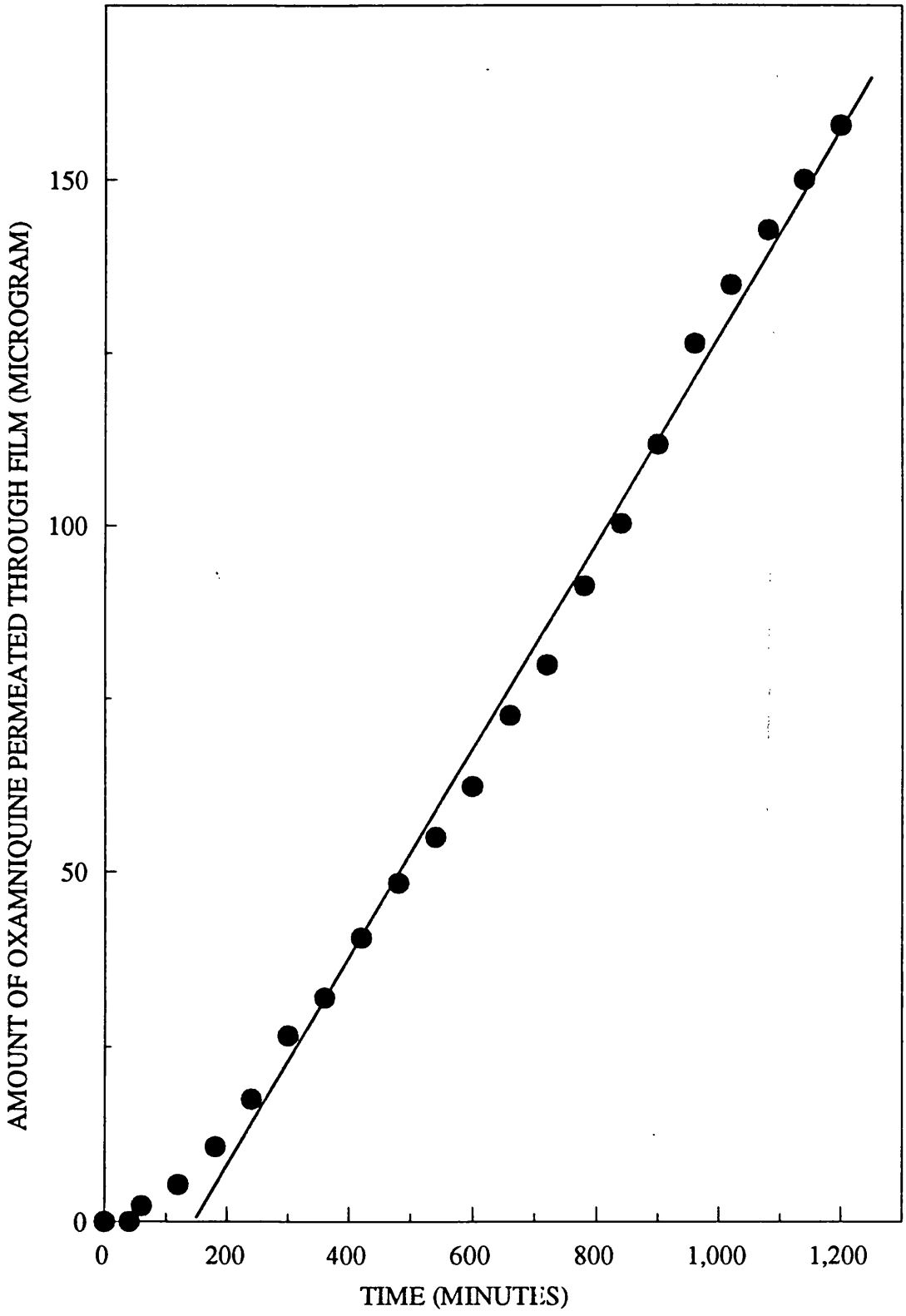

FILMS CONTAINED EQUAL PROPORTIONS OF EUDRAGIT RL AND RS

variability between films or variation in the analytical methods. Table 22 summarises the data obtained from these experiments.

TABLE 22 **SUMMARY OF PERMEABILITY AND DIFFUSION COEFFICIENTS OBTAINED FOR OXAMNIQUINE DIFFUSION THROUGH EUDRAGIT FILMS**

Plasticiser	Time Lag (min)	Diffusion coefficient D cm^2/sec	Permeability coefficient P cm^2/sec	Distribution coefficient K
Unplasticised	99.2	4.5×10^{-10}	5.7×10^{-11}	0.13
Dimethyl Phthalate	17.7	2.5×10^{-9}	1.3×10^{-9}	0.53
Diethyl Phthalate	-11.9	5.3×10^{-7}*	2.4×10^{-10}	4.52×10^{-4}*
Dibutyl Phthalate	1.7	2.6×10^{-8}	1.1×10^{-9}	0.04

* = calculated from "negative time lag" measurement.

In these experiments the membrane thickness was 0.004cm; the effective diffusional area was $12cm^2$; the concentration of oxamniquine in the donor solution was $0.0125gcm^{-3}$. The concentration of oxamniquine in the receptor phase remained less than 0.1% of that in the donor solution throughout the experiment. Hence sink conditions were assumed in the receptor solution and the concentration was taken as 0.

The measured values of the diffusion coefficient are in line with predicted values. For an organic permeant of molecular weight 280, diffusion coefficients in the range 10^{-8} - $10^{-9}cm^2/sec$ would be expected for diffusion in silicone rubber which is relatively permeable, $1)^{-14}cm^2/sec$

in polystyrene which is impermeable and 10^{-5} - $10^{-6}cm^2/sec$ in water, (BAKER AND LONSDALE, 1974). The diffusion coefficient obtained for oxamniquine in pH6.0 Citric Acid/Phosphate buffer was 8.6 x $10^{-6}cm^2/sec$ at 37°C (see Section 4.5).

As expected, incorporation of plasticisers in the film increases the diffusion coefficient by 1-2 orders of magnitude. Considering the calculated permeability coefficients, the rank of plasticisers in terms of increased film permeability is diethyl phthalate, dimethyl phthalate and dibutyl phthalate. This correlates with both the partition coefficients obtained for oxaminquine between aqueous buffers and plasticisers (Section 4.4) and with the release of oxamniquine from phthalate plasticised films, emphasising the importance of partitioning in the diffusion process.

Furthermore, in the case of dimethyl and diethyl phthalate, the plasticiser diffuses out of the film. Therefore the diffusion coefficient is time dependent and the value derived from the pre-steady state measurements must be regarded as an apparent diffusion coefficient. This is not likely to be the case for unplasticised films and for films containing dibutyl phthalate which is not substantially removed from the film. The high diffusion coefficient seen with dibutyl phthalate plasticised films suggests that partitioning between plasticiser and aqueous buffer within the film increases the efficiency of oxamniquine transport.

The calculated distribution coefficients derived are all less than unity, which indicates that the permeant concentration at the inner surface of the membrane is less than that at the outer surface. The very low distribution coefficients calculated for unplasticised and dibutyl phthalate plasticised films imply that the surface of the films is hydrophobic compared with dimethyl phthalate plasticised films.

Diethyl phthalate plasticised films exhibit an apparent negative time lag. This has been observed previously by SEROTA et al (1972) for permeation of polyethylene films by aniline derivatives and by DONBROW AND FRIEDMAN (1975b) for the permeation of caffeine through plasticised ethylcellulose membranes. In the former case the permeants were found to have low oil/water partition coefficients and in the latter caffeine had a low partition coefficient. There was, however, insufficient evidence to conclusively demonstrate that this is responsible for the negative time lag. Broadly speaking the results obtained from these experiments highlight the effect of partitioning of oxamniquine between the aqueous buffer and the plasticiser within the film and suggest that this is more significant than the solubility of the plasticiser in the aqueous medium.

5.7 Scanning Electron Microscopy Studies on Free Films

It has been proposed that deviations from established

mathematical models of drug release are the result of changes in the film structure with time. Scanning electron microscopy (SEM) provides a useful tool for examining the physical surface structure of films to evaluate the effects of such changes.

Figures 55 to 67 show scanning electron micrographs of the surface view of the films. Each of the film samples was examined at a range of magnifications between x220 and x13800 (actual magnification of the film transparency), and the micrographs shown represent sections which show features typical of the whole sample. A tilt correction of 30° for the beam angle was found to provide the best definition of the features of film surfaces.

Typically the air exposed surface of the films before extraction exhibited a fairly uniform mottled effect. This appearance, termed an orange peel effect, is due to the evaporative drying of the solvent during casting. There is no evidence of precipitation of the polymer or of oxamniquine at the film surface which demonstrates that a cohesive film has been formed. The PEG400 plasticised film appears to have a coarser structure than the glyceryl triacetate or dibutyl phthalate plasticised films. There may have been some bubbling of the dichloromethane during evaporation which gave rise to these inhomogeneities. The high magnifications required to visualise the surface structure suggest that the air exposed surfaces of all the films are relatively homogeneous.

FIGURE 55 Scanning electron micrograph showing the surface structure of the upper surface of a film containing equal proportions of Eudragit RL and RS with 10%w/w glyceryl triacetate and 5%w/w oxamniquine before extraction from the upper surface into pH6.0 Citric Acid-Phosphate buffer.
Magnification x 6900: Sample Tilt Correction 30°.

FIGURE 56 Scanning electron micrograph showing the surface structure of the lower surface of the film described in Figure 55. Magnification x 6900: Sample Tilt Correction 30°.

FIGURE 57 Scanning electron micrograph showing the surface structure of the upper surface of a film containing equal proportions of Eudragit RL and RS with 10%w/w PEG400 and 5%w/w oxamniquine before extraction from the upper surface into pH6.0 Citric Acid-Phosphate buffer. Magnification x 6900: Sample Tilt Correction 30°.

FIGURE 58 Scanning electron micrograph showing the surface structure of the lower surface of the film described in Figure 57. Magnification x 6900: Sample Tilt Correction 30°.

FIGURE 59 Scanning electron micrograph showing the surface structure of the upper surface of a film containing equal proportions of Eudragit RL and RS with 10%w/w dibutyl phthalate and 5%w/w oxamniquine before extraction from the upper surface into pH6.0 Citric Acid-Phosphate buffer.
Magnification x 13800: Sample Tilt Correction 30°.

FIGURE 60 Scanning electron micrograph showing the surface structure of the lower surface of the film described in Figure 59.
Magnification x 13800: Sample Tilt Correction 30°.

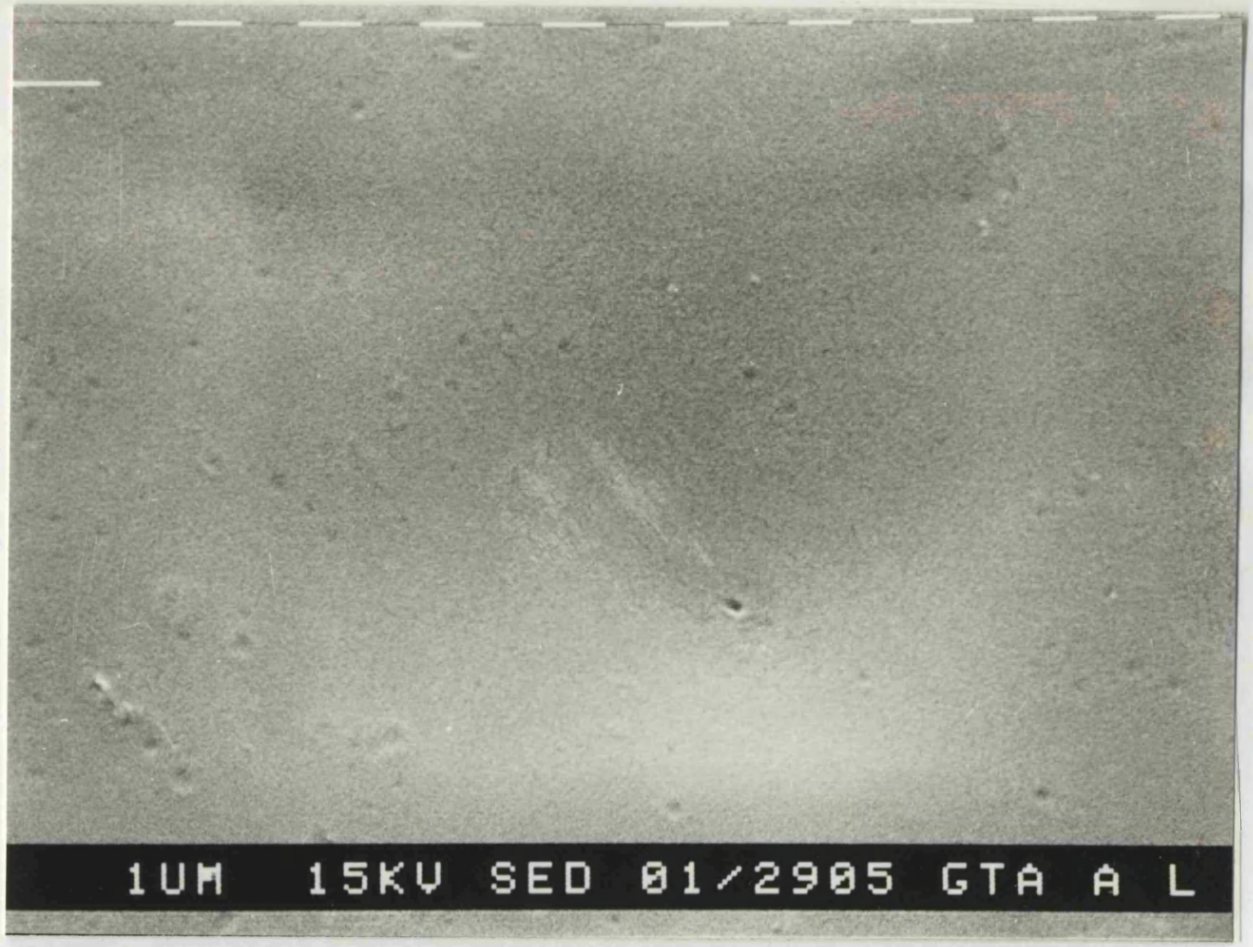

FIGURE 61 Scanning electron micrograph showing the surface structure of the upper surface of a film containing equal proportions of Eudragit RL and RS with 10%w/w glyceryl triacetate and 5%w/w oxamniquine after extraction from the upper surface into pH6.0 Citric Acid-Phosphate buffer.
Magnification x 3450: Sample Tilt Correction 30°.

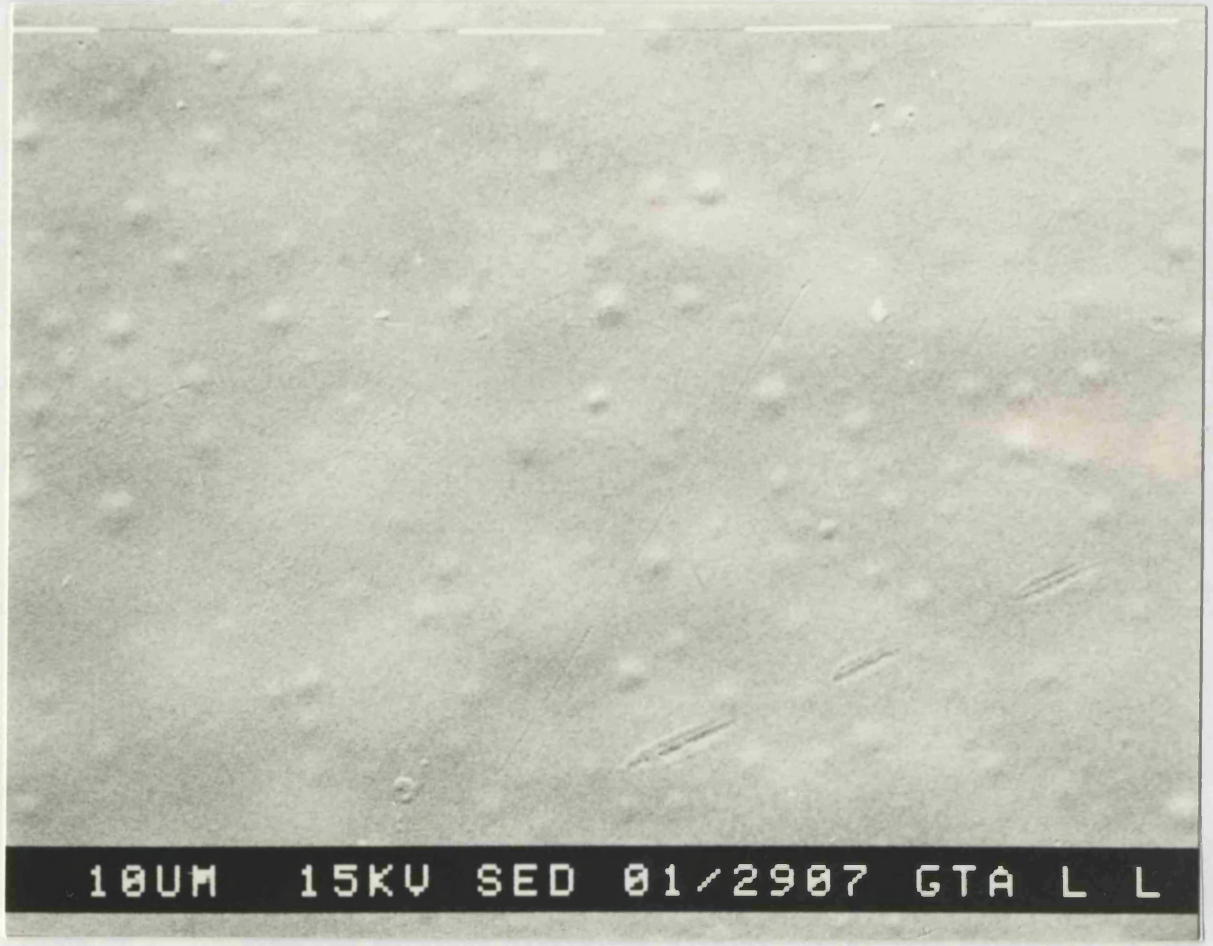

FIGURE 62 Scanning electron micrograph showing the surface structure of the lower surface of the film described in Figure 61. Magnification x 860: Sample Tilt Correction 30°.

FIGURE 63 Scanning electron micrograph showing the surface structure of the upper surface of a film containing equal proportions of Eudragit RL and RS with 10%w/w PEG 400 and 5%w/w oxamniquine after extraction from the upper surface into pH6.0 Citric Acid-Phosphate buffer. Magnification x 860 : Sample Tilt Correction 30°

FIGURE 64 Scanning electron micrograph showing the surface structure of the lower surface of the film described in Figure 63. Magnification x 860: Sample Tilt Correction 30°.

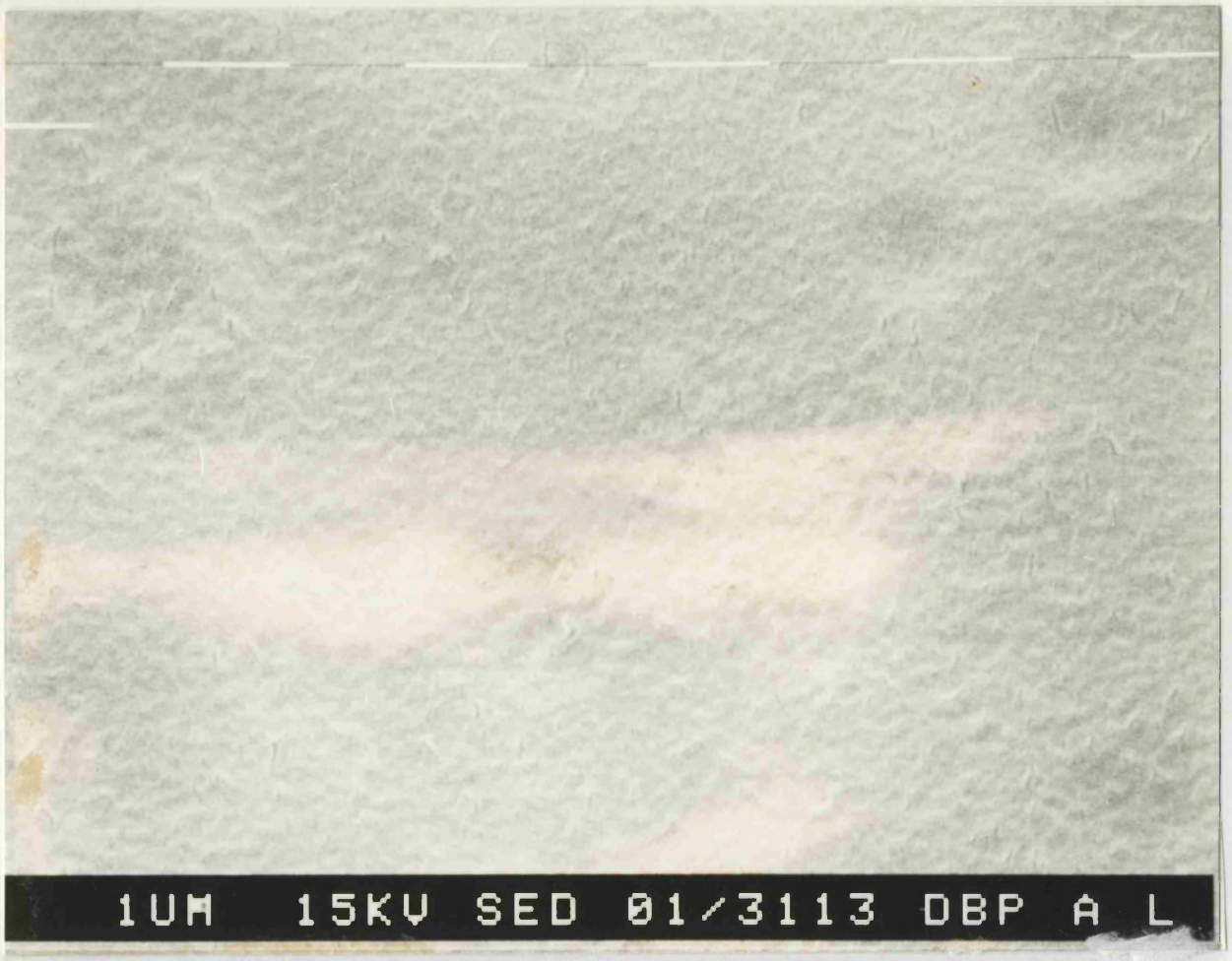

FIGURE 65 Scanning electron micrograph showing the surface structure of the upper surface of a film containing equal proportions of Eudragit RL and RS with 10%w/w dibutyl phthalate and 5%w/w oxamniquine after extraction from the upper surface into pH6.0 Citric Acid-Phosphate buffer.
Magnification x 860: Sample Tilt Correction 30°.

FIGURE 66 Scanning electron micrograph showing the surface structure of sample described in Figure 75.
Magnification x 6900: Sample Tilt Correction 30°.

FIGURE 67 Scanning electron micrograph showing the surface structure of the lower surface of the film described in Figure 65. Magnification x 3450: Sample Tilt Correction 30°.

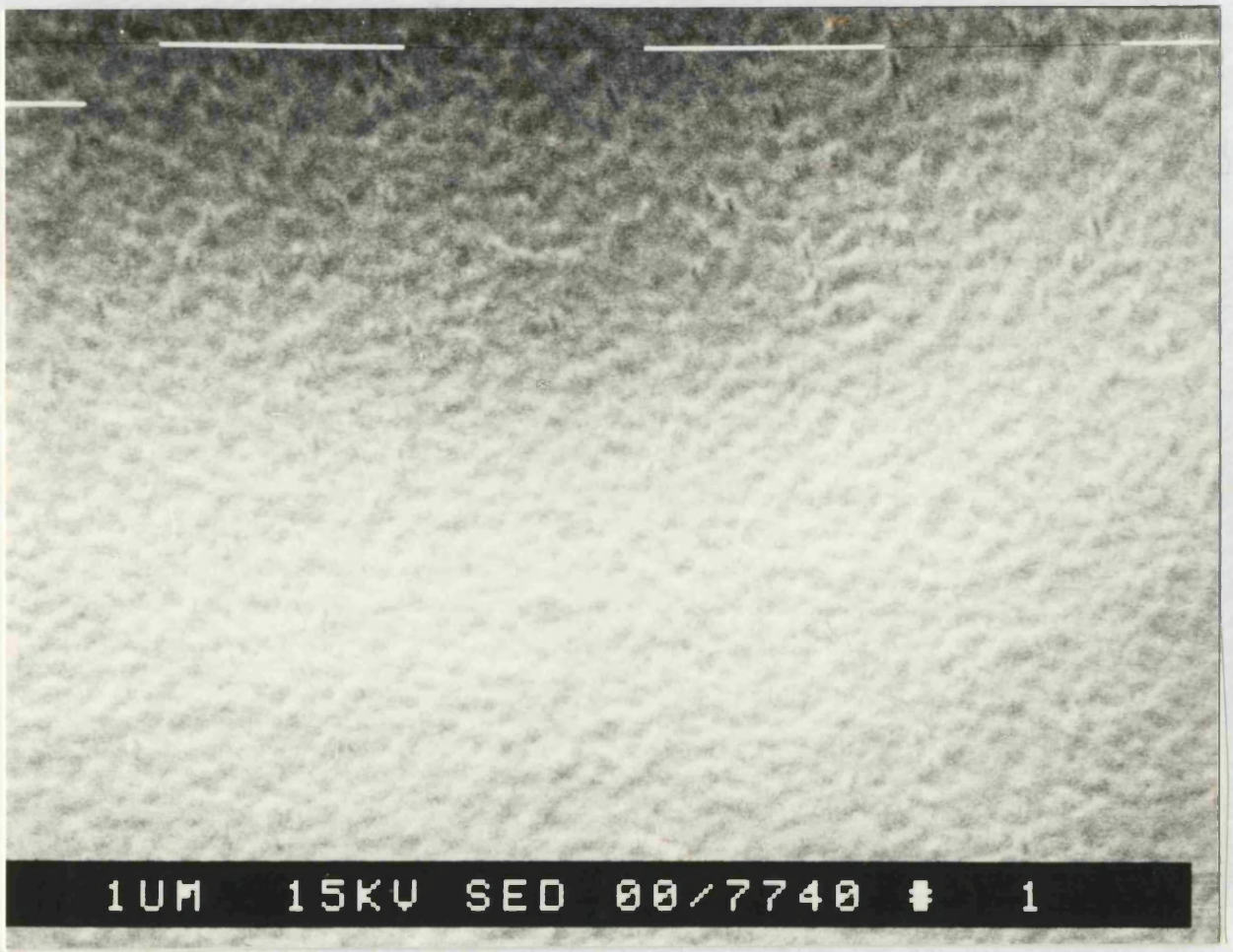

FIGURE 68 Scanning electron micrograph showing the surface structure of the upper surface of a film cast on PTFE containing Eudragit RL and RS in equal proportions with 10%w/w glyceryl triacetate and 5%w/w oxamniquine. Magnification x 13800: Sample Tilt Correction 0°.

FIGURE 69 Scanning electron micrographs showing the surface structure of the lower surface of a film cast on PTFE containing Eudragit RL and RS in equal proportions with 10%w/w glyceryl triacetate and 5%w/w oxamniquine.
Magnification x 55: Sample Tilt Correction 0°.

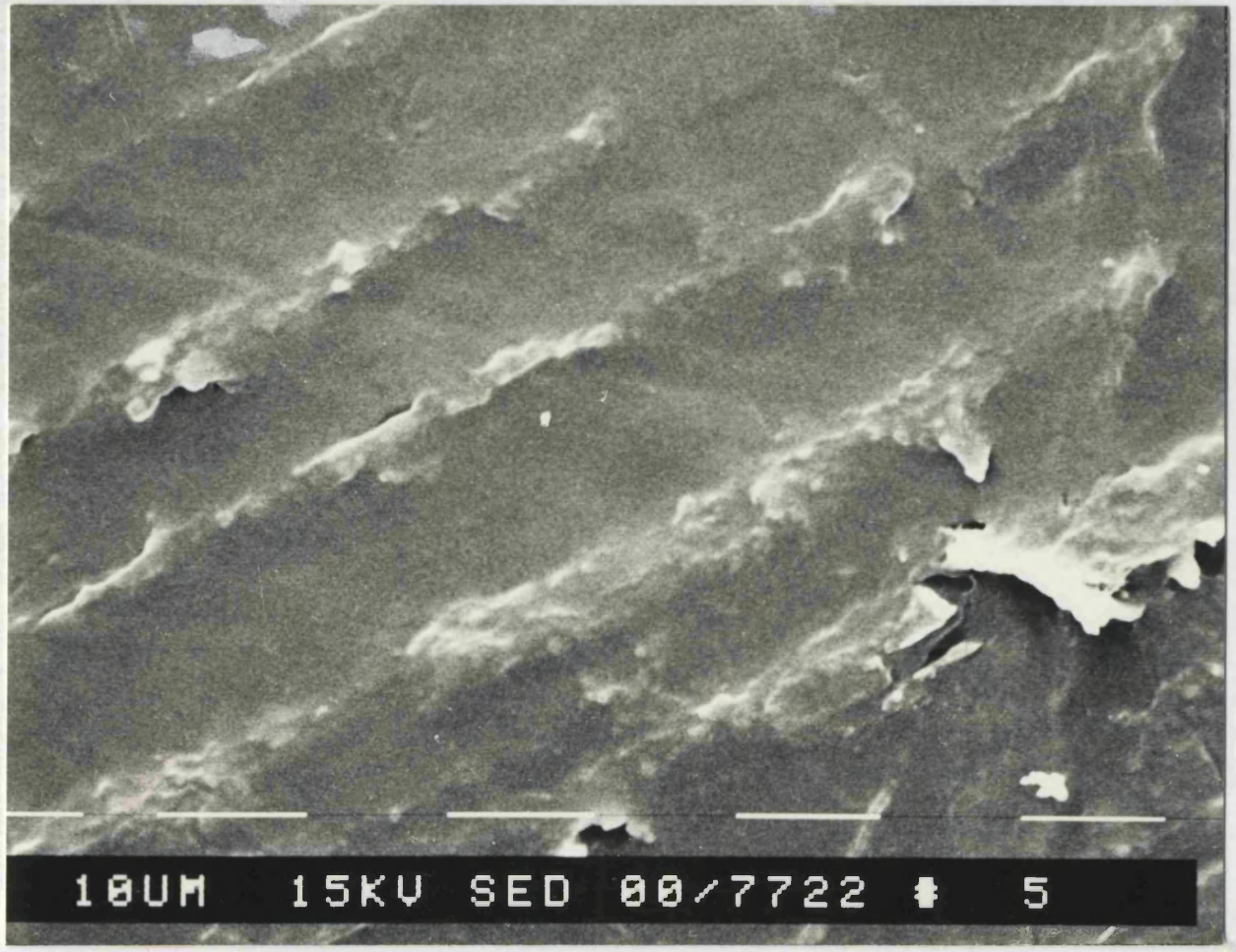

FIGURE 70 Scanning electron micrograph showing the surface structure of the film described in Figure 69.
Magnification x 862: Sample Tilt Correction 0°.

The mercury contact surface of each of the films before extraction shows a similar fine grained orange peel surface structure similar to the air exposed surface. There is again no evidence of precipitation of either the polymer or oxamniquine. The similarity between the surface structures of the air-exposed and mercury contact surfaces is notable. In similar studies ABDEL AZIZ et al (1975) examined the surfaces of Eudragit films which had been cast on PTFE surfaces. SEM of the lower surface showed an impression of the PTFE mould even though the PTFE surface had been machined to produce a fine finish. This effect was demonstrated in similar moulds constructed from machined PTFE, and the results are shown in Figures 68 to 70. This could in part account for the effect of surface differences on the permeability of films observed by these workers.

After oxamniquine has been extracted from the films by the buffer, there is a substantial change in the surface structure of the films. Differences can be seen between films containing different plasticisers.

The exposed surface of glyceryl triacetate plasticised films (Figure 61) shows the formation of relatively shallow depressions in the surface, which were not present before oxamniquine was extracted. The lower surface, however, shows the formation of considerably larger, pronounced blister like structures. Similar structures were observed by ABDEL-AZIZ et al (1975) after urea permeation through Eudragit films. The relationship between the crater and

blister like structures is uncertain, but it suggests that both permeation through and extraction from one surface of Eudragit films has been influenced by the internal structure of the film and consequently surface structure. The effect of oxamniquine leaching on the PEG400 plasticised films is even more dramatic. The upper surface (Figure 63) shows a mixture of the blister structures together with pin-hole crater structures. The lower surface (Figure 64) also shows the presence of blisters and pin-hole craters. These are less distinct than on the upper surface, but are still clearly present.

Lastly, an examination of films plasticised with dibutyl phthalate shows a different effect. Figure 65 shows the presence of crater like surface structures on the upper surface. However, in Figure 66, examined at higher magnification, these structures appear to be only slight surface depressions. These surface depressions are shallower than those seen with the GTA plasticised films. After extraction there appears to show no significant changes to the surface structure of the lower surface (Figure 67).

The inhomogenieties which have developed in the film surface after oxamniquine has been leached from the air exposed surface may be termed as "pores". These pores are not likely to be surface to surface channels which form continuous pathways through the film structure, but discontinuous internal channels which have formed within

the film as a result of the oxamniquine and plasticiser being extracted from the film. These channels become filled with the extracting fluid and form a pathway for the removal of further quantities of oxamniquine and plasticiser.

In dibutyl phthalate plasticised films, where it is proposed that the plasticiser is not extracted from the film, these pores are not formed, and there is relatively little change to the surface structure of the film after oxamniquine has been extracted.

It is difficult to exactly determine the distribution of pores over the entire surface of the film, but the photomicrographs represent typical areas of a appearance of the surfaces. This implies that the plasticiser and drug have been distributed reasonably uniformly throughout the film. SHAH AND SHETH (1972) stated that this condition is more likely to occur where films have been prepared by slow evaporative drying. Rapid drying may promote local pockets of polymer and/or plasticiser deposition which might be seen as clusters of pores after leaching.

5.8 Water Sorption Studies on Polymer Discs

In Section 5.5 a substantial difference was noted in the behaviour of films plasticised with glyceryl triacetate and PEG 400. Release from PEG 400 plasticised films was characterised by an initial rapid release of oxamniquine

followed by a slower release period. The initial rapid release was not seen in GTA plasticised films. It was considered that there may be an interaction between PEG 400 and Eudragit which causes this rapid release.

It is known that Eudragit RL undergoes a degree of swelling in contact with aqueous media (GURNY et al 1976). Swelling in water is typical of polymethacrylate polymers, but the sorption of water in hydrophobic Eudragit is not extensive as the swelling and dimensional change seen in hydrophillic polymethacrylates. To investigate differences in the swelling characteristics, polymer discs containing equal proportions of Eudragit RL and RS plasticised with 20%w/w of either glyceryl triacetate or PEG 400 were prepared.

50ml of solutions containing 150mg cm^{-3} of the polymers and 30mg cm^{-3} of the plasticiser in dichloromethane were poured into the deep PTFE moulds described in Chapter 3. The solvent was allowed to evaporate for 5 days at an ambient temperature in a low humidity environment (RH <30%), after which the discs were removed from the dishes. The centre portions of the discs were cut out using the punch and die cutter assembly described in Chapter 3, providing an exposed surface area of 11.5cm^2 per surface. The initial dry weights of the discs were recorded. Each disc was placed in 100ml of double distilled water maintained at 25°C in a water bath. The water in contact with the discs was agitated by magnetic stirring. At various intervals, discs were removed from the water, lightly dried of excess

surface moisture, weighed rapidly and then returned to the water bath. Discs were treated in this way for 2 hours.

Figure 71 shows the percentage weight increase plotted against the time the disc is immersed in water. It is evident that the discs plasticised with PEG 400 take up more water at a greater rate than those plasticised with glyceryl triacetate.

Water uptake may be considered as the combination of two processes. Firstly, as the plasticiser is removed from the discs it leaves a porous structure in which the pores are filled with water. If this were the only process taking place, there would be no significant weight change other than to compensate for density differences between the plasticiser and water. There is clearly a weight gain as the discs are immersed in water. Incorporation of the plasticiser has therefore made the discs more hydrophilic. The discs plasticised with PEG 400 take up approximately 3 times more water than those plasticised with glyceryl triacetate. It would be expected that unplasticised discs take up less water than plasticised discs. It is proposed that plasticisation of Eudragit RL and RS with PEG 400 renders the polymers more hydrophilic than plasticisation with glyceryl triacetate and that this effect is related to the rapid release oxamniquine from Eudragit films plasticised with PEG 400.

FIG 71: THE EFFECT OF PLASTICISERS ON WEIGHT INCREASE OF EUDRAGIT POLYMER DISCS AFTER IMMERSION IN WATER

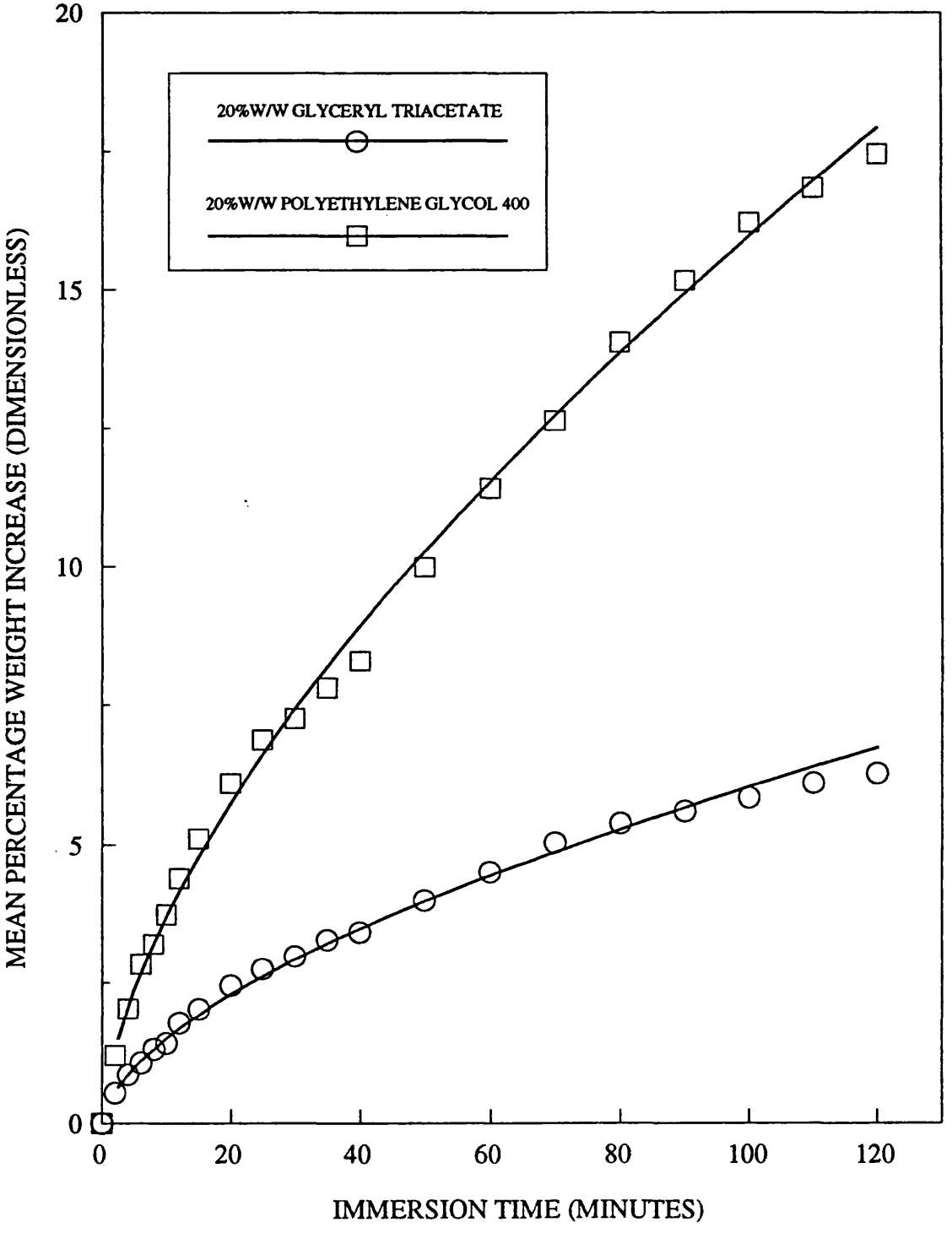

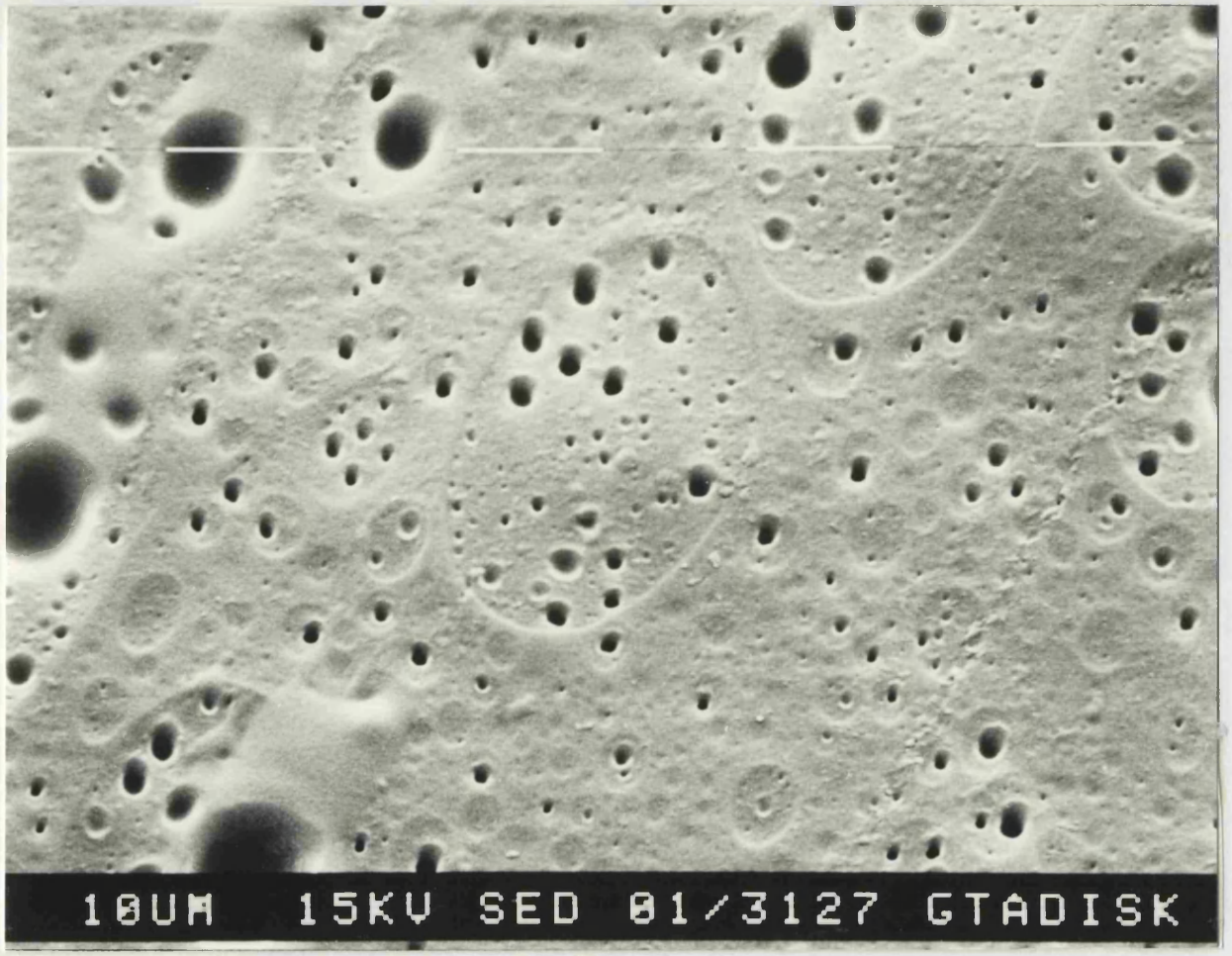

FIGURE 72 Scanning Electron Micrograph showing transverse section of a glyceryl triacetate plasticised Eudragit disc after immersion in water.
Magnification x 860: Sample Tilt Correction 30°.

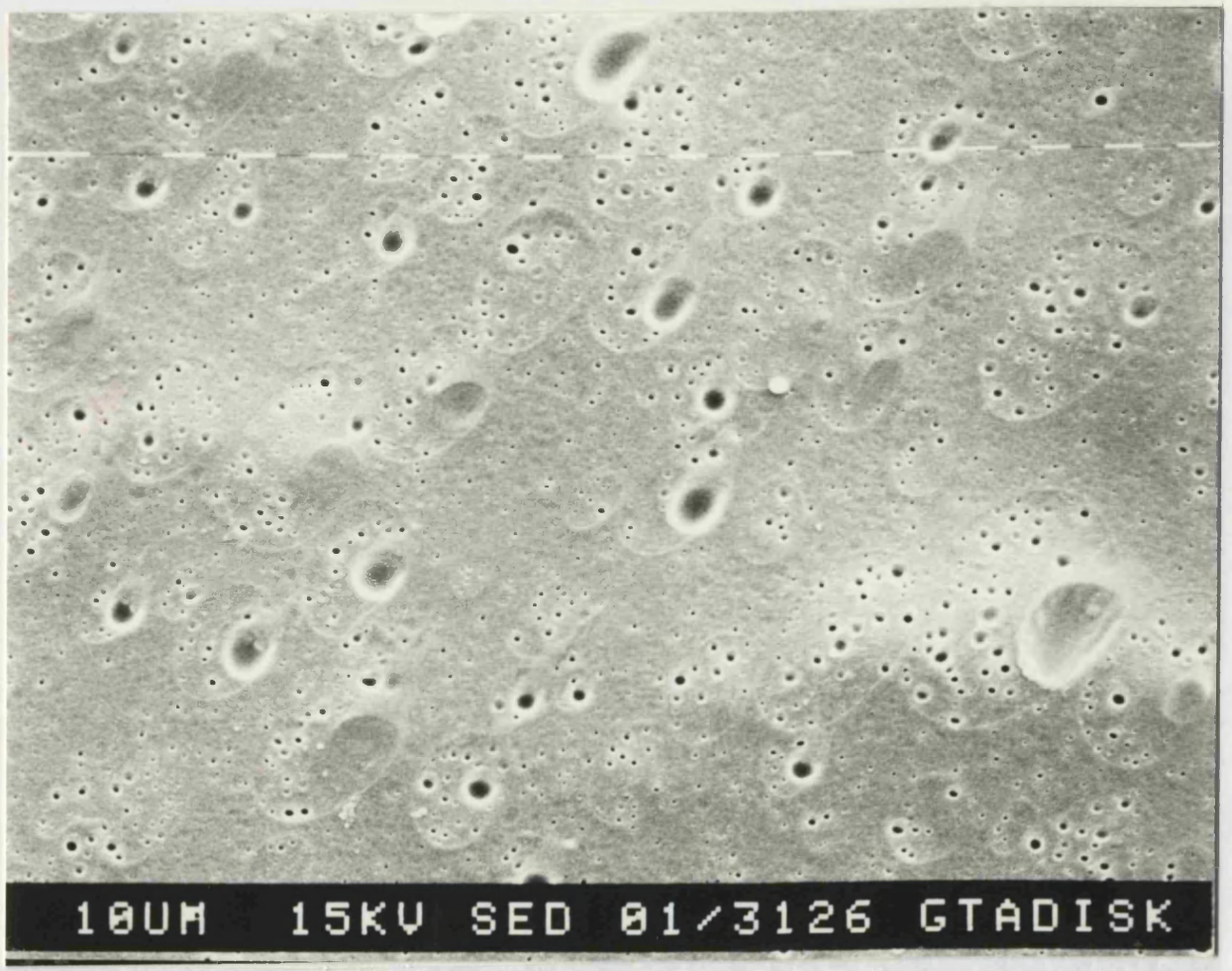

FIGURE 73 Scanning Electron Micrograph showing transverse section of a glyceryl triacetate plasticised Eudragit disc after immersion in water.
Magnification x 220: Sample Tilt Correction 0°.

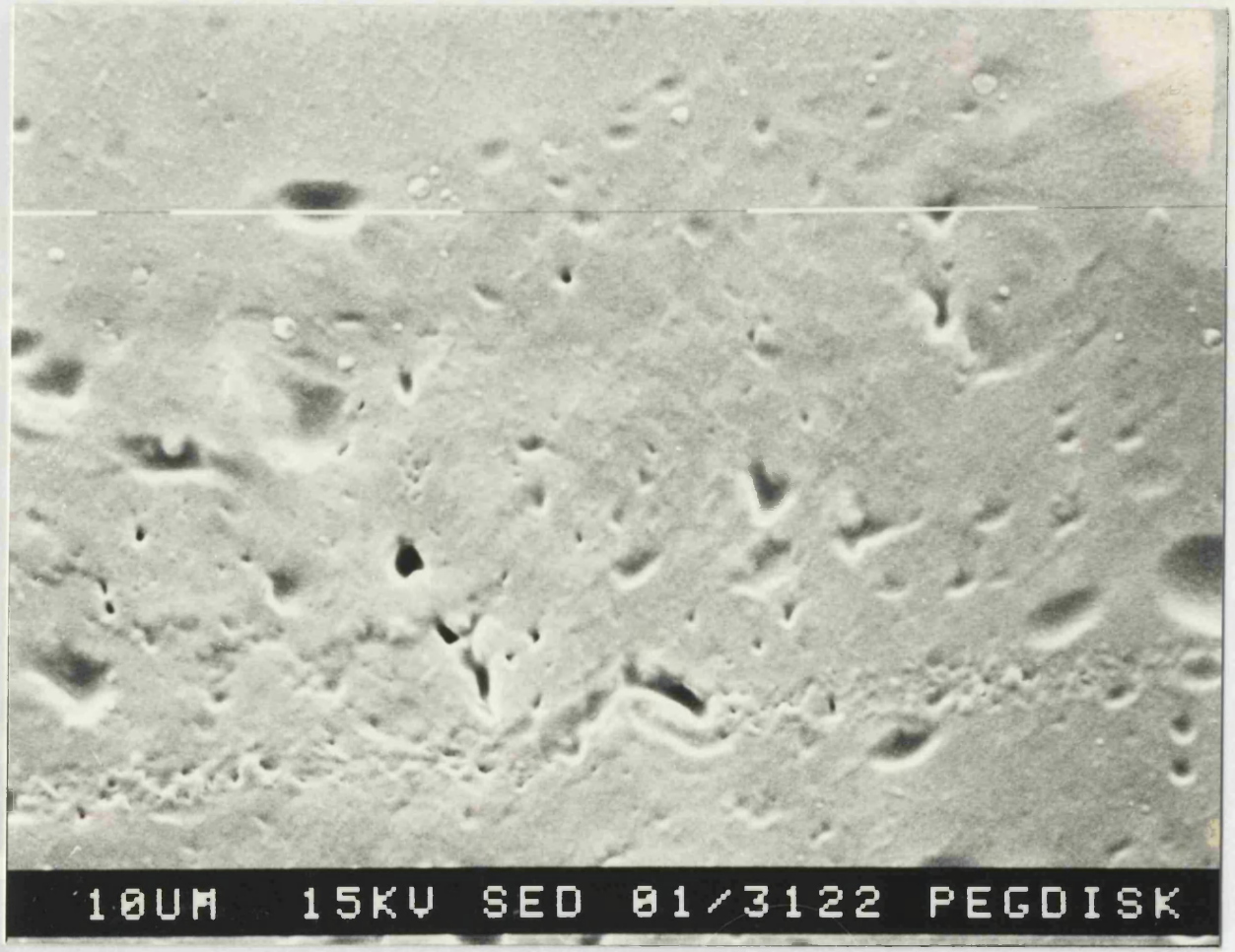

FIGURE 74 Scanning Electron Micrograph showing transverse section of a PEG 400 plasticised Eudragit disc after immersion in water. Magnification x 1720: Sample Tilt Correction 0°.

FIGURE 75 Scanning Electron Micrograph showing transverse section of a PEG 400 plasticised Eudragit disc after immersion in water. Magnification x 860: Sample Tilt Correction 0°.

To illustrate further the effect of water uptake on discs plasticised by PEG 400 and GTA, transverse sections through the centre of the discs were examined by scanning electron microscopy. Figures 72 to 75 show photographs of the scanning electron micrographs.

The scanning electron micrographs show that immersion of the plasticised discs in water causes definite structural inhomogeneities. This supports the hypothesis that extraction of oxamniquine and water soluble plasticisers from films causes discontinuous channels (pores) to develop within the film structure.

There appear to be differences betweem the transverse sections of the extracted glyceryl triacetate and PEG 400 discs. The differences are in the shape and apparent internal depth of the resulting inhomogeneities. It is possible that these differences result from the way in which the plasticisers were distributed within the discs. Although the discs were cast from solution, it is possible that plasticisers associate within the polymer structure differently as the discs are formed. This could affect the way in which oxamniquine is released from cast films and applied coatings.

5.9 Release of Oxamniquine from Coated Pellets

In this section, oxamniquine release from coated pellets, will be described and compared with the results of

oxamniquine release from isolated films. The preparation of coated pellets has been described in Chapter 3.

5.9.1 Theoretical Analysis

HIGUCHI (1963) has presented a theoretical analysis of the rate of release of drugs dispersed in solid, spherical matrices. An exact solution to this problem would involve deriving an exact co-ordinate system to describe the distribution pattern of the dispersed particles within the sphere. However a good approximation to the exact solution has been obtained using the assumptions used to develop the model for release from the planar system.

Higuchi made a number of observations based on the calculated relationships. Firstly, an initial surge of release from the spheres can be expected. Secondly a semilogarithmic plot of fraction remaining in pellet against time gives a sigmoidal relationship indicating a deviation from first order kinetics. He observed that any apparent linear relationship observed may be either coincidental or related to a difference in the overall mechanism of release from those used to derive the model.

Thirdly the release from the spherical model to the planar model was compared. On the basis that the total exposed surface area is $4\pi a_0^2$ it was observed that the two systems would predict a similar extent of release for up to 50% of the total drug content since a plane of the same area is a

good approximation to the sphere. It is only beyond 50% release that significant deviation is evident between the two systems. Therefore in the following experiments only this early portion of the data is considered.

It is important to note that other factors may modify the overall behaviour of real systems and lead to deviations from the behaviour predicted in the models. For example, a short lag time may be required to wet the interior of matrices. The lag time needs to be short compared with the overall duration of release for this not to be significant. Further it is assumed that matrices do not change significantly in the presence of moisture, for example swelling, or erosion by weakening of the matrix at the surface.

5.9.2 The Effect of Polymer Ratio

Since both Eudragit RL and RS were soluble in dichloromethane, it was possible to vary the composition of the polymer mixture in the film coating.

Figure 76 shows the effect of varying the proportions of Eudragit RL and RS in film coatings containing 5%w/w oxamniquine and 10%w/w glyceryl triacetate relative to the total weight of polymer. For all experiments, results reported are the mean of at least three individual determinations. Individual determinations were reproducible to within at least 5% of the mean.

The release of oxamniquine from the pellets becomes more rapid as the proportion of Eudragit RL in the coating is increased. This is as expected and agrees with the results obtained from isolated films.

Figure 77 shows the time taken to release between 10% and 70% of the oxamniquine from the coating, plotted as a function of the proportion of Eudragit RS in the coating. It is apparent that the relationship between the proportion of polymers in the coating and the release of oxamniquine is not linear. Inclusion of 20% Eudragit RS in the polymer mixture had no significant effect on the release of oxamniquine from the coating. The release of 50% of the oxamniquine content from the coating is approximately 24 times faster from a coating containing only Eudragit RL compared with a coating containing only Eudragit RS. The retarding effect is significant only when no Eudragit RL is present in the coating. This is similar to the results obtained using isolated films. It is possible that Eudragit RL acts by making the matrix more open to the penetration of aqueous buffer. This would encourage the extraction of oxamniquine from the coating. Alternately, there may be an interaction between Eudragit RL and oxamniquine which allows it to be more rapidly released from coatings.

Figure 78 shows the calculated rates of release of oxamniquine. Typically a high initial release rate followed by a rapid decrease to a slower rate can be seen.

FIG 76: THE EFFECT OF POLYMER RATIO ON THE RELEASE OF OXAMNIQUINE FROM COATED PELLETS: GRAPH OF FRACTION RELEASED AGAINST TIME

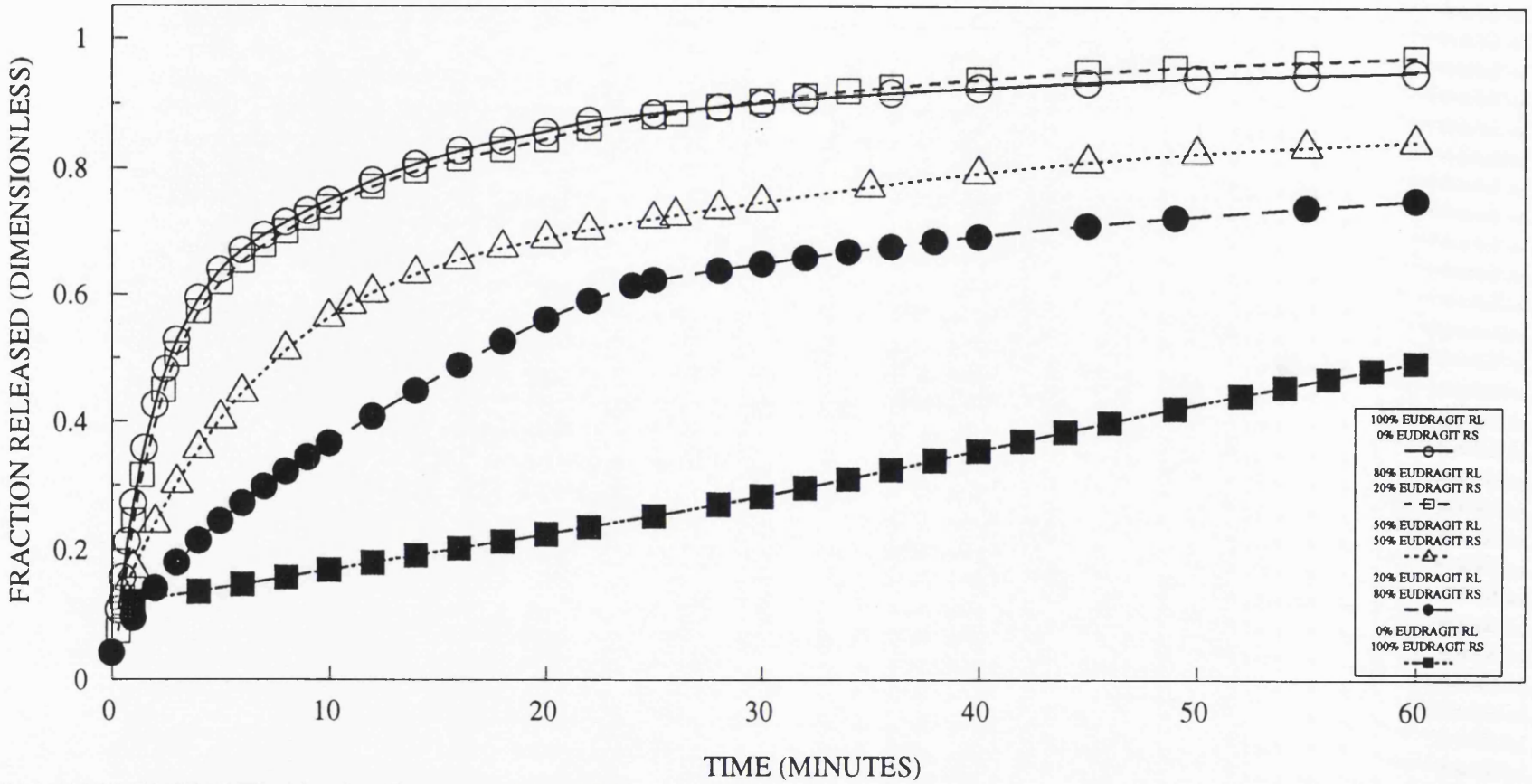

COATINGS CONTAINED 10% GLYCERYL TRIACETATE
AND 5% OXAMNIQUINE RELATIVE TO POLYMER WEIGHT
PELLET SIZE 14-18 US MESH

FIG 77: THE EFFECT OF POLYMER RATIO ON THE TIME TAKEN TO RELEASE OXAMNIQUINE FROM COATED PELLETS

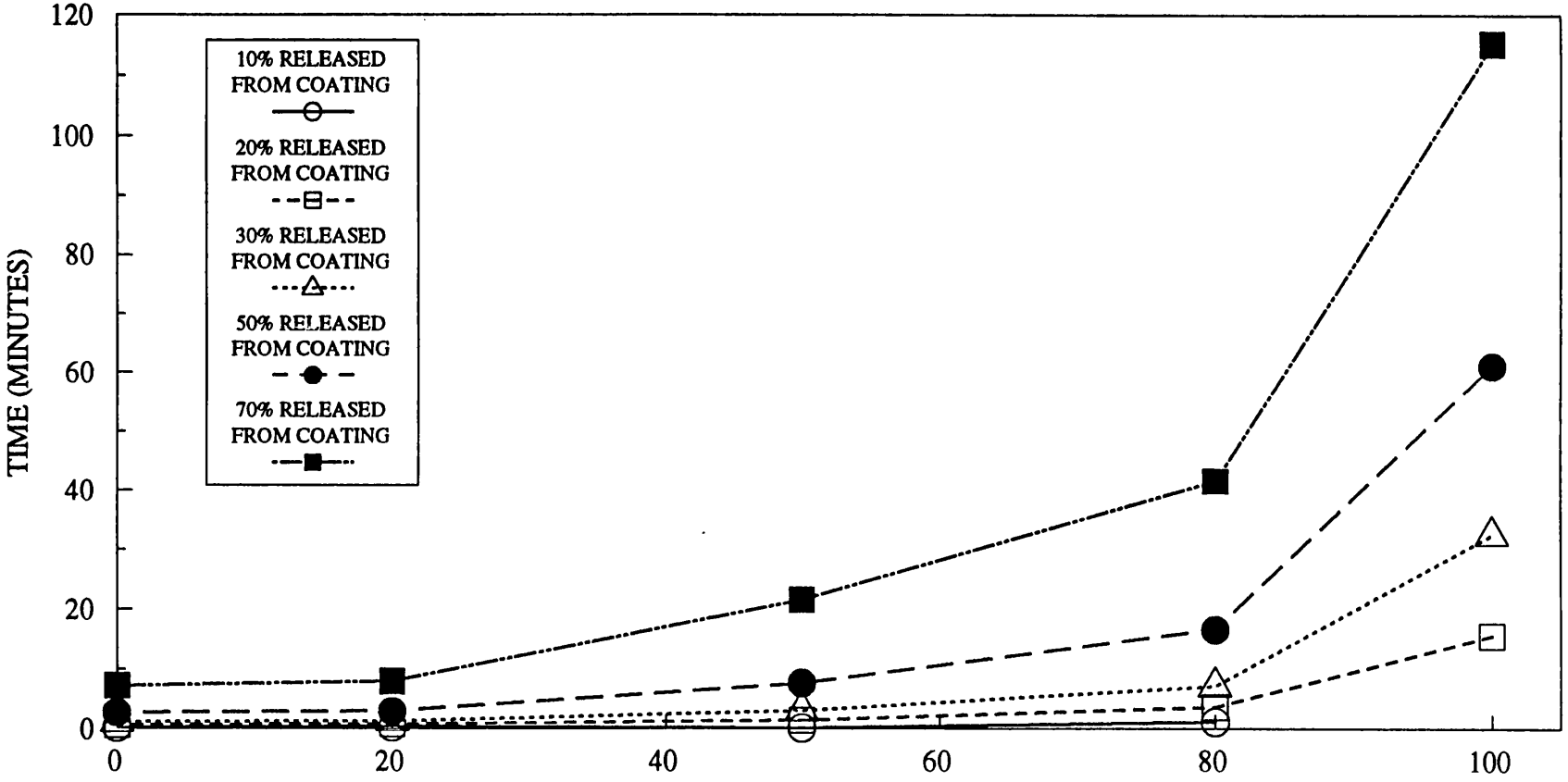

COATINGS CONTAINED 10% GLYCERYL TRIACETATE AND
5% OXAMNIQUINE RELATIVE TO POLYMER WEIGHT
PELLET SIZE 14-18 US MESH

This is evident when the ratio of Eudragit RL to Eudragit RS in the coating is 100:0 or 80:20. It is only when the coating contains no Eudragit RL that a low and approximately constant release rate is evident. The initial surge of release is apparently in agreement with Higuchi's prediction about the release from spherical matrices.

It is also interesting to note that the release of oxamniquine is more rapid from the spherical coatings than from planar films of equivalent composition. Whilst this may be explained by Higuchi's prediction it is also possible that the structure of the films are different. This will be discussed further in Section 5.10 where the surface structure of coated pellets is described.

Since the mechanism of oxamniquine release is important to these studies, release of oxamniquine from the coatings will be examined to see whether it can be described by any of the mathematical models detailed earlier in this chapter.

Figure 79 shows the fraction of oxamniquine released plotted as a function of √(time). If the matrix controlled model was applicable then these plots should be linear for up to 50% of the oxamniquine released.

Figure 79 shows that the matrix controlled model is apparently a good fit for the first 50% of oxamniquine

FIG 78: THE EFFECT OF POLYMER RATIO ON THE RELEASE OF OXAMNIQUINE FROM COATED PELLETS: GRAPH OF RATE OF FRACTIONAL RELEASE AGAINST TIME.

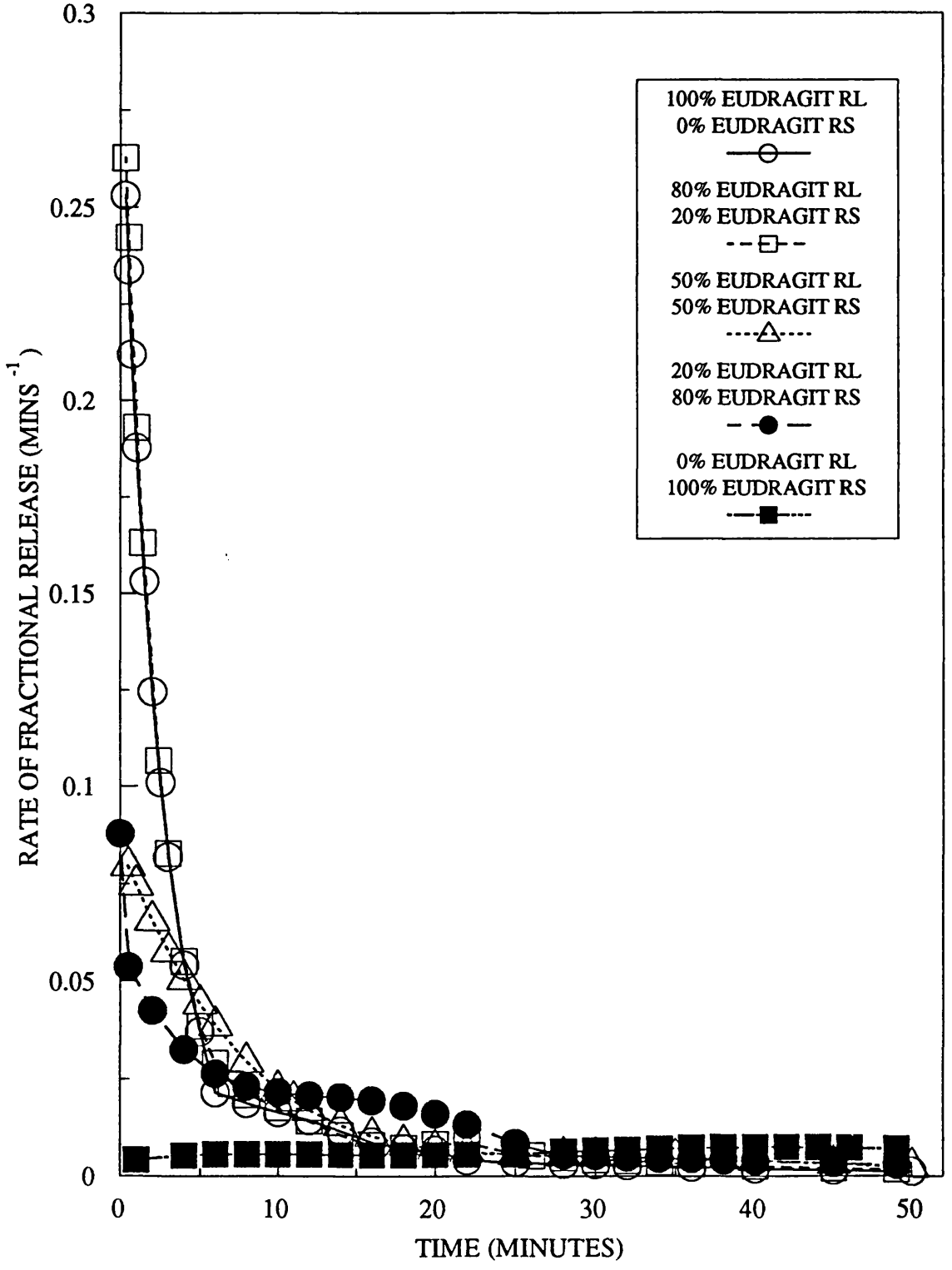

COATINGS CONTAINED 5% OXAMNIQUINE AND 10% GLYCERYL TRIACETATE RELATIVE TO TOTAL POLYMER WEIGHT. PELLET SIZE 14-18 US MESH.

release from the coatings, which contain at least 20% of Eudragit RL in the polymer mixture. In Figure 79 it can be seen that the linear relationship holds well for coatings containing up to 50% of Eudragit RS in the polymer mixture. There is some deviation from linearity when the coating composition contains 80% Eudragit RS. The curve is distinctly sigmoidal for the coating containing only Eudragit RS.

It is interesting to note that there is a slight lag time preceding the oxamniquine release. This effect is likely to be due to a delay in wetting the matrix.

Figure 80 shows fraction of oxamniquine remaining (log scale) plotted against time to evaluate the dissolution controlled model. The curves shown in Figure 80 suggest that although the dissolution controlled model may be a reasonable fit to the data for up to 50% of the oxamniquine. However, there is some curvature in the plots, which suggests that the matrix controlled model therefore appears to be a better fit to the data. This can be further tested using the differential rate plots shown in Figures 81 and 82.

These graphs indicate that the dissolution controlled model is a good fit to the release of oxamniquine from coatings containing up to 50% of Eudragit RS in the polymer mixture. When there is more than 50% of Eudragit RS in the polymer mixture, the dissolution controlled model appears to break

FIG 79: THE EFFECT OF POLYMER RATIO ON THE RELEASE OF OXAMNIQUINE FROM COATED PELLETS: GRAPH OF FRACTION RELEASED AGAINST ROOT TIME

PLOT TO EVALUATE THE MATRIX CONTROLLED RELEASE MODEL.

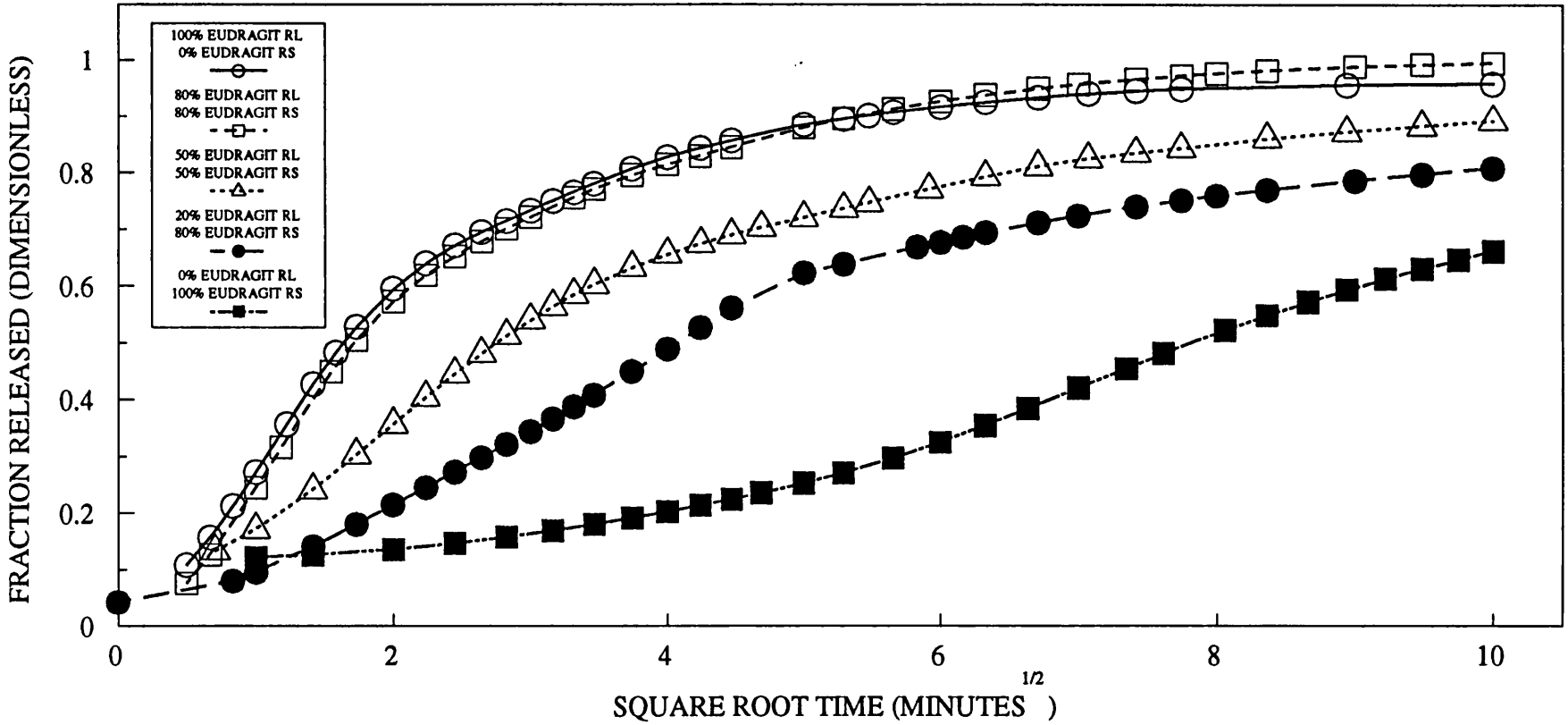

COATINGS CONTAINED 10% GLYCEYL TRIACETATE AND 5% OXAMNIQUINE RELATIVE TO POLYMER WEIGHT.
PELLET SIZE 14-18 US MESH.

FIG 80: THE EFFECT OF POLYMER RATIO ON THE RELEASE OF OXAMNIQUINE FROM COATED PELLETS: GRAPH OF LOG FRACTION REMAINING AGAINST TIME

PLOT TO EVALUATE THE DISSOLUTION CONTROLLED RELEASE MODEL.

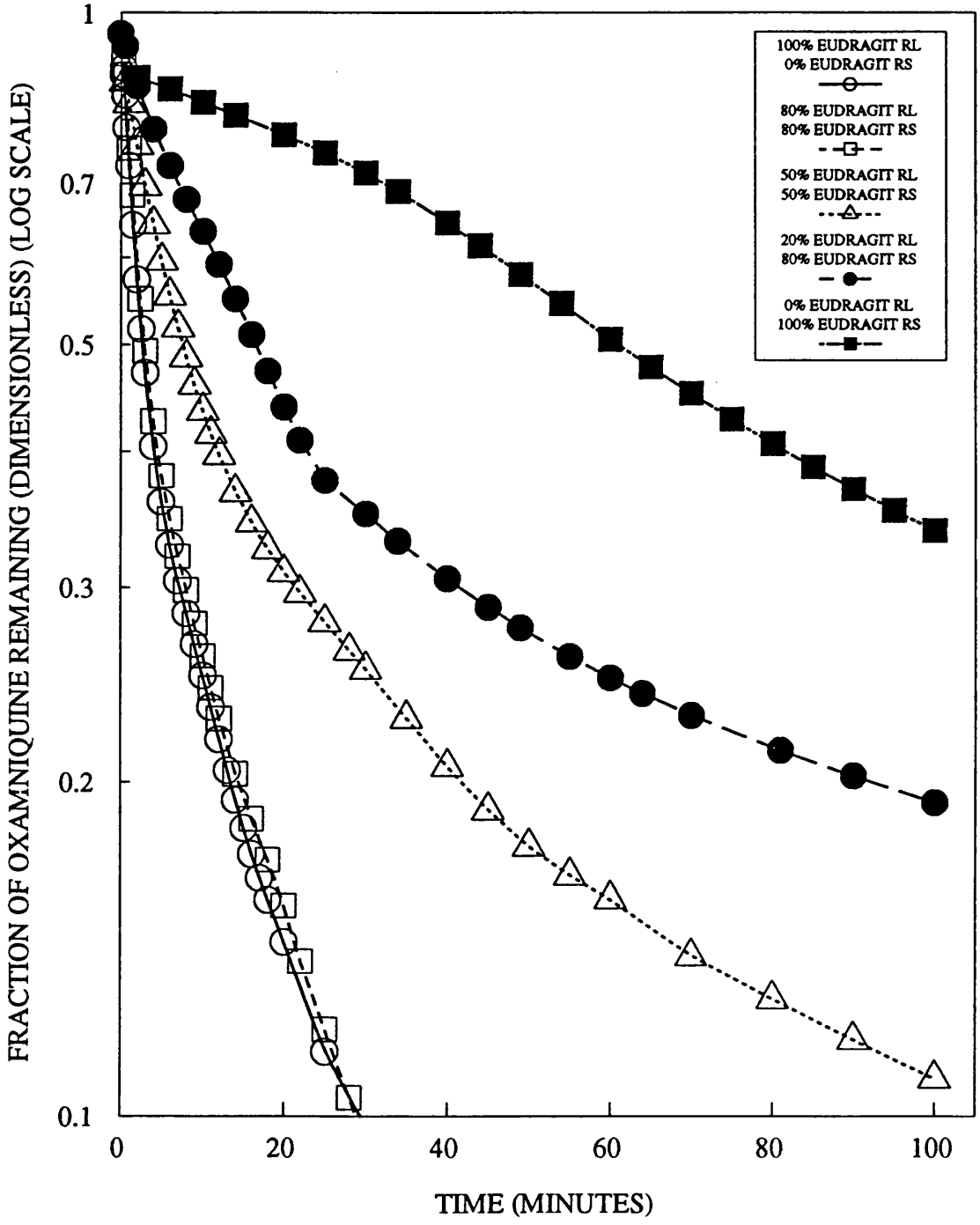

COATINGS CONTAINED 10% GLYCEYL TRIACETATE AND 5% OXAMNIQUINE RELATIVE TO POLYMER WEIGHT.
PELLET SIZE 14-18 US MESH.

FIG 81: THE EFFECT OF POLYMER RATIO ON THE RELEASE OF OXAMNIQUINE FROM COATED PELLETS: GRAPH OF RATE OF FRACTIONAL RELEASE AGAINST RECIPROCAL FRACTION RELEASED

DIFFERENTIAL RATE PLOT TO TEST THE VALIDITY OF THE MATRIX CONTROLLED MODEL.

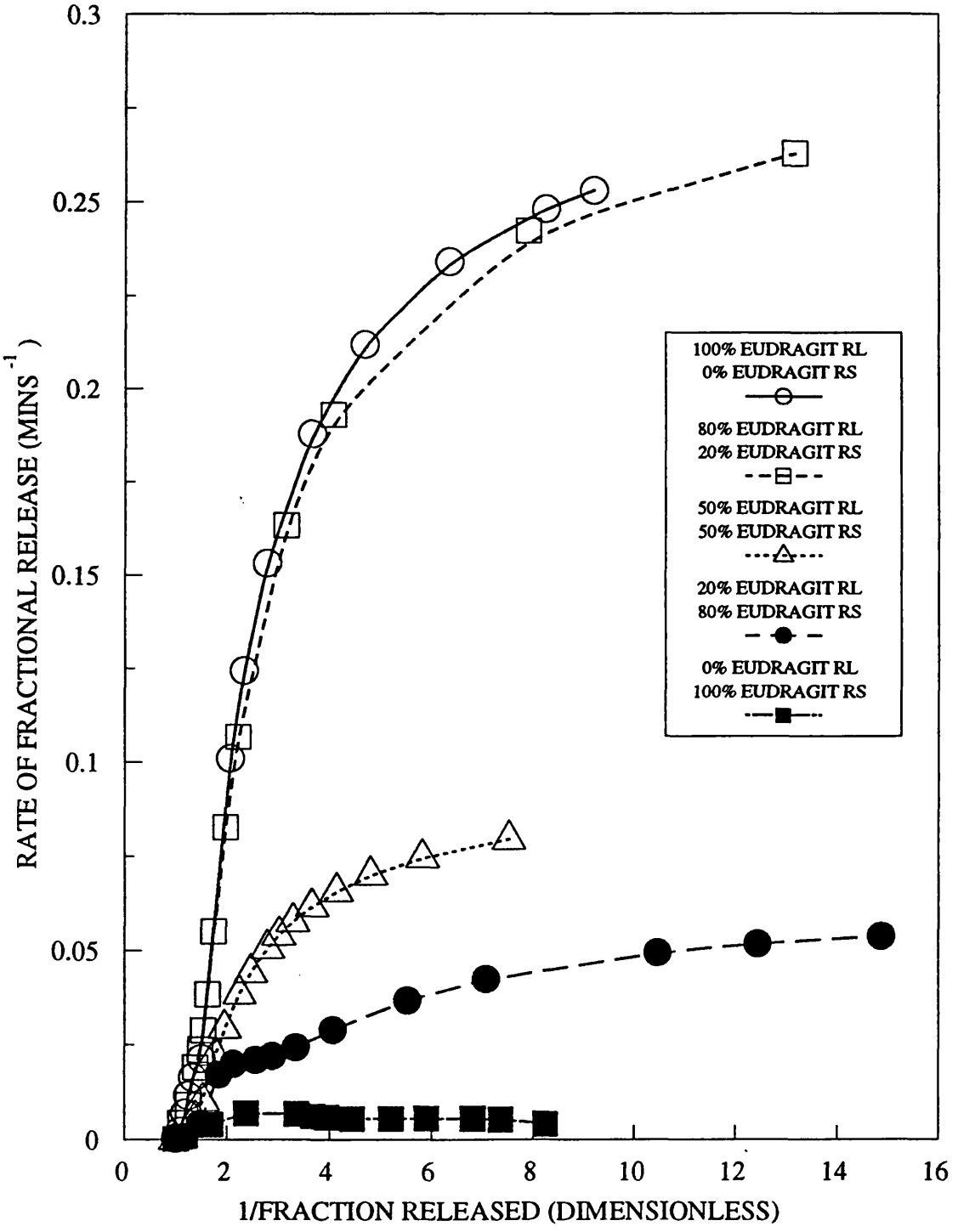

COATINGS CONTAINED 5% OXAMNIQUINE AND 10% GLYCERYL TRIACETATE RELATIVE TO TOTAL POLYMER WEIGHT. PELLET SIZE 14-18 US MESH.

FIG 82: THE EFFECT OF POLYMER RATIO ON THE RELEASE OF OXAMNIQUINE FROM COATED PELLETS: GRAPH OF RATE OF FRACTIONAL RELEASE AGAINST FRACTION RELEASED

DIFFERENTIAL RATE PLOT TO TEST THE VALIDITY OF THE DISSOLUTION CONTROLLED MODEL.

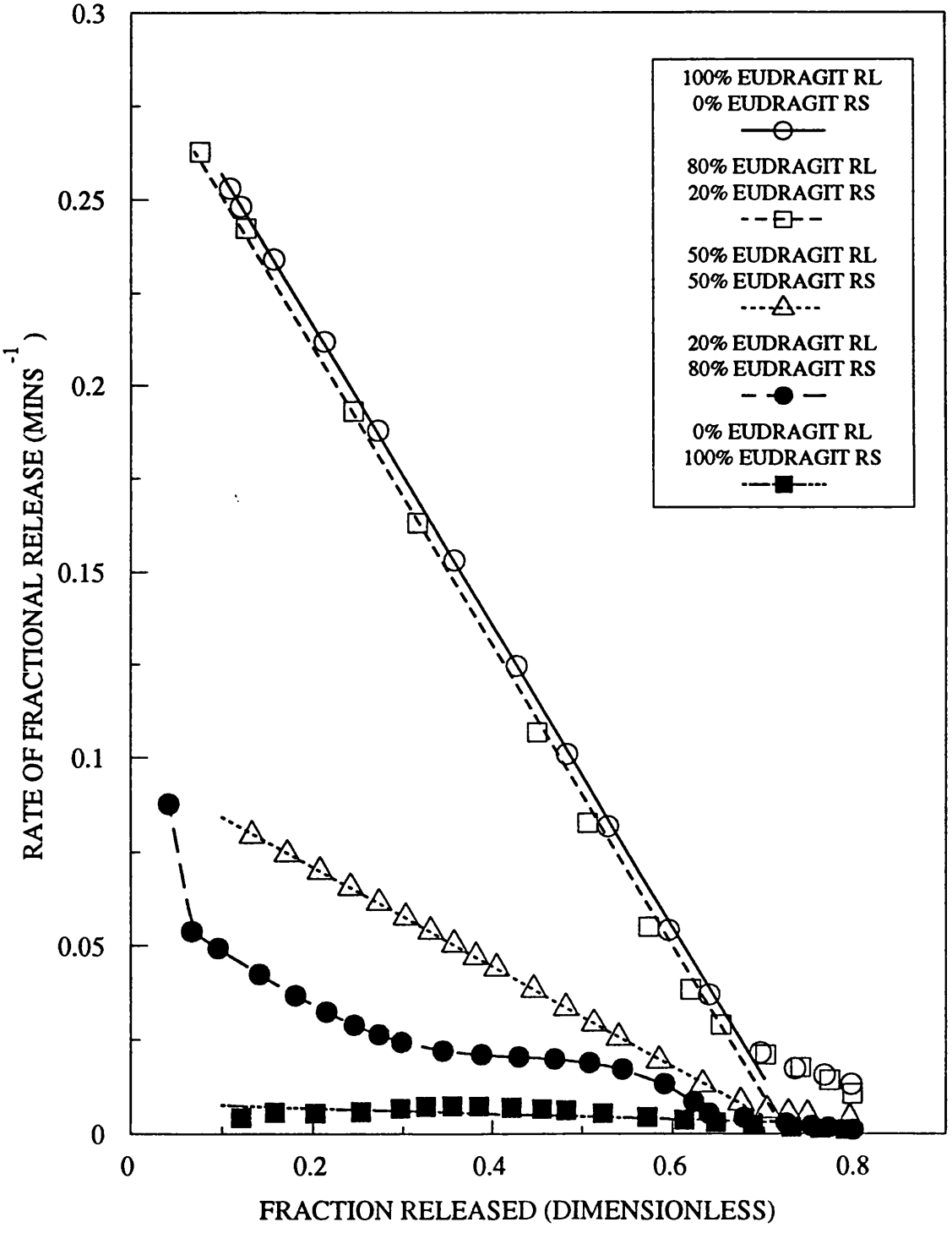

COATINGS CONTAINED 5% OXAMNIQUINE AND 10% GLYCERYL TRIACETATE RELATIVE TO TOTAL POLYMER WEIGHT. PELLET SIZE 14-18 US MESH.

down. The matrix controlled model does not appear to be applicable to any of these formulations.

This suggests that the differential rate plot method does not apply consistently to the systems tested. The methods described by DONBROW AND FRIEDMAN (1975a) were used to describe the effects on planar systems, and may not be applicable to spherical geometry, even up to 50% release where the kinetics are claimed to be analogous.

Coatings containing higher proportions of Eudragit RS in the polymer mixture do not appear to be adequately described by either matrix control or dissolution controlled kinetics. The reason for this is uncertain and requires further investigation.

5.9.3 The Effect of Glyceryl Triacetate Content

The coatings prepared to examine the effect of the relative proportion of Eudragit RL and RS contained 10%w/w glyceryl triacetate relative to polymer content as plasticiser.

The incorporation of plasticisers was shown to exert a significant effect on the release of oxamniquine from isolated films. To evaluate whether similar effects occurred with applied coatings, batches of pellets were spray coated with formulations containing up to 20%w/w relative to polymer content of glyceryl triacetate. The coatings contained equal proportions of Eudragit RL and

Eudragit RS and contained 5% w/w of oxamniquine relative to polymer content.

Figure 83 shows the fraction of oxamniquine released plotted as a function of time. As expected, the presence of glyceryl triacetate increases the extent of oxamniquine release from the coatings. Figure 84 shows that glyceryl triacetate also increase the rate of release of oxamniquine. There is little difference in the release behaviour of coatings containing 5% and 10% glyceryl triacetate. However, when the glyceryl triacetate content is increased to 20%, the amount and rate of oxamniquine release is significantly increased.

The rate of release of oxamniquine is initially high and diminishes rapidly. This is typical of matrix systems which have a source of drug not at constant thermodynamic activity and a receding diffusion boundary. With the unplasticised coating the release rate of oxamniquine diminishes more slowly. A possible explanation for this is that a significant proportion of the oxamniquine exists dissolved in the plasticiser within the coating and is then extracted from the coating with the plasticiser in an analogous manner to the free films. With unplasticised coatings, however, oxamniquine is released from the coatings only by diffusion from the matrix or by dissolution in the buffer solution in contact with the pellets.

Figure 85 shows the fraction of oxamniquine released as a function of √(time) to test the matrix controlled model. Figure 85 shows that for the first 50% of oxamniquine release the matrix controlled model may be an acceptable fit to this data tor each of these formulations since a linear relationship can be constructed. An intercept is apparent on the √(time) axis in Figure 85. This can be considered to be a measure of a 'lag time' or time to allow penetration of the aqueous buffer into the coating. Although this lag time is very short, it is notable that they are shorter for the more hydrophillic plasticised coatings.

Graphs to examine the applicability of the dissolution controlled model are shown in Figure 86. Comparing Figures 85 and 86 for the first 50% of oxamniquine release implies that either the matrix or dissolution controlled models may be equally valid. Application of the differential rate plots should determine which of the models best applies. Figures 87 and 88 show the differential rate plots to test the applicability of the dissolution and matrix controlled models respectively.

The differential rate plot to test the matrix controlled model shows significant curvature which indicates that this model is not applicable. The differential rate plots to test the dissolution controlled model shows linear relationships for the plasticised coatings. However, both of the rate plots show curvature for the unplasticised

FIG 83: THE EFFECT OF GLYCERYL TRIACETATE CONTENT ON THE RELEASE OF OXAMNIQUINE FROM COATED PELLETS: GRAPH OF FRACTION RELEASED AGAINST TIME.

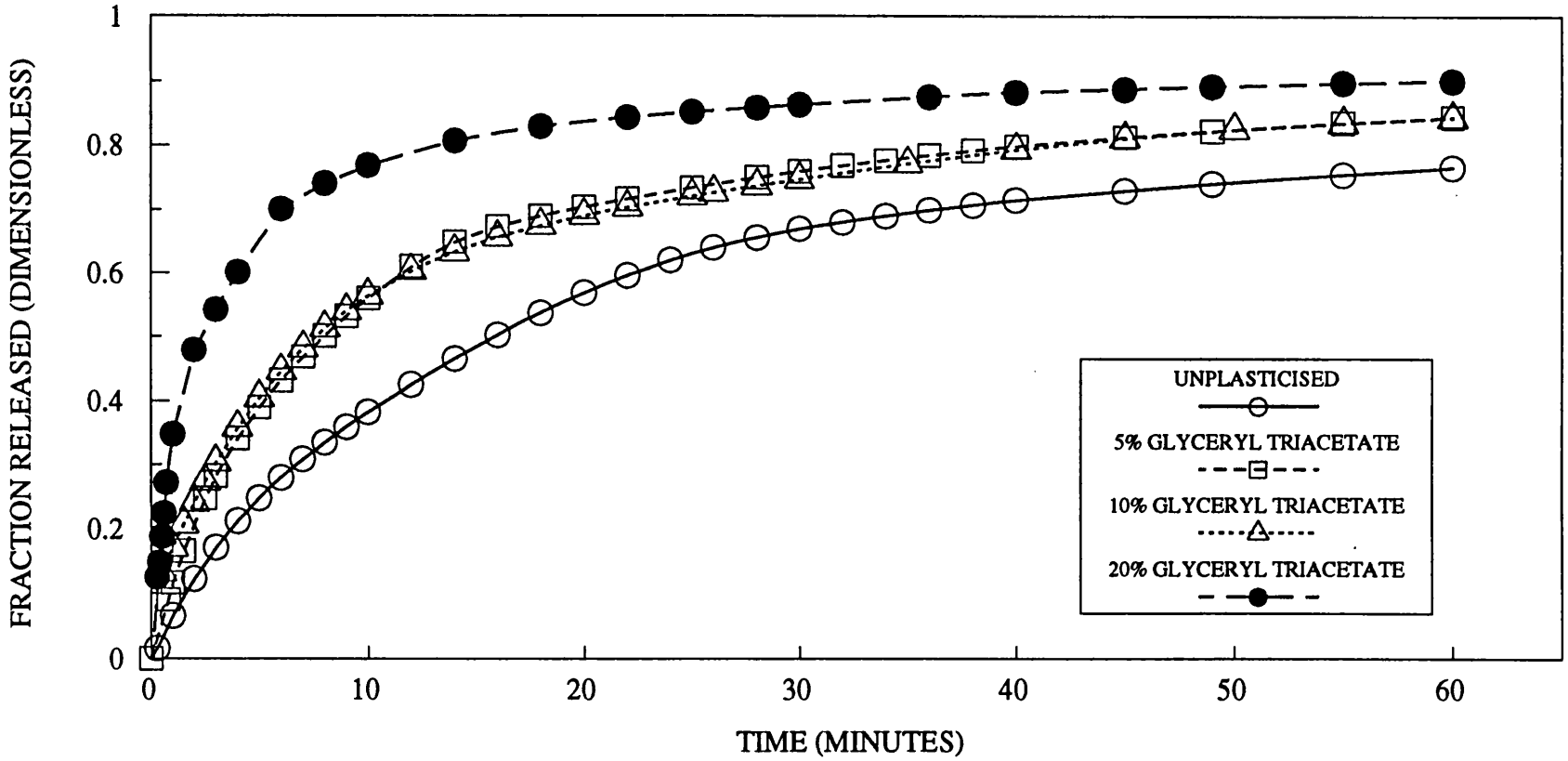

COATINGS CONTAINED EQUAL PROPORTIONS OF EUDRAGIT RL AND RS WITH 5% OXAMNIQUINE RELATIVE TO POLYMER WEIGHT. PELLET SIZE 14-18 US MESH.

FIG 84: THE EFFECT OF GLYCERYL TRIACETATE CONTENT ON THE RELEASE OF OXAMNIQUINE FROM COATED PELLETS: GRAPH OF RATE OF FRACTIONAL RELEASE AGAINST TIME

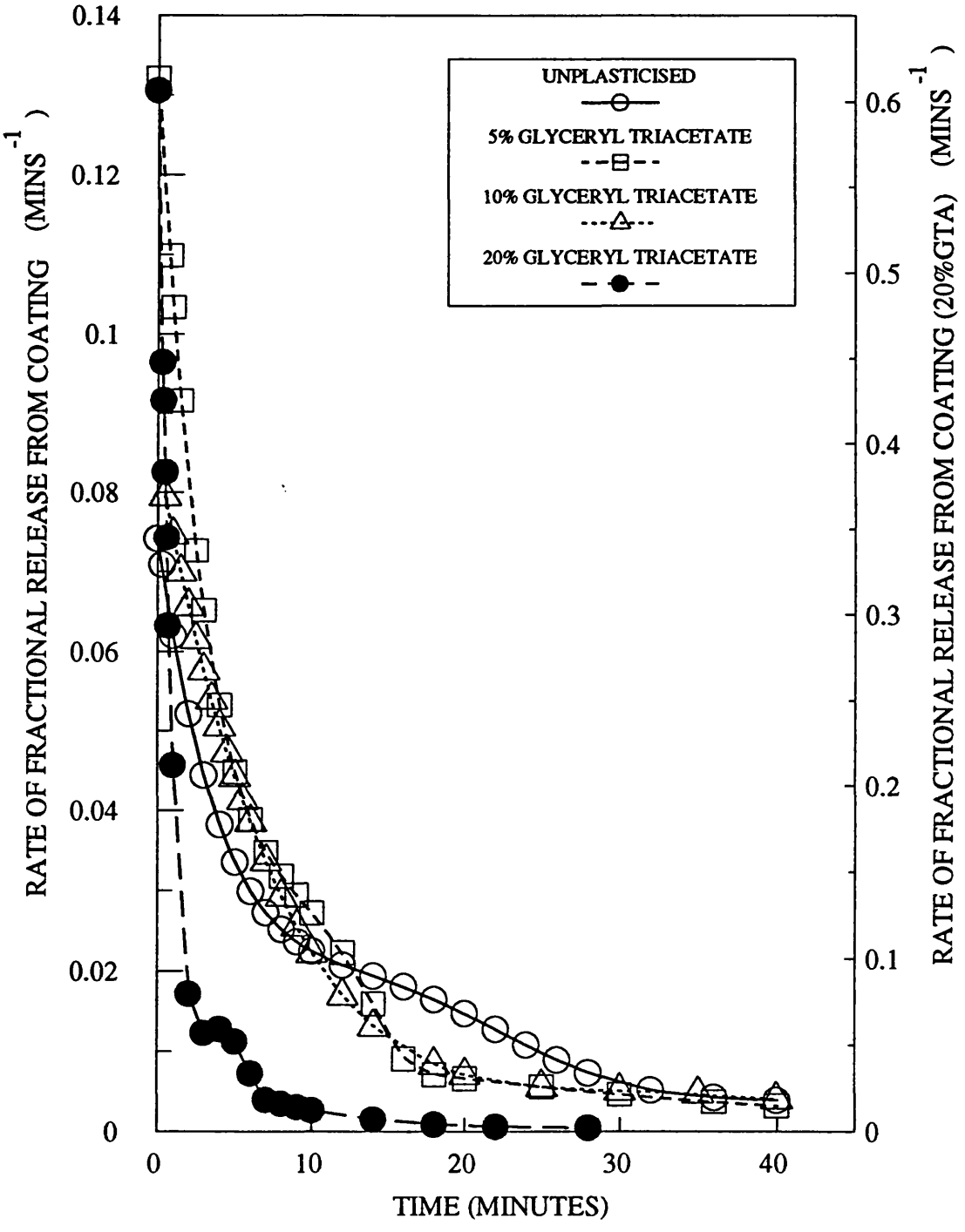

COATINGS CONTAINED EQUAL PROPORTIONS OF EUDRAGIT RL AND RS WITH 5% OXAMNIQUINE RELATIVE TO POLYMER WEIGHT. PELLET SIZE 14-18 US MESH.

FIG 85: THE EFFECT OF GLYCERYL TRIACETATE CONTENT ON THE RELEASE OF OXAMNIQUINE FROM COATED PELLETS: GRAPH OF FRACTION RELEASED AGAINST SQUARE ROOT TIME

PLOT TO TEST THE VALIDITY OF THE MATRIX CONTROLLED MODEL

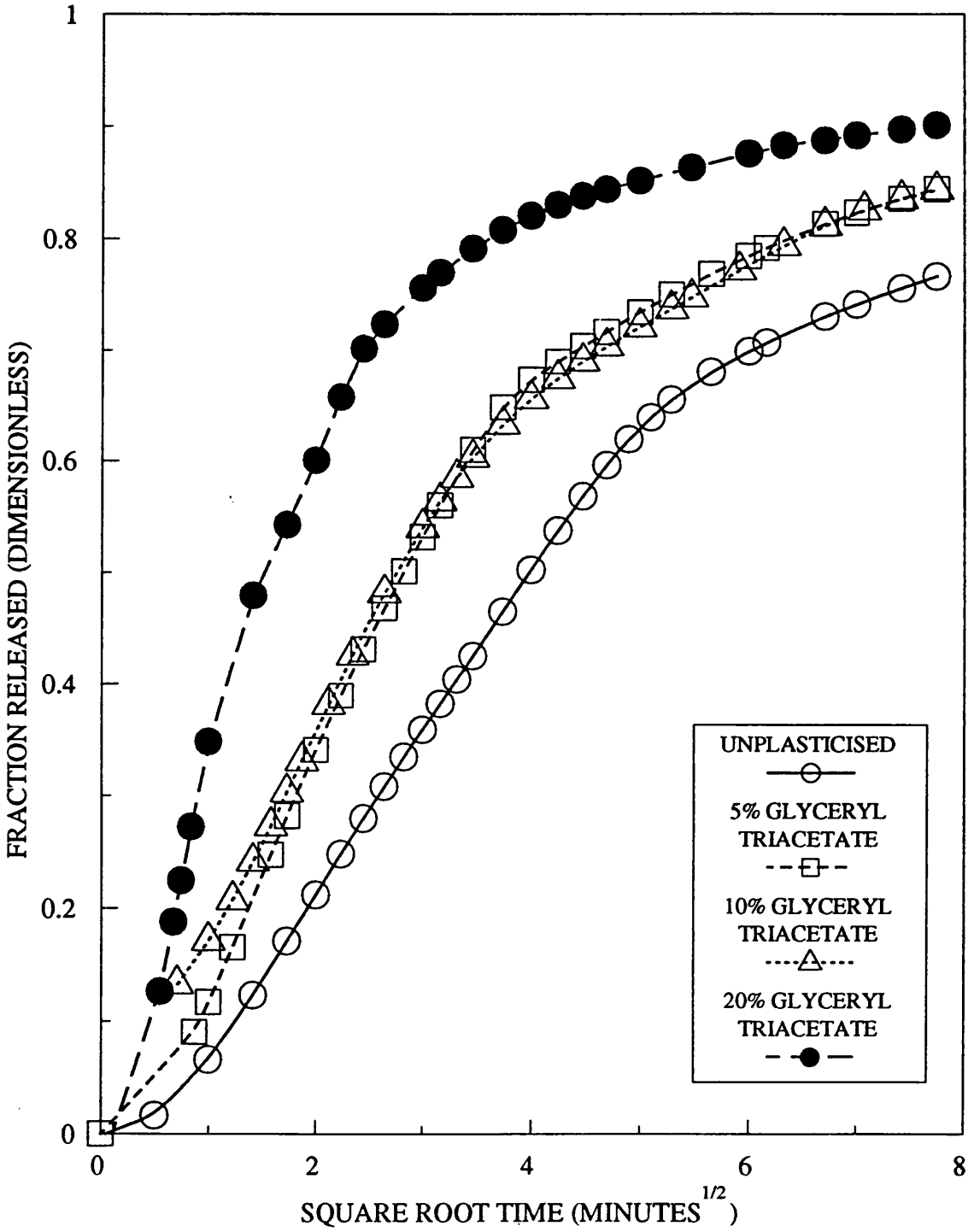

COATINGS CONTAINED EQUAL PROPORTIONS OF EUDRAGIT RL AND RS WITH 5% OXAMNIQUINE RELATIVE TO TOTAL POLYMER WEIGHT. PELLET SIZE 14-18 US MESH.

FIG 86: THE EFFECT OF GLYCERYL TRIACETATE CONTENT ON THE RELEASE OF OXAMNIQUINE FROM COATED PELLETS: GRAPH OF LOG FRACTION REMAINING IN COATING AGAINST TIME

PLOT TO TEST THE VALIDITY OF THE DISSOLUTION CONTROLLED MODEL

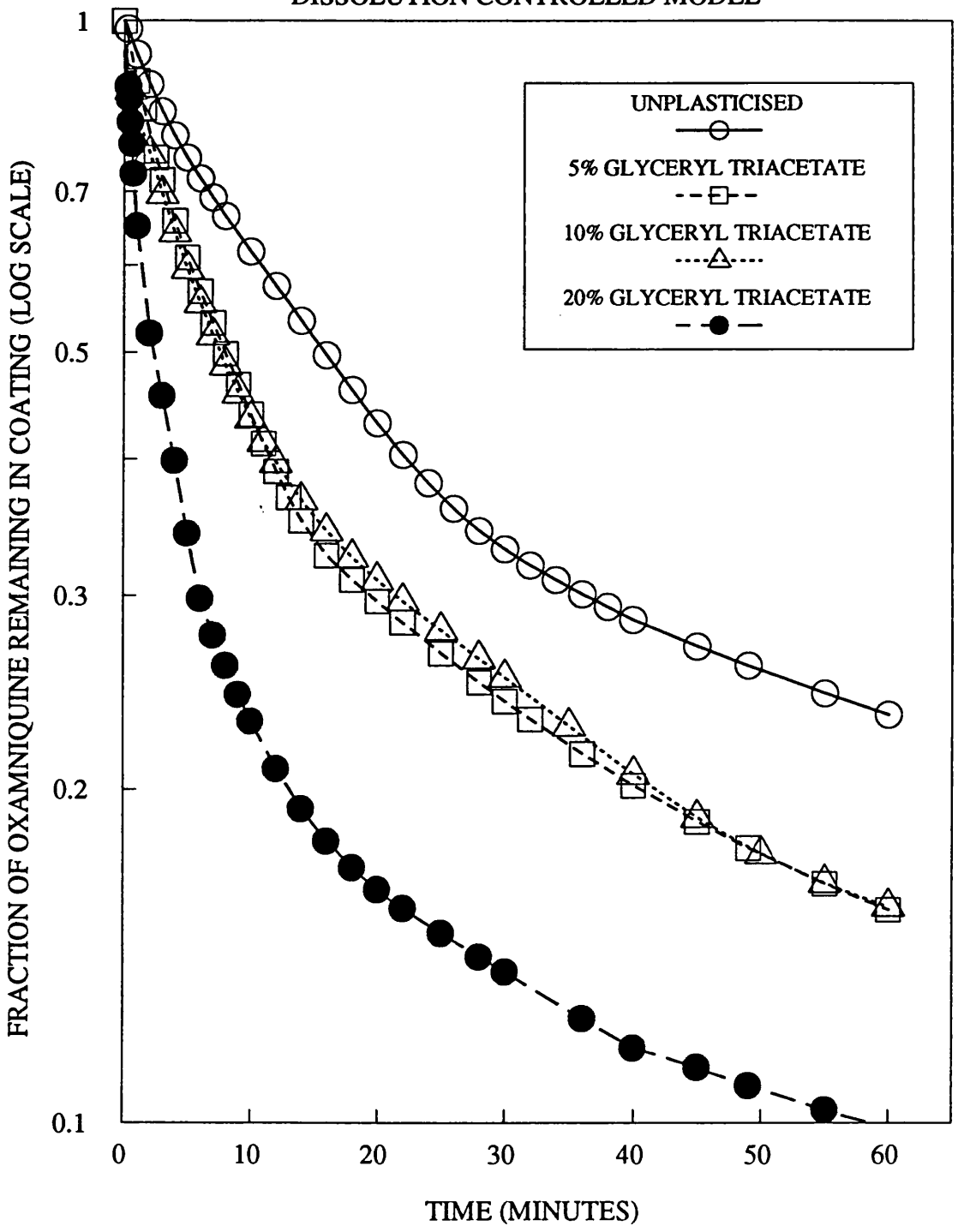

COATINGS CONTAINED EQUAL PROPORTIONS OF EUDRAGIT RL AND RS WITH 5% OXAMNIQUINE RELATIVE TO POLYMER WEIGHT. PELLET SIZE 14-18 US MESH.

FIG 87:THE EFFECT OF GLYCERYL TRIACETATE CONTENT ON THE RELEASE OF OXAMNIQUINE FROM COATED PELLETS: GRAPH OF RATE OF FRACTIONAL RELEASE AGAINST FRACTION RELEASED

DIFFERENTIAL RATE PLOT TO TEST THE VALIDITY OF THE DISSOLUTION CONTROLLED MODEL

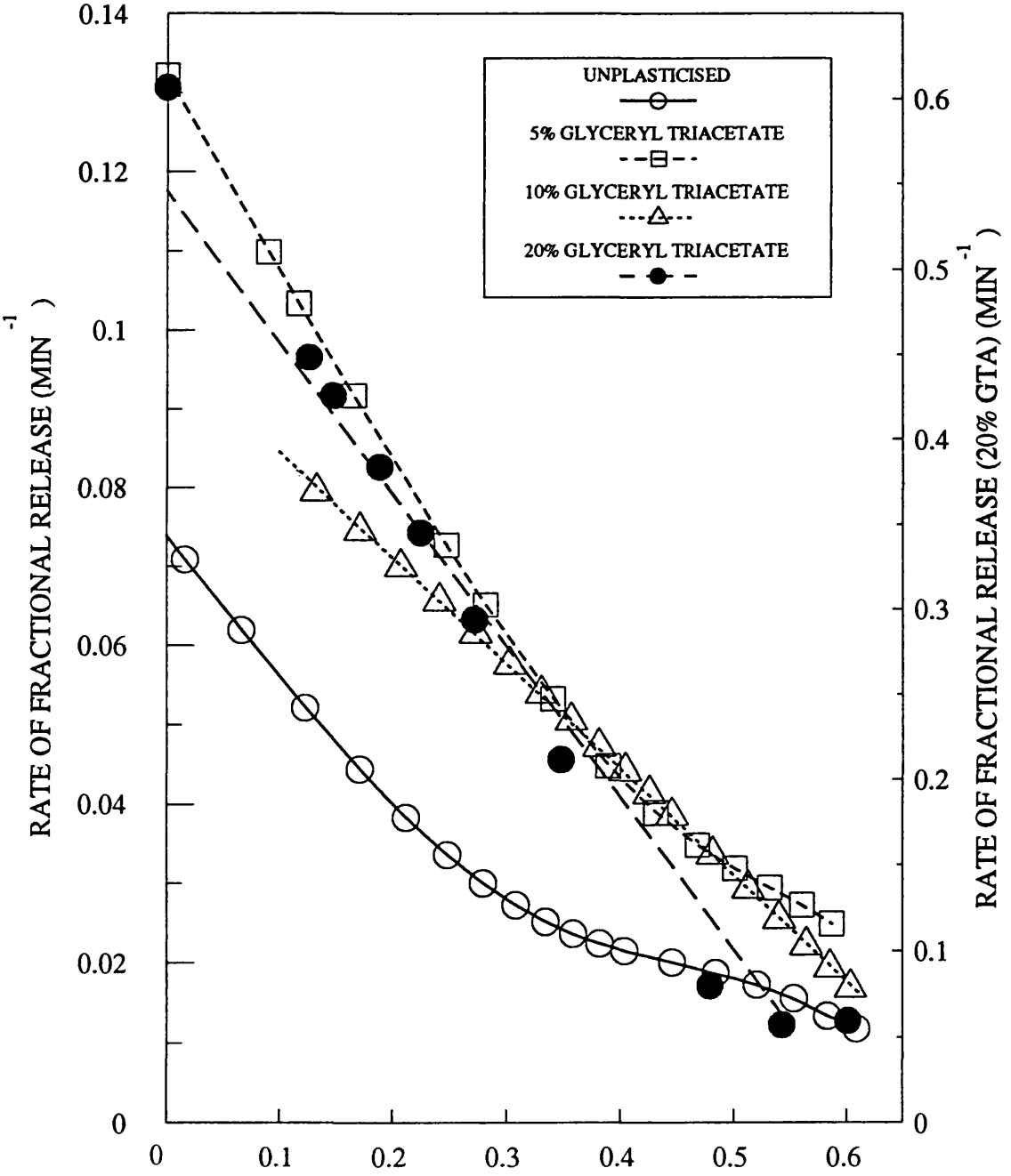

COATINGS CONTAINED EQUAL PROPORTIONS OF EUDRAGIT RL AND RS WITH 5% OXAMNIQUINE RELATIVE TO POLYMER WEIGHT. PELLET SIZE 14-18 US MESH.

FIG 88: THE EFFECT OF GLYCERYL TRIACETATE CONTENT ON THE RELEASE OF OXAMNIQUINE FROM COATED PELLETS:GRAPH OF RATE OF FRACTIONAL RELEASE AGAINST RECIPROCAL FRACTION RELEASED

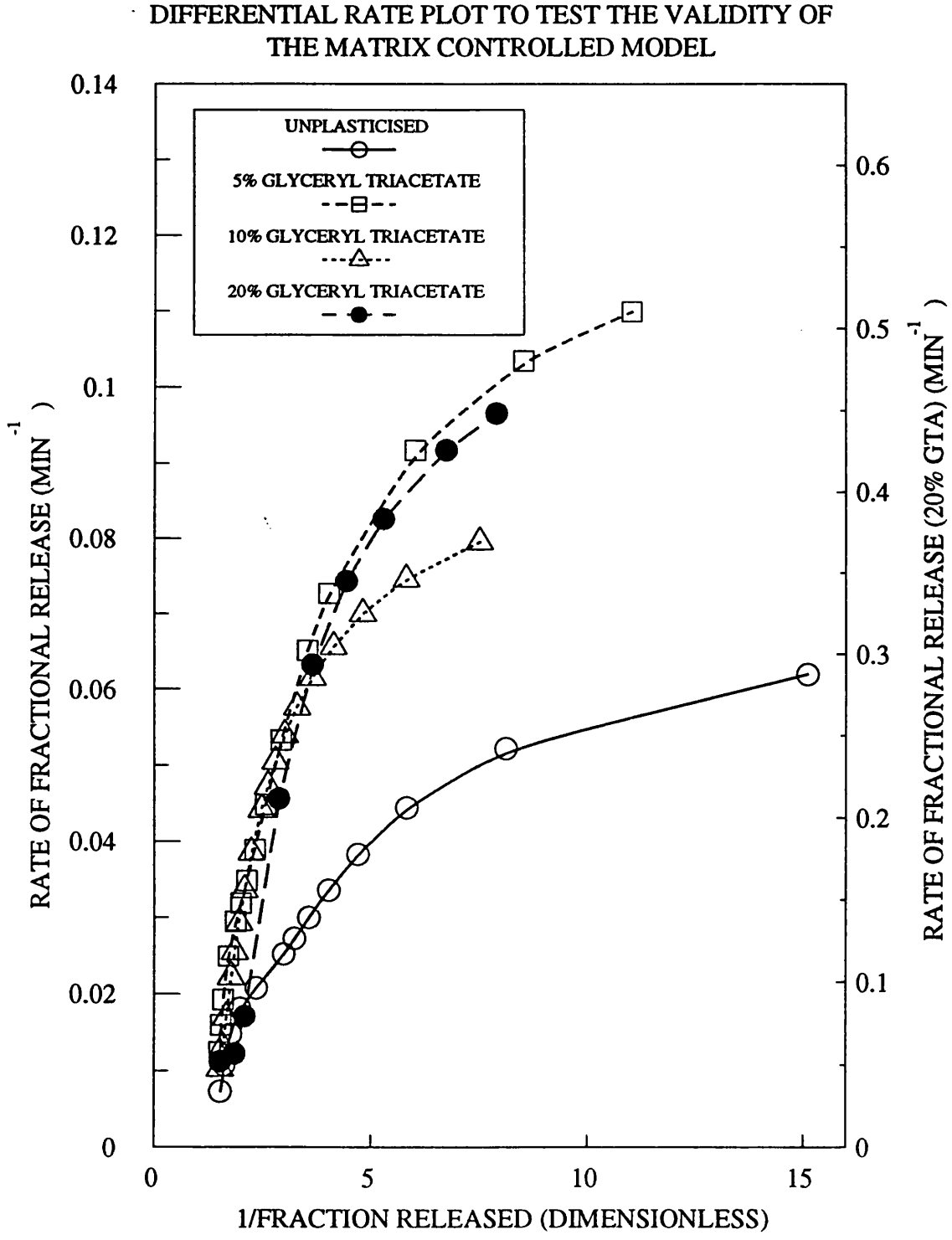

COATINGS CONTAINED EQUAL PROPORTIONS OF EUDRAGIT RL AND RS WITH 5% OXAMNIQUINE RELATIVE TO POLYMER WEIGHT. PELLET SIZE 14-18 US MESH.

coating which implies that neither of the models are directly applicable.

Another model may be applicable to describe the kinetics. This is the Hixson-Crowell cube root law. This law has been applied to the release of water soluble compounds from ethyl cellulose microcapsules by BENITA AND DONBROW (1982). This law which was derived by HIXSON AND CROWELL (1931) may describe the oxamniquine from coated pellets since

(i) access of the extracting medium is enhanced by the formation of pores,

(ii) the surface area of the extracting boundary decreases,

(iii) the shape of the pellet remains unchanged,

(iv) sink conditions are maintained throughout the experiment.

This law can be expressed by equation 33

$$W^{1/3} = W_o^{1/3} - kt \qquad (33)$$

where W is the amount of drug remaining in the pellets at time t

W_o is the initial amount of drug in the pellet

k is a constant

k is defined by equation 34

$$k = \frac{DC_s}{\rho h}\left[\frac{4\pi\rho}{3}\right]^{1/3} \qquad (34)$$

where D = diffusion coefficient and

C_s = solubility of the drug in the dissolution medium

ρ = density of the dissolution medium

h = thickness of any unstirred boundary layer.

A plot of $W^{1/3}$ against t would be linear if the Hixson-Crowell cube root law was applicable. Figure 89 shows such a series of plots for coatings plasticised with glyceryl triacetate. The curvature of the lines demonstrates that the Hixson-Crowell law is not applicable to oxamniquine release from these coated pellets.

In summary, dissolution controlled kinetics appears to describe the release of oxamniquine from coated pellets plasticised with glyceryl triacetate. From the Higuchi type plots, matrix controlled kinetics apparently describe the release from the unplasticised coating.

This is not supported by the differential rate plots which suggest that neither model describes release from the unplasticised coating. The dissolution controlled model is quite feasible where the oxamniquine content of the coating is partially dissolved in the plasticiser which is extracted from the coating by the dissolution medium.

5.9.4 The Effect of Plasticiser Solubility and Oxamniquine Solubility in Plasticisers

In Section 5.5.3, the type of plasticiser included in formulations of isolated Eudragit films was demonstrated to influence significantly the kinetics of oxamniquine release from these films. It was proposed that a combination of the solubility of the plasticiser in the extracting medium

FIG 89: THE EFFECT OF GLYCERYL TRIACETATE CONTENT ON THE RELEASE OF OXAMNIQUINE FROM COATED PELLETS: GRAPH OF CUBE ROOT FRACTION REMAINING IN COATING AGAINST TIME

PLOT TO TEST THE VALIDITY OF THE HIXSON-CROWELL CUBE ROOT LAW

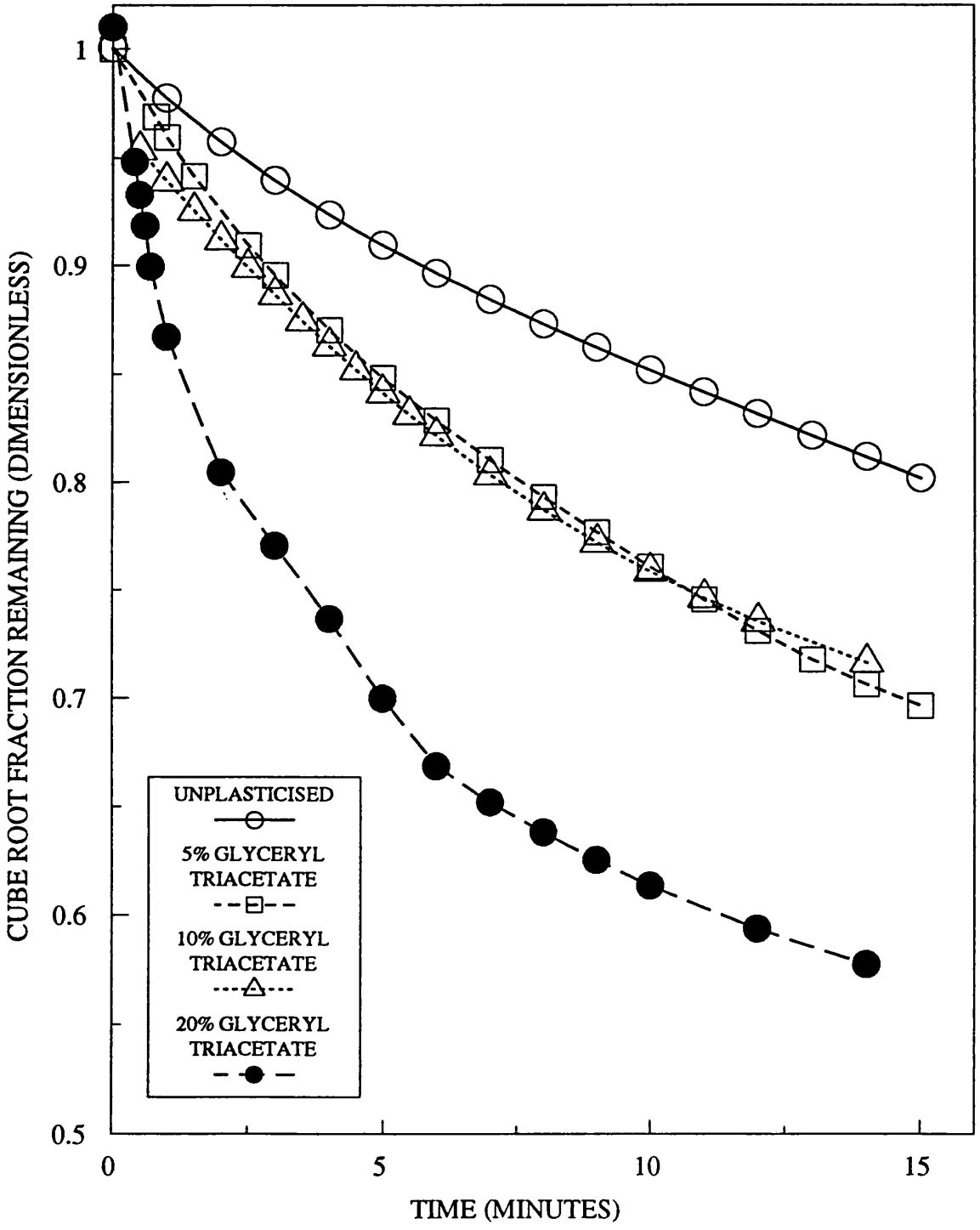

COATINGS CONTAINED EQUAL PROPORTIONS OF EUDRAGIT RL AND RS WITH 5% OXAMNIQUINE RELATIVE TO TOTAL POLYMER WEIGHT. PELLET SIZE 14-18 US MESH.

and the solubility of oxamniquine in the plasticiser determined the release kinetics.

Experiments were performed to determine whether similar effects occurred with coatings of equivalent composition to the isolated films applied to pellets. Batches of pellets were coated with films containing equal proportions of Eudragit RL and RS with 5%w/w oxamniquine and 10% w/w plasticiser (both relative to total polymer content). Plasticisers tested were as detailed in Section 5.5.3.

Figure 90 shows the release of oxamniquine from these coated pellets plotted against time. Clearly inclusion of any of the plasticisers tested increases the rate and extent of oxamniquine release from the coatings. Table 23 summarises the time taken to release between 10% and 70% of the oxamniquine for each of the plasticisers tested.

TABLE 23 **SUMMARY OF TIME TAKEN TO RELEASE BETWEEN 10% AND 70% OF OXAMNIQUINE CONTENT FROM PLASTICISED COATINGS APPLIED TO PELLETS**

Plasticiser Type	Time Taken To Release 10% of Oxamniquine Content from Coating (min)				
	10%	20%	30%	50%	70%
Unplasticised	1.57	3.69	6.70	15.85	36.37
Glyceryl Triacetate	0.09	1.39	2.95	7.57	21.50
Polyethylene Glycol 400	0.21	0.63	1.35	8.00	19.48
Dimethyl Phthalate	0.44	1.07	2.20	6.01	13.29
Diethyl Phthalate	0.35	0.85	1.67	5.94	15.49
Dibutyl Phthalate	0.25	0.57	1.12	5.46	12.72

Figure 91 shows the rate of fractional release of

oxamniquine from the coated plotted against time and Table 24 summarises the rate of release at 10%, 20%, 30%, 50% and 70% of the oxamniquine release for each of the plasticisers tested.

TABLE 24 **SUMMARY OF RATES OF RELEASE OF OXAMNIQUINE BETWEEN 10% AND 70% OXAMNIQUINE RELEASE FROM PLASTICISED COATINGS APPLIED TO PELLETS**

Plasticiser Type	Rate of Release of Oxamniquine after 10% 20% 30% 50% 70% of Oxamniquine released ($min^{-1} \times 10^{-3}$)				
Unplasticised	56.08	40.00	27.98	18.17	4.19
Glyceryl Triacetate	83.66	70.98	58.00	31.08	6.42
Polyethylene Glycol 400	282.28	195.37	92.81	26.60	9.24
Dimethyl Phthalate	195.57	124.54	63.75	51.99	14.47
Diethyl Phthalate	235.91	164.13	90.02	42.76	8.57
Dibutyl Phthalate	359.80	249.44	130.38	39.00	17.33

The first 10% of oxamniquine is released more rapidly from coatings containing the water miscible plasticisers than from those containing water immiscible plasticisers. For the water immiscible plasticisers, it appears that the less soluble the plasticiser is in the buffer, the more rapidly oxamniquine is released from the coating. This relationship is broadly correct for the release of up to 50% of oxamniquine content from the coatings. A similar trend can be seen with the rates of release. Generally the highest rate of release is seen from dibutyl phthalate plasticised coatings, whereas the slowest release is seen from glyceryl triacetate plasticised coatings. Dibutyl phthalate has the highest affinity for oxamniquine and is the least water miscible, which would suggest that oxamniquine would be retained in these coatings. However,

FIG 90: THE EFFECT OF PLASTICISERS ON THE RELEASE OF OXAMNIQUINE FROM COATED PELLETS: GRAPH OF FRACTION RELEASED AGAINST TIME.

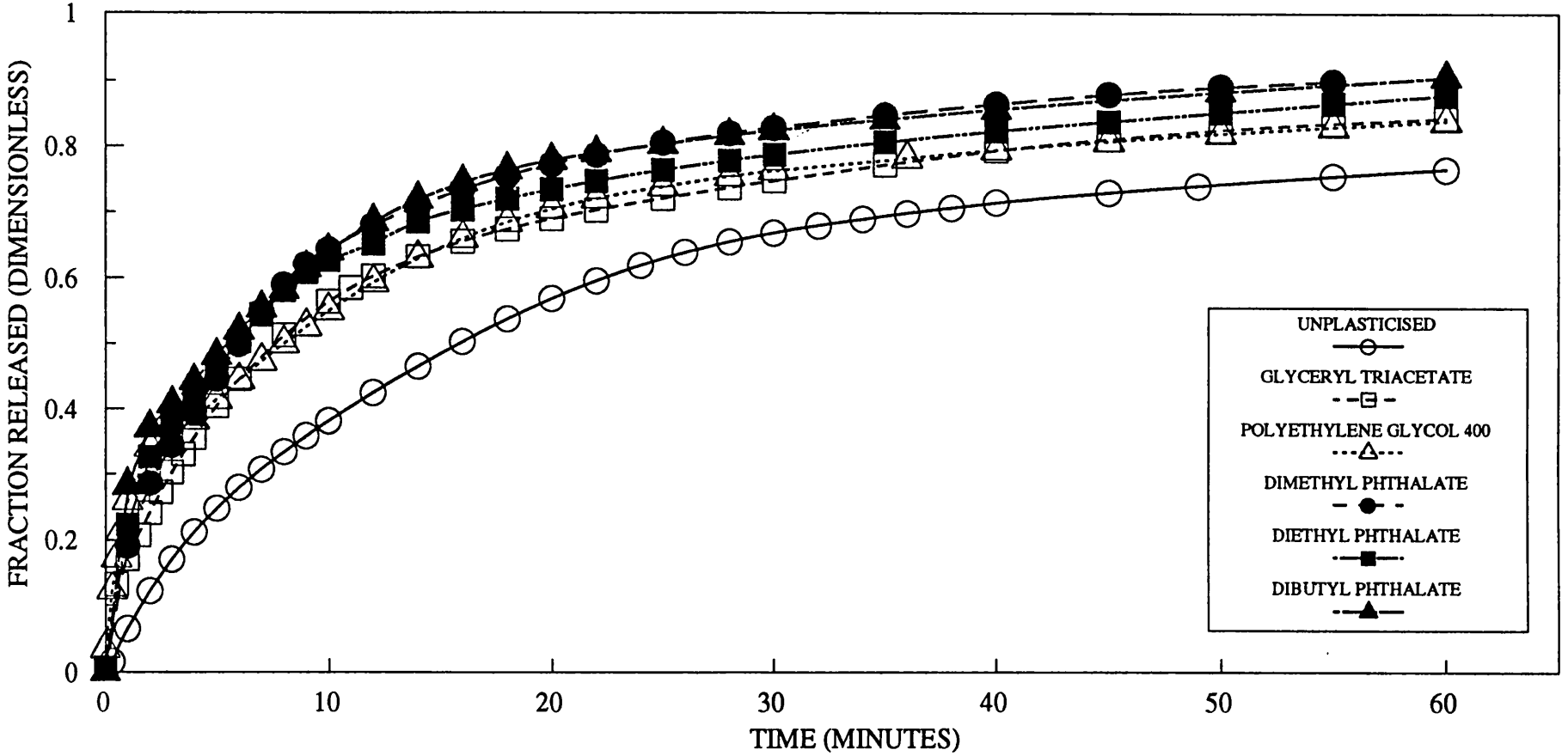

COATINGS CONTAINED EQUAL PROPORTIONS OF EUDRAGIT RL AND RS WITH 10% PLASTICISER AND 5% OXAMNIQUINE RELATIVE TO TOTAL POLYMER WEIGHT.

FIG 91:THE EFFECT OF PLASTICISERS ON THE RELEASE OF OXAMNIQUINE FROM COATED PELLETS: GRAPH OF RATE OF FRACTIONAL RELEASE AGAINST TIME

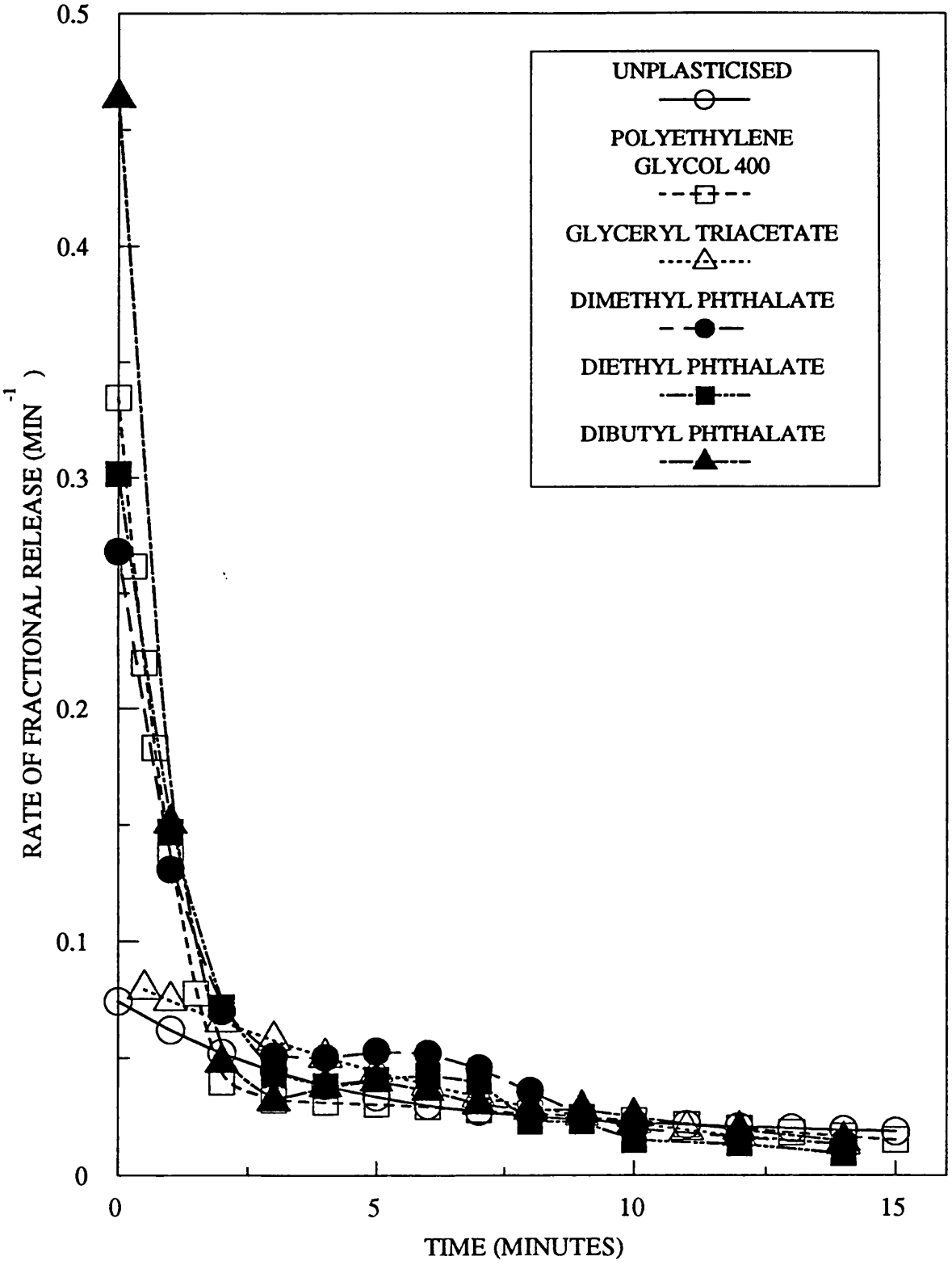

COATINGS CONTAINED EQUAL PROPORTIONS OF EUDRAGIT RL AND RS WITH 5% OXAMNIQUINE AND 10% PLASTICISER RELATIVE TO TOTAL POLYMER WEIGHT. PELLET SIZE 14-18 US MESH

it would appear that partitioning of oxamniquine between the aqueous buffer and plasticiser within the coating extracts oxamniquine more efficiently than when the plasticiser is rapidly removed from the matrix.

The situation present with dimethyl and diethyl phthalates is more complex as discussed in Section 5.5.3. Figure 92 shows the release of dimethyl and diethyl phthalate from coated pellets. The plasticiser release was analysed simultaneously with oxamniquine release by HPLC, using the method and assay described in Chapter 3.

It is evident that the more water soluble dimethyl phthalate is extracted from the coatings faster than diethyl phthalate. In another experiment dibutyl phthalate release could not be detected from coated pellets. Since the HPLC method had been validated for detecting dibutyl phthalate, it is apparent that this plasticiser is retained within the coating for the duration of the release experiments.

Figure 93 shows the release of oxamniquine from the pellets plotted against $\sqrt{(time)}$ to evaluate the matrix controlled model. The matrix controlled model appears to be a good fit to the data for all of the plasticisers except PEG 400 and dibutyl phthalate.

Figure 94 shows graphs to test the dissolution controlled model.

FIG 92: THE RELEASE OF WATER IMMISCIBLE PLASTICISERS FROM COATED PELLETS CONTAINING OXAMNIQUINE: GRAPH OF FRACTION OF PLASTICISER RELEASED AGAINST TIME

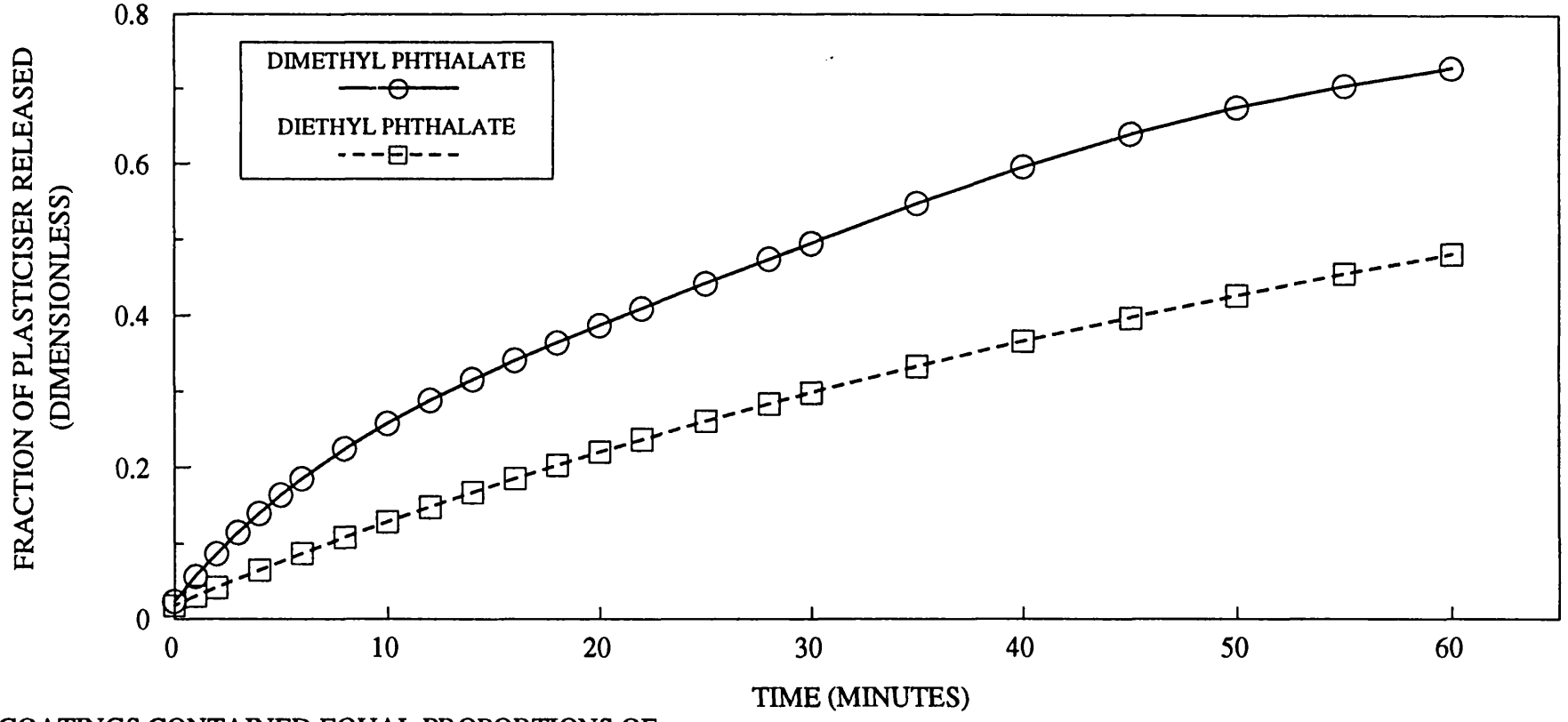

COATINGS CONTAINED EQUAL PROPORTIONS OF EUDRAGIT RL AND RS WITH 5% OXAMNIQUINE AND 10% PLASTICISER RELATIVE TO POLYMER WEIGHT.
PELLET SIZE 14-18 US MESH

FIG 93:THE EFFECT OF PLASTICISERS ON THE RELEASE OF OXAMNIQUINE FROM COATED PELLETS: GRAPH OF FRACTION RELEASED AGAINST SQUARE ROOT TIME

PLOT TO TEST THE VALIDITY OF THE MATRIX CONTROLLED MODEL.

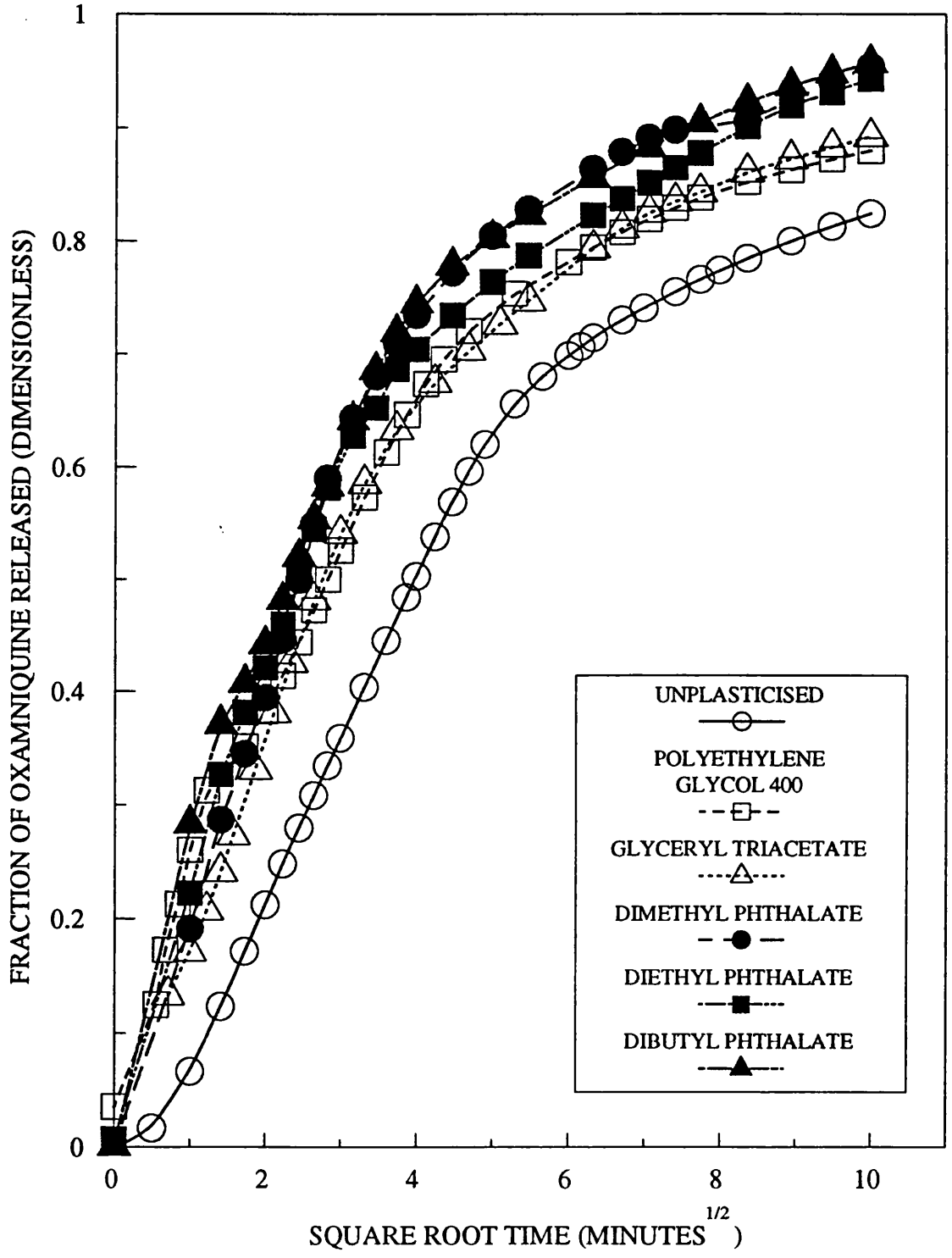

COATINGS CONTAINED EQUAL PROPORTIONS OF EUDRAGIT RL AND RS WITH 5% OXAMNIQUINE AND 10% PLASTICISER RELATIVE TO TOTAL POLYMER WEIGHT. PELLET SIZE 14-18 US MESH

FIG 94:THE EFFECT OF PLASTICISERS ON THE RELEASE OF OXAMNIQUINE FROM COATED PELLETS: GRAPH OF LOG FRACTION REMAINING IN COATING AGAINST TIME

PLOT TO TEST THE VALIDITY OF THE DISSOLUTION CONTROLLED MODEL.

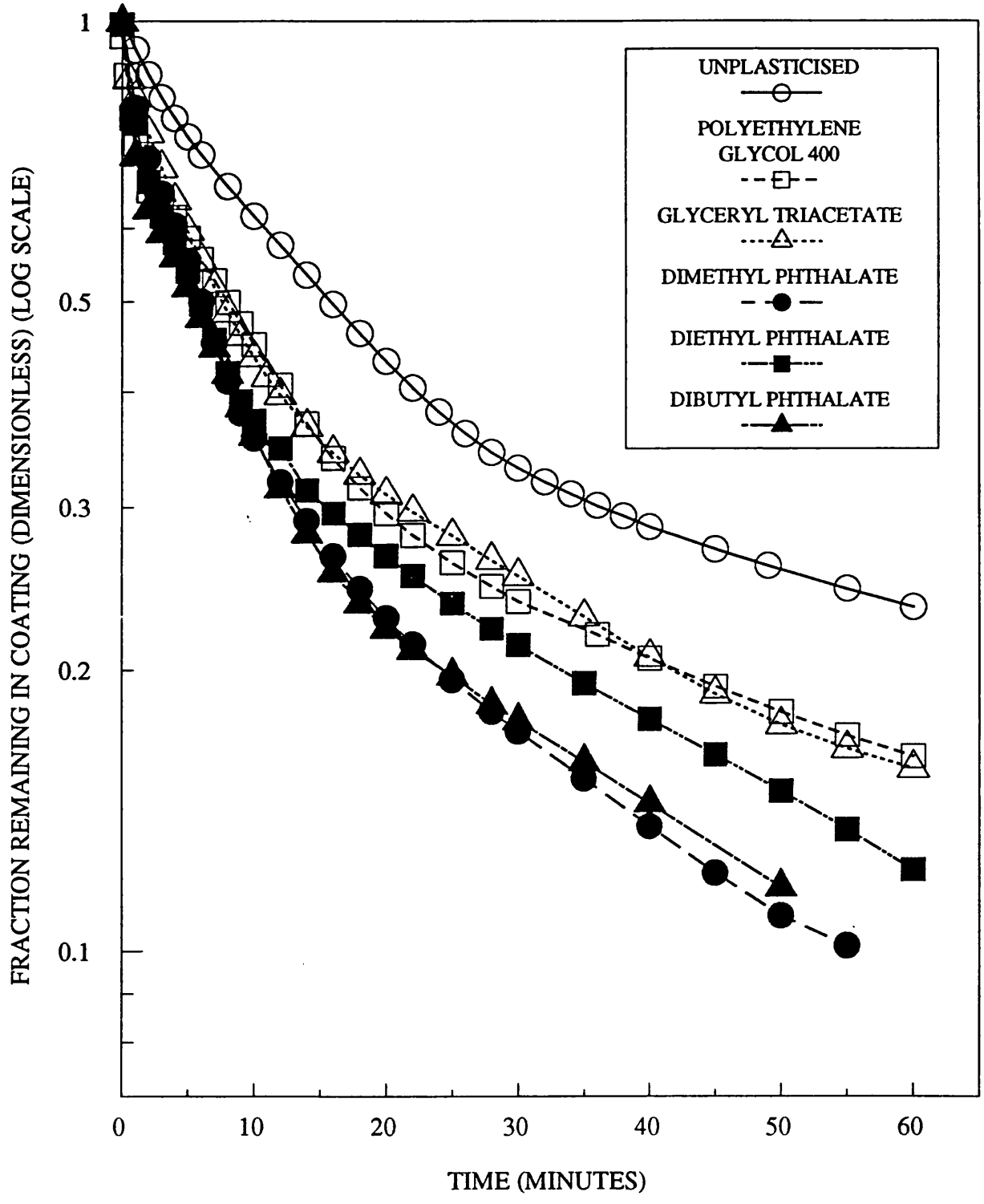

COATINGS CONTAINED EQUAL PROPORTIONS OF EUDRAGIT RL AND RS WITH 5% OXAMNIQUINE AND 10% PLASTICISER RELATIVE TO TOTAL POLYMER WEIGHT. PELLET SIZE 14-18 US MESH

FIG 95: THE EFFECT OF PLASTICISERS ON THE RELEASE OF OXAMNIQUINE FROM COATED PELLETS: GRAPH OF CUBE ROOT FRACTION REMAINING IN COATING AGAINST TIME

PLOT TO TEST THE VALIDITY OF THE HIXSON-CROWELL CUBE ROOT LAW

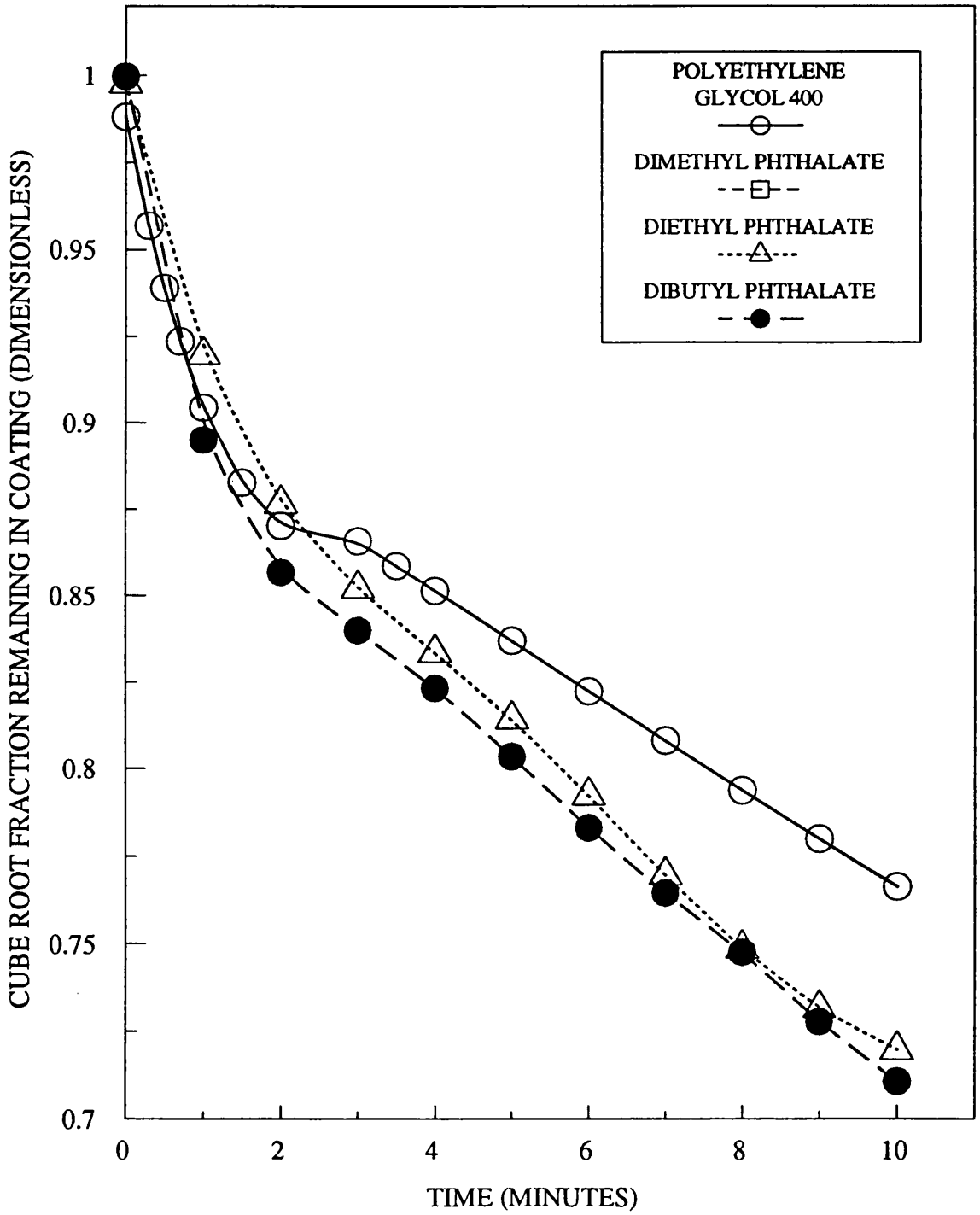

COATINGS CONTAINED EQUAL PROPORTIONS OF EUDRAGIT RL AND RS WITH 5% OXAMNIQUINE AND 10% PLASTICISER RELATIVE TO POLYMER WEIGHT. PELLET SIZE 14-18 US MESH

The dissolution controlled model appears not to describe the release of oxamniquine other than from unplasticised coatings or those containing glyceryl triacetate.

Figure 95 shows the data plotted to evaluate the Hixson-Crowell cube root law. The curvature of the lines indicates that this model does not describe oxamniquine release from these coating formulations. The release of oxamniquine from unplasticised coatings and coatings plasticised with glyceryl triacetate have been previously established not to fit this model.

To summarise, the following hypotheses have been made concerning oxamniquine release from coatings containing plasticisers.

1. Unplasticised coatings and coatings plasticised with glyceryl triacetate fit both the matrix and dissolution control modes.

2. Coatings plasticised with dimethyl or diethyl phthalate fit only the matrix controlled model.

3. PEG 400 and dibutyl phthalate plasticised coatings do not fit either model.

Figures 96 and 97 show differential rate plots to test these observations further.

Oxamniquine release from glyceryl triacetate plasticised coatings more closely fits the dissolution controlled model than the matrix controlled model. Release from unplasticised coatings does not conclusively fit either model, but is closer to the dissolution control than matrix control. With the other plasticisers the mechanism of release is uncertain. For PEG 400 plasticised coatings, release of the initial 30% of the oxamniquine content appears to be under dissolution control. There follows a period where the rate of release of oxamniquine does not change significantly. It is possible that these events may represent an initial surge of oxamniquine which is located at or near the surface of the coating, followed by a more prolonged release of the remaining oxamniquine from the coating which has lost substantially all of its plasticiser.

The release from phthalate containing coatings is even more complex. The differential rate plots suggest that neither the dissolution controlled or the matrix controlled model adequately describe the release kinetics.

For all of these formulations, the rate of release falls initially, and then starts to rise after approximately 40% of the oxamniquine has been released. This may be again related to the presence of oxamniquine near to the surface of the coating which is initially released fairly rapidly followed by a more protracted release of the remaining drug. In the case of phthalate plasticised coatings, this

is complicated by the possibility of partitioning between the plasticiser and the dissolution medium both within and at the surface of the coating as well as the prolonged liberation of the plasticiser itself. It may therefore be concluded that either the formulations tested or the experimental conditions used to determine the release kinetics do not exactly meet the conditions imposed by the model being evaluated, and that the true release mechanism is uncertain.

It is, however, of further interest to examine whether the release of the plasticisers dimethyl or diethyl phthalate from the coatings can be described by either the matrix controlled or dissolution models. Figures 98 and 99 show graphs to test these models. It appears that the dissolution controlled model best describes the release of dimethyl phthalate from the coatings, whereas the matrix controlled model best describes the release of diethyl phthalate from the coatings.

Figures 100 and 101 show the corresponding differential rate plots for these data.

The differential rate plots confirm these conclusions adequately but not with the accuracy predicted by DONBROW AND FRIEDMAN (1975a), from which it would be expected that the matrix controlled differential rate plot for dimethyl phthalate plasticised coatings would be linear. The significant deviation from linearity observed may be due

FIG 96: THE EFFECT OF PLASTICISERS ON THE RELEASE OF OXAMNIQUINE FROM COATED PELLETS: GRAPH OF RATE OF FRACTIONAL RELEASE AGAINST RECIPROCAL FRACTION RELEASED

DIFFERENTIAL RATE PLOT TO EXAMINE THE VALIDITY OF THE MATRIX CONTROLLED MODEL.

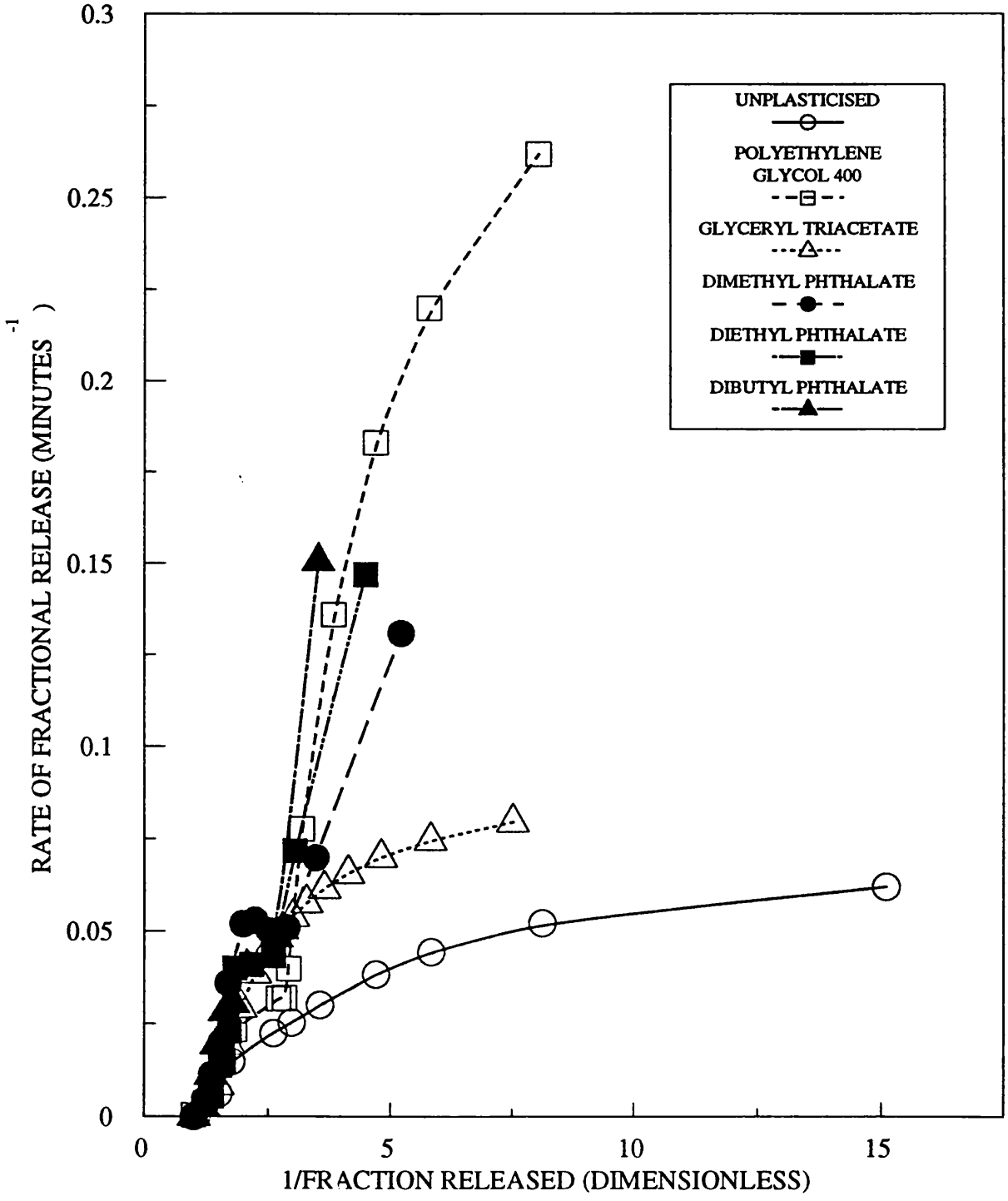

COATINGS CONTAINED EQUAL PROPORTIONS OF EUDRAGIT RL AND RS WITH 5% OXAMNIQUINE AND 10% PLASTICISER RELATIVE TO POLYMER WEIGHT. PELLET SIZE 14-18 US MESH

FIG 97: THE EFFECT OF PLASTICISERS ON THE RELEASE OF OXAMNIQUINE FROM COATED PELLETS: GRAPH OF RATE OF FRACTIONAL RELEASE AGAINST FRACTION RELEASED

DIFFERENTIAL RATE PLOT TO TEST THE VALIDITY OF THE DISSOLUTION CONTROLLED MODEL.

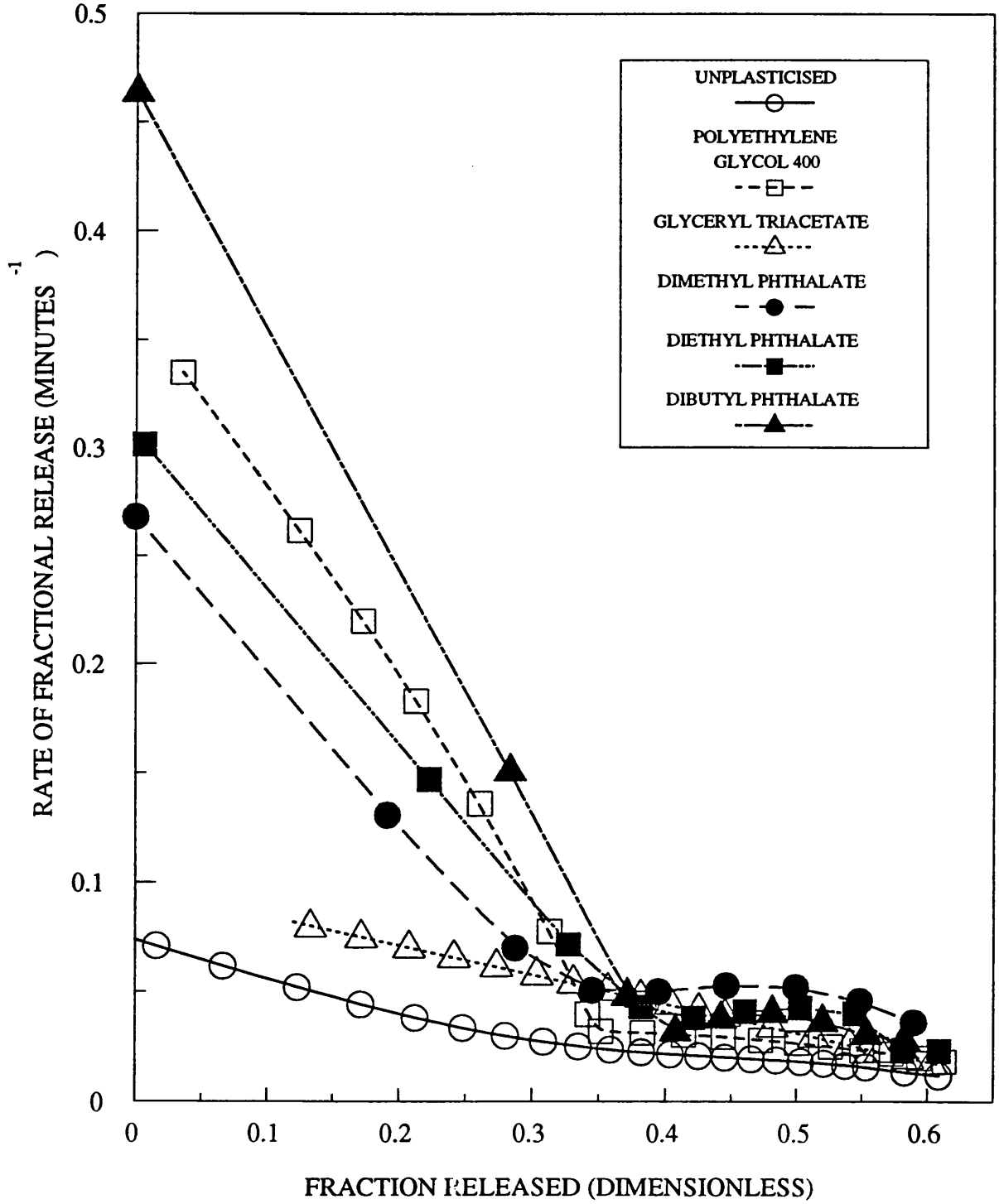

COATINGS CONTAINED EQUAL PROPORTIONS OF EUDRAGIT RL AND RS WITH 5% OXAMNIQUINE AND 10% PLASTICISER RELATIVE TO POLYMER WEIGHT. PELLET SIZE 14-18 US MESH

FIG 98: THE RELEASE OF WATER IMMISCIBLE PLASTICISERS FROM COATED PELLETS CONTAINING OXAMNIQUINE: GRAPH OF FRACTION OF PLASTICISER RELEASED FROM COATING AGAINST SQUARE ROOT TIME

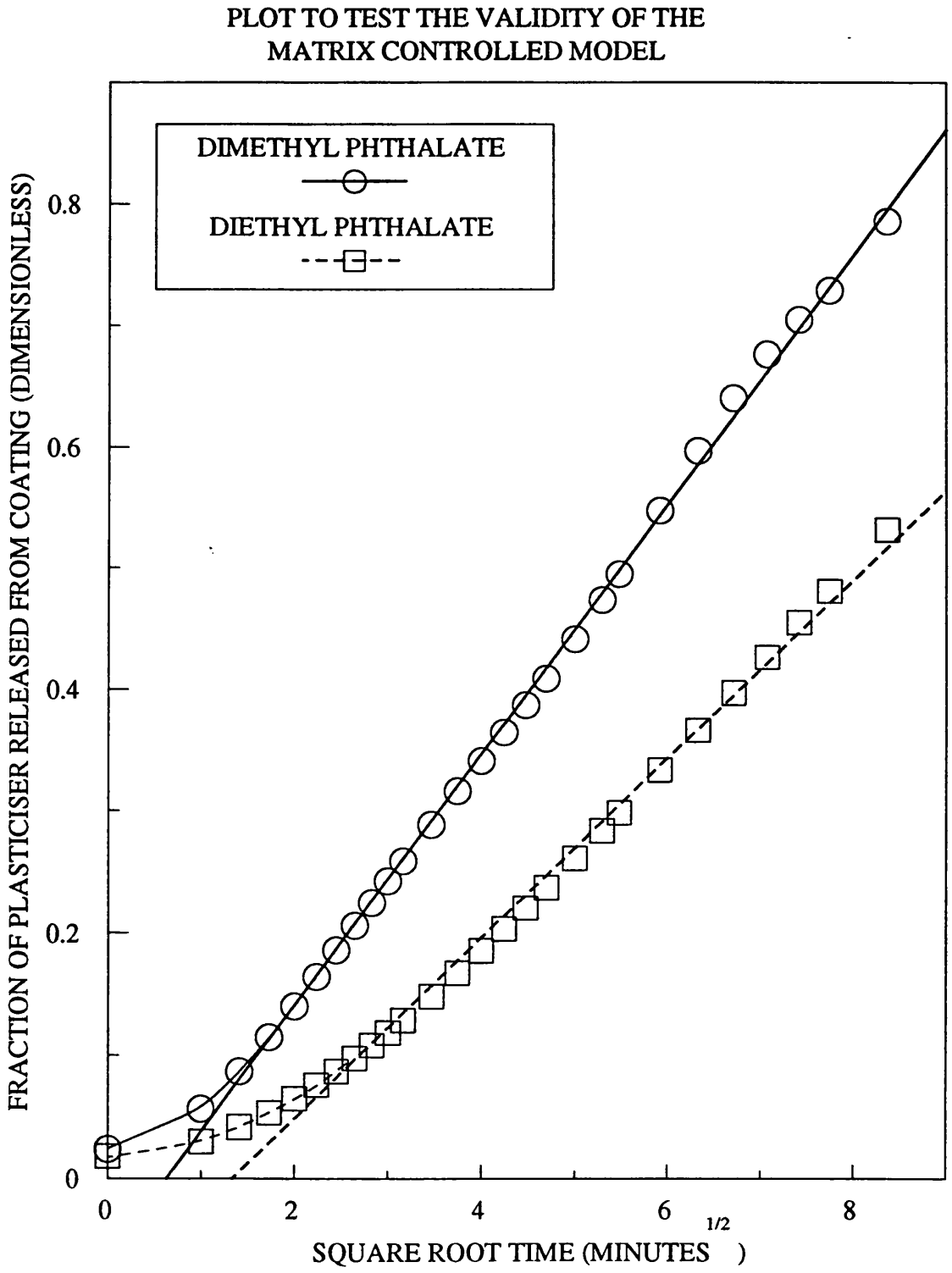

COATINGS CONTAINED EQUAL PROPORTIONS OF EUDRAGIT RL AND RS WITH 5% OXAMNQUINE AND 10% PLASTICISER RELATIVE TO POLYMER WEIGHT.
PELLET SIZE 14-18 US MESH

FIG 99: THE RELEASE OF WATER IMMISCIBLE PLASTICISERS FROM COATED PELLETS CONTAINING OXAMNIQUINE: GRAPH OF LOG FRACTION OF PLASTICISER REMAINING IN COATING AGAINST TIME

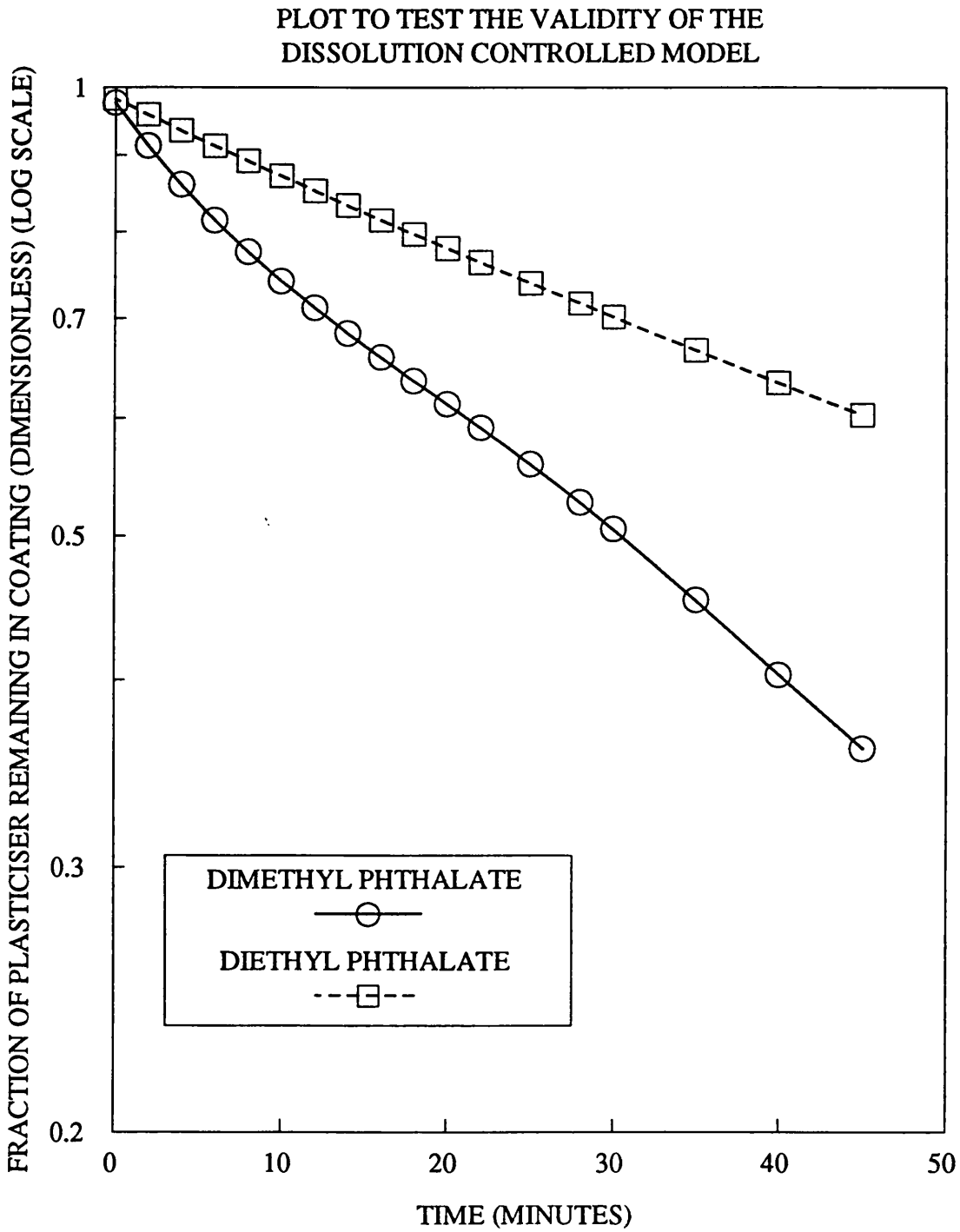

COATINGS CONTAINED EQUAL PROPORTIONS OF EUDRAGIT RL AND RS WITH 5% OXAMNIQUINE AND 10% PLASTICISER RELATIVE TO POLYMER WEIGHT.
PELLET SIZE 14-18 US MESH

FIG 100: THE RELEASE OF WATER IMMISCIBLE PLASTICISERS FROM COATED PELLETS CONTAINING OXAMNIQUINE: GRAPH OF RATE OF FRACTIONAL PLASTICISER RELEASE AGAINST RECIPROCAL FRACTION RELEASED

DIFFERENTIAL RATE PLOT TO TEST THE MATRIX CONTROLLED MODEL FOR PLASTICISER RELEASE.

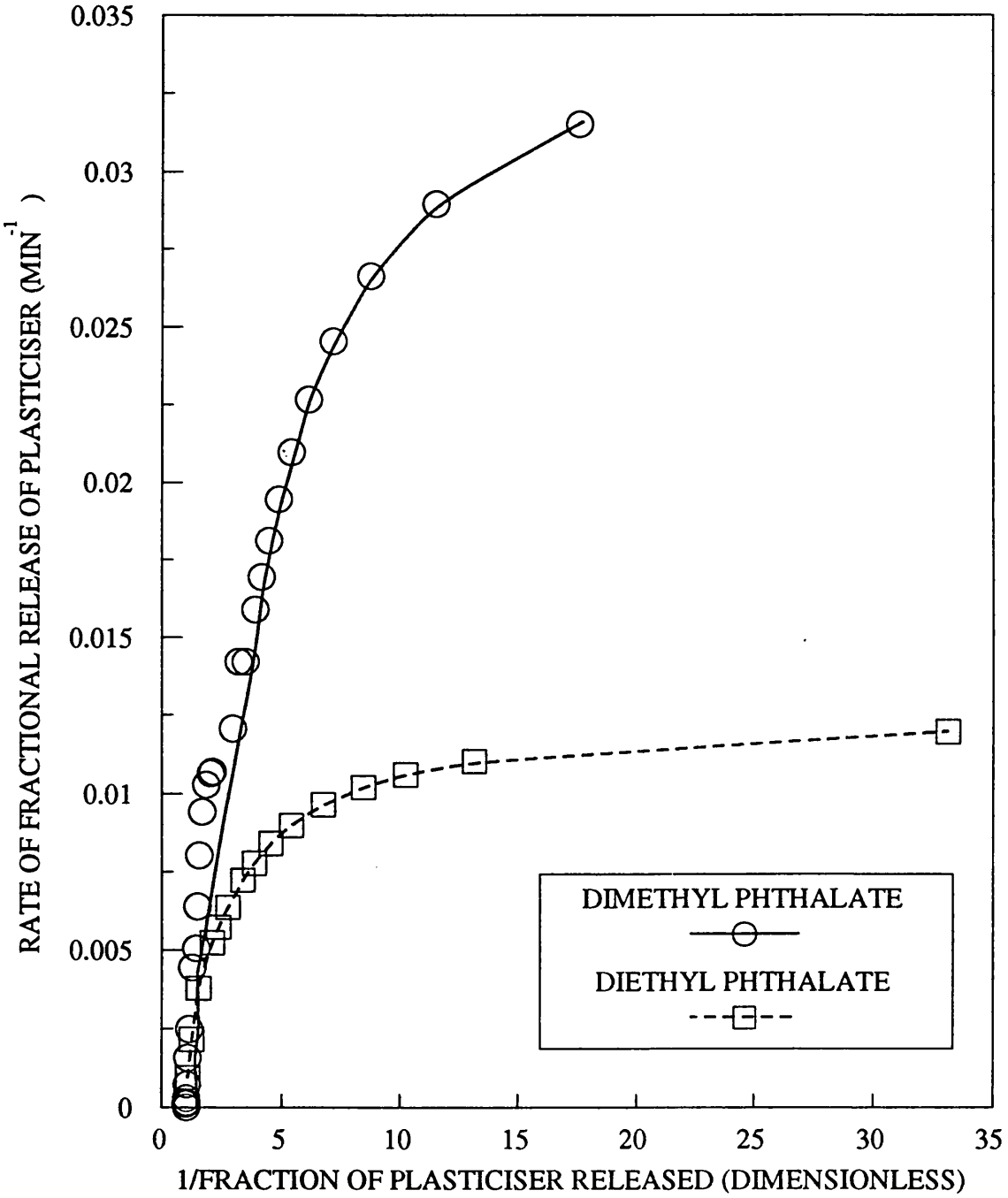

COATINGS CONTAINED EQUAL PROPORTIONS OF EUDRAGIT RL AND RS WITH 5% OXAMNIQUINE AND 10% PLASTICISER RELATIVE TO POLYMER WEIGHT.
PELLET SIZE 14-18 US MESH

FIG 101:THE RELEASE OF WATER IMMISCIBLE PLASTICISERS FROM COATED PELLETS CONTAINING OXAMNIQUINE: GRAPH OF RATE OF FRACTIONAL PLASTICISER RELEASE AGAINST FRACTION RELEASED

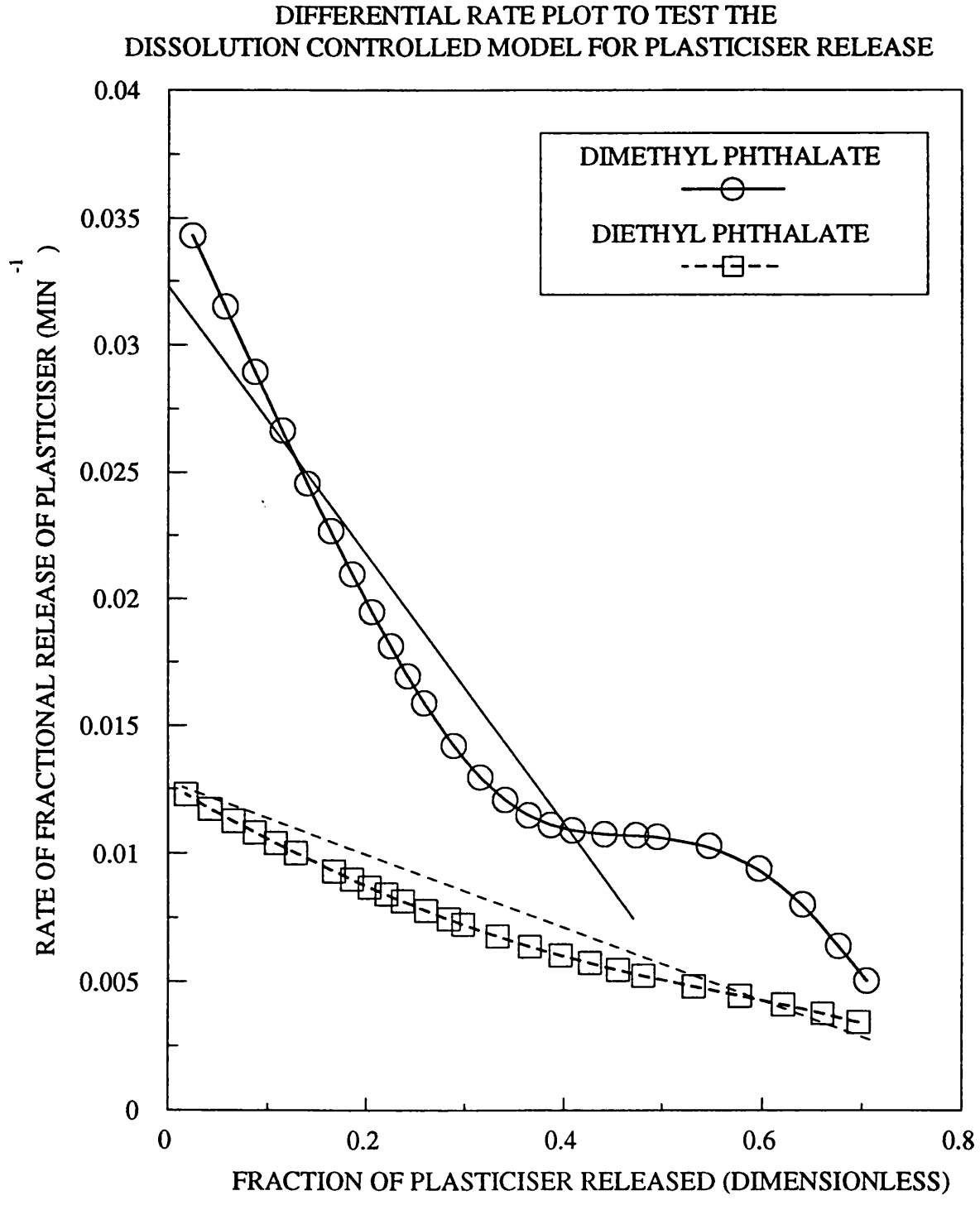

COATINGS CONTAINED EQUAL PROPORTIONS OF EUDRAGIT RL AND RS WITH 5% OXAMNIQUINE AND 10% PLASTICISER RELATIVE TO POLYMER WEIGHT.
PELLET SIZE 14-18 US MESH

to a long lag time required to set up equilibrium between the plasticiser and dissolution medium within the coating.

The difference in model describing the release of dimethyl and diethyl phthalates from the coatings is interesting. Dimethyl phthalate is considerably more soluble in water than diethyl phthalate. It is therefore possible that sink conditions exist for dimethyl phthalate throughout the release experiment, which is a necessary condition for the matrix model to be applicable. Dissolution of diethyl phthalate may be rate limiting in these systems. It is likely that this is the reason for conformity with the dissolution controlled model.

In summary, the release of oxamniquine from plasticised coatings is complex, and it is not easy to define distinct trends in the data. The presence of plasticiser increases the rate of release of oxamniquine from the coatings. Other than for dibutyl phthalate plasticised coatings, the plasticiser and oxamniquine are released simultaneously from the coatings. Additionally for phthalate plasticised coatings, partitioning of oxamniquine can occur between the dissolution medium and the plasticiser within the matrix.

Release of oxamniquine is most rapid from coatings plasticised with either PEG400 which is rapidly released and from dibutyl phthalate which is apparently retained within the coatings. It is not possible to define a logical order of release from coatings containing the other

plasticisers tested from the data.

Data from the release experiments have been analysed to determine whether a matrix controlled or dissolution controlled model is appropriate. In some cases results were ambiguous. Differential rate plots, which are claimed to readily distinguish between those two models also produced ambiguous results.

The release of dimethyl and diethyl phthalate from the coatings has also been analysed. Dimethyl phthalate is released more rapidly from the coatings than diethyl phthalate. The apparent mechanism of release is also different, with the less soluble diethyl phthalate dissolution controlled compared with matrix controlled release for dimethyl phthalate plasticised coatings.

5.9.5 The Effect of Oxamniquine Content In Polymer Coatings

All of the data reported so far has been generated using coatings containing 5% w/w of oxamniquine relative to total polymer weight. Coatings containing high drug loadings, up to 15% w/w of oxamniquine were prepared as described in Chapter 3 and tested. These coatings contained equal proportions of Eudragit RL and Eudragit RS with 10% w/w of glyceryl triacetate relative to total polymer weight. Data generated from these experiments have been analysed to determine the effect of oxamniquine content on the rate, extent or mechanism of release.

Figure 102 shows the fraction of oxamniquine released from the coatings plotted against time. It is evident that at the two higher loadings, increasing the oxamniquine content results in a greater fraction of oxamniquine is released at a given time.

There is a more significant difference between coatings containing 5% and 10% oxamniquine than between coatings containing 10% and 15% oxamniquine. This is illustrated more clearly in Figure 103 where the time taken to release between 10% and 70% of the oxamniquine content is plotted as a function of the drug content in the film.

Figure 104 shows the rate of release of oxamniquine plotted as a function of time. During the early phase of release, higher release rates of oxamniquine are seen with coatings containing higher drug loadings. However, during the later phase as the drug content of the coatings become exhausted, the release rates are similar for different loadings. It is possible that this effect is due to accumulation of the drug near the surface of the pellet coating. If this is the case, then the drug must be located within the coating near to surface rather than spray dried on the surface. This is supported by the absence of excessive fine material collected from the coatings after abrasion tests and sieve analysis described in Section 5.3.

Figures 105 and 106 show graphs to evaluate the matrix and dissolution controlled models respectively.

FIG 102: THE EFFECT OF OXAMNIQUINE CONTENT ON RELEASE OF OXAMNIQUINE FROM COATED PELLETS: GRAPH OF FRACTION RELEASED AGAINST TIME.

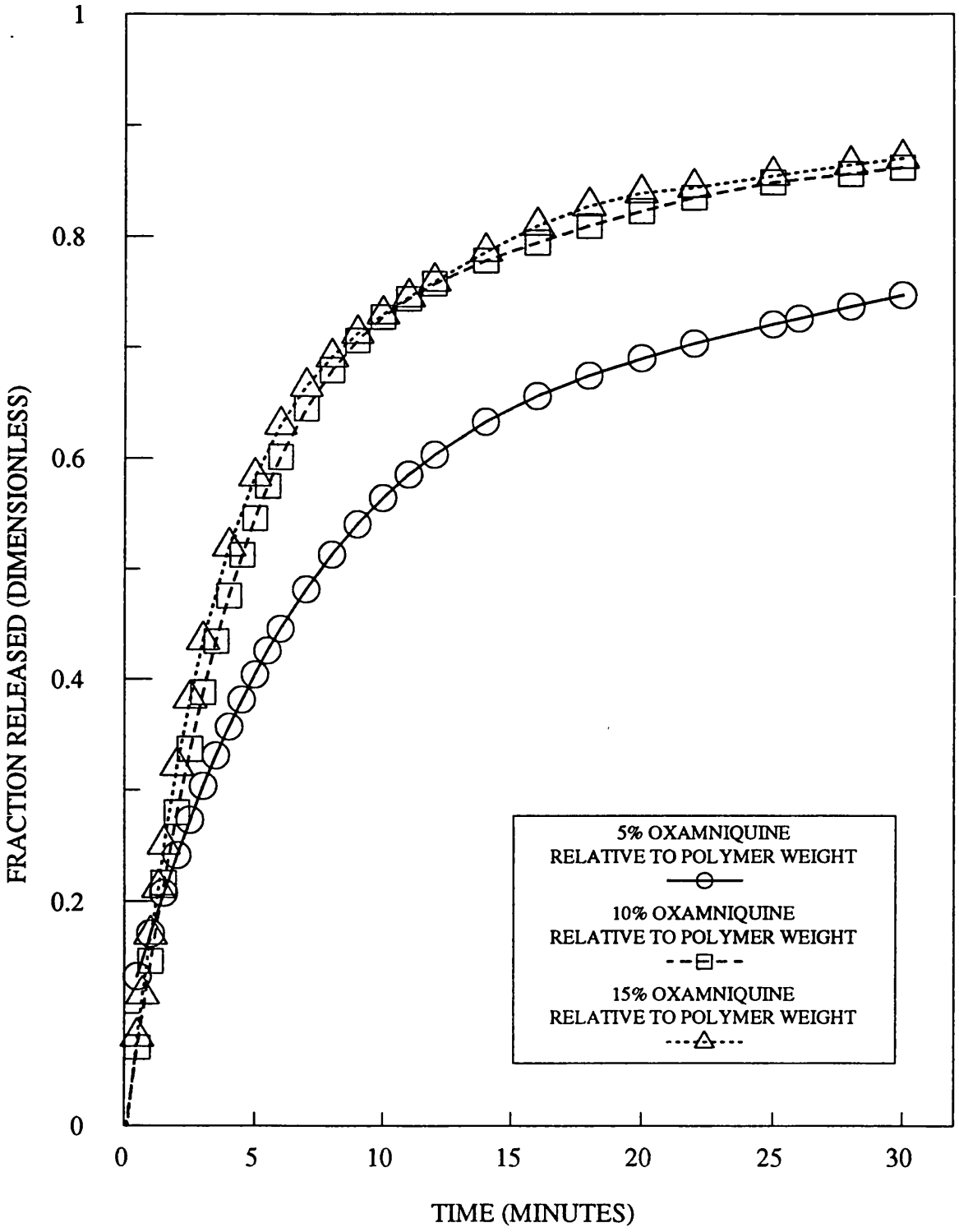

COATINGS CONTAINED EQUAL PROPORTIONS OF EUDRAGIT RL AND RS AND 10% GLYCERYL TRIACETATE RELATIVE TO POLYMER WEIGHT. PELLET SIZE 14-18 US MESH.

FIG 103:THE EFFECT OF OXAMNIQUINE CONTENT ON THE TIME TAKEN TO RELEASE OXAMNIQUINE FROM COATED PELLETS

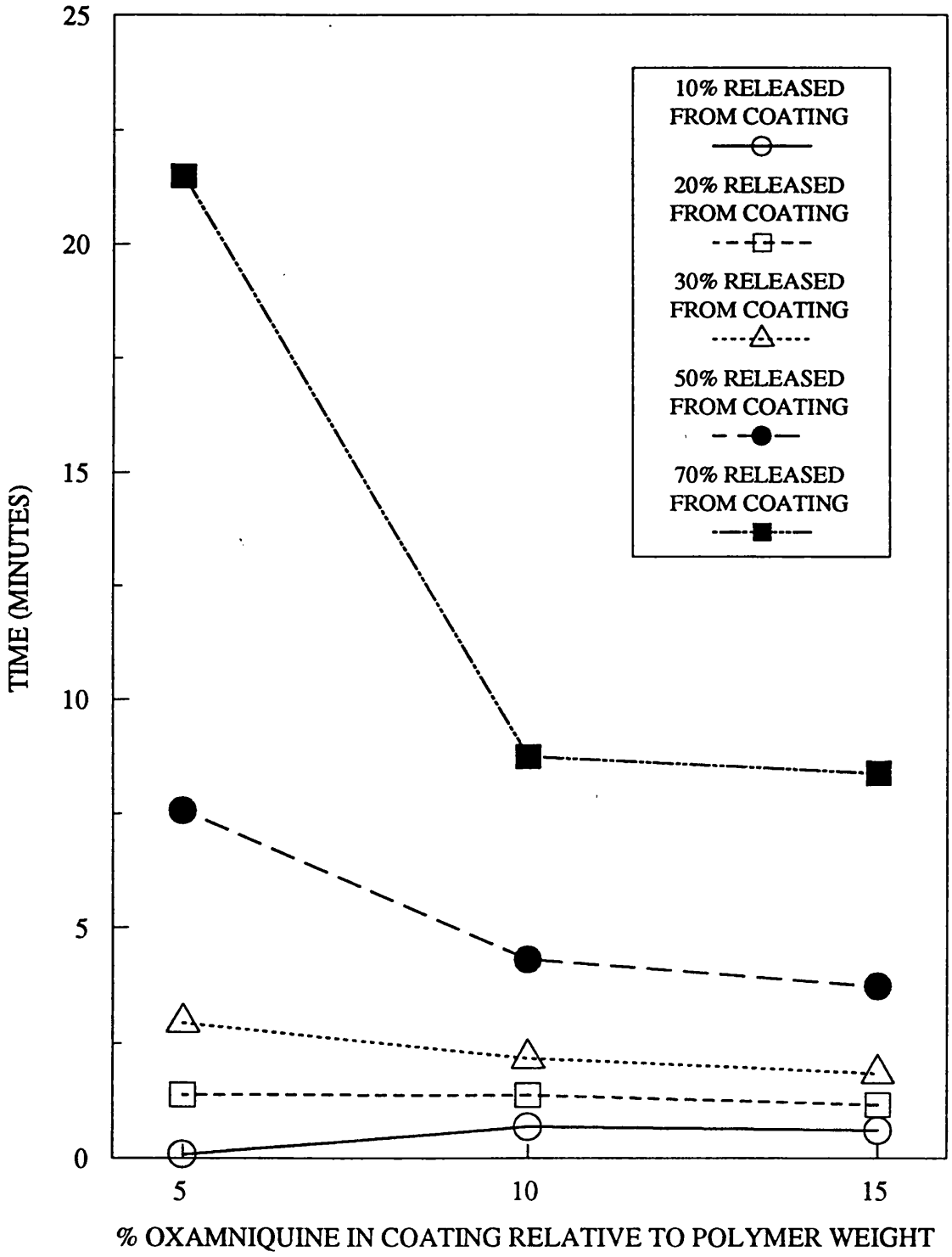

COATINGS CONTAINED EQUAL PROPORTIONS OF EUDRAGIT RL AND RS AND 10% GLYCERYL TRIACETATE RELATIVE TO POLYMER WEIGHT. PELLET SIZE 14-18 US MESH.

FIG 104:THE EFFECT OF OXAMNIQUINE CONTENT ON THE RELEASE OF OXAMNIQUINE FROM COATED PELLETS: GRAPH OF RATE OF FRACTIONAL RELEASE AGAINST TIME.

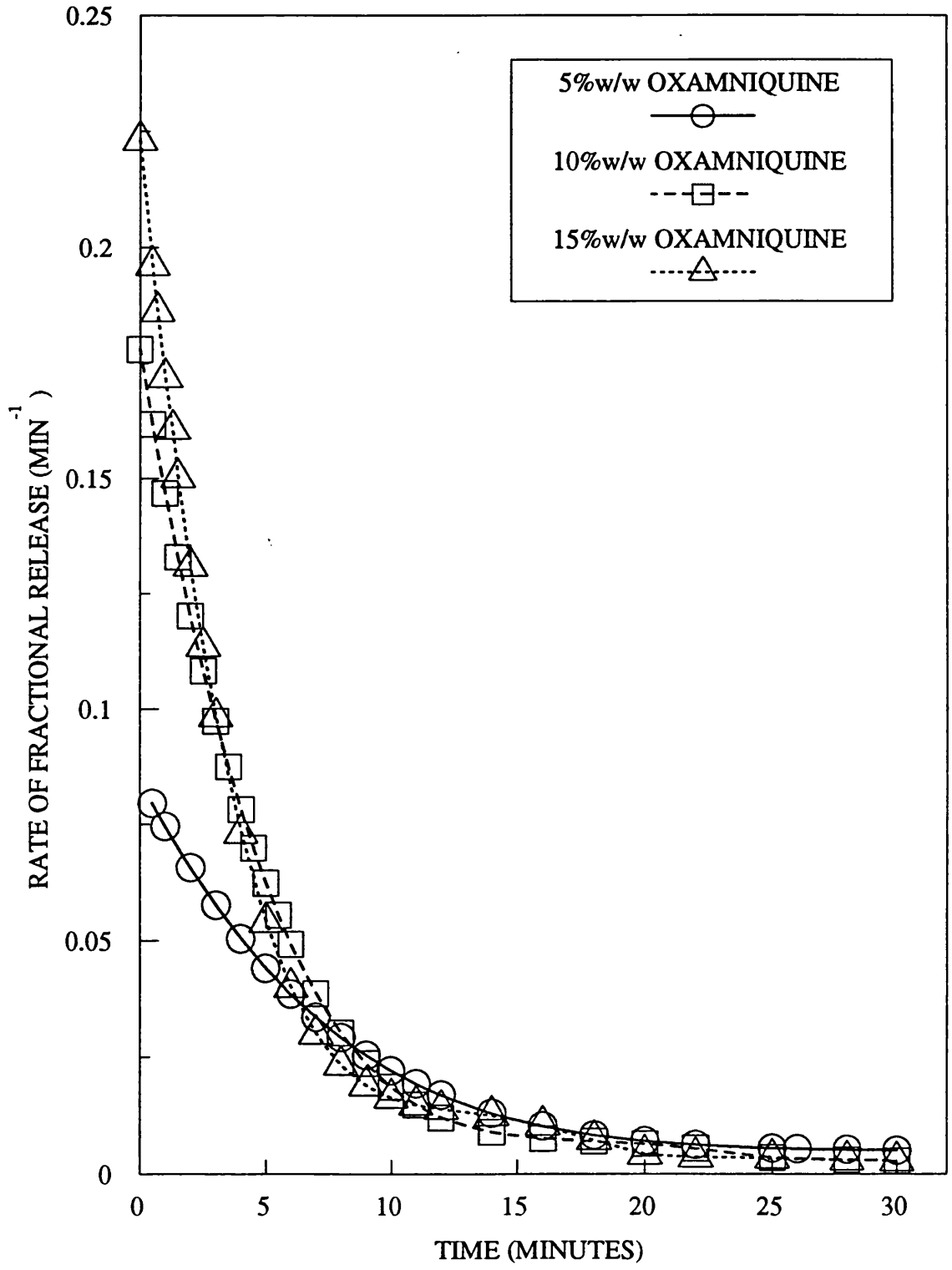

COATINGS CONTAINED EQUAL PROPORTIONS OF EUDRAGIT RL AND RS WITH 10% GLYCERYL TRIACETATE
PELLET SIZE 14-18 US MESH

FIG 105:THE EFFECT OF OXAMNIQUINE CONTENT ON THE RELEASE OF OXAMNIQUINE FROM COATED PELLETS: GRAPH OF FRACTION RELEASED AGAINST SQUARE ROOT OF TIME

PLOT TO EVALUATE THE MATRIX CONTROLLED MODEL.

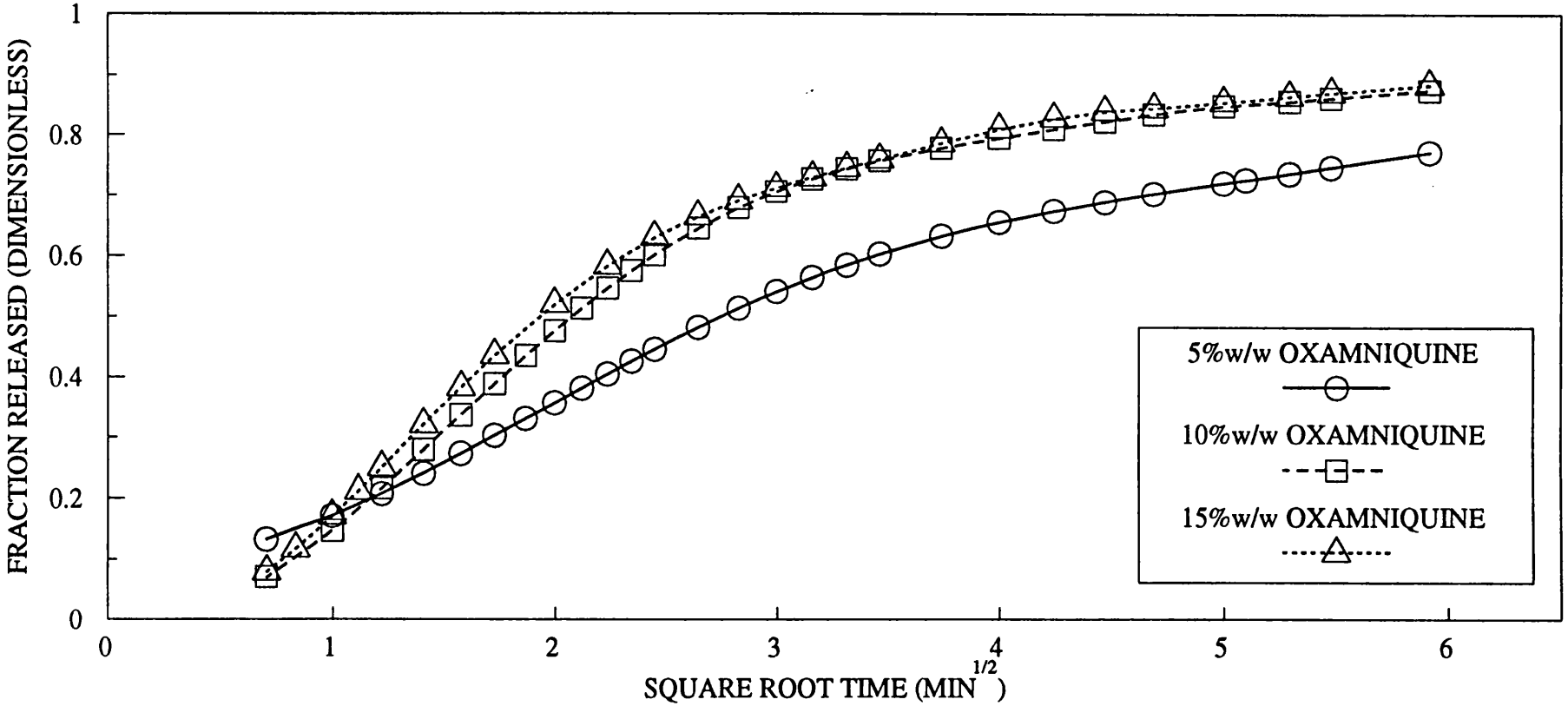

COATINGS CONTAINED EQUAL PROPORTIONS OF
EUDRAGIT RL AND RS WITH 10% GLYCERYL TRIACETATE
PELLET SIZE 14-18 US MESH

FIG 106:THE EFFECT OF OXAMNIQUINE CONTENT ON THE RELEASE OF OXAMNIQUINE FROM COATED PELLETS: GRAPH OF LOG FRACTION REMAINING IN COATING AGAINST TIME.

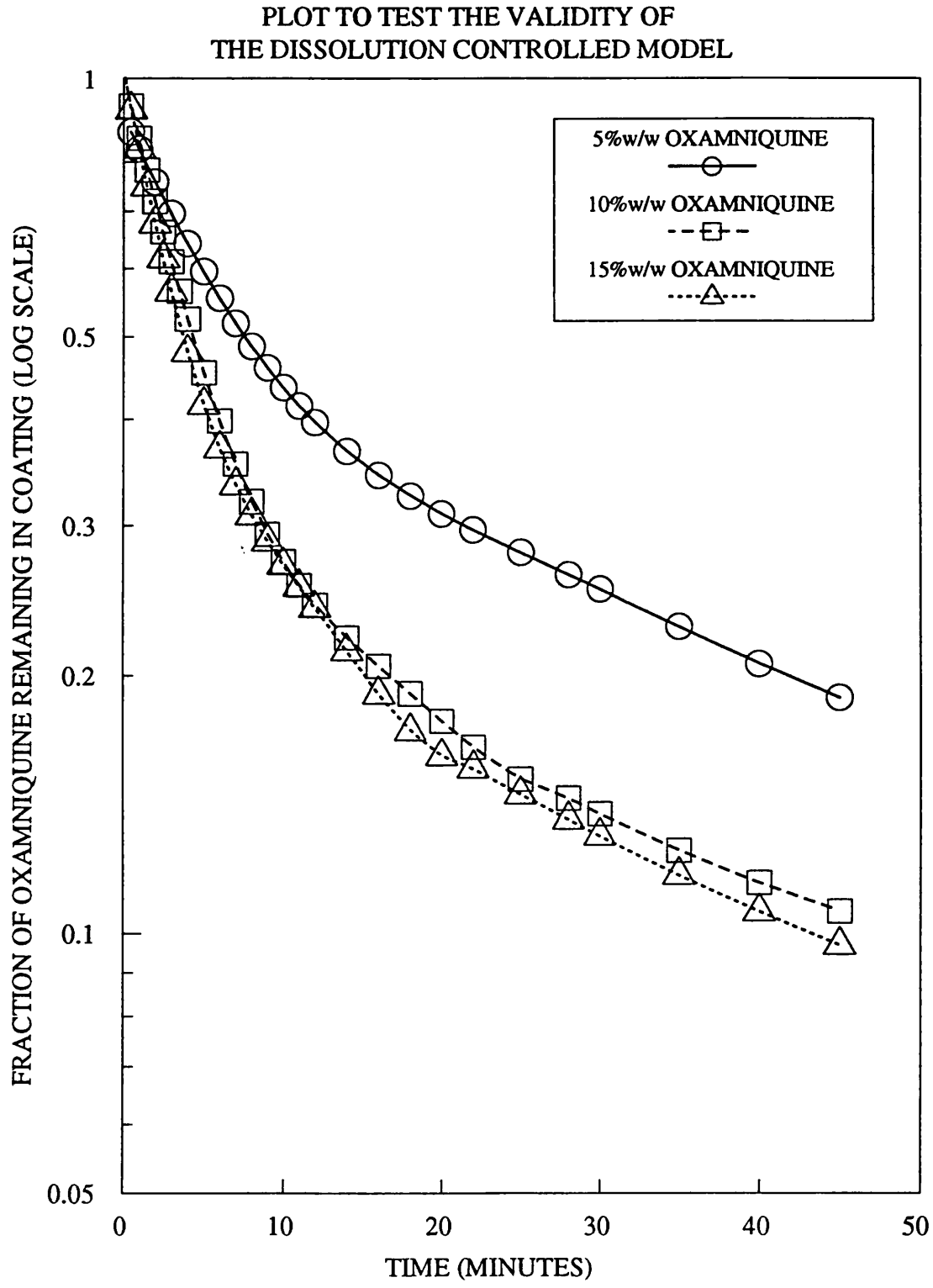

COATINGS CONTAINED EQUAL PROPORTIONS OF EUDRAGIT RL AND RS WITH 10% GLYCERYL TRIACETATE
PELLET SIZE 14-18 US MESH

Considering the first 50% of drug release it would appear that either the dissolution controlled or the matrix controlled model could be applicable to this data. If matrix controlled kinetics are applicable, the slope of the Q versus $t^{1/2}$ profile is defined by equation 35.

$$\frac{Q}{t^{1/2}} = \sqrt{[D_m(2A-C_s)C_s]} \qquad (35)$$

where Dm is the diffusivity in the matrix

A is the drug loading

C_s is the saturation solubility in the extraction medium

For high drug loadings $A>>C_s$, equation 35 may be rewritten

$$\frac{Q}{t^{1/2}} = \sqrt{(2D_mAC_s)}$$

and taking the square of both sides results in

$$\frac{Q^2}{t} = 2AD_mC_s \qquad (36)$$

so that a plot of Q^2/t against A should be linear with slope $2D_mC_s$.

These data are plotted for oxamniquine in Figure 107. As the resulting plot is not linear, this suggests that the matrix controlled model may not be applicable to the release of oxamniquine from the coated pellets.

Further evidence of this can be seen from the differential rate plots, shown in Figures 108 and 109, for the matrix controlled and dissolution controlled models respectively. These graphs indicate that the dissolution controlled model describes the release of oxamniquine from the coatings at all three drug loadings.

It is possible that dissolution controlled release may have been seen at the lowest drug loading, if the oxamniquine content did not exceed the saturation solubility within the matrix. However, this is unexpected where the oxamniquine content incorporated in the coating is 15% w/w relative to the total polymer weight of the coating, which is likely to exceed its saturation solubility within the coating. It is possible that this effect is due to the way oxamniquine exists within the coating. This will be discussed further in Section 5.10 when experiments on surface scanning electron microscopy are described.

5.9.6 The Effect of Core Pellet Size

All of the experiments reported previously were performed using 14-18 US mesh pellet cores. After coating oxamniquine release was measured from coated pellets in the 1200-1400 micron size fraction.

To evaluate the effect of changing the surface area of the pellet cores, 20-25 US Mesh pellets were coated as described in Chapter 3. The coated pellets were sieved,

FIG 107:THE EFFECT OF OXAMNIQUINE CONTENT ON THE RELEASE OF OXAMNIQUINE FROM COATED PELLETS: GRAPH OF (SLOPE) ^{2}OF MATRIX CONTROLLED MODEL PLOT AGAINST OXAMNIQUINE CONTENT

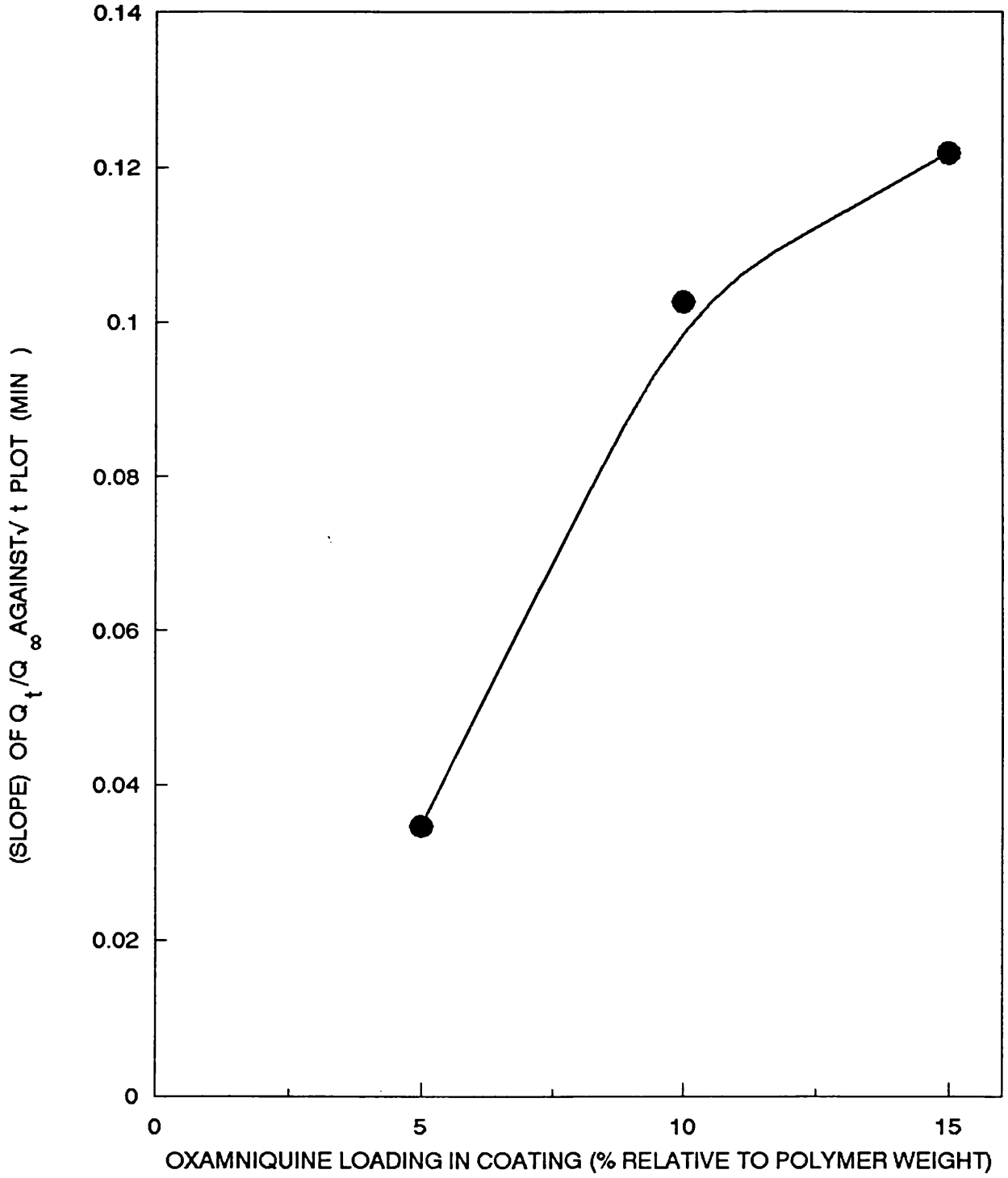

COATINGS CONTAINED EQUAL PROPORTIONS OF EUDRAGIT RL AND EUDRAGIT RS WITH 10% GLYCERYL TRIACETATE RELATIVE TO POLYMER WEIGHT.

FIG 108:THE EFFECT OF OXAMNIQUINE CONTENT ON THE RELEASE OF OXAMNIQUINE FROM COATED PELLETS. PLOT OF RATE OF FRACTIONAL RELEASE AGAINST RECIPROCAL FRACTION RELEASED

DIFFERENTIAL RATE PLOT TO EVALUATE
THE MATRIX CONTROLLED MODEL.

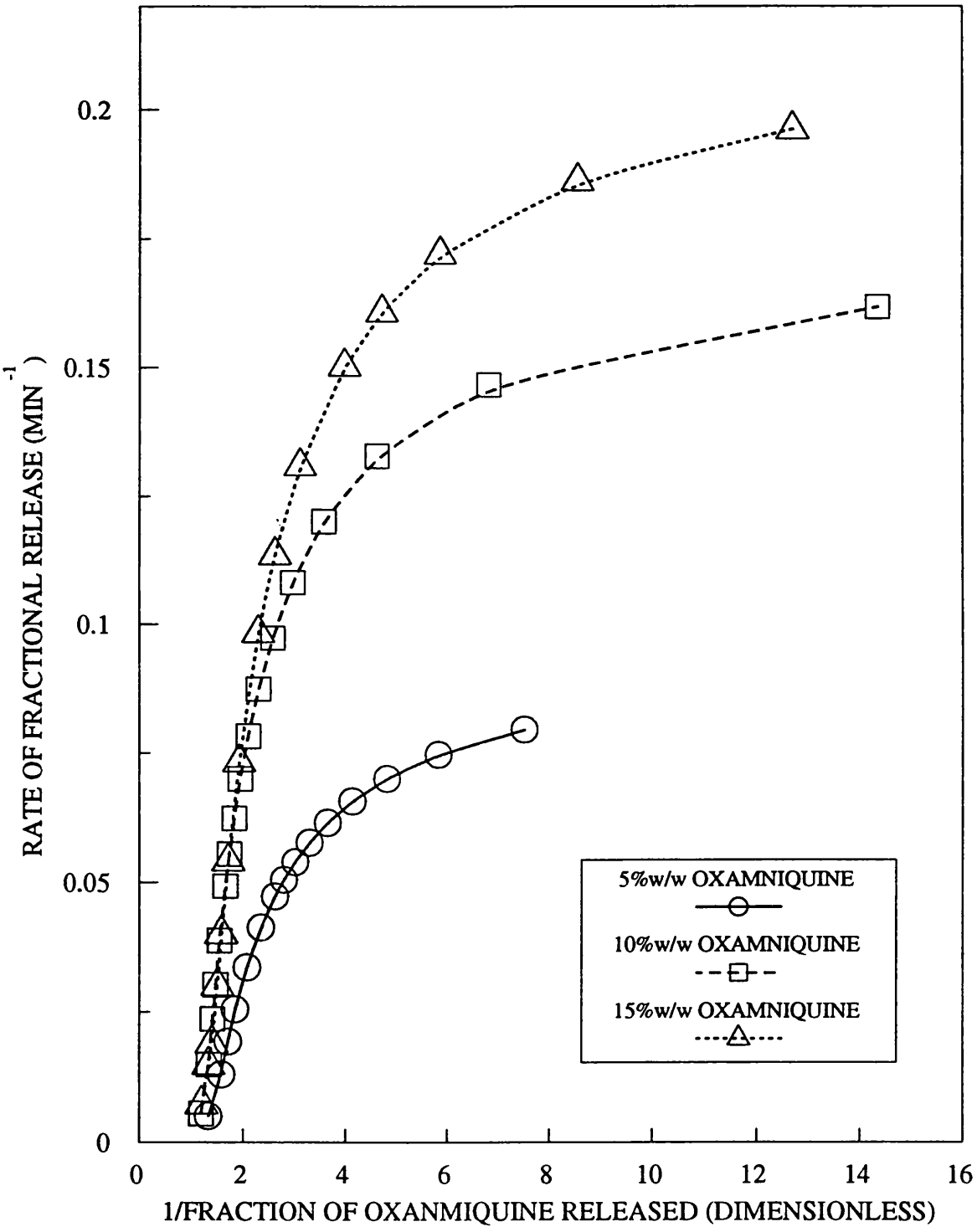

COATINGS CONTAINED EQUAL PROPORTIONS OF
EUDRAGIT RL AND RS WITH 10% GLYCERYL TRIACETATE
PELLET SIZE 14-18 US MESH

FIG 109: THE EFFECT OF OXAMNIQUINE CONTENT ON THE RELEASE OF OXAMNIQUINE FROM COATED PELLETS: PLOT OF RATE OF FRACTIONAL RELEASE AGAINST FRACTION RELEASED

DIFFERENTIAL RATE PLOT TO EVALUATE
THE DISSOLUTION CONTROLLED MODEL.

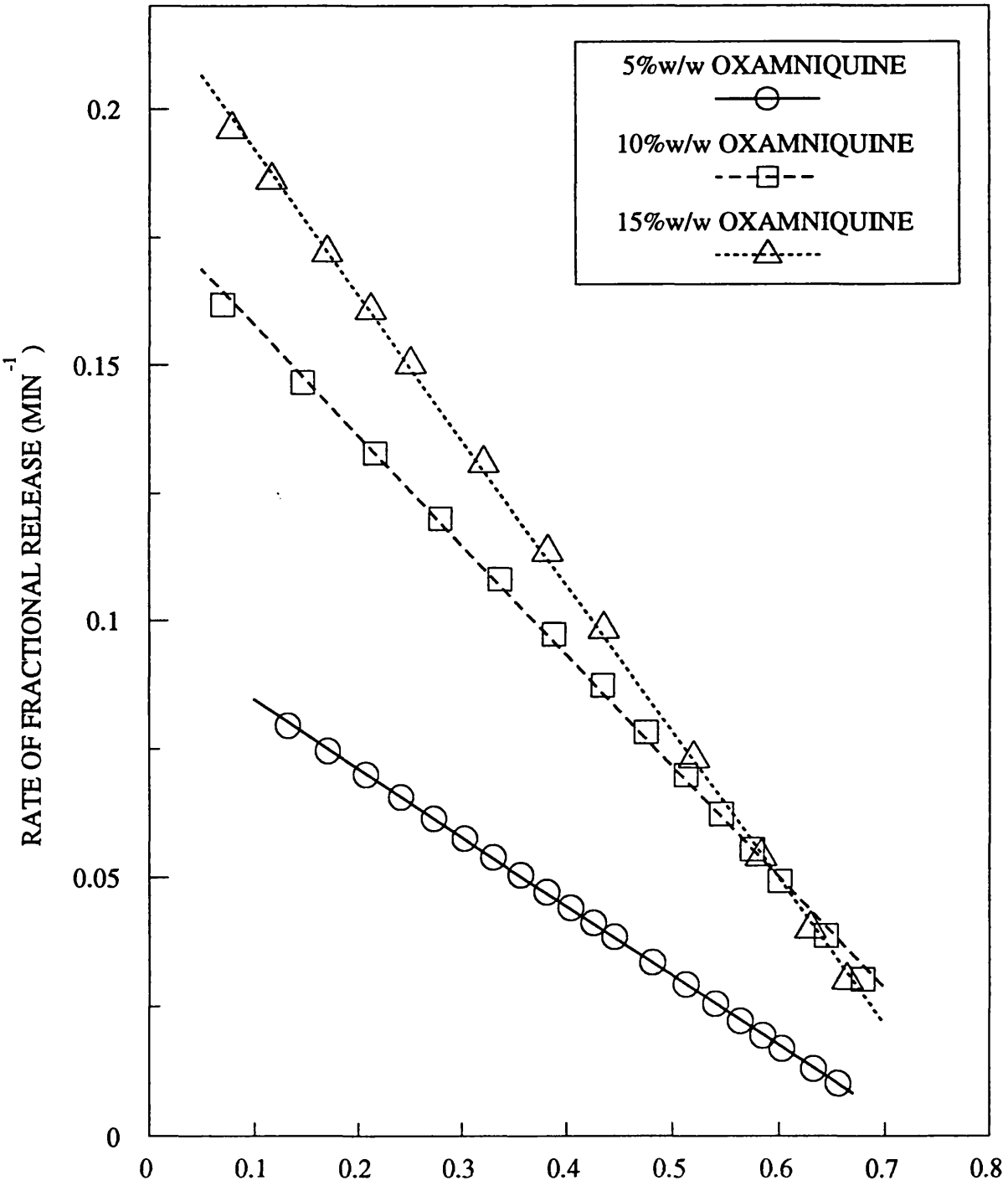

COATINGS CONTAINED EQUAL PROPORTIONS OF
EUDRAGIT RL AND RS WITH 10% GLYCERYL TRIACETATE
PELLET SIZE 14-18 US MESH

and the release of oxamniquine from pellets in the 841-1000 micron size fraction was measured.

Figure 110 shows the release of oxamniquine from each of the pellet sizes. There appears to be little difference in the oxamniquine release profile for the first 60% of oxamniquine released. However, at later times when the oxamniquine content becomes depleted the smaller pellets appear to release the remaining oxamniquine more rapidly.

Figure 111 shows the rate of oxamniquine release plotted against time. Differences in the shape of the rate profiles are evident. At early times the rate of release of oxamniquine is higher from the smaller pellets. The rates of release appear to be linearly related to the increased surface area of the pellet available for release. This is illustrated in Figure 112.

Figure 112 shows the ratio of fractional release rates for various fractions released from the coatings plotted against the percentage of oxamniquine released from the coating. The significance of the linear relationship between the release rate ratio and the percentage of oxamniquine release is uncertain.

Figures 113 and 114 show graphs to evaluate the matrix controlled and dissolution controlled models for oxamniquine release. It has been established previously that oxamniquine release from the 1200-1400μm pellets is

FIG 110: EFFECT OF PELLET CORE SIZE ON THE RELEASE OF OXAMNIQUINE FROM COATED PELLETS: GRAPH OF FRACTION RELEASED AGAINST TIME

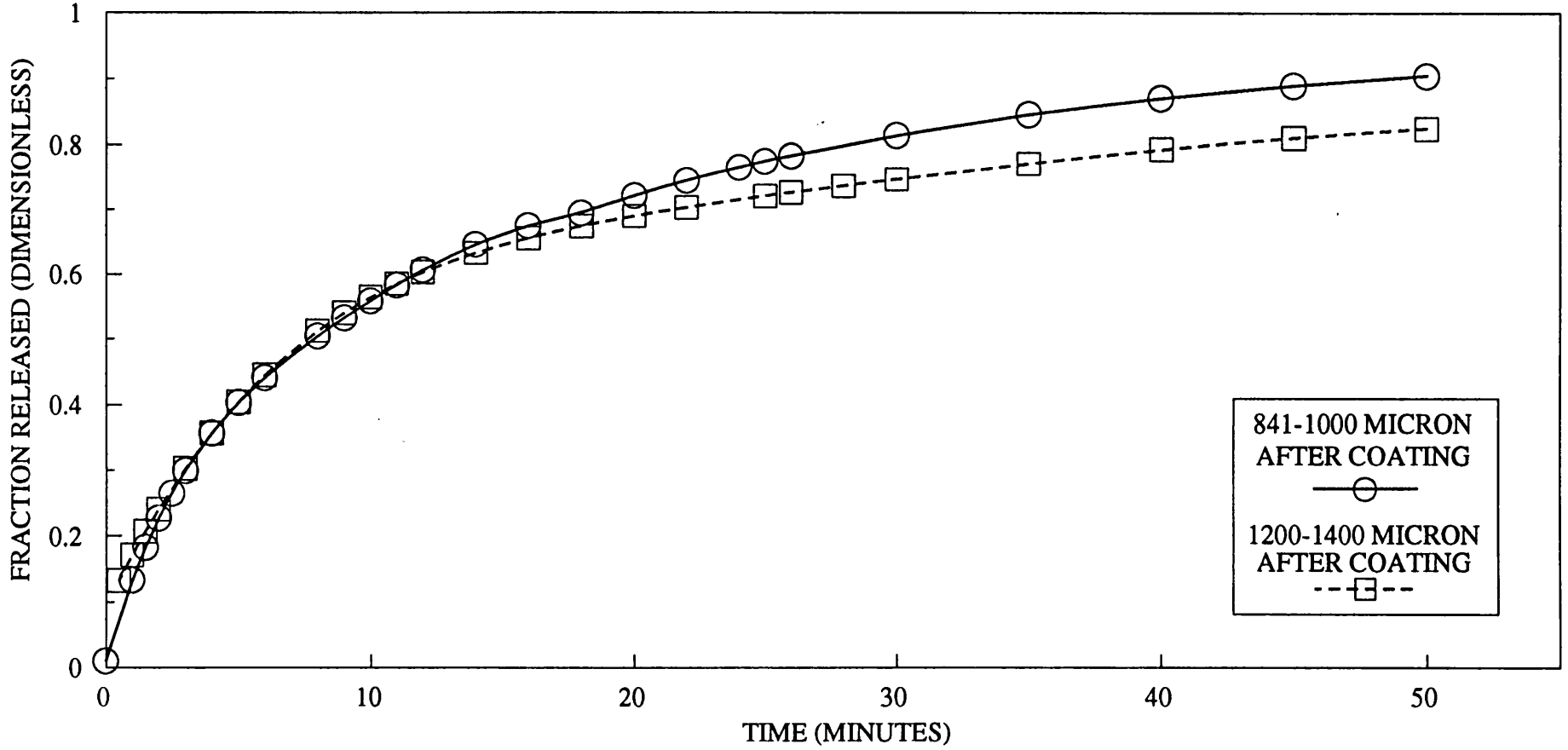

COATINGS CONTAINED EQUAL PROPORTIONS OF EUDRAGIT RL AND RS WITH 10% GLYCERYL TRIACETATE AND 5% OXAMNIQUINE RELATIVE TO POLYMER WEIGHT

FIG 111: EFFECT OF PELLET CORE SIZE ON THE RELEASE OF OXAMNIQUINE FROM COATED PELLETS: GRAPH OF RATE OF FRACTIONAL RELEASE AGAINST TIME

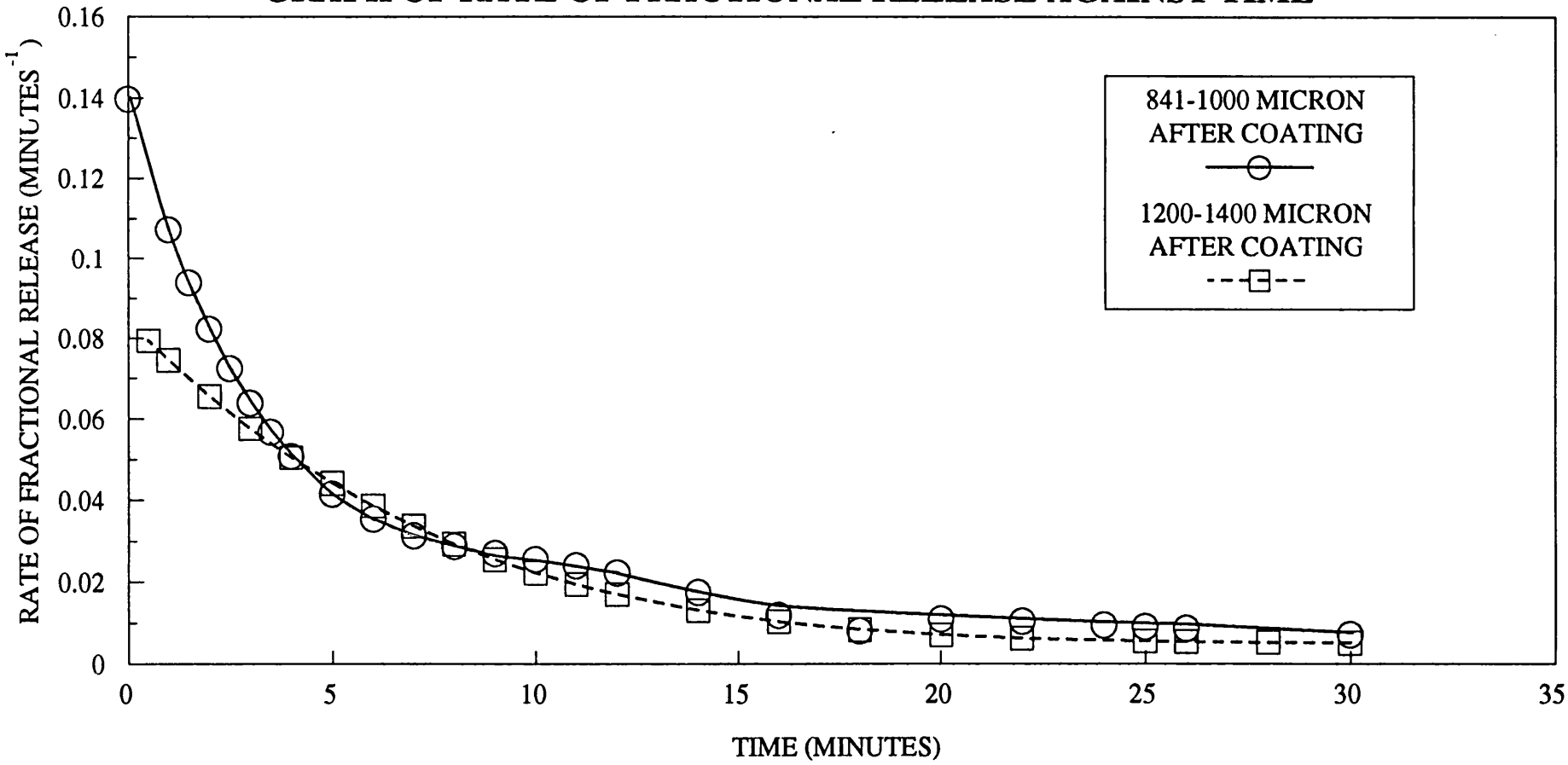

COATINGS CONTAINED EQUAL PROPORTIONS OF EUDRAGIT RL AND RS WITH 10% GLYCERYL TRIACETATE AND 5% OXAMNIQUINE RELATIVE TO POLYMER WEIGHT

FIG 112:THE EFFECT OF PELLET CORE SIZE ON THE RELEASE OF OXAMNIQUINE FROM COATED PELLETS: GRAPH OF RATIO OF RATES OF FRACTIONAL RELEASE AGAINST PERCENTAGE RELEASED

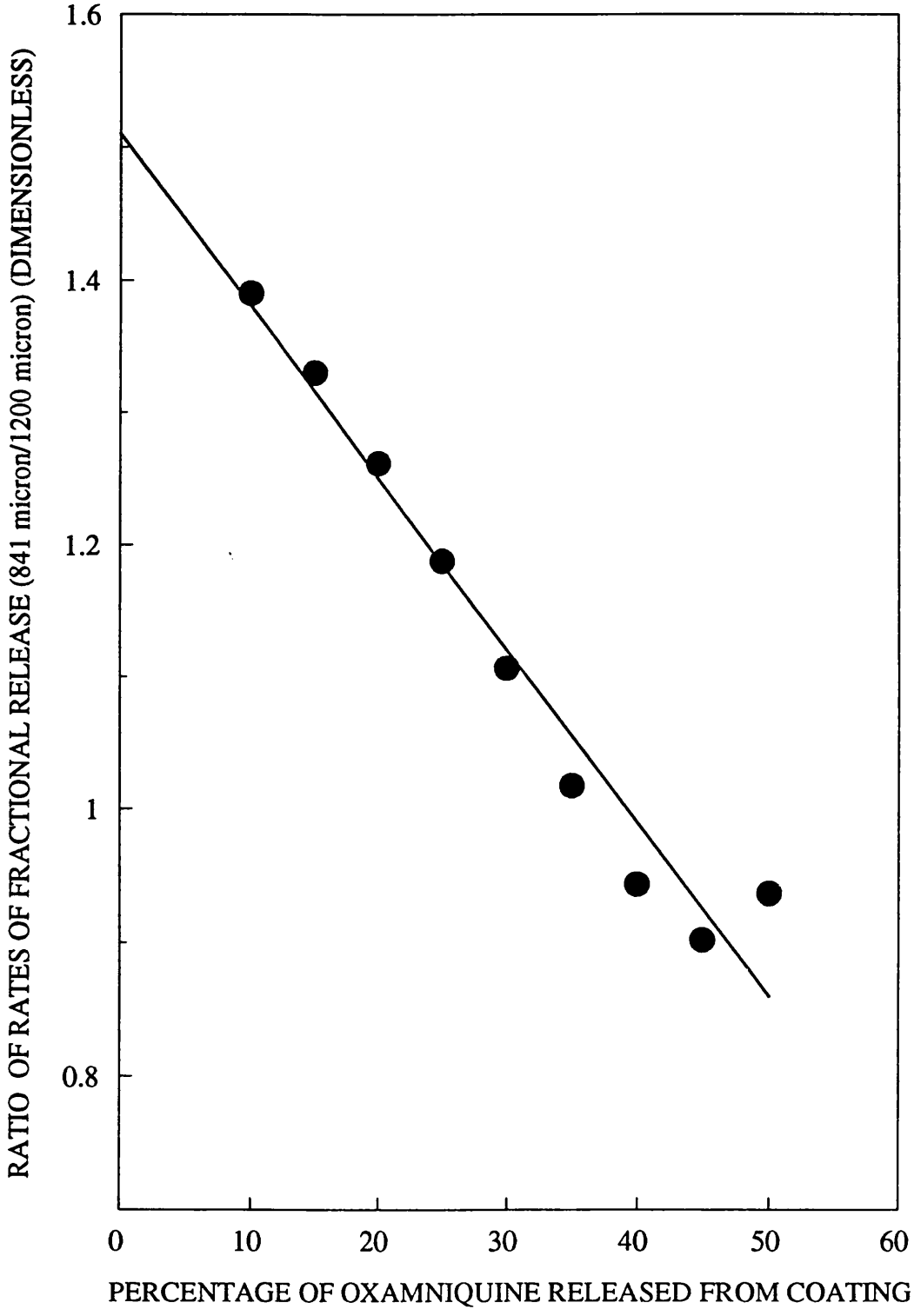

FIG 113: THE EFFECT OF PELLET CORE SIZE ON THE RELEASE OF OXAMNIQUINE FROM COATED PELLETS: GRAPH OF FRACTION RELEASED AGAINST SQUARE ROOT TIME

PLOT TO TEST THE VALIDITY OF THE MATRIX CONTROLLED MODEL

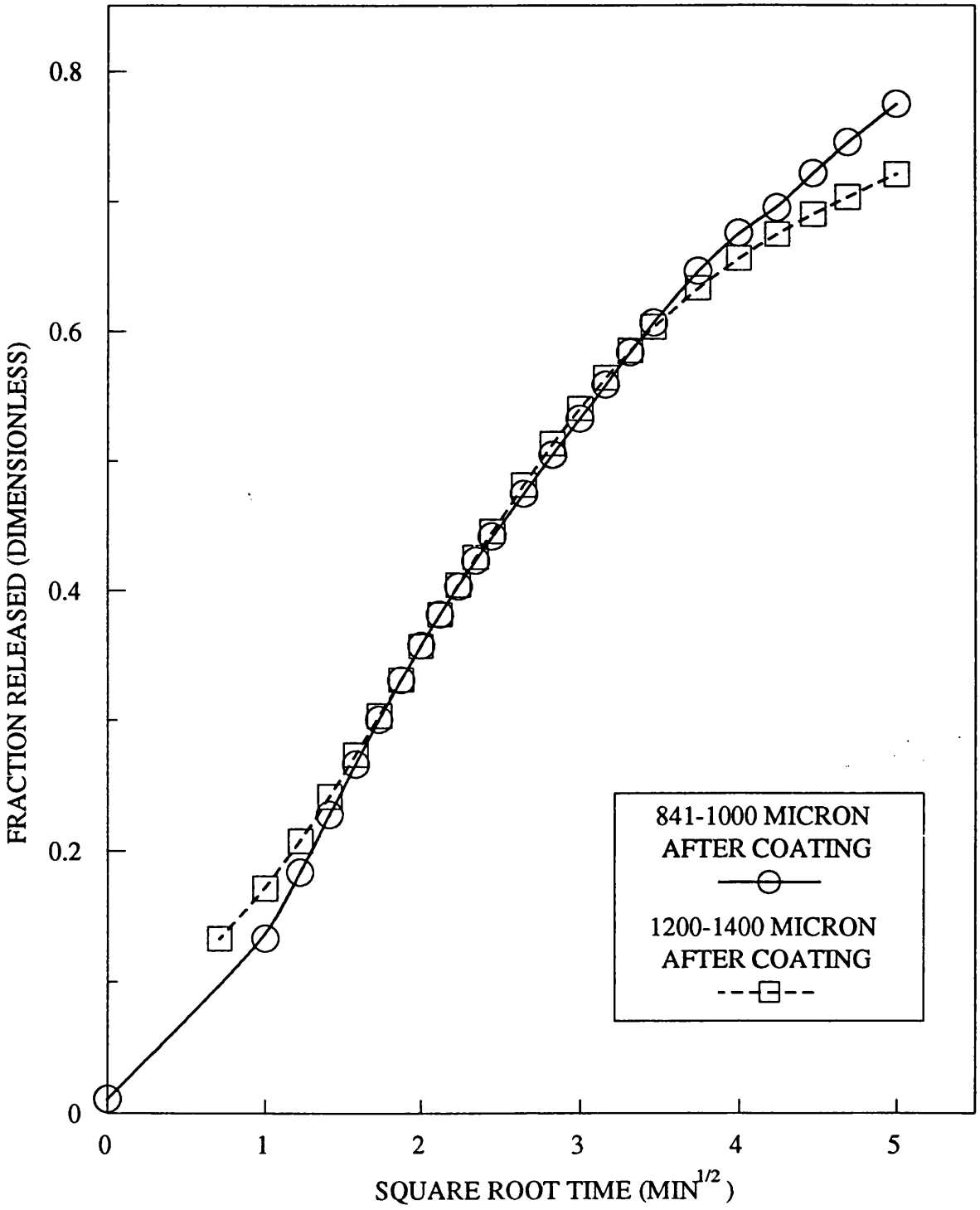

COATINGS CONTAINED EQUAL PROPORTIONS OF EUDRAGIT RL AND RS WITH 10% GLYCERYL TRIACETATE AND 5% OXAMNIQUINE RELATIVE TO POLYMER WEIGHT.

FIG 114: THE EFFECT OF PELLET CORE SIZE ON THE RELEASE OF OXAMNIQUINE FROM COATED PELLETS: PLOT OF LOG FRACTION REMAINING IN COATING AGAINST TIME

GRAPH TO TEST THE VALIDITY OF THE DISSOLUTION CONTROLLED MODEL

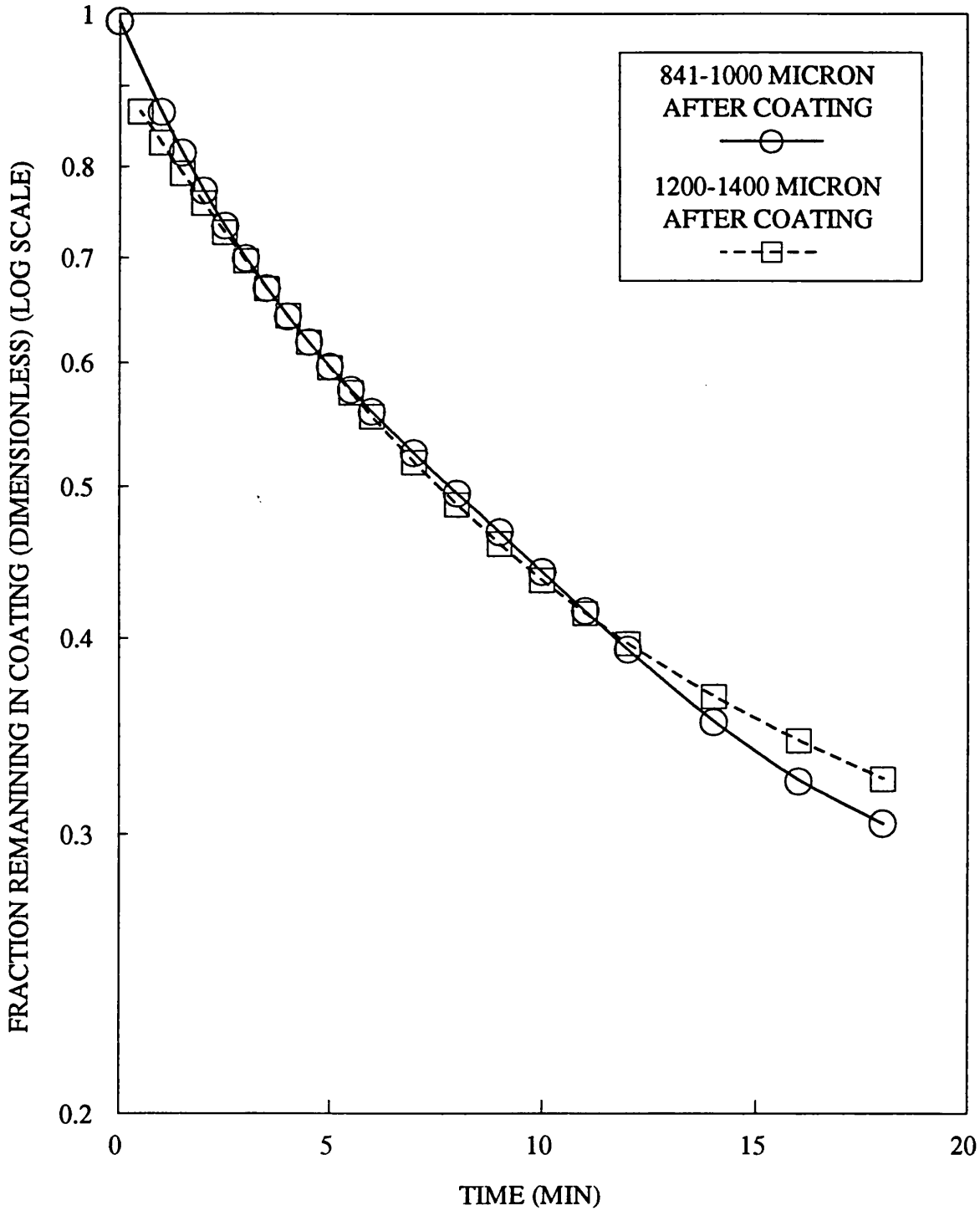

COATINGS CONTAINED EQUAL PROPORTIONS OF EUDRAGIT RL AND RS WITH 10% GLYCERYL TRIACETATE AND 5% OXAMNIQUINE RELATIVE TO POLYMER WEIGHT.

best described by the dissolution controlled model. Considering the first 50% of release, Figures 113 and 114 suggest that the matrix controlled model is a better fit to data for the 841-1000μm size fraction pellets. However, if the differential rate plots shown in Figures 115 and 116 are examined, it would appear that the dissolution controlled models described the release of oxamniquine from the smaller pellets better than the matrix controlled model. This contradicts the primary data shown in Figure 113. This is a further example of how, for this type of system, differential rate plots do not definitively establish whether data fits a dissolution controlled or matrix controlled model.

5.10 Scanning Electron Microscopy of Coated Pellets

The formation of isolated polymer films represents a somewhat idealised situation in which the carrier solvents are allowed to evaporate slowly and uniformly, often unidirectionally, from a uniform surface. This allows polymer chains to be arranged within the film structure in a consistent manner. The result is an apparent physically homogeneous film structure. This apparent homogeneity was seen as an 'orange peel' effect in scanning electron micrographs of films and is discussed in Section 5.7.

The various processes of obtaining coating films onto substrates by spraying techniques, will almost certainly result in non-homogeneous films. Polymer solutions are

FIG 115: THE EFFECT OF PELLET CORE SIZE ON THE RELEASE OF OXAMNIQUINE FROM COATED PELLETS: PLOT OF RATE OF FRACTIONAL RELEASE AGAINST RECIPROCAL FRACTION RELEASED

DIFFERENTIAL RATE PLOT TO TEST THE VALIDITY OF THE MATRIX CONTROLLED MODEL

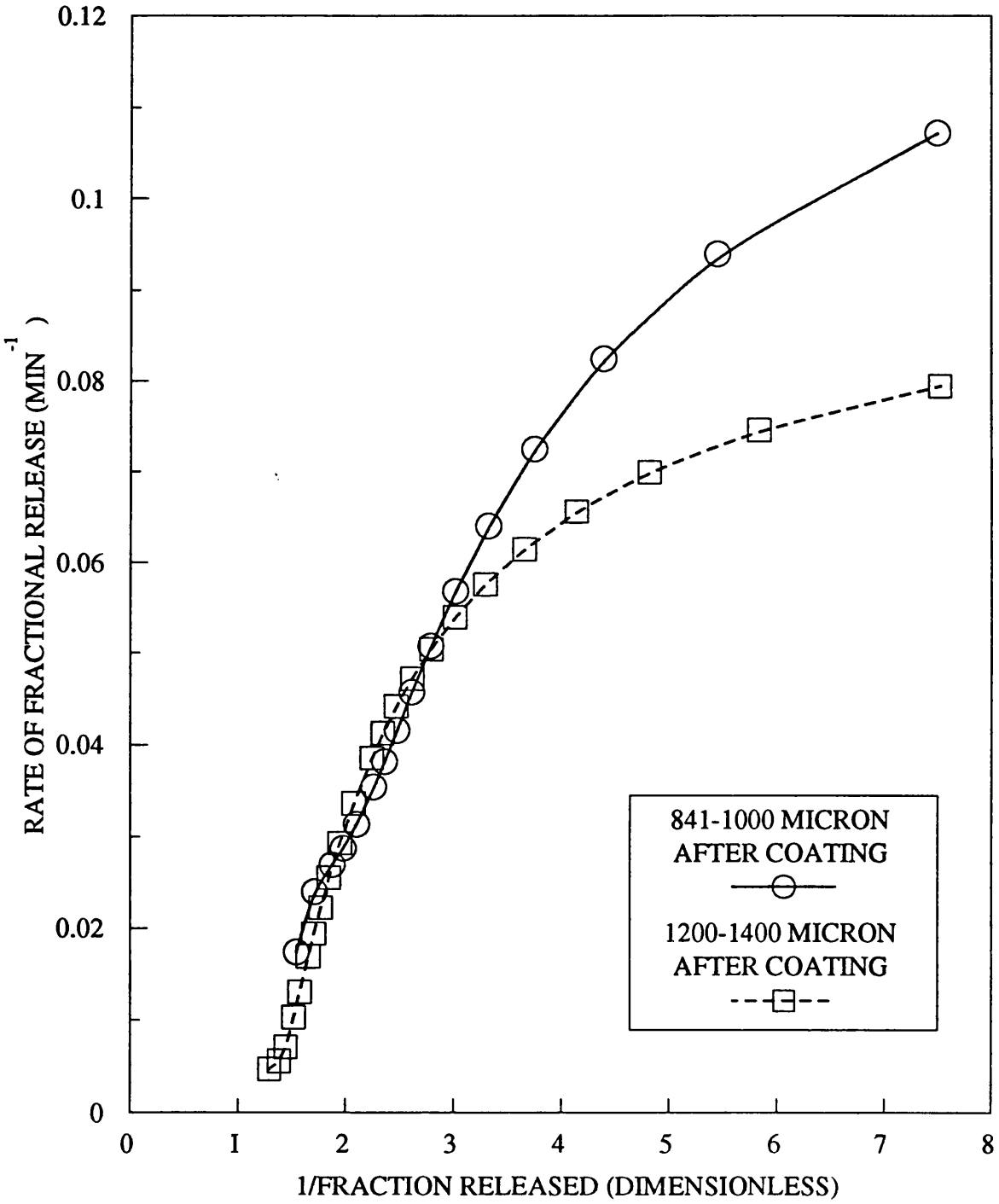

COATINGS CONTAINED EQUAL PROPORTIONS OF EUDRAGIT RL AND RS WITH 10% GLYCERYL TRIACETATE AND 5% OXAMNIQUINE RELATIVE TO POLYMER WEIGHT.

FIG 116:THE EFFECT OF PELLET CORE SIZE ON THE RELEASE OF OXAMNIQUINE FROM COATED PELLETS: PLOT OF RATE OF FRACTIONAL RELEASE AGAINST FRACTION RELEASED

DIFFERENTIAL RATE PLOT TO TEST THE VALIDITY OF THE DISSOLUTION CONTROLLED MODEL

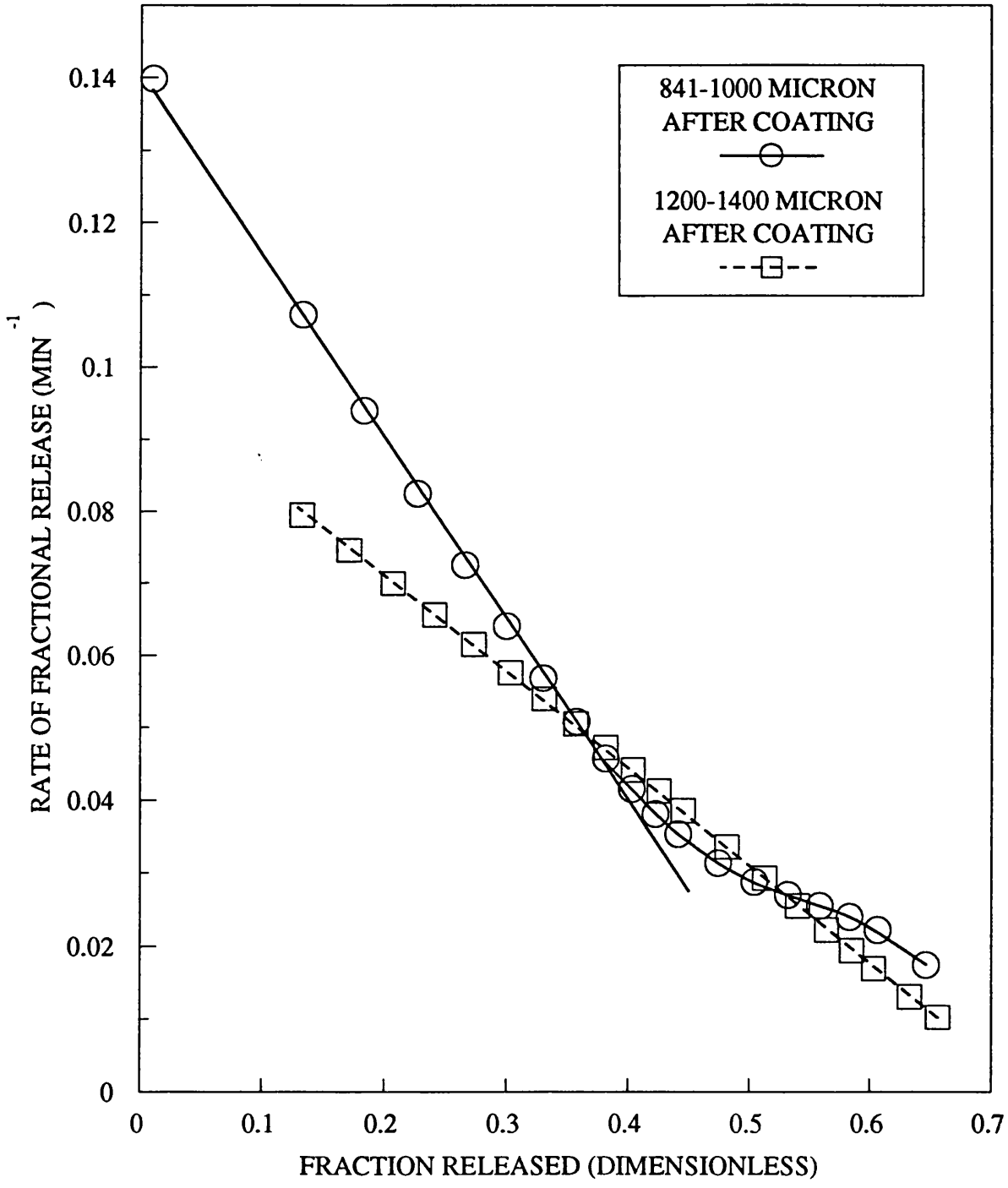

COATINGS CONTAINED EQUAL PROPORTIONS OF EUDRAGIT RL AND RS WITH 10% GLYCERYL TRIACETATE AND 5% OXAMNIQUINE RELATIVE TO POLYMER WEIGHT.

delivered rapidly in the form of atomised droplets to moving surfaces. Solvents are evaporated rapidly from the coating area, which may lead to premature spray drying of coating on surfaces. Pores may be present, produced by solvent evaporation from within coatings. Film structures are built up by multiple applications of small quantities of polymer within the coating region of coating chambers, which may result in the gross failure of contiguous polymer coats to form on particles, or the formation of microscopic voids within the film coating. Abrasion tests on coated pellets prepared for these studies did not indicate the gross failure of a film to form on the surface of pellets.

Reflected light microscopy does not have adequate resolution to identify defects within film coats. Examination of the coatings by light microscopy, also used to characterise the thickness of the coating applied to pellets, did not reveal any defects in the film coatings. Scanning electron microscopy has been used in these studies to examine the structure of films which have formed on pellet surfaces and possibly to explain some of the observations made during the release studies.

Figures 117 to 125 show examples of scanning electron micrographs of the surfaces of uncoated pellets, coated pellets and transverse sections through coated pellets.

The scanning electron micrographs of the uncoated pellets

at low magnification show an apparently smooth surface. The photomicrographs also illustrate the variation in pellet shape, which is assumed to be spherical. The variation in shape may be responsible for some deviation from the theoretical models used to describe release of oxamniquine from the coating.

Figure 118 shows the surface of an uncoated pellet at higher magnification. The photomicrograph shows a granular and heterogeneous surface typical of a sugar/starch comprimate. The heterogeneous surface may assist in the bonding of the coating to the pellet surface.

At low magnification the surface view of coated pellets does not appear any different from uncoated pellets. This was apparent from both visual inspection and also a comparison of the photomicrographs in Figures 117 and 119.

Figures 120 to 125 show photomicrographs of transverse sections through coated pellets from three of formulations of coated pellets prepared for these studies. Scanning electron microscopy was found to be a useful method of determining coating thickness. Other methods which were attempted included micrometry of coated and uncoated pellets, light microscopy, and sieve analysis.

Micrometry was unsuccessful because the size variation within samples of coated and uncoated pellets was greater than the average thickness of the coating. Reflected light

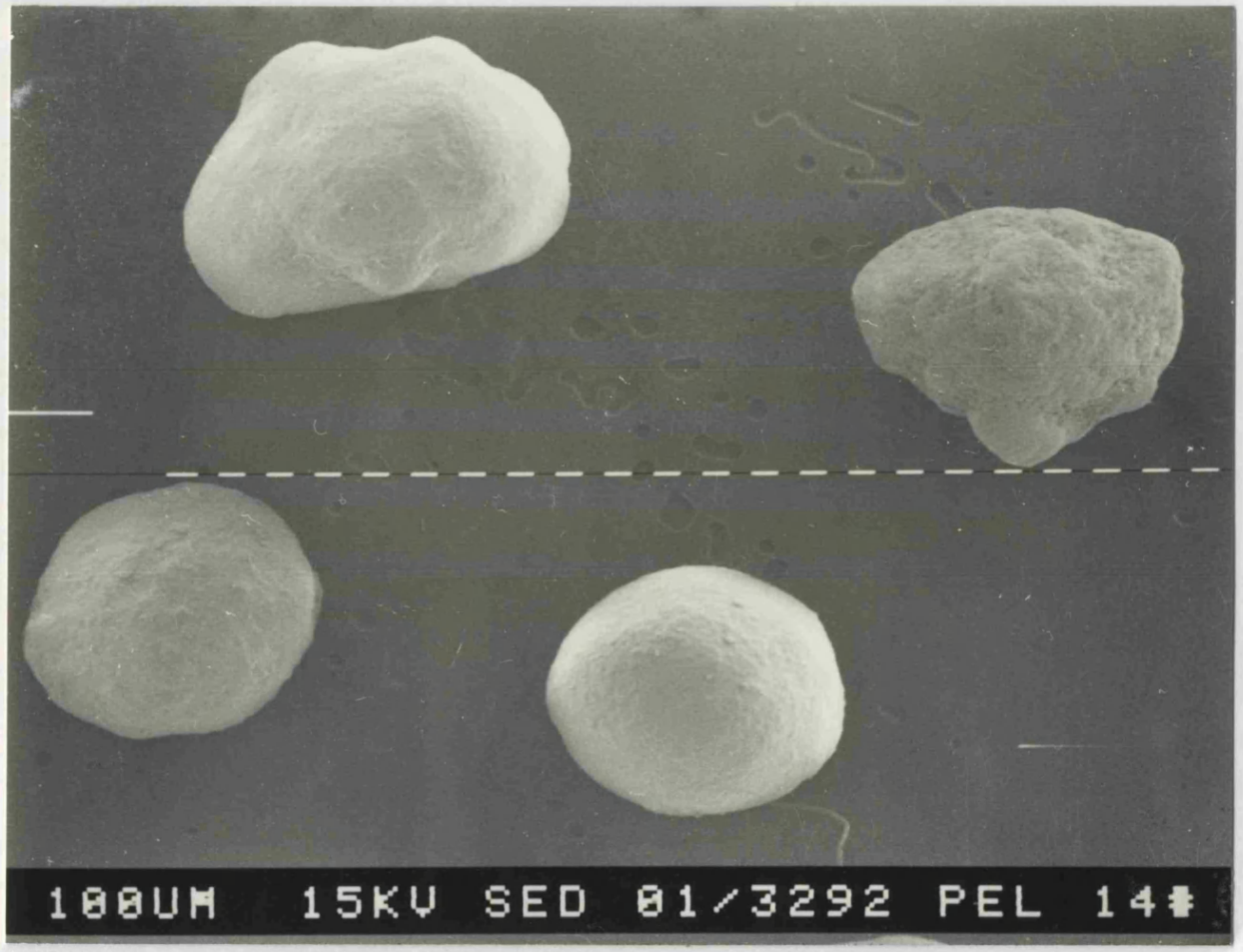

FIGURE 117 Scanning electron micrograph showing the surface structure of an uncoated non-pareil pellet (14-18 US Mesh).
Magnification x 14: Sample Tilt Correction 0°.

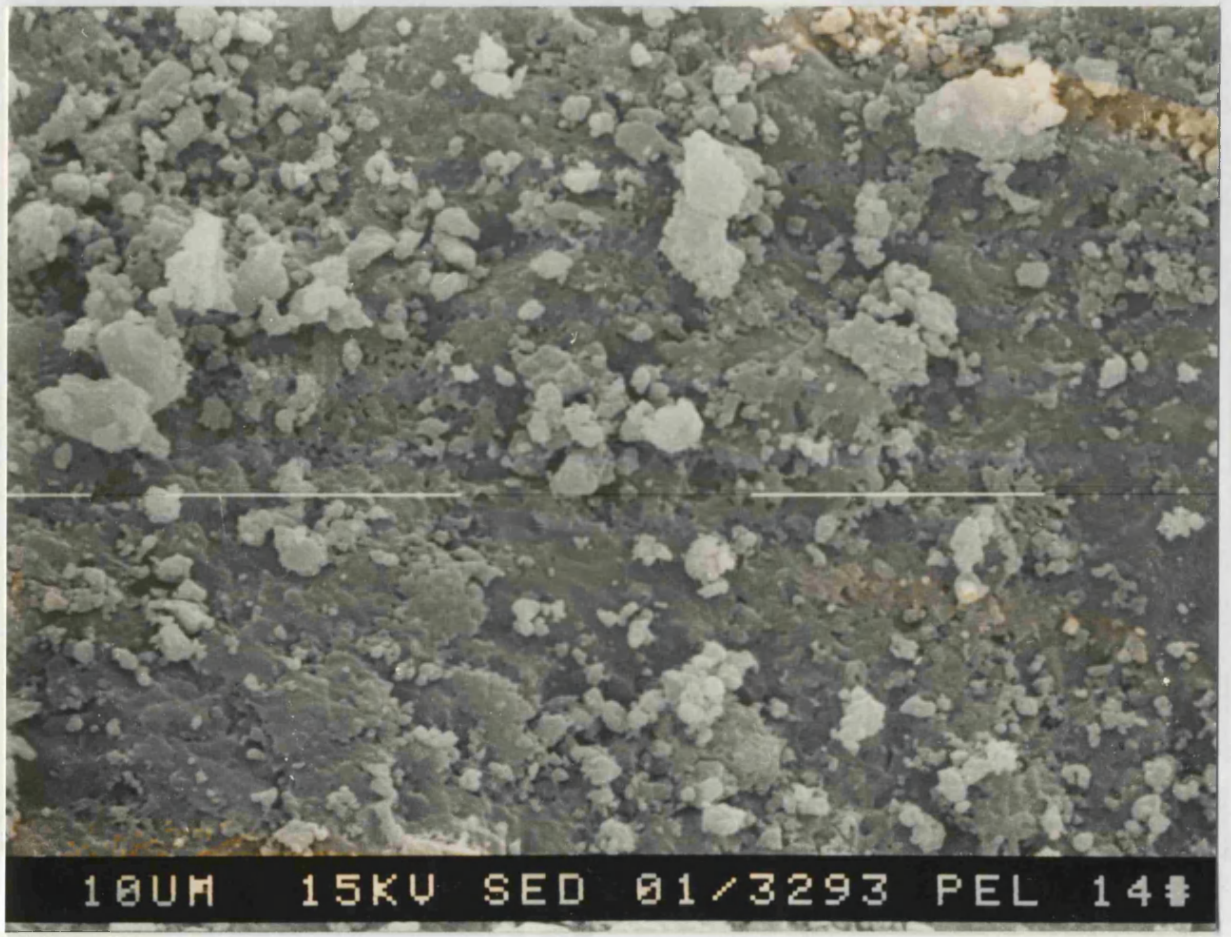

FIGURE 118 Scanning electron micrograph showing the surface structure of an uncoated non-pareil pellet (14-18 US Mesh).
Magnification x 1720: Sample Tilt Correction 0°.

FIGURE 119 Scanning electron micrograph showing the surface structure of a non-pareil pellet coated with a film containing equal proportions of Eudragit RL and Eudragit RS with 10% w/w glyceryl triacetate and 5% w/w oxamniquine (relative to total polymer weight). (FORMULATION A1).
Magnification x 14: Sample Tilt Correction 0°.

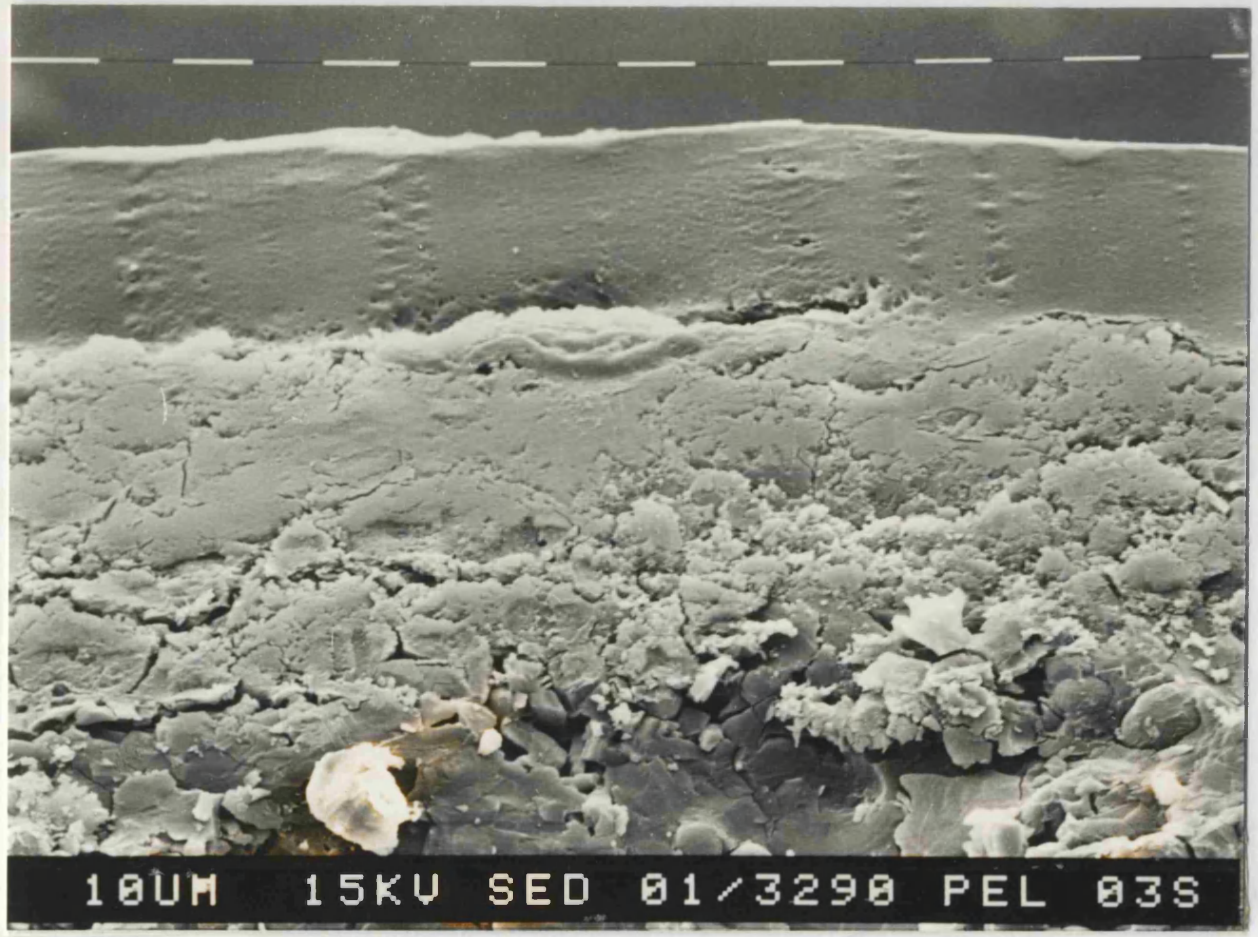

FIGURE 120 Scanning electron micrograph showing a transverse section through a coated non-pareil pellet described in Figure 119.
Magnification x 430: Sample Tilt Correction 0°.

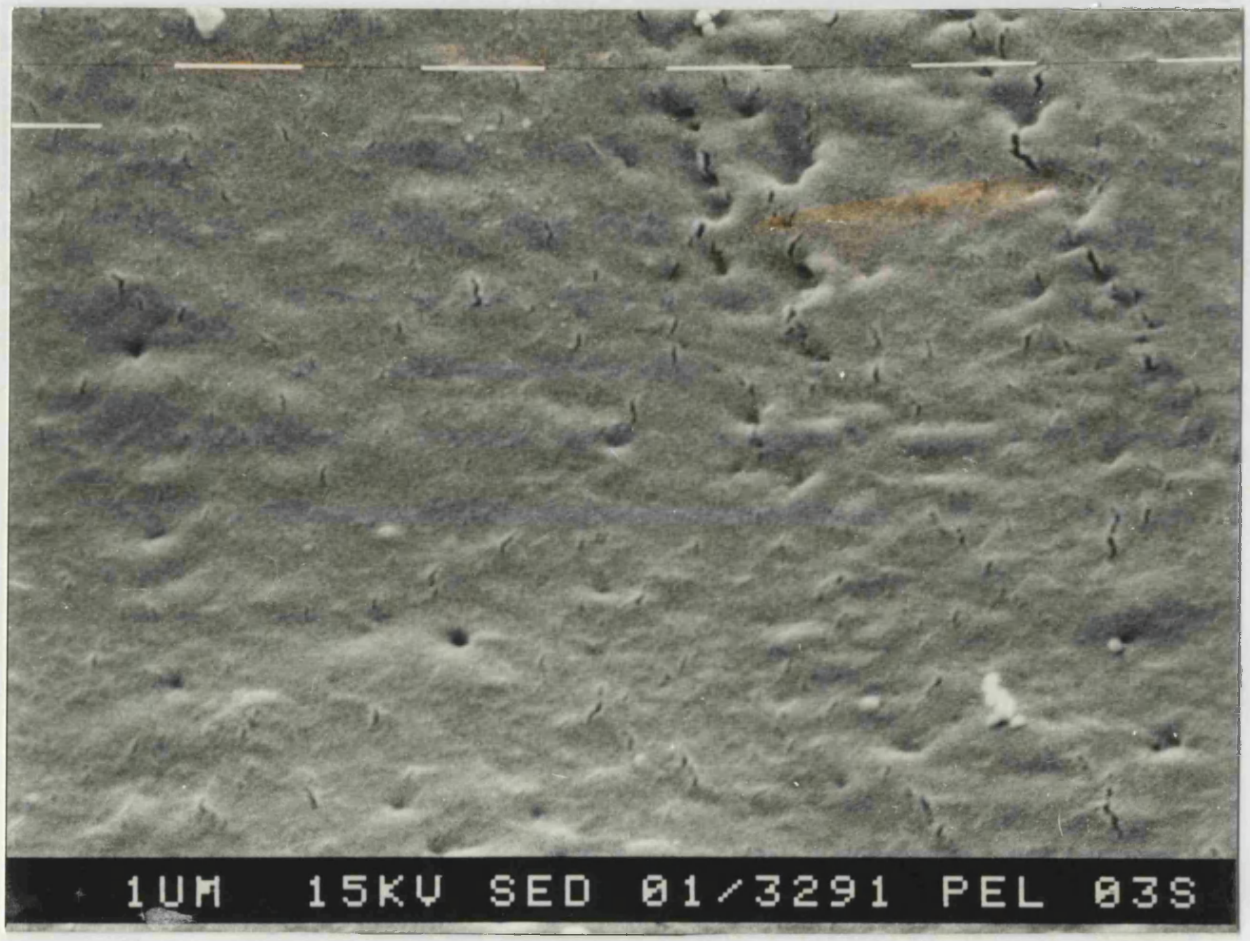

FIGURE 121 Scanning electron micrograph showing a transverse section through a coated non pareil pellet described in Figure 119. High magnification to illustrate film coating.
Magnification x 6900: Sample Tilt Correction 0°.

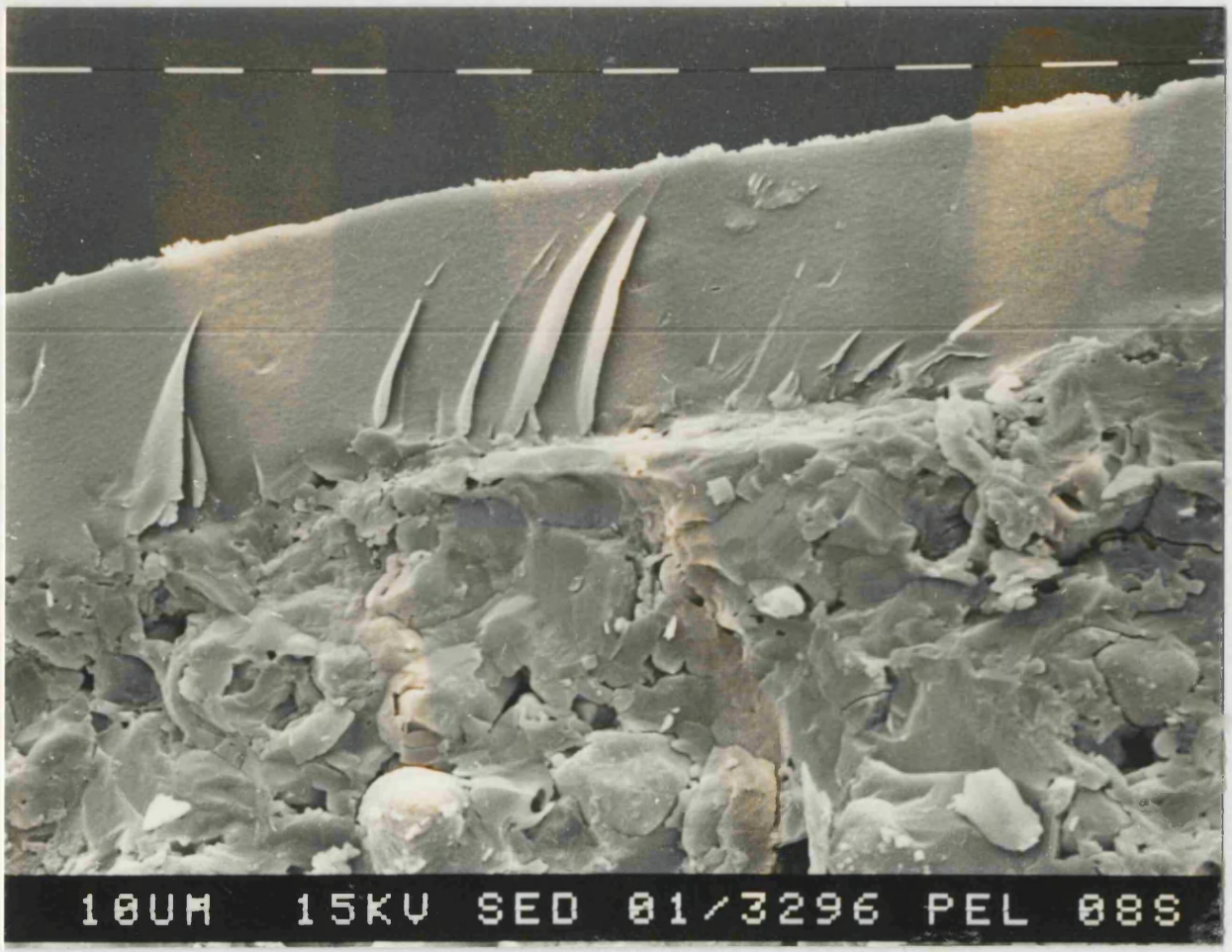

FIGURE 122 Scanning electron micrograph showing a transverse section through a coated non-pareil pellet coated with a film containing Eudragit RS with 10% w/w Glyceryl Triacetate and 5% w/w Oxamniquine (relative to polymer weight). (FORMULATION B4).
Magnification x 430: Sample Tilt Correction 0°.

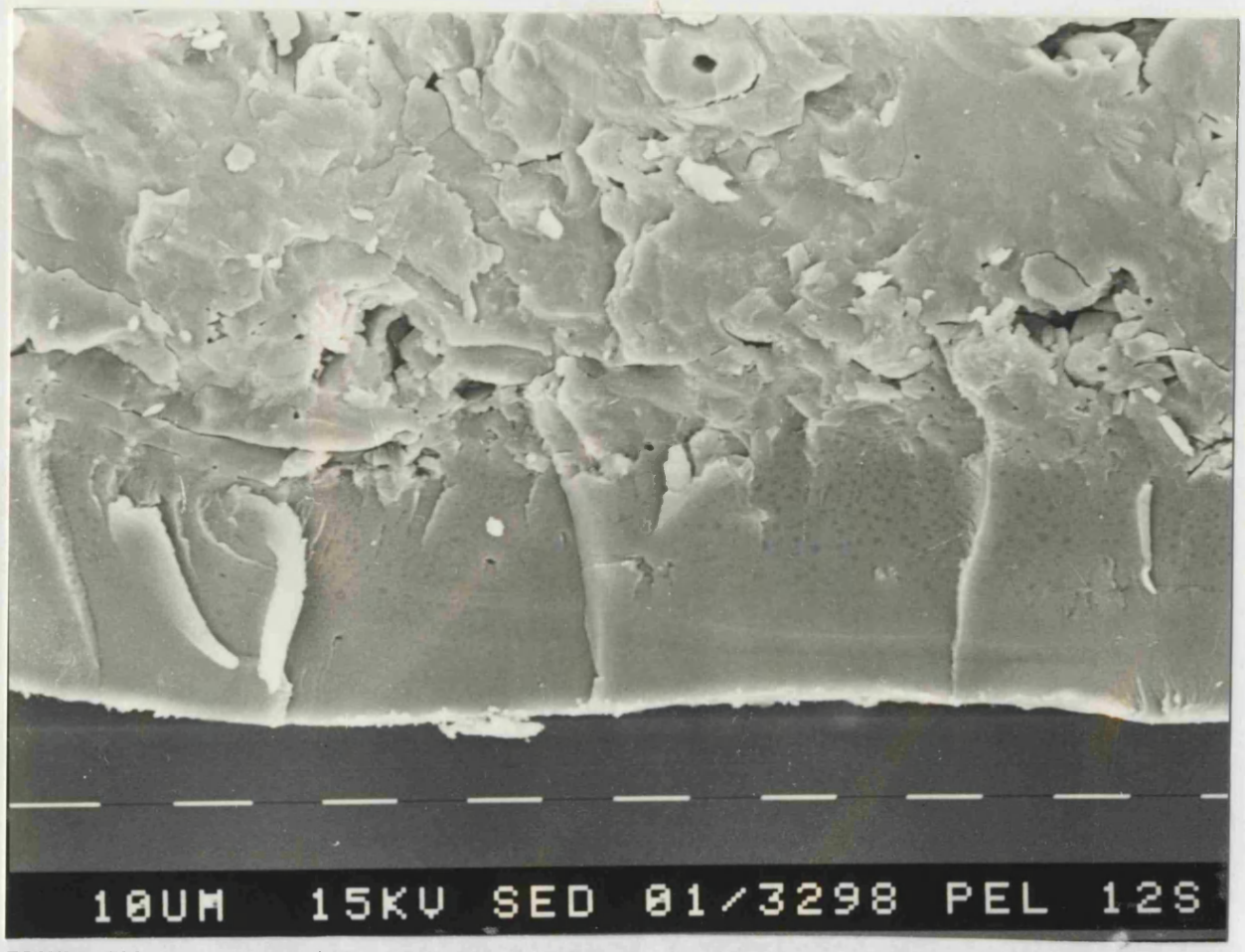

FIGURE 123 Scanning electron micrograph showing a transverse section through a coated non-pareil pellet coated with a film containing equal proportions of Eudragit RL and Eudragit RS with 10% w/w Polyethylene Glycol 400 and 5%w/w Oxamniquine (relative to polymer weight). (FORMULATION D1).
Magnification x 430; Sample Tilt Correction 0°.

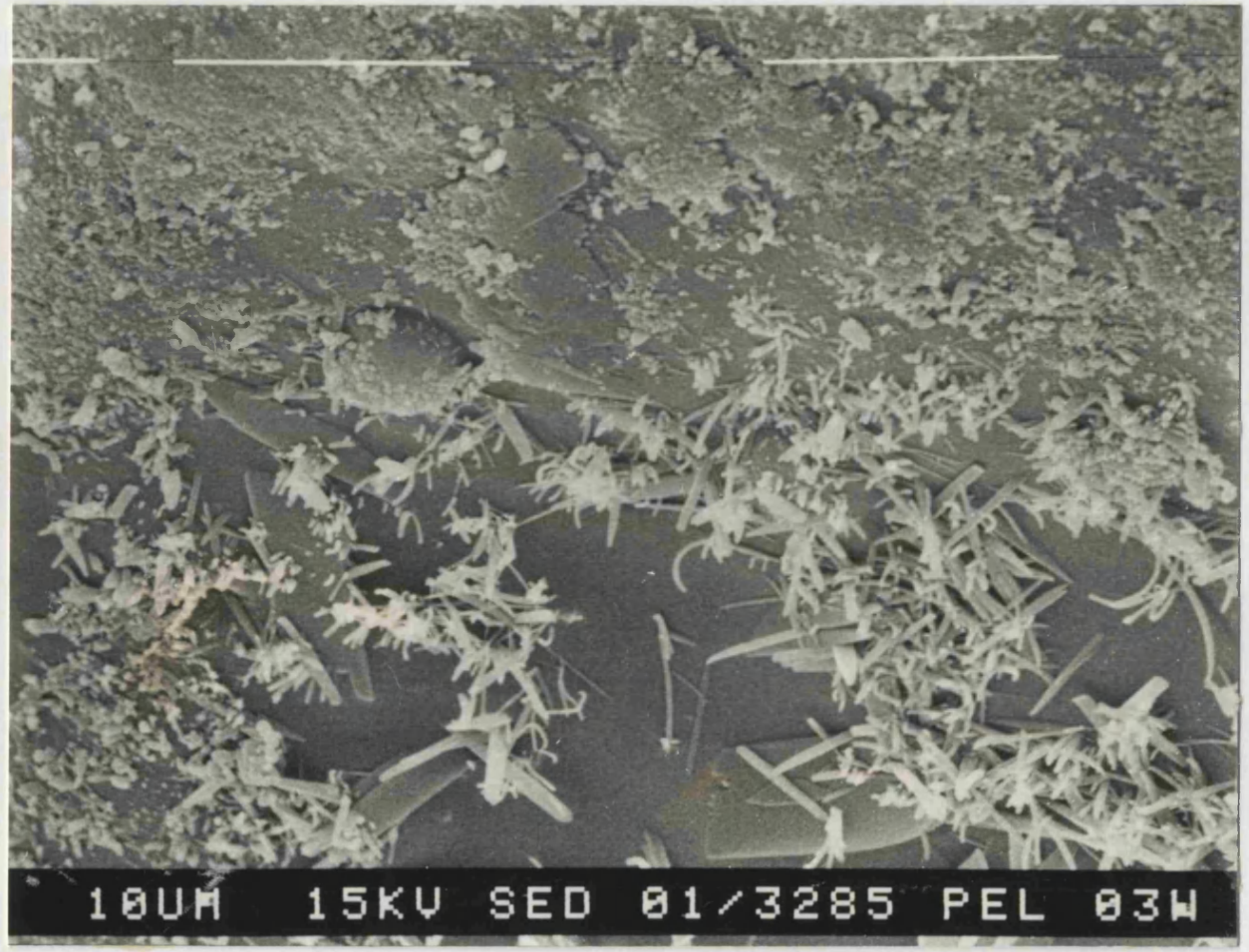

FIGURE 124 Scanning electron micrograph showing the surface structure of non pareil pellets coated with a film described in Figure 119. Magnification x 1720: Sample Tilt Correction 0°.

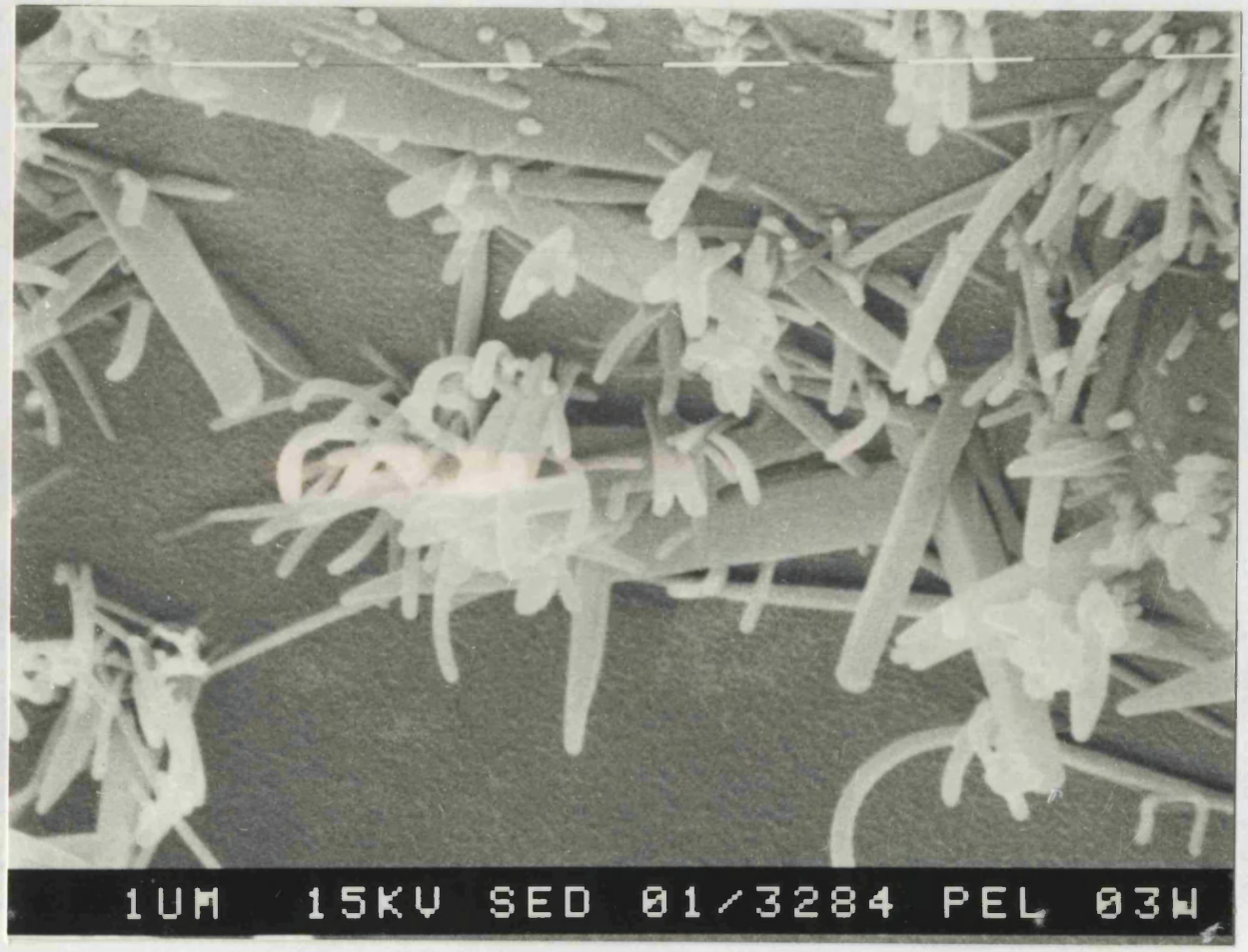

FIGURE 125 Scanning electron micrograph showing the surface structure of non pareil pellets coated with a film described in Figure 119. Magnification x 6900; Sample Tilt correction 0°.

microscopy was unable to resolve the interface between the core and the coating. Furthermore, it was not possible to cut a transverse section through the pellet sufficiently thin to measure coating thickness using transmitted light. From sieve analysis measurements the difference between coated and uncoated pellets was approximately 100μm at 50% cumulative weight oversize was detected, which could be attributed to the coating thickness. However the size distribution curves required considerable interpolation which reduced the reliability of this method. Sieves with a sufficient resolution between 1000, 1200, and 1400 microns to make a more precise determination of coating thickness using this method were not available.

Table 25 summarises thickness determinations made on the coatings measured using the scanning electron micrographs. Typically the coating thickness applied to the pellets was around 30μm. The variation in coating thickness from between 20 and 44μm is probably due to variations from true spherical shape of the coatings caused during manufacture and during the early stages of coating when abrasion of the pellets is most likely.

It has been estimated (ROHM PHARMA 1979a,b) that application of 1mg of polymer per square centimeter of tablet surface produces a layer of 8μm in thickness. On tablets an 8μm layer will provide a very short sustained release effect.

TABLE 25 **SUMMARY OF COATING THICKNESS DETERMINATIONS MADE ON TRANSVERSE SECTIONS THROUGH COATED PELLETS BY SCANNING ELECTRON MICROSCOPY**

Coating Formulation	Individual Thickness Determinations (μm)	Mean Thickness (μm)	Standard Deviation (μm)	Coefficient of Variation %
A1	27, 28, 32, 35, 35 21, 25, 27, 30, 34 23, 23, 23, 25, 23 29, 33, 33, 33, 32	28.55	4.64	16.25
B4	31, 33, 37, 31, 28 38, 30, 29, 32, 27 37, 37, 33, 33, 30	30.40	9.09	29.90
D1	33, 44, 36, 33, 30 20, 23, 23, 24, 22 32, 28, 28, 30, 29	29.20	6.33	21.68

Rounded pellets or granules require the application of 1 to 5mg of dry polymer per square centimeter of surface area, which should be equivalent to 8 to 40μm of coating thickness. Given that polymer solution equivalent to 5mg/cm^2 was applied to the pellets, and that this resulted in a coating approximately 30μm thick, suggests that the process used was only 75% efficient. Using the calculation based on weight increase of the pellets after detailed in Section 5.3.2, the process efficiency was calculated to be approximately 90%. In either case, the result demonstrates that there was a high loss of coating material and that the coating process requires further investigation.

Figures 120 to 122 showing transverse sections through pellets demonstrate good interfacial contact between the film and the substrate. A contiguous film was formed which

could clearly be differentiated from the pellet surface. Some inhomogeneities can be seen within the film, which may be due to the coating process or damage to the pellets caused during sample preparation. Figure 121 shows a higher magnification of the coating surface in transverse section. An array of crater, pore and hill like structures are visible in the surface. These are more typical of the structure of a coating from which drug has been extracted. This appearance may be due to the rapid removal of the solvent during the coating process leading to bubbles of polymer solution which collapse at the surface leaving discontinuities in the film coating structure. Figures 124 and 125 shows views the surface structure of coated pellets at higher magnification. The photomicrographs show a coarse granular structure containing needle like crystals layered over a finer 'orange peel' structure. This structure was not apparent visually or by light microscopy. It is proposed that this structure represents crystals of oxamniquine within a surface layer of Eudragit caused by rapid evaporation of the carrier solvent during coating. As the solvent evaporates, the concentration of oxamniquine within the carrier mixture increases and eventually exceeds the solubility, depositing oxamniquine at the surface.

It is further proposed that this surface layer is responsible for the initial rapid release of oxamniquine from the coatings, and the apparent conformity with a dissolution controlled model for oxamniquine release observed for many of the coatings.

5.11 X-Ray Crystallography Studies

5.11.1 Introduction

Polymers very rarely exhibit a regular crystal lattice structure. Regardless of chemical structural factors which promote molecular order and crystallinity within films, it is extremely unlikely that any polymer is 100% crystalline.

The majority of pharmaceutically significant polymers are composed of both crystalline and amorphous regions. The properties of polymers depend upon the relative proportions of crystalline and amorphous domains. The 'supermolecular structure' (BANKER, 1966) is a description of the placement of laterally ordered groups of chains in a polymer structure and is related to the overall crystallinity of that polymer. In general highly crystalline polymers are more difficult to solvate than amorphous polymers.

A number of chemical factors promote crystallinity in polymers. Strongly polar groups or hydrogen bonding groups which are regularly distributed along the chains tend to form ordered groups of chains. Greater order between groups of chains will promote a greater degree of crystallinity within the polymer.

It was considered that the presence of polar quaternary ammonium functions in Eudragit RL and Eudragit RS might induce crystallinity in these polymers, and that the extent

of crystallinity in the two polymers might be different.

The regular ordering of molecules in the crystalline state can be used to determine the degree of crystallinity in materials by X-ray diffraction. X-ray diffraction patterns of perfect ionic crystals give sharp, narrow, diffraction peaks. Strongly crystalline polymers yield broad diffraction peaks superimposed on a diffuse halo. The broadness is due to the relatively small size of, and imperfections within, the crystalline regions of the polymer. As the degree of polymer crystallinity decreases the diffraction peaks become broader. Thus amorphous polymers, like low molecular weight liquids, give broad diffraction peaks associated with the average distances between atoms in the liquid state. The diffraction peaks are broad because of the statistical distribution of these distances and because they are not periodic in nature.

5.11.2 Materials Tested

A series of Eudragit films were cast from solution in dichloromethane. The composition of these films is summarised in Table 26.

In addition, a series of physical mixtures of oxamniquine with finely powdered pure Eudragit RL (Batch 6732/22/RL;

Röhm Pharma) were prepared and examined by X-Ray crystallography. The sample of finely powdered pure Eudragit RL 100 was specially provided by Röhm Pharma GmbH.

The composition of the powder samples is summarised in Table 27.

TABLE 26 **COMPOSITION OF EUDRAGIT FILMS EXAMINED BY X-RAY CRYSTALLOGRAPHY**

Sample Code	COMPOSITION % w/w			
	Eudragit RL	Eudragit RS	Glyceryl Triacetate	Oxamniquine
A1	-	100.0	-	-
A2	100.00	-	-	-
A3	50.00	50.00	-	-
A4	40.00	40.00	20.00	-
B1	-	80.00	20.00	-
B2	80.00	-	20.00	-
B3	80.00	-	20.00 (Note 1)	-
B4	80.00	-	20.00 (Note 2)	-
C1	-	80.00	20.00 (Note 2)	-
C2	38.46	38.46	15.38	7.69
C3	45.45	45.45	-	9.09
C4	-	-	-	100.00 (Note 3)

NOTES TO TABLE 26

1. The film was stored <u>in vacuo</u> at 35°C for 1 week before examination by X-Ray crystallography.

2. Films were washed in distilled water for 4 hours. Excess surface moisture was removed using blotting paper, and the films dried in a vacuum oven for 6 hours at 35°C.

3. Oxamniquine drug substance as received from Pfizer without further purification or treatment.

TABLE 27 **COMPOSITION OF OXAMNIQUINE/EUDRAGIT RL POWDER MIXTURES EXAMINED BY X-RAY CRYSTALLOGRAPHY**

Formulation Code	COMPOSITION % w/w	
	Oxamniquine	Eudragit RL
1	0.0	100.0
2	1.0	99.0
3	5.0	95.0
4	10.0	90.0
5	100.0 (Note 1)	0.0
6	100.0 (Note 2)	0.0

NOTES TO TABLE 27

1. Oxamniquine drug substance as received from Pfizer without further purification or treatment.

2. Oxamniquine drug substance dissolved in and recrystallised from dichloromethane.

5.11.3 Results and Discussion

Figures 126 to 131 show photographs of the diffraction patterns of the cast films. Figure 129 shows a photograph of the diffraction pattern of an empty sample holder as reference. The 'diffraction pattern' seen in Figure 129 is an artefact and therefore be excluded from patterns in samples A1-A4.

None of the film formulations show any crystalline diffraction pattern and are therefore substantially amorphous. No diffraction pattern was seen in films from which the plasticiser was removed either by vacuum treatment or washing. Pure oxamniquine (sample C4) has

strong crystalline pattern, which is absent from films C2 and C3, which contained 7.69% w/w and 9.09% w/w oxamniquine respectively. It is possible that the oxamniquine concentration in the films is too low to be detected by the X-Ray Camera.

Examination of the powder samples provided further interesting information. Eudragit RL has no diffraction pattern and therefore appears to be substantially amorphous.

As Eudragit RL contains twice as many quarternary ammonium groups as Eudragit RS, it would be expected that pure Eudragit RS is substantially amorphous. There may be a few crystalline domains within the polymers, but the proportion may be too low to be detected by this method. Figure 130 shows photographs of the diffraction patterns of physical powder mixtures of oxamniquine with Eudragit RL and illustrate increasing intensity of the oxamniquine diffraction pattern with increasing oxamniquine concentration. The diffraction pattern of the physical mixture containing 1% w/w oxamniquine shows the oxamniquine pattern quite clearly. Therefore the concentration of oxamniquine present in the cast films is not below the limit of detection for the drug.

Oxamniquine is therefore present either dispersed in the films in an amorphous (high energy) state or entirely dissolved in the films.

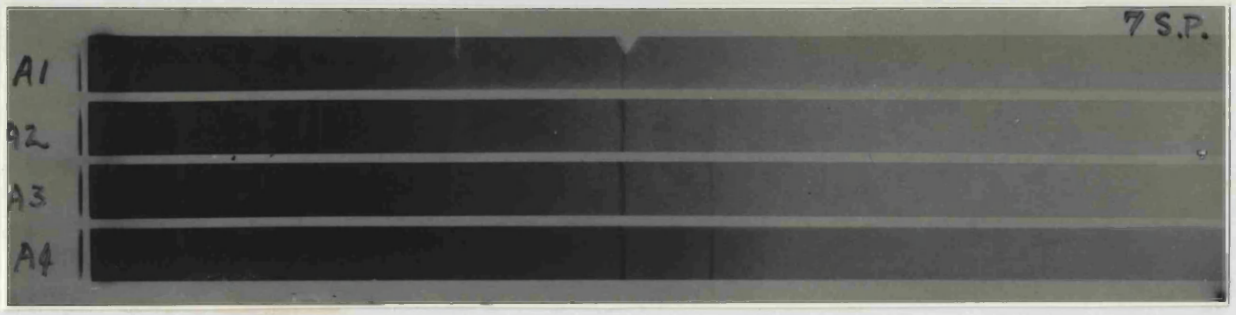

FIGURE 126 Photograph of X-Ray Diffraction Pattern of Cast Films Codes A1 to A4

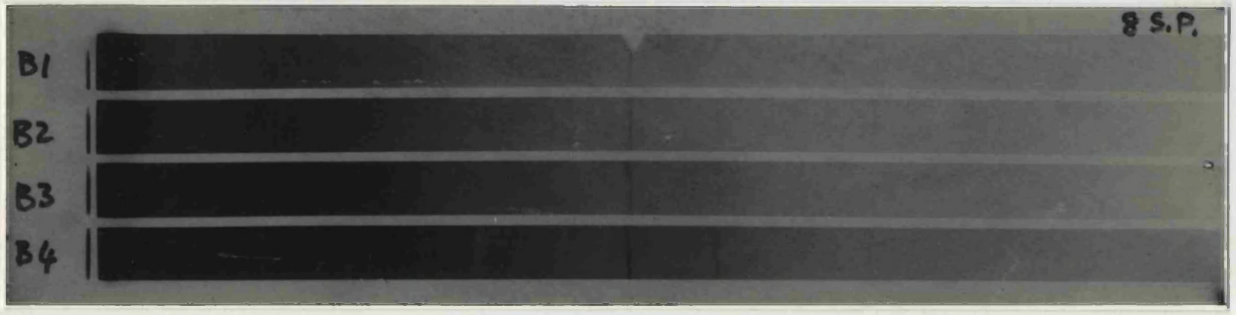

FIGURE 127 Photograph of X-Ray Diffraction Pattern of Cast Films Codes B1 to B4

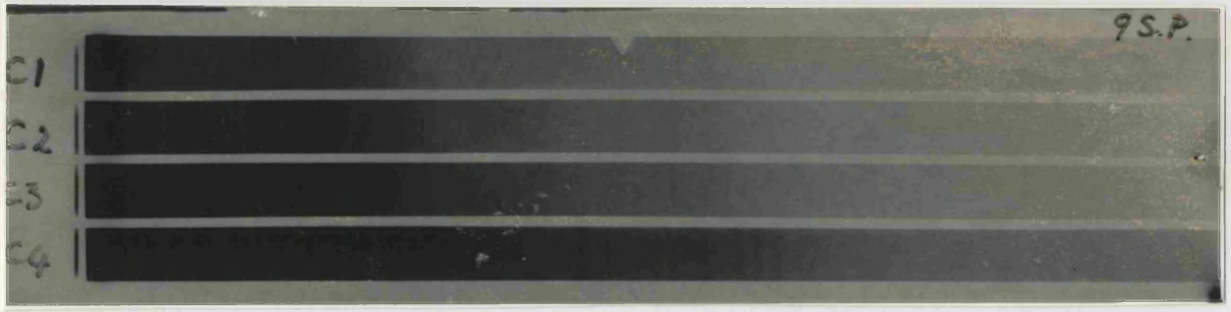

FIGURE 128 Photograph of X-Ray Diffraction Pattern of Cast Films Codes C1 to C4

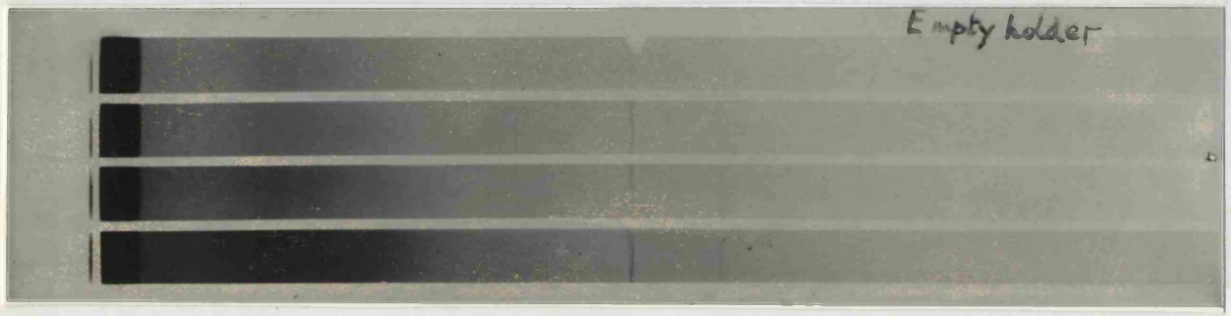

FIGURE 129 Photograph of X-Ray Diffraction Pattern of Empty Sample Holder

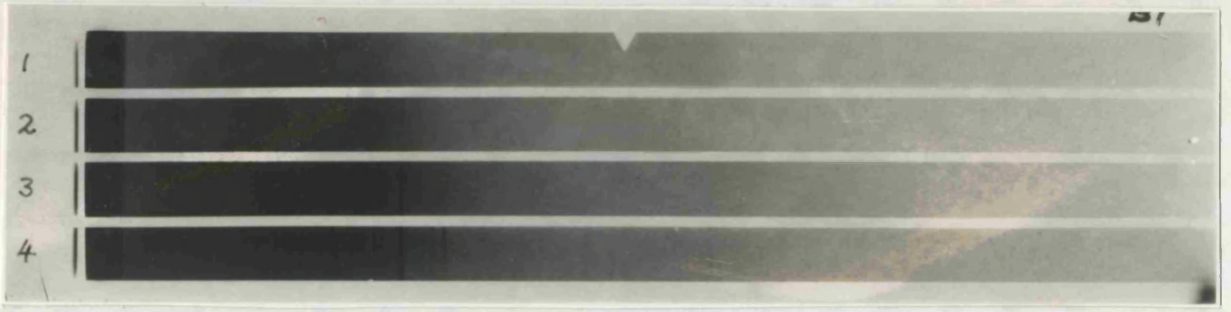

FIGURE 130 Photograph of X-Ray Diffraction Pattern of Oxamniquine/Eudragit RL powder mixtures samples 1 to 4

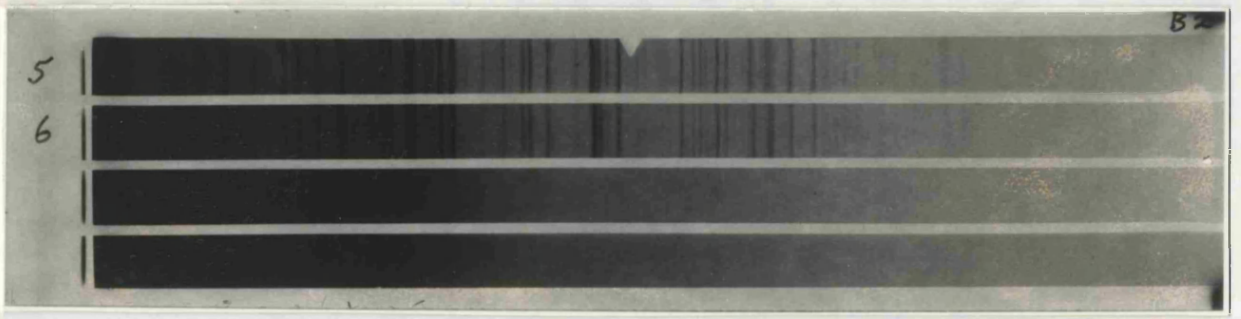

FIGURE 131 Photograph of X-Ray Diffraction Pattern of Oxamniquine powder samples 5 and 6.

The solubility of oxamniquine in glyceryl triacetate is approximately 1.5mg cm^{-3} (Chapter 4). Oxamniquine is present in the films examined by X-Ray diffraction in a proportion of 50%w/w relative to the glyceryl triacetate content, which is considerably in excess of its solubility in the plasticiser. Unless the drug has completely dissolved in the polymer, which is unlikely, then the physical form of oxamniquine has changed within the film. The crystallisation of oxamniquine has been inhibited by co-evaporation in the presence of polymer. A similar effect has been reported in the literature (DeFILIPPAS et al, 1991) for co-evaporates of Indomethacin with Eudragit E which showed on absence of drug crystallinity compared with physical mixtures. This contrasts sharply with the apparent presence of crystalline oxamniquine observed in the scanning electron micrographs of coated pellets. Figure 146 demonstrates that there was no difference in the diffraction pattern of oxamniquine as received and after recrystallisation from dichloromethane. This suggests that the casting process itself is not responsible for the change of physical form of the drug within the film.

5.12 Determination of Glass Transition Temperatures

Two methods were used to attempt to measure the glass transition temperature of Eudragit RL and RS. These were differential scanning calorimetry and change in hardness using micro-indentation.

5.12.1 Glass Transition Temperatures by Differential Scanning Calorimetry

Approximately 5mg of polymer was placed in standard flat bottomed aluminium DSC pans, by repeated application of polymer solutions. The pans were crimped closed with aluminium lids. Thermograms were recorded using a Perkin Elmer DSC-1B (Perkin Elmer Ltd, Beaconsfield, England) over the temperature range 240K to 320K (-33°C to +47°C) at a rate of 8K/min. The DSC cell was cooled with liquid nitrogen.

Two apparent transitions were observed for both Eudragit RS (at 279K and 298K) and for Eudragit RL (at 281 and 298K). The transitions which appear as baseline slope changes indicate that they are not melting changes which would be seen as sharp peaks. It is unlikely that the transitions which are apparently seen at 279K and 281K are glass transition temperatures. It is possible that the transitions seen at 298K represent glass transitions, although this cannot be stated with certainty as the results were not reproducible.

In a subsequent experiment, polymer samples were prepared in aluminium DSC pans from solution in dichloromethane as described above, and examined using the Perkin Elmer DSC-2 (Perkin Elmer Ltd, Beaconsfield, England). Thermograms were recorded over the temperature range 253K to 310K (-20°C to +35°C). The DSC head was cooled using solid

carbon dioxide/acetone and the sample cells maintained at low humidity to prevent moisture condensation. The scanning rate was 4K/min and the instrument was calibrated for temperature using indium melting. Under these conditions, no transitions were detected.

The physical properties of unplasticised Eudragit films suggest that at typical ambient room temperatures (18-22°C), Eudragit RL and RS are below their glass transition temperatures since polymer films formed at ambient temperatures are mechanically fragile and brittle.

5.12.2 Glass Transition Temperatures by Micro-indentation

Micro-indentation was used to measure glass transition temperatures by monitoring the change in hardness of a sample under an applied load at or around the glass transition temperature. Figure 132 shows two types of reaction which were observed under indentation load.

Figure 132A shows the reaction of a thermoplastic polymer above its glass transition point. Application of the load results in a deep indentation, rising slowly to a maximum which recovers slowly and incompletely after removal of the load. The polymer is soft and undergoes non-recoverable plastic deformation. By contrast, Figure 132B shows the results of an indentation on a polymer below its glass transition temperature. Application of load results in a small indentation which does nct deepen over the period

that the load is applied. Recovery is instantaneous and complete after the load is removed. These reactions are characteristic of a hard material.

Three measurements can be made, as illustrated in Figure 132. Firstly the depth of indentation under load h_1, which is measured after a fixed arbitrary period. After the load is removed, sample recovery takes place. After a fixed recovery time, the non recoverable (plastic) deformation h_2 and the recoverable (elastic) deformation Δh can be measured. The Brinnell Hardness depends upon the indentation under load and can be calculated from equation 37.

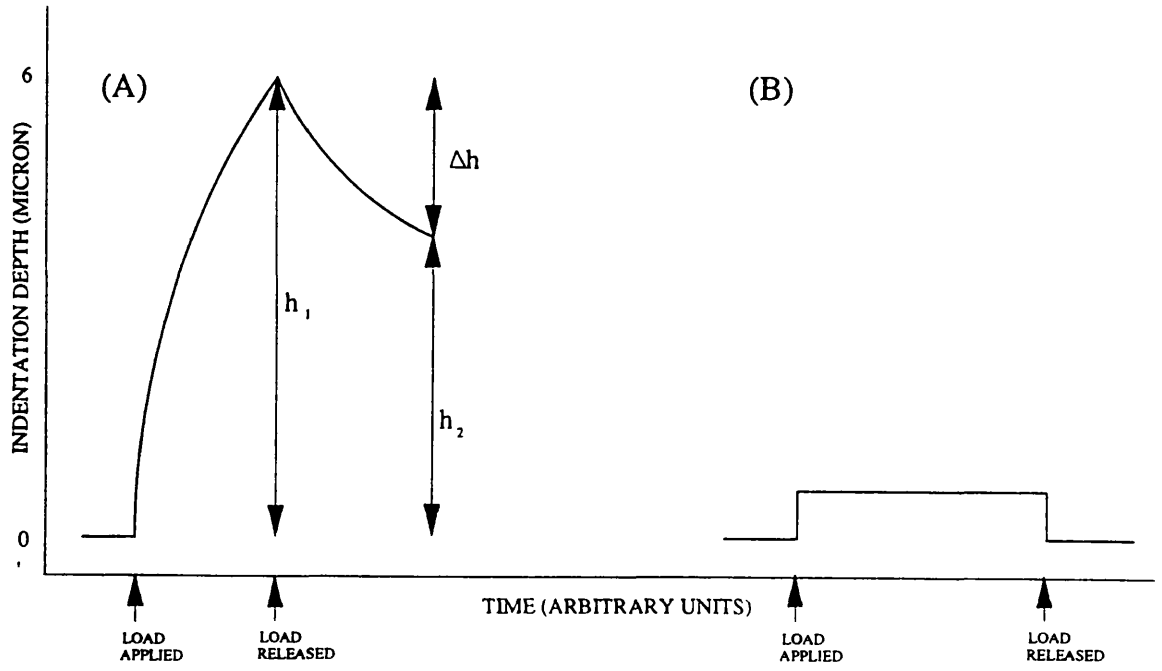

FIGURE 132 Typical indentation reactions of a polymer under load

$$BH = \frac{W}{\pi D h_1} \qquad (37)$$

Where W g is the load force applied with the mass measured in grams. D is the diameter of the indenter (1.5875mm) and h_1 the indentation under load measured in microns.

Hence

$$BH = \frac{W \times 9.81 \times 10^{-3}}{\pi \times 1.5875 \times 10^{-3} \times h_1 \times 10^{-6}} \quad Nm^{-2}$$

$$= \frac{1.967W}{h_1} \quad MNm^{-2} \text{ (MPa)}$$

Equation 38 relates the modulus of elasticity E to indentation and recovery under load of a spherical indenter (PORTER, 1980).

$$E = \frac{0.333\ W}{\Delta h \sqrt{(h_1 D)}} \qquad (38)$$

where Δh is the recoverable indentation measured in microns and other symbols have been defined previously.

Applying numeric substitutions as before

$$E = \frac{0.333 \times W \times 9.81 \times 10^{-3}}{\Delta h \times 10^{-6} \sqrt{(h_1 \times 10^{-6} \times 1.5875 \times 10^{-3})}} \quad Nm^{-2}$$

$$= \frac{81.989 \times 10^{6}\ W}{\Delta h \sqrt{h_1}} \quad Nm^{-2} \qquad \text{or}$$

$$E = \frac{81.989\ W}{\Delta h \sqrt{h_1}} \quad MNm^{-2} \text{ (MPa)}$$

Figures 133 to 142 show the effect of sample temperature on the modulus of elasticity and Brinnell Hardness of unplasticised films of Eudragit RL and Eudragit RS and mixed films plasticised with glyceryl triacetate.

Table 28 summarises glass transition temperatures derived from measurements of the Brinnell Hardness, modulus of elasticity and thermal measurements.

TABLE 28 **COMPARISON OF GLASS TRANSITION TEMPERATURES DETERMINED FROM BRINNELL HARDNESS, MODULUS OF ELASTICITY, AND THERMAL ANALYSIS MEASUREMENTS OF EUDRAGIT FILMS**

Film composition (% w/w)			Glass Transition Temperature (°C)		
Eudragit RL	Eudragit RS	Glyceryl Triacetate	Brinnell Hardness Number Measurements	Modulus of Elasticity Measurements	DSC Measurements (Note 3)
100	0	0	29.5	29.0	25.0
0	100	0	25.5	28.5	25.0
50	50	0	28.5	30.5	NT
47.62	47.62	4.76	14.8	16.5	NT
45.45	45.45	9.09	(-1.0) Note 1	N/A Note 2	NT

NOTES TO TABLE 28

1. Brinnell Hardness values were continually decreasing. It was not readily possible to detect a sharp transition which could be categorised as a glass transition.

2. Continually decreasing values of modulus of elasticity with temperature made it impossible to detect a glass transition point.

3. Data from DSC was not reproducible. It was not always possible to detect transition points.

FIG 133: THE EFFECT OF TEMPERATURE ON THE BRINNELL HARDNESS NUMBER OF EUDRAGIT RL FILMS

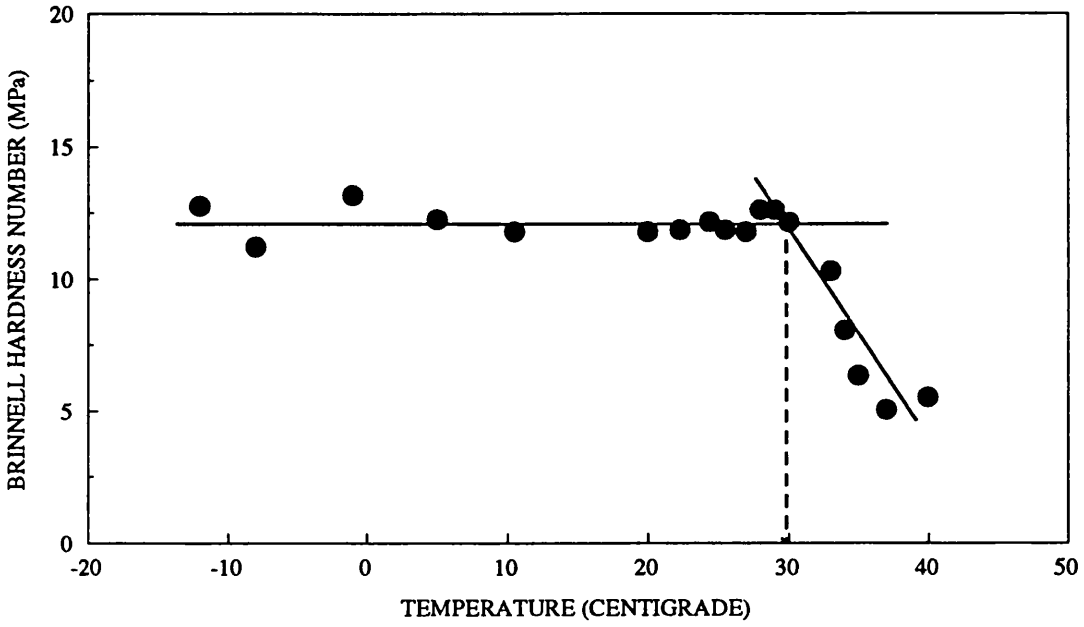

FIG 134: THE EFFECT OF TEMPERATURE ON THE MODULUS OF ELASTICITY OF EUDRAGIT RL FILMS

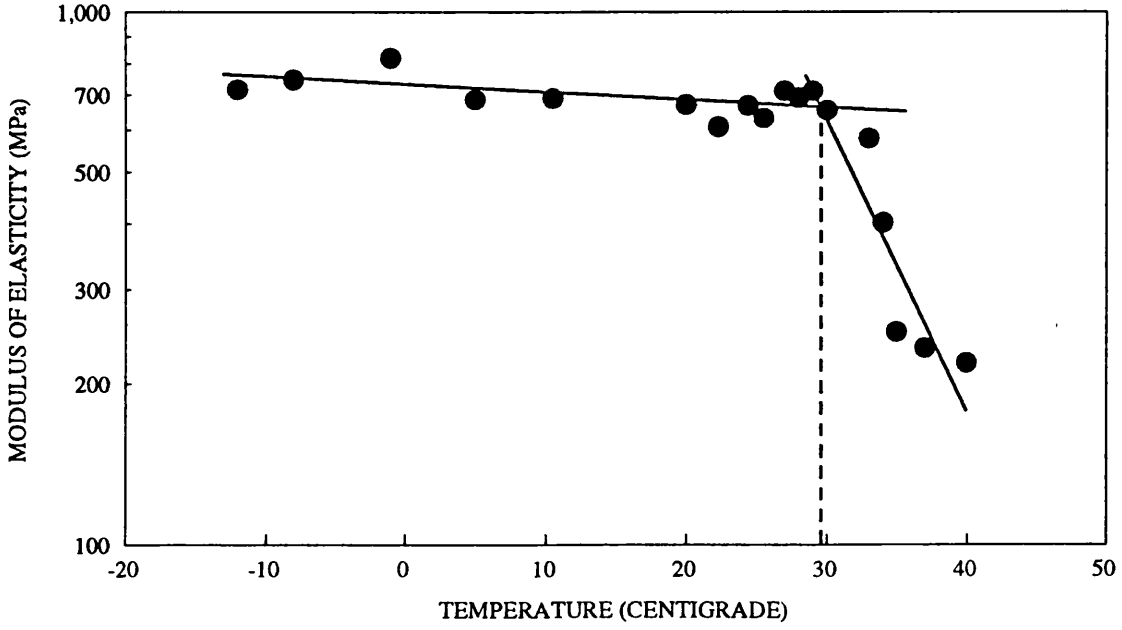

FILMS CAST ONTO DURAL DISCS FROM SOLUTION
IN DICHLOROMETHANE

FIG 135: THE EFFECT OF TEMPERATURE ON THE BRINNELL HARDNESS NUMBER OF EUDRAGIT RS FILMS

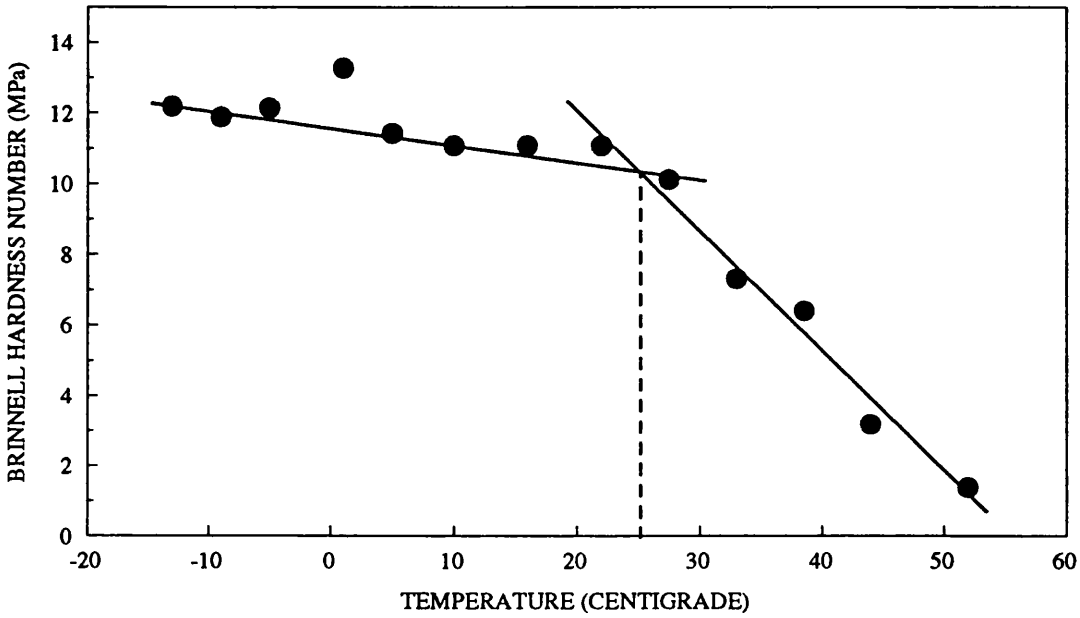

FIG 136: THE EFFECT OF TEMPERATURE ON THE MODULUS OF ELASTICITY OF EUDRAGIT RS FILMS

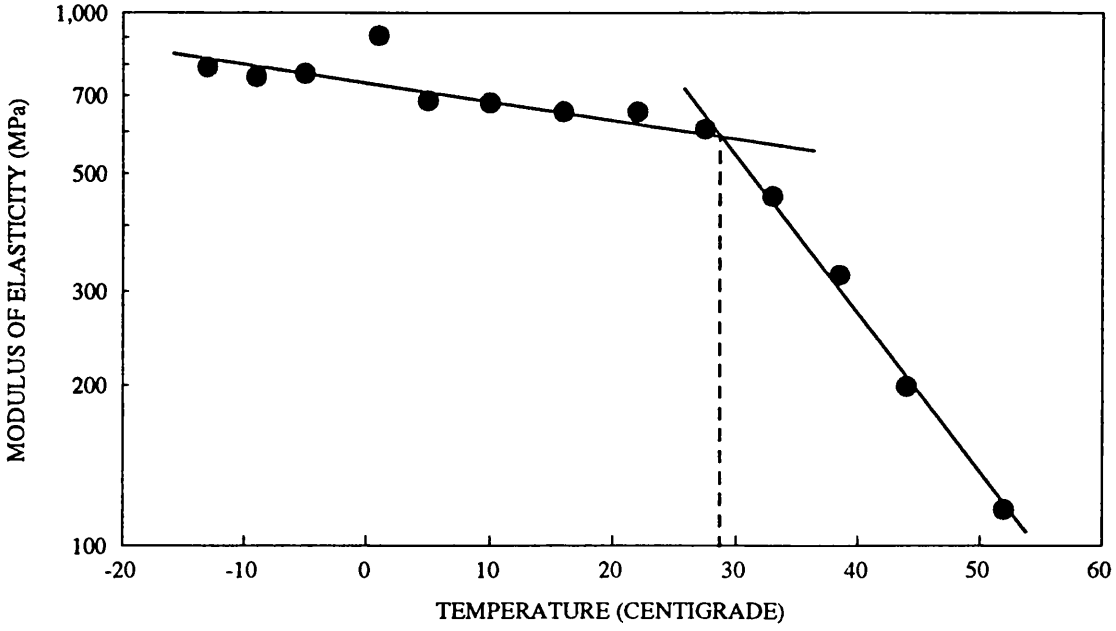

FILMS CAST ONTO DURAL DISCS FROM SOLUTION
IN DICHLOROMETHANE

FIG 137: THE EFFECT OF TEMPERATURE ON THE BRINNELL HARDNESS NUMBER OF FILMS CONTAINING EQUAL PROPORTIONS OF EUDRAGIT RL AND EUDRAGIT RS

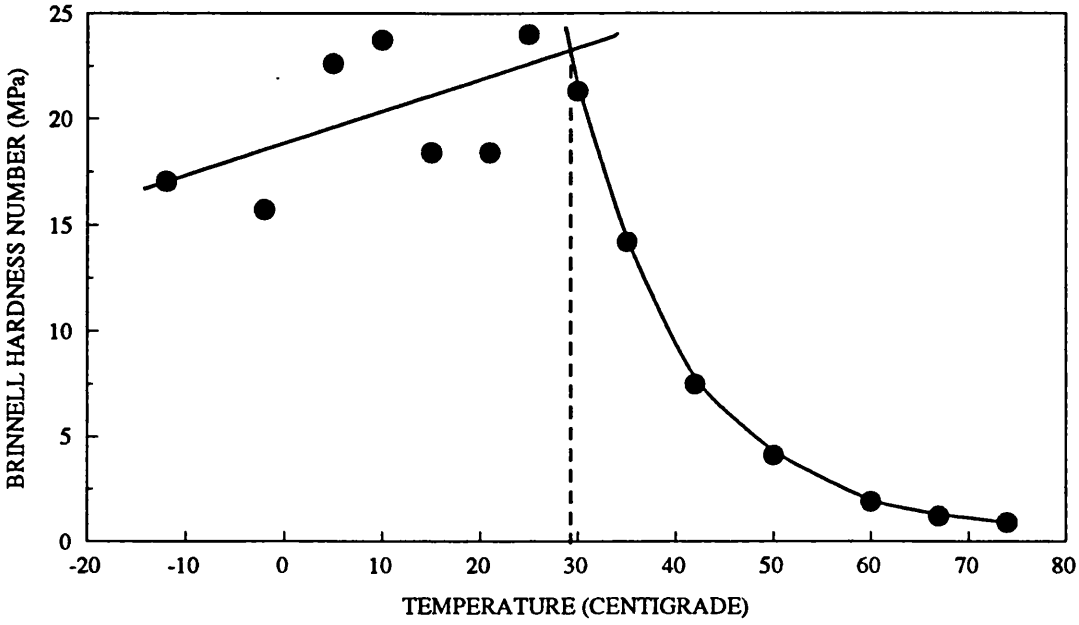

FIG 138: THE EFFECT OF TEMPERATURE ON THE MODULUS OF ELASTICITY OF FILMS CONTAINING EQUAL PROPORTIONS OF EUGRAGIT RL AND EUDRAGIT RS

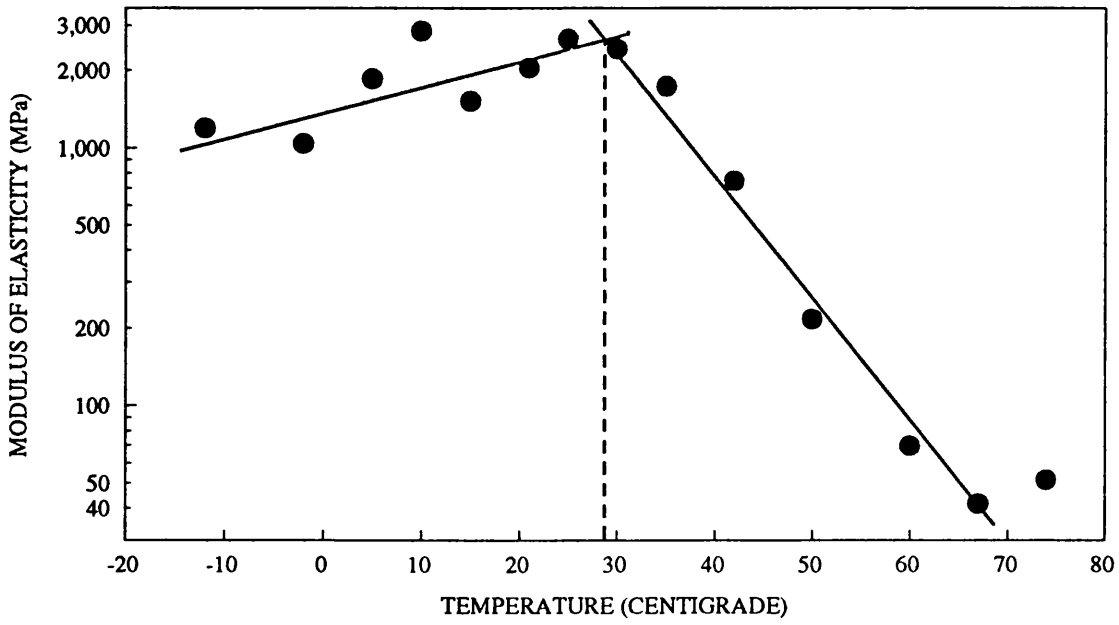

FILMS CAST ONTO DURAL DISCS FROM SOLUTION IN DICHLOROMETHANE

FIG 139: THE EFFECT OF TEMPERATURE ON THE BRINNELL HARDNESS NUMBER OF FILMS CONTAINING EQUAL PROPORTIONS OF EUDRAGIT RL AND EUDRAGIT RS WITH 5% GLYCERYL TRIACETATE RELATIVE TO TOTAL POLYMER WEIGHT

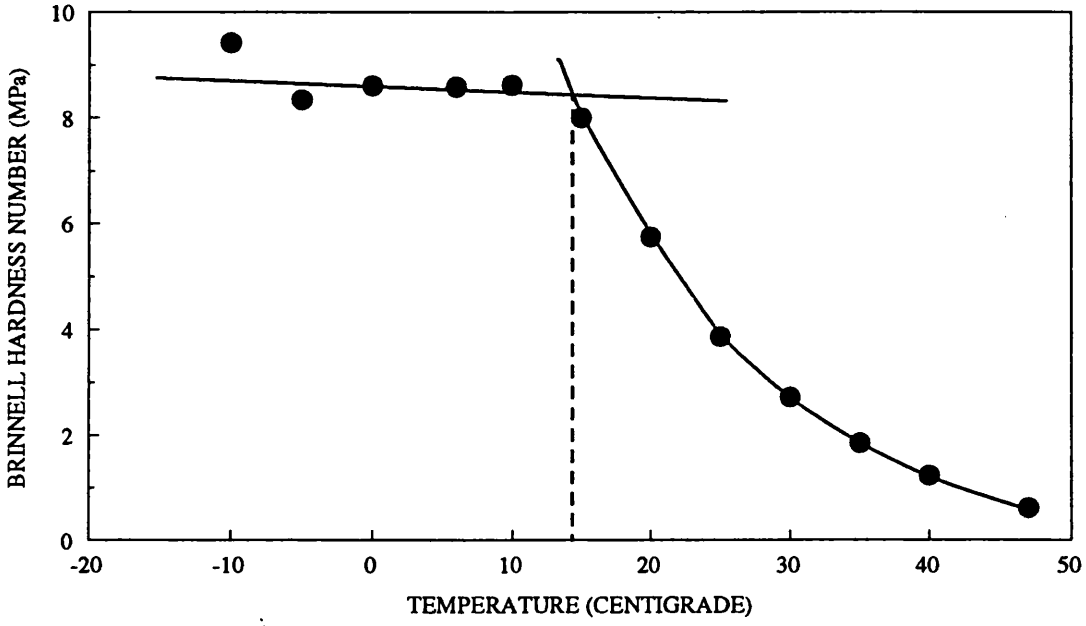

FIG 140: THE EFFECT OF TEMPERATURE ON THE MODULUS OF ELASTICITY OF FILMS CONTAINING EQUAL PROPORTIONS OF EUGRAGIT RL AND EUDRAGIT RS WITH 5% GLYCERYL TRIACETATE RELATIVE TO TOTAL POLYMER WEIGHT

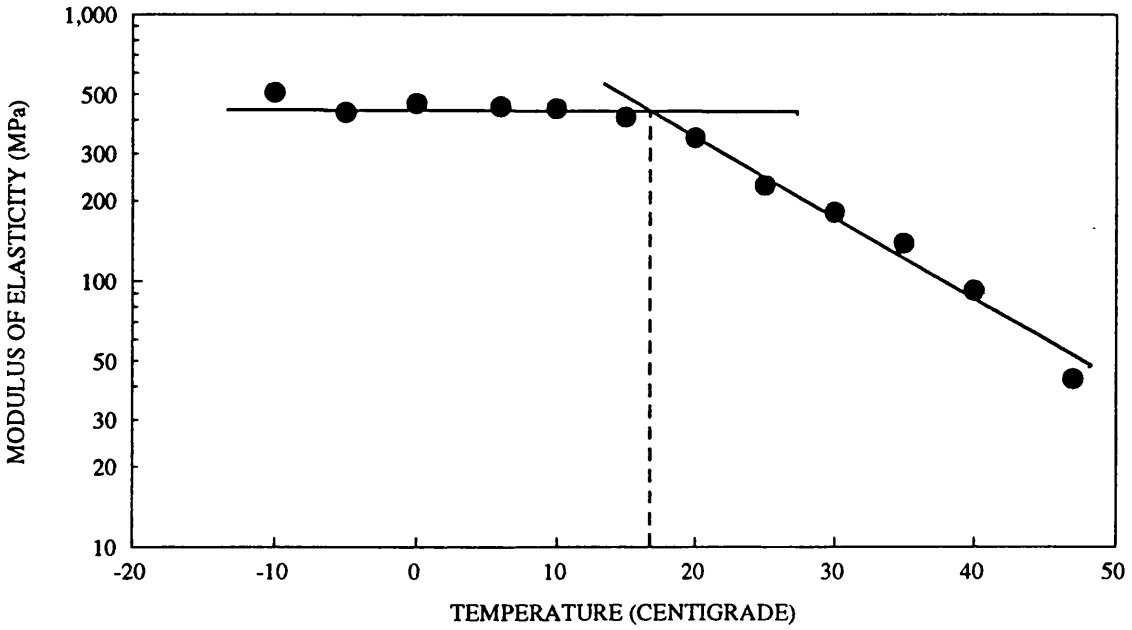

FILMS CAST ONTO DURAL DISCS FROM SOLUTION
IN DICHLOROMETHANE

FIG 141: THE EFFECT OF TEMPERATURE ON THE BRINNELL HARDNESS NUMBER OF FILMS CONTAINING EQUAL PROPORTIONS OF EUDRAGIT RL AND EUDRAGIT RS WITH 10% GLYCERYL TRIACETATE RELATIVE TO TOTAL POLYMER WEIGHT

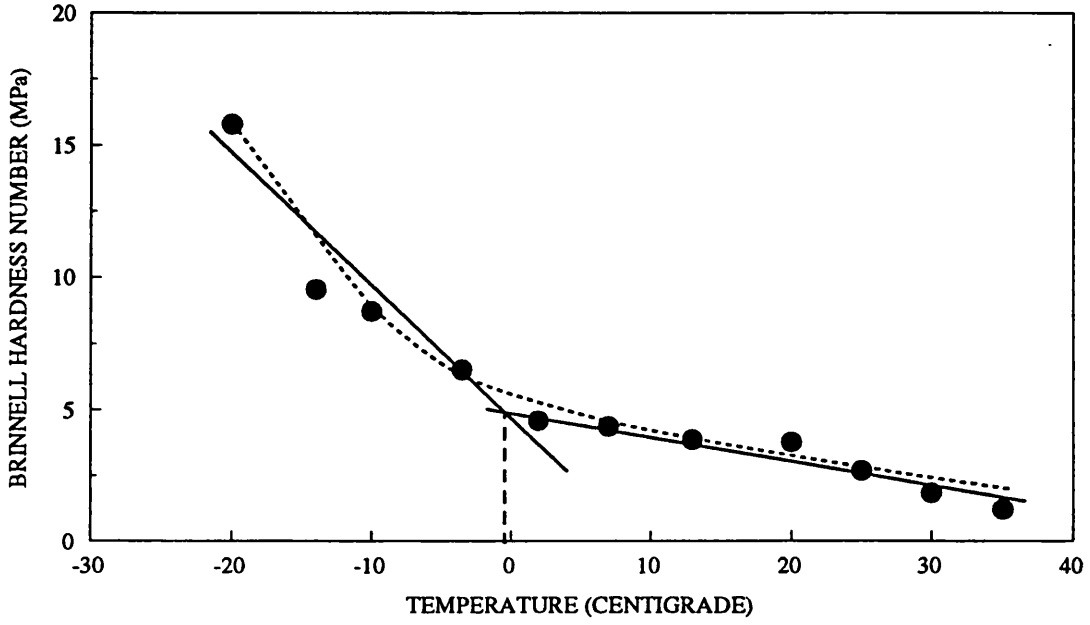

FIG 142: THE EFFECT OF TEMPERATURE ON THE MODULUS OF ELASTICITY OF FILMS CONTAINING EQUAL PROPORTIONS OF EUGRAGIT RL AND EUDRAGIT RS WITH 10% GLYCERYL TRIACETATE RELATIVE TO TOTAL POLYMER WEIGHT

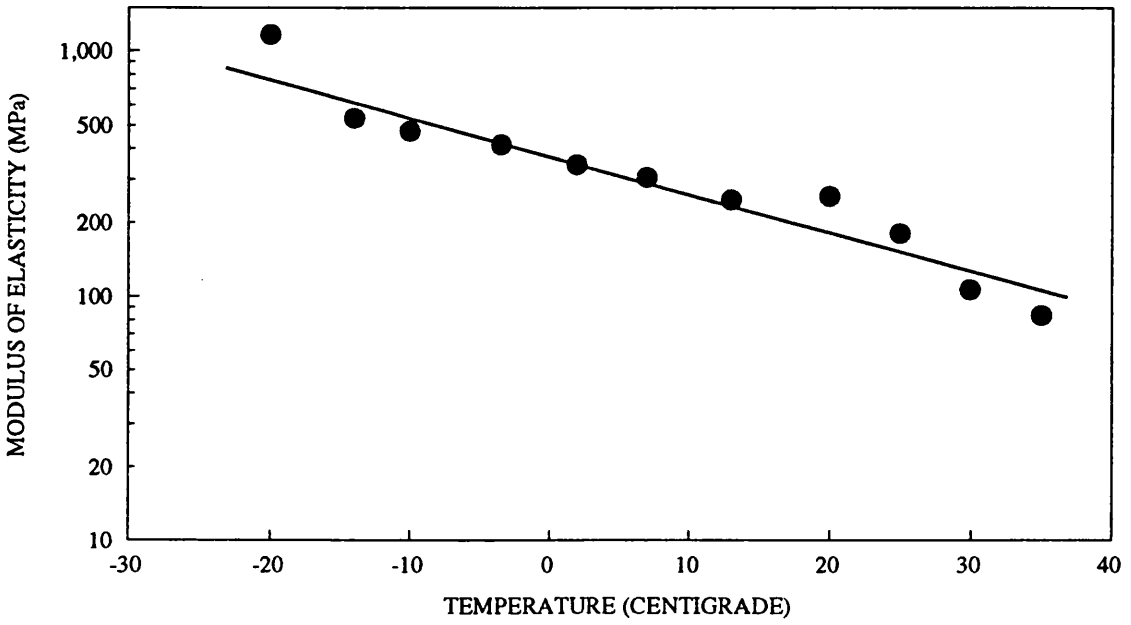

FILMS CAST ONTO DURAL DISCS FROM SOLUTION
IN DICHLOROMETHANE

From Table 28 it is apparent that Eudragit RL and Eudragit RS have similar glass transition temperatures. From X-Ray diffraction studies, both polymers are essentially amorphous as the pure powdered polymer, as well as after casting from solution in dichloromethane and should therefore undergo a glass transition. The values of the glass transition temperature determined are considerably lower than those which have been subsequently reported in the literature. KASSEN et al (1986) determined Tg for Eudragit RL and RS to be 55.1°C and 52.1°C respectively. Differences in determined values of glass transition temperature are possible. Residual solvents and water present in sample preparations may shift the determined by 40-50°C. PORTER AND RIDGEWAY (1983) indicated that difficulties were encountered with glass transition temperatures determined by differential scanning calorimetry. These are due to the small specific heat changes being measured, the failure to establish near-equilibrium conditions during measurement, and the use of too high a scanning temperature which is faster than the changes in molecular motion.

The difference in the degree of quarternary ammonium substitution present in Eudragit RL and Eudragit RS does not appear to affect the glass transition point of the polymers either individually or mixed together in a cast film.

One interesting consequence of the low glass transition

temperature of unplasticised Eudragit copolymers is that diffusion and release experiments were all carried out at 37°C, which is above the determined glass transition. This may account for the observation that although unplasticised films were glassy and difficult to prepare, they did not exhibit notably anamolous release properties.

It must also be noted that hydration of the films also acts as a form of plasticisation. The consequence of these observations is that at 37°C an increase in the polymer free volume and hence its diffusivity over that at room temperature would be expected.

It was possible to infer a glass transition temperature by indentation measurements for the film containing 4.76% glyceryl triacetate, but not for the film containing 9.09%. In the latter case, both the hardness and elasticity of the films decreased progressively with temperature, rather than at a sharp point, suggesting that segmental mobility was increased considerably at higher plasticiser concentration.

The importance of the polymer-plasticiser mixture in determining glass transition temperatures has been discussed by BONDI AND TOBOLSKY (1971) who described the use of mixture rule models. If the mixture is ideal then the contribution of the individual components to the measured value of Tg is determined by that of the component with the greater free volume, whether that free volume is determined by low molecular weight or high internal

molecular mobility. KELLEY AND BUECHE (1961) have proposed a simplified form of mixture rule which relates the composite glass transition temperature of the polymer-plasticiser mixture to the coefficient of volumetric expansion, volume fraction and the glass transition temperature of the components.

With further experimentation it should be possible to predict the glass transition temperatures of mixtures and compare them to measured values to identify the most appropriate plasticiser and concentration.

CHAPTER 6

CONCLUSIONS

6.1 Overall Conclusions

The work described in this thesis is the basis of an evaluation of the polymethacrylate copolymers Eudragit RL (ERL) and Eudragit RS (ERS) in a controlled release formulation. The use of these polymers with oxamniquine dispersed in a coating solution of the polymer subsequently applied to inert pellets is a novel application.

Studies on isolated films of the polymer indicated that this system could effectively control the release of the schistosomicidal drug oxamniquine. The rate of release could be varied by altering the ratio of the two polymers and by including plasticisers in the formulation. Films of ERL and ERS were very brittle and it was necessary to include plasticisers in the formulation. The nature of the plasticiser had a significant effect on the release of oxamniquine, depending upon the solubility of oxamniquine in the plasticiser and the solubility of the plasticiser in aqueous extraction medium. The mechanism of release was not readily predictable. It was expected that this system would behave according to the matrix controlled model developed by HIGUCHI (1963). In several cases, it was possible that a form of dissolution controlled model best described the release kinetics. A mathematical test to

distinguish between the two models was not conclusive. The likely explanation for this is suggested by SCHWARTZ et al (1968) and DONBROW AND FRIEDMAN (1975a) that not all of the conditions defined in these models were met. It is probable that the diffusion coefficient of the drug within the matrix was not constant throughout the duration of the experiments as the composition of the matrix changed as plasticiser was extracted. This is particularly true for phthalate plasticisers where oxamniquine is capable of dimerising in the plasticiser and partitioning between the plasticiser and aqueous buffer within the film.

On first inspection, it appeared that the coating process used to prepare the pellets was successful. A coherent film was formed around the pellets which did not appear to be easily abraded from the surface of the pellet. The presence of a coherent coating was confirmed by examination of sections through the pellet visually and by scanning electron microscopy. The release of oxamniquine was, however, faster than from the corresponding films by factors of several hundred times. Once again, it is difficult to identify a suitable model to describe the release kinetics of oxamniquine from the coated pellets, particularly where phthalate plasticisers were used.

An examination of the pellets by scanning electron microscopy revealed possible reasons for this. Although the coating was coherent and formed a distinct boundary with the pellet, crystals of oxamniquine had evidently

precipitated within the film structure. These crystals might be expected to dissolve rapidly, leading to a fast rate of release.

By contrast, scanning electron microscopy of the surface of isolated films revealed a uniform mottled 'orange skin' appearance, with no evidence of drug precipitations. Furthermore, comparative X-ray crystallography studies on physical mixtures of oxamniquine with ERL and ERS demonstrated that the strongly crystalline pattern of oxamniquine disappeared in the films leaving an apparently amorphous structure.

In conclusion ERL and ERS copolymers exhibit potential for preparing controlled release dosage forms as films containing dispersed oxamniquine but considerable work is required to develop these into films applied to inert pellets.

6.2 Suggestions for Further Work

It would be appropriate for further studies to continue from this work. Since coated pellets released oxamniquine considerably faster than the equivalent free films, it would be useful to prepare free films by a spraying method and examine the structure and release properties of these films. This information might then be applied to produce coatings which did not contain crystals of drug. This may involve changes to the coating conditions used or to the

choice of carrier solvent.

It was not possible to evaluate the mechanical properties of these films with the available equipment, since the films were either too brittle or too plastic. It would be interesting to characterise the mechanical properties of the films, both on preparation and after accelerated and prolonged storage.

It was also not possible to obtain reproducible measurements of the glass transition temperature of the polymers and the effect of plasticisers and dispersed drugs on this parameter. Further studies on glass transitions, perhaps using alternative methods such as the torsional braid pendulum or dielectric relaxation would be useful, particularly to evaluate possible interactions between the polymers, plasticisers and drug.

The range of formulations studied has necessarily been limited, leaving scope for further studies particularly with different plasticisers and using different solvents to prepare films and coatings.

Finally, since the trend in preparing coatings is towards aqueous based systems, these studies could be usefully extended towards examining pseudo-latices of ERL and ERS containing dispersed drugs.

Bibliography

Abdel-Aziz, S.A. M., (1976) Ph.D. Thesis, University of Strathclyde.

Abdel-Aziz, S.A. M. , Anderson, W., and Armstrong, P.A. M. (1975) J. Appl. Polym. Sci. **19**, 1181.

Abdel-Aziz, S.A. M. , and Anderson, W. (1976) J. Pharm. Pharmacol. **28**, 801.

Abdel-Aziz, S.A. M. , Armstrong, P.A. M. , and Anderson, W. (1974) J. Pharm. Pharmacol. **26 Suppl.**, 131P.

Akbuga, J. (1989) Int. J. Pharm. **53**, 99.

Allcock, H.R., and Lampe, F.W. (1981) in Contemporary Polymer Chemistry, Prentice-Hall, New Jersey.

Anderson, W., and Abdel-Aziz, S.A. M. (1976) J. Pharm. Pharmacol. **28 Suppl.**, 22P.

Anderson, W., Armstrong, P.A. M. , and Abdel-Aziz, S.A. M. (1973) J. Pharm. Pharmacol. **25 Suppl.**, 137P.

Azoury, R., Elkayam, R., and Friedman, M. (1988) J. Pharm. Sci. **77**, 424.

Baker, R.W., and Lonsdale, H.K. (1974) in Controlled Release Of Biologically Active Agents, Advances In Experimental Medicine And Biology Volume 47 Edited by Tanquery, A.C., and Lacey, S.R., Plenum, New York. Page 13.

Ballard, B.E. (1978) in Sustained And Controlled Delivery Systems, Edited by Robinson, J.R., Marcel Dekker, New York. Page 1.

Banker, G.S. (1966) J. Pharm. Sci. **55**, 81.

Banker, G.S. (1978) in Polymeric Delivery Systems, Midland Macromolecular Monographs Volume 5 Edited by Kostelnik, R.J., Gordon and Breach, New York. Page 25.

Banker, G.S., Gore, A.Y., and Swarbrick, J. (1966a) J. Pharm. Pharmacol. **18**, 457.

Banker, G.S., Gore, A.Y., and Swarbrick, J. (1966b) J. Pharm. Pharmacol. **18 Suppl.**, 205S.

Barkai, A., Pathak, Y.V., and Benita, S. (1990) Drug Dev. Ind. Pharm. **16**, 2057.

Barnett, R.P., Carless, J.E., and Summers, M.P. (1984) J. Pharm. Pharmacol. **36 Suppl.**, 6P.

Barrer, R.M. (1951) in Diffusion In And Through Solids, Cambridge University Press, London.

Baxter, C.A. R. , and Richards, H.C. (1971) J. Med. Chem. **14**, 1033.

Baxter, C.A. R. , and Richards, H.C. (1972) J. Med. Chem. **15**, 351.

Bayer, K., Soliva, M., and Speiser, P. (1972) Pharm. Ind. **34**, 677.

Benet, L.Z. (1973) in Drug Design Volume IV, Edited by Ariens, E.J., Academic, New York. Page 1.

Benita, S., Barkai, A., and Pathak, Y.V. (1990) J. Controlled Release **12**, 213.

Benita, S., and Donbrow, M. (1982) J. Pharm. Pharmacol **34**, 77.

Benita, S., Hoffman, A., and Donbrow, M. (1985) J. Pharm. Pharmacol. **37**, 391.

Bodmeier, R., and Paeratakul, O. (1990b) Int. J. Pharm. **59**, 197.

Bodmeier, R., and Paeratakul, O. (1990a) J. Pharm. Sci. **79**, 32.

Bondi, A., and Tobolsky, A.V. (1971) in Polymer Science and Materials, Wiley Interscience, New York, Page 118.

Borodkin, S., and Tucker, F.E. (1975) J. Pharm. Sci. **64**, 1289.

Burrell, H. (1975) in Polymer Handbook, 2nd Edition, Edited by Bandrup, J.Immergut, E. H., Wiley Interscience, New York. Page IV 337.

Cadman, A.D., Fleming, R., and Guy, R.H. (1981) J. Pharm. Pharmacol. **33**, 121.

Caldwell, H.C., and Rosen, H.C. (1964) J. Pharm. Sci. **53**, 1387.

Carnell, P.H., and Cassidy, H.G. (1961) J. Polym. Sci. **55**, 233.

Chafi, N., Montheard, J.P., and Vergnaud, J.M. (1988) Int. J. Pharm. **45**, 229.

Chafi, N., Montheard, J.P., and Vergnaud, J.M. (1989a) Int. J. Pharm. **52**, 203.

Chafi, N., Montheard, J.P., and Vergnaud, J.M. (1989b) Drug Dev. Ind. Pharm. **15**, 629.

Chafi, N., Montheard, J.P., and Vergnaud, J.M. (1991) Int. J. Pharm. **67**, 265.

Chandrasekeran, S.K., and Hillman, R. J. Pharm. Sci. **69**, 1311.

Chandrasekaran, S.K., and Paul, D.R. (1982) J. Pharm. Sci. **71**, 1399.

Chandrasekeran, S., Wright, R.M., and Yuen, M.J. (1983) in Controlled Release Delivery Systems, Edited by Roseman, T.J., and Mansdorf, S.Z., Marcel Dekker, New York. Page 1.

Chang, N.J., and Himmelstein, K.J. (1990) J. Controlled Release **12**, 201.

Chang, R.K., Price, J.C., and Hsiao, C. (1989) Drug Dev. Ind. Pharm. **15**, 361.

Chien, Y.W. (1976) in Controlled Release Polymeric Formulations, ACS Symposium Series No. 33 Edited by Paul, D.R., and Harris, F.W., American Chemical Society, Washington DC. Pge 53.

Chien, Y.W., and Lambert, H.J. (1974) J. Pharm. Sci. **63**, 515.

Chien, Y.W., Lambert, H.J., and Grant, D.E. (1974) J. Pharm. Sci. **63**, 365.

Chien, Y.W., Lambert, H.J., and Lin, T.K. (1975) J. Pharm. Sci. **64**, 1643.

Chien, Y.W., Rozek, L.F., and Lambert, H.J. (1976) in Controlled Release Polymeric Formulations, ACS Symposium Series No 33 Edited by Paul, D.R., and Harris, F.W., American Chemical Society, Washington, DC. Page 72.

Colletta, V., and Rubin, H. (1964) J. Pharm. Sci. 53, 953.

Colombo, P., Conte, U., Caramella, C., Gazzaniga, A., and LaManna, A. (1985) J. Controlled Release **1**, 283.

Cooper, J., Swartz, C.J., and Suydam, W.Jr (1961) J. Pharm. Sci **50**, 67.

Crank, J. (1975) in The Mathematics Of Diffusion, Clarendon, Oxford, England.

Crank J. , and Park, G.S. (1968) in Diffusion In Polymers, Edited by Crank, J., and Park, G.S., Academic, New York. Page 1.

DeFillipas, P., Boscolo, M., Gibellini, M., Rupena, P., Rubessa, F., and Moneghini, M. (1991) Drug Dev. Ind. Pharm. **17**, 2017.

Delporte, J.P., and Jaminet, F. (1978a) J. Pharm. Belg. **33**, 179.

Delporte, J.P., and Jaminet, F. (1978b) J. Pharm. Belg. **33**, 227.

Desai, S.J., Simonelli, A.P., and Higuchi, W.I. (1965) J. Pharm. Sci. **54**, 1459.

Desai, S.J., Singh, P., Simonelli, A.P., and Higuchi, W.I. (1966a) J. Pharm. Sci. **55**, 1224.

Desai, S.J., Singh, P., Simonelli, A.P., and Higuchi, W.I. (1966b) J. Pharm. Sci. **55**, 1230

Desai, S.J., Singh, P., Simonelli, A.P., and Higuchi, W.I. (1966c) J. Pharm. Sci. **55**, 1235.

Donbrow, M., and Benita, S. (1982) J. Pharm. Pharmacol. **34**, 547.

Donbrow, M., and Friedman, M. (1974) J. Pharm. Pharmacol. **26**, 148.

Donbrow, M., and Friedman, M. (1975a) J. Pharm. Sci. **64**, 76.

Donbrow, M., and Friedman, M. (1975b) J. Pharm. Pharmacol. **27**, 463.

Donbrow, M., and Samuelov, Y. (1980) J. Pharm. Pharmacol. **32**, 463.

El-Fattah, S.A., El-Massik, M., and Salib, N.N. (1984b) Drug Dev. Ind. Pharm. **10**, 809.

El-Fattah, S.A., Salib, N.N., and El-Massik, M. (1984a) Drug Dev. Ind. Pharm. **10**, 649.

Ellis, J.R., Prillig, E.B., and Amann, A.H. (1976) in Theory and Practice of Industrial Pharmacy, Edited by Lachman, H.A., Lieberman, and Kanig, J.A., Lea and Febiger, Philadelphia. Page 359.

Fanger, G.O. (1974) in Proc. Controlled Release Pesticide Symposium, Edited by Cardarelli, N.F., University of Akron, Ohio. Page 1.18.

Farhadieh, B., Borodkin, S., and Buddenhagen, J.D. (1971a) J. Pharm. Sci. **60**, 209.

Farhadieh, B., Borodkin, S., and Buddenhagen, J.D. (1971b) J. Pharm. Sci. **60**, 212.

Fessi, H., Marty, J-P, Puisieux, F., and Carstenson, J.T. (1982) J. Pharm. Sci. **71**, 749.

Fites, A.L., Banker, G.S., and Smolen, V.F. (1970) J. Pharm. Sci. **59**, 610.

Flynn, G.L. (1974) in Controlled Release Of Biologically Active Agents, Advances In Experimental Medicine And Biology Volume 47 Edited by Tanquery, A.C., and Lacey, S.R., Plenum, New York. Page 73.

Flynn, G.L., Yalkowsky, S.H., and Roseman, T.J. (1974) J. Pharm. Sci. **63**, 479.

Friedman, M., and Donbrow, M. (1978) Drug Dev. Ind. Pharm. **4**, 319.

Friedman, M., Donbrow, M., and Samuelov, Y. (1979) J. Pharm. Pharmacol. **31**, 396.

Garcia, R., Siquerios, A., and Benet, L.Z. (1978) Pharm. Acta Helv. **53**, 99.

Geigy Scientific Tables (1984) Volume 3 Geigy Ltd., Basle. Page 58.

Gibaldi, M., and Feldman, S. (1967) J. Pharm. Sci. **56**, 1238.

Gibaldi, M., and Perrier, D. (1975) in Pharmacokinetics, Marcel Dekker, New York. Page 166.

Gillard, J., Tamba Vemba, and Roland, M. (1980) Pharm. Acta Helv. **55**, 231.

Gonzales, M.A., Nematollahi, J., Guess, W.L., and Autian, J. (1967) J. Pharm. Sci. **56**, 1288.

Good, W.R. (1978) in Polymeric Delivery Systems, Midland Macromolecular Monographs Volume 5 Edited by Kostelnik, R.J., Gordon and Breach, New York. Page 139.

Goodhard, F.W., Harris, M.R., Murthy, K.S., and Nesbitt, R.V. (1984) Pharm. Tech. **4**, 64.

Gould, P.L. (1983) Br. Polym. J. **15**, 172.

Gurny, R. (1976) Pharm. Acta Helv. **51**, 1.

Gurny, R., Buri, P., Sucker, H., Guitard, P., and Leuenberger, P. (1977a) Pharm. Acta Helv. **52**, 175.

Gurny, R., Buri, P., Sucker, H., Guitard, P., and Leuenberger, P. (1977b) Pharm. Acta Helv. **52**, 247.

Gurny, R., Guitard, P., Buri, P., and Sucker, H. (1977c) Pharm. Acta Helv. **52**, 182.

Gurny, R., Mordier, D., and Buri, P. (1976) Pharm. Acta Helv. **51**, 384.

Haleblain, J., Runkel, R., Mueller, N., Christopherson, J., and Ng, K. (1971) J. Pharm. Sci. **60**, 541.

Hall, H.S., and Pondell, R.E. (1980) in Controlled Release Technology: Methods, Theory, and Applications, Volume 2 Edited by Kydoneius, A.F., CRC Press, Boca Ratan. Page 133.

Hannula, A-M (1983a) Acta Pharm. Fenn. **92**, 37.

Hannula, A-M (1983b) Acta Pharm. Fenn. **92**, 45.

Hannula, A-M, and Iivanaienen, H. (1983a) Acta Pharm. Fenn. **92**, 85.

Hannula, A-M, and Iivanaienen, H. (1983b) Acta Pharm. Fenn. **92**, 105.

Harbert, F.C. (1974) Manufacturing Chemist and Aerosol News January 23.

Harris, F.W. (1976) in Proc. Controlled Release Pesticide Symposium, Edited by Cardarelli, N.F., University of Akron, Ohio. Page 1.33.

Higuchi, T. (1960) J. Soc. Cosmet. Chem. **11**, 85.

Higuchi, T. (1961) J. Pharm. Sci. **50**, 874.

Higuchi, T. (1963) J. Pharm. Sci. **53**, 1145.

Higuchi, W.I. (1961) J. Pharm. Sci. **51**, 802.

Higuchi, W.I. (1967) J. Pharm. Sci. **56**, 315.

Hildebrand, J.H., and Scott, R.L. in Solubility of Non-Electrolytes, 3rd Edition, Reinhold, New York. Page 124.

Hixson, A.W., and Crowell, J.H. (1931) Ind. Eng. Chem. **2**, 923.

Hopfenberg, H.B. (1978) in Polymeric Delivery Systems, Midland Macromolecular Monographs Volume 5 Edited by Kostelnik, R.J., Gordon and Breach, New York. Page 1.

Hopfenberg, H.B., Apicella, A., and Saleeby, D.E. (1981) J. Membrane Sci. **8**, 273.

Hopfenberg, H.B., and Hsu, K.C. (1978) Polym. Eng. Sci. **18**, 1186.

Jain, S.K., and Vyas, S.P. Dixit, V. K. (1990) J. Controlled Release **12**, 257.

Johnston, H.K., and Sourirajan, S. (1973) J. Appl. Polymer Sci. **17**, 2485.

Jones, D.M. (1985) Pharm. Tech. **9**, 50.

Kanig, J.L., and Goodman, H. (1962) J. Pharm. Sci. **51**, 77.

Kassen, M.A., Attia, M.A., and Safwat, S.M. (1986) J. Pharm. Belg. **41**, 106.

Kawashima, Y., Niwa, T., Kanda, T., Takeuchi, H., Iwamoto, T., and Itoh, K. (1989) J. Pharm. Sci. **78**, 68.

Kaye, B. (1978) in Advances In Pharmacology and Therapeutics, Edited by Adolphe, M., Pergamon Press, New York. Page 41.

Kaye, B., and Roberts, D.W. (1980) Xenobiotica **10**, 97.

Kelley, F.N., and Bueche, F. (1961) J. Polym. Sci. **50**, 549.

Kent, D.J., and Rowe, R.C. (1978) J. Pharm. Pharmacol. **30**, 308.

Kofitsekpo, W.M. (1980) Drugs Exptl. Clin. Res. **6**, 421.

Kolonits, V. (1968) Kolloid Z. Z. Polymere **226**, 40.

Korsemeyer, R.W., Gurny, R., Doelker, E., Buri, P., and Peppas, N.A. (1983) J. Pharm. Sci. **72**, 1189.

Korsemeyer, R.W., and Peppas, N.A. (1983) in Controlled Release Delivery Systems, Edited by Roseman, T.J., and Mansdorf, S.Z., Marcel Dekker, New York. Page 77.

Krebs, H.A., and Speakman, J.C. (1945) J. Chem. Soc. **159**, 593.

Kuelling, W., and Simon, E.J. (1980) Pharm. Tech. Int. **3**, 29.

Kumins, C.A., and Roteman, J. (1961) J. Polym. Sci. **55**, 683.

Kydoneius, A.F. (1980) in Controlled Release Technology: Methods, Theory, and Applications, Edited by Kydoneius, A.F., CRC Press, Boca Ratan. Page 1.

Lachman, L., and Drubulis, A. (1964) J. Pharm. Sci. **53**, 639.

Laguna, O., Luong Thanh Thuy , Duchene, D., and Seiller, M. (1975) R. Sci. Techn. Pharm. **T.4**, 91.

Langer, R. (1980) Chem. Eng. Commun. **6**, 1.

Lapidus, H., and Lordi, N.G. (1966) J. Pharm. Sci. **55**, 840.

Lapidus, H., and Lordi, N.G. (1968) J. Pharm. Sci. **57**, 1292.

Lappas, L., and McKeehan, W. (1965) J. Pharm. Sci. **54**, 176.

Launo, J.A. K. , Agrawal, D.K., and Emenige, I.V. (1990) Drug Dev. Ind. Pharm. **16**, 1375.

Lazarus, J., and Cooper, J. (1959) J. Pharm. Pharmacol. **11**, 257.

Lee, P.I. (1980a) J. Membrane Sci. **7**, 255.

Lee. P. I. (1980b) in Controlled Release of Bioactive Materials, Edited by Baker, R.W., Academic, New York. Page 135.

Lee, W.A., and Knight, G.J. (1965) in Polymer Handbook, Edited by Brandrup, J., and Immergut, E.H., Wiley Interscience, New York. Page III-62.

Lehmann, K. (1971) Pharma International **3** 1.

Lehmann, K. (1975) Acta Pharm. Tech. **21**, 255.

Lehmann, K. (1982) Acta Pharm. Fenn. **91**, 225.

Lehmann, K. (1984) Acta Pharm. Fenn. **93**, 55.

Lehmann, K. (1968) Drugs Made In Germany **11**, 34.

Lehmann, K.O. R. , Bossler, H.M., and Dreher, D.K. (1978) in Polymeric Delivery Systems, Midland Macromolecular Monographs Volume 5 Edited by Kostelnik, R.J., Gordon and Breach, New York. Page 111.

Lehmann, K., and Dreher, D. (1981) Int. J. Pharm. Tech. Prod. Manf. **2**, 31.

Lehmann, K., and Dreher, D. (1979) Pharm. Tech. **2**, 33.

Lehr, C-M, Boustra, J.A., Tunner, J.J., and Junginger, H.E. (1990) J. Controlled Release **12**, 51.

Levich, V.G. (1962) in Physicochemical Hydrodynamics, Prentice Hall, Englewood Cliffs, NJ.

Li, L.C., and Peck, G.E. (1989) Drug Dev. Ind. Pharm. **15**, 65.

Lippold, B.C., Lippold, B.H., and Sgoll, G.B. (1980) Pharm. Ind. **42**, 745.

Malamataris, S., and Avgerinos, A. (1990) Int. J. Pharm. **62**, 105.

Martindale (1989) in The Extra Pharmacopoeia, 29th Edition, The Pharmaceutical Press, London. Page 61.

Mehta, A.M., and Jones, D.M. (1985) Pharm. Tech. **9**, 52.

Mishell, D.R., Jr. , Moore, D.R., Roy, S., Brenner, P.F., and Page, M.A. (1978) Am. J. Obstet. Gyned. **130**, 55.

Mishell, D.R., Jr. , Talas, M., Parlow, A.F., and Mayer, D.L. (1970) Am. J. Obstet. Gynec. **107**, 100.

Monk, C.H. J. , and Wright, T.A. (1965) J. Oil and Colour Chemists Assn. **48**, 520.

Munden, B.J., DeKay, H.G., and Banker, G.S. (1964) J. Pharm. Sci. **53**, 395.

Naidoo, N.T., and McGinity, J.W. (1985) S.A. Pharm. J. February **73**.

Nixon, J.R., and Wong, K.T. Int. J. Pharm. **58**, 31.

Okor, R.S. (1982a) J. Pharm. Pharmacol. **34**, 83.

Okor, R.S. (1982b) Int. J. Pharm. **11**, 1.

Okor, R.S. (1990) J. Controlled Release **12**, 195.

Okor, R.S. (1991) J. Pharm. Pharmacol. **43**, 198.

Okor, R.S., and Anderson, W. (1978a) J. Pharm. Pharmacol. **30 Suppl.**, 4P.

Okor, R.S., and Anderson, W. (1978b) J. Pharm. Pharmacol. **30 Suppl.**, 6P.

Okor, R.S., and Anderson, W. (1979) J. Pharm. Pharmacol. **31 Suppl.**, 78P.

Okor, R.S., and Obi, C.E. (1990) Int. J. Pharm. **58**, 89.

Okor, R.S., and Yahahya, M.A. (1990) Pharm. Res. **7**, 1208.

Oth, M.P., Moes, and A. J. (1989) Int. J. Pharm. **55**, 157.

Park, G.S. (1968) in Diffusion In Polymers, Edited by Crank, J., and Park, G.S., Academic, New York. Page 141.

Patel, M., Patel, J.M., and Lemberger, A.P. (1964) J. Pharm. Sci. **53**, 286.

Paul, D.R. (1976) in Controlled Release Polymeric Formulations, ACS Symposium Series No. 33 Edited by Paul, D.R., and Harris, F.W., American Chemical Society, Washington DC. Page 1.

Paul, D.R., and McSpadden, S.K. (1976) J. Membrane Sci. **1**, 33.

Peters, M. (1963a) Aust. J. Pharm. **44**, 52.

Peters, M. (1963b) Aust. J. Pharm. **44**, 514.

Peters, R.H. (1968) in Diffusion In Polymers, Edited by Crank, J., and Park, G.S., Academic, New York. Page 315.

Pickard, J.F., (1979) Ph.D. Thesis, Sunderland Polytechnic.

Pondell, R.E. (1984) Drug Dev. Ind. Pharm. **10**, 191.

Pongpaibul, Y., Price, J.C., and Whitworth, C.W. (1984) Drug Dev. Ind. Pharm. **10**, 1597.

Porter, S.C., (1980) Ph.D. Thesis, University of London.

Porter, S.C., and Ridgeway, K. (1983) J. Pharm. Pharmacol. **35**, 341.

Richards, H.C., and Foster, R. (1969) Nature **222**, 581.

Ritschell, W.A. (1973) in Drug Design Volume IV, Edited by Ariens, E.J., Academic, New York. Page 38.

Robinson, J.R. in Chem. Marketing And Economic Reprints, Edited by Long, F.W., O'Neill, W.P., and Stewart, R.D., American Chemical Society, San Francisco. Page 212.

Robinson, M.J., Grass, G.M., and Lantz, R.J. (1965) J. Pharm. Sci. **57**, 1983.

Robinson, R.A., and Stokes, R.H. (1965) in Electrolyte Solutions, Volume 2nd Edition (rev.) Butterworths, London. Page 253.

Rohm Pharma (1979a) Information Sheet RL 3/e

Rohm Pharma (1979b) Information Sheet RS 3/e

Roseman, T.J. (1972) J. Pharm. Sci. **61**, 46.

Roseman, T.J., and Cardarelli, N.F. (1980) in Controlled Release Technology: Methods, Theory, and Applications, Edited by Kydoneius, A.F., CRC Press, Boca Ratan. Page 21.

Roseman, T.J., and Higuchi, W.I. (1970) J. Pharm. Sci. **59**, 353.

Roseman, T.J., and Yalkowsky, S.H. (1976) in Controlled Release Polymeric Formulations, ACS Symposium Series No. 33 American Chemical Society, Washington DC. Page 33.

Samuelov, Y., Donbrow, M., and Friedman, M. (1979) J. Pharm. Pharmacol. **31**, 120.

Schwartz, J.B., Simonelli, A.P., and Higuchi, W.I. (1968) J. Pharm. Sci. **57**, 274.

Sciarra, J.J., and Gidwani, R. J. Pharm. Sci. **61**, 759.

Sciarra, J.J., and Gidwani, R. J. Soc. Cosmet. Chem. **21**, 66.

Seager, H., Taskis, C.B., and Way, T.J. R. (1976) Manufacturing Chemist and Aerosol News **47** (2), 31.

Serota, D.G., Meyer, C.M., and Autian, J. (1972) J. Pharm. Sci. **57**, 274.

Seymour, R.W., and Minter, J.R. (1980) Polym. Eng. Sci. **20**, 1188.

Shah, N.B., and Sheth, B.B. (1972) J. Pharm. Sci. **53**, 790.

Shangraw, R.F. (1967) Hosp. Pharm. **2**, 19.

Shaw, J.E., Chandrasekeran, S., and Taskovitch, L. (1975) Pharm. J.,**215** 325.

Singh, P., Desai, S.J., Simonelli, A.P., and Higuchi, W.I. (1967a) J. Pharm. Sci. **56**, 1542.

Singh, P., Desai, S.J., Simonelli, A.P., and Higuchi, W.I. (1967b) J. Pharm. Sci. **56**, 1548.

Singiser, R.E., and Lowenthal, W. (1961) J. Pharm. Sci. **50**, 168.

Spilman, C.H., Beuving, D.C., Forbes, A.D., Roseman, T.J., and Larion, L.J. (1976) Prostaglandins, Suppl. **12**, 1.

Spitael, J., and Kinget, R. (1977a) J. Pharm. Belg. **32**, 569.

Spitael, J., and Kinget, R. (1977b) Pharm. Acta Helv. **52**, 106.

Spitael, J., and Kinget, R. (1980) Pharm. Acta Helv. **55**, 157.

Sprockel, O.L., Prapaitrakul, W., and Shivnand, P. (1990) J. Pharm. Pharmacol. **42**, 152.

Stricker, H. (1969) Pharm. Ind. **51**, 794.

Stricker, H. (1971) Pharm. Ind. **33**, (3) 157.

Tamba Vemba , Gillard, J., and Roland, M. (1980) Pharm. Acta Helv. **55**, 65.

Theeuwes, F., and Bayne, W. J. Pharm. Sci. **66**, 1388.

Wagner, G.J. (1961) J. Pharm. Sci. **50**, 359.

Watts, P.J., Davies, M.C., and Melia, C.D. (1991) J. Controlled Release **16**, 311.

Weast, R.C. (1980) in CRC Handbook of Chemistry And Physics Students Edition, Edited by Weast, R.C., CRC Press, Boca Ratan.

Wendlandt, W.W., and Gallagher, P.K. (1981) in Thermal Characterisation of Polymeric Materials, Edited by Turi, E.A., Academic, New York. Page 33.

Wolkoff, H.N., Pinchuk, G., and Shapiro, P.H. (1968) J. Pharm. Sci. **57**, 317.

Wurster, D.E. (1959) J. Am. Pharm. Assn. (Sci. Ed.) **48**, 451.

Zaffaroni, A. (1973) Fifteenth Annual National Industrial Pharmaceutical Conference, through Swarbrick, J. Aust J. Pharm. Sci. (1976) **NS5**, 73.

Zatz, J.L., Wiener, N.D., and Gibaldi, M. (1969) J. Pharm. Sci. **58**, 1493.